the role and regulation of the Atypical Chemokine Receptor 2 in psoriasiform inflammation

Kave Shams
MBChB *hons.* (*Edin.*), BSc (*hons.*), MRCP (Dermatology)

Submitted in fulfilment of the requirements for the Degree of Doctor of Philosophy

Institute of Infection, Immunity and Inflammation
College of Medical, Veterinary and Life Sciences,
University of Glasgow

July 2016

Abstract

Psoriasis is a common, debilitating systemic inflammatory disorder that is characterised by sharply demarcated, thick, erythematous scaly skin plaques. Such plaques commonly appear on skin that is subjected to repeated tensile trauma, such as elbows, knees and flexures. The mechanism by which these inflammatory lesions are spatially restricted is not known and yet knowledge of this could be of critical importance for our understanding of this disease. Chemokines are the principal regulators of leukocyte migration and play a critical role in the initiation and maintenance of inflammation. The atypical chemokine receptor ACKR2 (formerly D6) binds inflammatory CC-chemokines, but does not signal upon ligand binding; instead ACKR2 internalises and helps degrade such chemokines, after which it continues to cycle back to the cell surface. ACKR2 acts, through this mechanism, as a high-capacity scavenger of chemokines, and plays an important role in regulating inflammation. It is known that ACKR2 expression is high in unaffected skin of patients with psoriasis (remote from inflammatory plaques) and concurrently deficient in the plaques themselves. Additionally, human studies have shown that simple skin trauma in psoriasis patients causes a reduction in cutaneous ACKR2 expression at the site of trauma. However, the functional significance and the molecular mechanism by which it occurs are not understood. This thesis explored the role of ACKR2 in the spatial restriction of psoriasiform inflammation and the molecular mechanisms for its differential regulation. Through the use of disease relevant mouse models, primary human cell cultures and novel cell migration assays, the results presented here show that localised psoriasiform inflammation upregulates ACKR2 in remote tissues through the systemic release of cytokines. This remotely upregulated ACKR2 expression protects tissues from the further spread of inflammation. This protective effect is mediated by stromally expressed ACKR2 that acts to control inflammatory T-cell positioning within the skin. Tensile trauma of keratinocytes however, acted to reduce ACKR2 expression in the context of inflammation, which in turn provides a novel mechanism for the well-characterised phenomenon that occurs in psoriasis (and a range of skin condition) termed ‘koebnerisation’. Koebnerisation refers to the phenomenon by which

relatively simple skin trauma induces the development of disease-specific skin lesions. Furthermore, this thesis defines novel disease-relevant regulators of ACKR2 expression. *In silico* analyses identified psoriasis-associated microRNAs that bound to the 3'-UTR of ACKR2, and reduced its expression at transcriptional and protein level. Importantly, trauma of keratinocytes induced ACKR2 downregulation concurrent with a substantial and significant increase in the expression of the identified ACKR2 targeting microRNAs. Together, this thesis defines a novel mechanism by which ACKR2-mediated regulation of chemokine function, cutaneous trauma, microRNAs and systemic cytokines, co-ordinately modulate the predisposition of remote tissue sites to the development of new lesions. Importantly, the results presented here have profound implications for how spatial restriction is imposed on inflammation. The data also highlight therapeutic ACKR2 induction as a plausible novel strategy for the limitation and treatment of psoriasiform- and potentially other forms of inflammation.

Table of contents

Abstract **2**

List of figures and tables **9**

Acknowledgements **13**

Author's statements **14**

List of abbreviations **15**

1 Introduction **18**

1.1 Chemokines **18**

1.1.1 Chemokines and chemokine receptors: evolution, nomenclature and classification 18

1.1.2 Chemokines-chemokine receptor interactions: intracellular signalling events; PI3K pathways 21

1.1.3 Intracellular signalling events; non-PI3K pathways 22

1.1.4 Chemokine haptotactic gradient formation 22

1.1.5 Homeostatic chemokines in skin 23

1.1.6 Chemokines in inflamed skin and psoriasis 24

1.2 Immune cells and chemokines **25**

1.2.1 Dendritic Cells: chemokines and DC entry into and localisation in skin 25

1.2.2 Dendritic Cells: chemokines and trafficking to draining lymph nodes (LN); a CCR7-dependent process 26

1.2.3 T-cell migration: the role of chemokines 28

1.3 The atypical chemokine receptors **30**

1.3.1 Atypical Chemokine Receptor family: nomenclature and overview 30

1.3.2 ACKR2: molecular mechanism of chemokine scavenging 32

1.3.3 ACKR2: expression patterns and disease associations 35

1.3.4 ACKR2: *in vivo* function: lymphatic endothelial cells 39

1.3.5 ACKR2: *in vivo* function: skin and keratinocytes 39

1.3.6 ACKR2: *in vivo* function: leukocytes 41

1.3.7 ACKR2: regulators of expression 41

1.3.8 The Atypical Chemokine Receptor 1 42

1.3.9 The Atypical Chemokine Receptor 3 42

1.3.10 The Atypical Chemokine Receptor 4 43

1.3.11 Chemokines as therapeutic targets 44

1.4 Clinical aspects of psoriasis **45**

1.4.1 Overview 45

1.4.2 Structure and function of skin in health and psoriasis 45

1.4.3 Diagnosing psoriasis 50

1.4.4 Features of clinical variants of psoriasis 51

1.4.5 Quantification of disease severity 52

1.5 Treatment of psoriasis **53**

1.5.1 Principles of treating psoriasis 53

1.5.2 Biological agents 54

1.5.3 Small molecule antagonists 57

1.6 Genetics of psoriasis **58**

1.6.1 Heritability of psoriasis 58

1.6.2 Genetic determinants of psoriasis: PSORS1 and HLA-C 59

1.6.3 Genetic determinants beyond HLA-C 60

1.7 Environmental triggers of psoriasis **60**

1.8 Immunopathogenesis of psoriasis **61**

1.8.1 T-cells in psoriasis: overview 64

1.8.2 T-cells subsets in healthy skin 65

1.8.3 Cytotoxic CD8+ T-cells in psoriasis; early arrivals in the epidermis.... 65
1.8.4 Th17 cells in psoriasis; the IL-23/Th17 axis..... 66
1.8.5 γδT-cells in psoriasis: innate-like pro-inflammatory cells 67
1.8.6 Regulatory T-cells..... 68
1.8.7 Resident memory T-cells; initiators of psoriasiform inflammation..... 68
1.8.8 Keratinocytes in health and disease: overview..... 69
1.8.9 Keratinocytes in psoriasis; environmental and immune sensors 70
1.8.10 Keratinocytes in psoriasis; amplifiers of immune signals and recruiters of leukocytes..... 71
1.8.11 Dendritic cells in psoriasis; bridging adaptive and innate immune systems 72
1.8.12 DC activation in psoriasis by antimicrobial peptides 72
1.8.13 Neutrophils in psoriasis..... 73
1.8.14 Macrophages in psoriasis 74
1.9 Laboratory models of psoriasis 75
1.9.1 Animal models of psoriasiform inflammation..... 75
1.9.2 Imiquimod mouse model: the conception of the IMQ model 76
1.9.3 Imiquimod mouse model: characteristics 77
1.9.4 Spontaneous mouse models 78
1.9.5 Xenotransplantation mouse model 79
1.9.6 Transgenic mouse models..... 81
1.9.7 Exogenous IL-23 induced mouse model 81
1.10 Overview of thesis 82

2 Methods and materials..... 86
2.1 Animal work 86
2.1.1 General principles of experiments involving mice 86
2.1.2 Imiquimod mouse model 86
2.1.3 Cytokine treatment of mice 87
2.1.4 Assessment of skin inflammation *in vivo* 87
2.1.5 Infection of mouse skin with Bunyamwera virus 87
2.1.6 Processing of tissues post cull..... 87
2.2 Protein quantification in murine skin..... 88
2.2.1 Dermal-epidermal skin splitting 88
2.3 Immunohistochemistry..... 89
2.3.1 Immunohistochemistry of tissues 89
2.3.2 Fluorescent immunocytochemistry..... 89
2.4 Cell culture 90
2.4.1 Primary cell cultures: keratinocytes (KC) 90
2.4.2 Primary cell cultures: lymphatic endothelial cells (LEC) 90
2.4.3 Cell line culture; HEK293 and HEK293 ACKR2 transfectants 91
2.4.4 Freezing of cells..... 91
2.4.5 Thawing of cells 91
2.4.6 Subculture protocols..... 91
2.4.7 Cytokine treatment of cells 92
2.4.8 Generation of skin equivalents..... 92
2.4.9 Tensile stress of cells..... 93
2.4.10 Isolation and stimulation of human T-cells 94
2.5 Cell migration 94
2.5.1 Preparation of migration chambers 94
2.5.2 Preparation of cell layers 95
2.5.3 Analysis of cell migration 95
2.6 microRNAs 96
2.6.1 microRNA *in silico* selection..... 96
2.6.2 microRNA transfection of cells..... 96
2.6.3 Luciferase microRNA assay 96
2.7 Western Blots 97

2.7.1 Lysis of Cell cultures..... 97
2.7.2 Preparation of Western Blot Gel..... 98
2.7.3 Antibody staining of Western Blot (for ACKR2)..... 98
2.7.4 Antibody staining of Western Blot (for ß-tubulin, housekeeping gene) 99
2.7.5 Western blot band densitometry 99
2.8 RNA extraction.....99
2.8.1 RNA purification from cell cultures 99
2.8.2 RNA purification from skin and solid organs 100
2.8.3 Reverse transcription of RNA.....101
2.9 Polymerase chain reaction 102
2.9.1 Quantitative Polymerase Chain Reaction (PCR) primer design.....102
2.9.2 Polymerase Chain Reaction (PCR) 103
2.9.3 Generation of standard curve for QPCR 103
2.9.4 Quantitative Polymerase Chain Reaction (PQCR) protocol 104
2.9.5 Primer sequences 105
2.9.6 QPCR data analysis.....106
2.10 Statistical analyses..... 106

3 ACKR2 determines the severity of psoriasiform cutaneous inflammation *in vivo* and T-cell positioning in skin. 108
3.1 Contents 108
3.2 Hypotheses 108
3.3 Aims..... 109
3.4 Introduction 109
3.5 Results..... 111
3.5.1 A murine model of cutaneous inflammation for studying the *in vivo* role of ACKR2.....111
3.5.2 ACKR2 expression levels in the IMQ mouse model of psoriasiform inflammation. 113
3.5.3 ACKR2 expression in remote internal organs in the IMQ mouse model of psoriasiform inflammation.....114
3.5.4 Absence of ACKR2 was associated with more severe psoriasiform inflammation in the IMQ mouse model. 115
3.5.5 Absence of ACKR2 was associated with enhanced epidermal thickening and basal keratinocyte hyperproliferation. 116
3.5.6 ACKR2-/- mice demonstrated enhanced CD3+ T-cell positioning in epidermal skin layers in response to topical IMQ. 117
3.5.7 A novel *in vitro* model of T-cell migration towards a chemokine stimulus.....118
3.5.8 A barrier layer of cells expressing ACKR2 regulated T-cell migration towards a chemokine stimulus. 120
3.6 Summary Chapter 3..... 144

4 Focal psoriasiform inflammation limits the spread of inflammation to remote tissues *in vivo*, in ACKR2-dependent manner. 149
4.1 Contents 149
4.2 Hypotheses 149
4.3 Aims..... 150
4.4 Introduction 150
4.5 Results..... 152
4.5.1 Th1 and Th17 cytokines upregulate ACKR2 expression in skin. 152
4.5.2 IFNγ is the principal T-cell derived cytokine inducer of ACKR2 expression. 154
4.5.3 IFNγ upregulates cutaneous ACKR2 expression when administered exogenously *in vivo*. 155
4.5.4 Induced ACKR2 upregulation limits psoriasiform skin inflammation *in vivo*. 156

4.5.5 IFNγ co-administered with topical IMQ in mice, leads to a remote upregulation of ACKR2. 157
4.5.6 Remotely upregulated ACKR2 protects against the spread of psoriasiform cutaneous inflammation. 158
4.6 Summary Chapter 4 176

5 Psoriasis associated microRNAs regulate expression of ACKR2 in human primary keratinocytes and lymphatic endothelial cells. 181
5.1 Contents 181
5.2 Hypothesis 181
5.3 Aims 182
5.4 Introduction 182
5.5 Results 183
5.5.1 Three microRNAs, predicted to bind the ACKR2 3'-UTR are differentially expressed in psoriatic lesions. 183
5.5.2 A microRNA transfection protocol was developed for use in primary human cells. 185
5.5.3 miR-146b and miR-10b reduce the expression of ACKR2 mRNA in primary human KC and LEC respectively. 186
5.5.4 A Dual-Glo™ Luciferase Assay was optimised to determine whether miR-10b/miR-146b modulate ACKR2 expression through directly binding the ACKR2 3'-UTR. 188
5.5.5 Cytoplasmic ACKR2 can be visualised in ACKR2 transfected HEK293 cells through immunofluorescent antibody staining. 189
5.5.6 miR-146b transfection of KC and miR-10b transfection of LEC reduce cytoplasmic ACKR2 expression. 190
5.5.7 miR-146b transfection of KC and miR-10b transfection of LEC reduce ACKR2 protein expression by Western Blot. 192
5.6 Summary Chapter 5 222

6 Tensile stretching of inflamed KC and LEC differentially regulates expression of ACKR2. 226
6.1 Contents 226
6.2 Hypothesis 226
6.3 Aims 226
6.4 Introduction 226
6.4.1 An *in vitro* model of repeated tensile trauma of primary human keratinocytes. 227
6.4.2 Tensile trauma of inflamed KC leads to a rapid reduction in ACKR2 mRNA expression. 228
6.4.3 Tensile trauma of inflamed KC led to a significant increase in miR-146a and miR-146b expression. 229
6.4.4 Tensile trauma of LEC did not affect ACKR2 expression. 230
6.4.5 Incisional trauma of remote unaffected skin of mice in the IMQ mouse model of psoriasiform inflammation led to a downregulation of ACKR2. 231
6.5 Summary Chapter 6 242

7 General discussion 246

Bibliography 246

List of figures and tables

CHAPTER 1

Table 1.1 Table of chemokine-receptor interactions. **p 19**

Table 1.2 Chemokine binding profiles of atypical chemokine receptors. **p** 34

Table 1.3. Overview of ACKR2 expression. **p 38**

Table 1.4 Common anti-psoriasis therapies currently used. **p 55**

Figure 1.1 Key pathways in psoriatic plaque initiation and maintenance. **p 27**

Figure 1.2 Summary of ACKR2 function. **p 33**

Figure 1.3 Typical psoriatic plaques. **p 47**

Figure 1.4 Anatomical sites typically involved with psoriasis. **p 48**

Figure 1.5 Schematic representation of psoriatic plaque development. **p 49**

Figure 1.6 Summary of interactions between somatic cells and leukocytes in psoriasis. **p 62**

CHAPTER 3

Figure 3.1 Schematic representation of the IMQ mouse model of psoriasiform inflammation. **p 122**

Figure 3.2 Details of the modified PASI used to quantity the severity of psoriasiform pathology in murine skin. **p 123**

Figure 3.3 Modified PASI in wild-type mice treated with imiquimod cream. **p 124**

Figure 3.4 Correlation between modified PASI and histopathological changes. **p 125**

Figure 3.5 Effect of topical IMQ treatment on ACKR2 expression *in vivo*. **p 126**

Figure 3.6 Treatment of explanted WT mouse skin with pure imiquimod *in vitro*. **p 127**

Figure 3.7 Effect of topical IMQ treatment on ACKR2 expression in inguinal lymph nodes and spleen. **p 128**

Figure 3.8 Effect of topical IMQ treatment on ACKR2 expression the heart and liver. **p 129**

Figure 3.9 Modified PASI in ACKR2-/- mice treated with imiquimod. **p 130**

Figure 3.10 Exaggerated psoriasiform inflammation in IMQ treated ACKR2-/- mice. **p 131**

Figure 3.11 Exaggerated psoriasiform pathology in IMQ treated ACKR2-/- mice. **p 132**

Figure 3.12 Exaggerated psoriasiform pathology in IMQ treated ACKR2-/- mice; enlarged views. **p 133**

Figure 3.13 CD3+ T-cells in epidermis of ACKR2-/- mice following IMQ treatment. **p 134**

Figure 3.14 Enhanced epidermal CD3+ positioning in ACKR2-/- mice following IMQ treatment. **p 135**

Figure 3.15 Diagram of the design of the novel T-cell migration assay. **p 136**

Figure 3.16 Details of the novel T-cell migration assay. **p 137**

Figure 3.17 Details of the novel T-cell migration assay methodology. **p 138**

Figure 3.18 Details of the novel T-cell migration assay methodology: schematic examples of migration plots. **p 139**

Figure 3.19 Determination of optimal CCL5 concentration for migration assay. **p 140**

Figure 3.20 Accumulated distance travelled of all T-cells in one field-of-view. **p 141**

Figure 3.21 Effect of ACKR2 expression in barrier layer on T-cell migration. **p 142**

Figure 3.22 Effect of ACKR2 expression in barrier layer of primary human keratinocytes on T-cell migration. **p 143**

CHAPTER 4

Figure 4.1 Differential expression of ACKR2 in skin is dependent on products of activated T-cells. **p 162**

Figure 4.2 Th1/Th17 cytokines upregulate ACKR2 expression, with IFNγ being the single most potent ACKR2 inducing T-cell product. **p 163**

Figure 4.3 The IMQ mouse model of psoriasis is not associated with increased IFNγ transcript/protein in skin. **p 164**

Figure 4.4 IFNγ induced ACKR2 expression in mice protects against IMQ induced psoriasiform skin inflammation. **p 165**

Figure 4.5 IFNγ failed to protect against IMQ induced psoriasiform skin inflammation in ACKR2-/- mice. **p 166**

Figure 4.6 Induced ACKR2 expression in mice limits production of psoriasis-associated soluble CC-chemokines. **p 167**

Figure 4.7 Human psoriatic ACKR2 expression patterns can be successfully modelled *in vivo* by topical IMQ at one site plus exogenous IFNγ in mice. **p 168**

Figure 4.8 Focal psoriasiform inflammation protected remote unaffected skin from the spread of inflammation. **p 169**

Figure 4.9 Focal psoriasiform inflammation plus IFNγ did not protect remote unaffected ear skin from the spread of inflammation in the absence of ACKR2. **p 170**

Figure 4.10 ACKR2 is essential for focal psoriasiform inflammation protecting remote unaffected skin from the spread of inflammation. **p 171**

Figure 4.11 IFNγ induced ACKR2 expression limits epidermal thickening and restricts epidermal CD3+ T-cell positioning. **p 172**

Figure 4.12 IFNγ induced ACKR2 expression limits epidermal thickening and restricts epidermal CD3+ T-cell positioning: quantitative data. **p 173**

Figure 4.13 Immunohistochemical characterisation of immune cells in skin. **p 174**

Supplementary Figure 4.1 Supplied by Dr Mark Singh. IFNγ levels were increased in patients with psoriasis as compared to healthy controls. **p 175**

CHAPTER 5

Figure 5.1 TargetScan *in silico* predictions of microRNAs potentially binding the ACKR2 3'-UTR. **p 195**

Figure 5.2 Summary of microRNAs predicted to bind the ACKR2 3'-UTR with associated microRNA specific data from previous psoriasis publications. **p 196**

Figure 5.3 Three microRNAs (miR-10, miR-146 and miR-203) are predicted to bind the ACKR2 3'-UTR and are differentially expressed in psoriasis. **p 197**

Figure 5.4 MicroRNAs can be successfully transfected into primary human keratinocytes. **p 198**

Figure 5.5 MicroRNAs can be successfully transfected into primary human keratinocytes at 8, 24 and 48 hour time points. **p 199**

Figure 5.6 miR-146b transfection of primary human keratinocytes for 24 and 48 hours leads to reduction in ACKR2 mRNA. **p 200**

Figure 5.7 miR-146a as well as miR-146b transfection of primary human keratinocytes for 48 hours leads to reduction in ACKR2 mRNA. **p 201**

Figure 5.8 miR-10 and miR-203 do not differentially regulate ACKR2 expression in keratinocytes. **p 202**

Figure 5.9 miR-10b reduces ACKR2 mRNA expression in lymphatic endothelial cells. **p 203**

Figure 5.10 Schematic representation of Dual-Glo™ Luciferase reporter assay. **p 204**

Figure 5.11 Schematic representation of Dual-Glo™ Luciferase reporter vector showing results of sequencing of the ACKR2 3'-UTR. **p 205**

Figure 5.12 Representative images of stable transfected HEK293 clones. **p 206**

Figure 5.13 miR-146b can be successfully transfected into HEK293 cells. **p 207**

Figure 5.14 miR-146b and miR-10b bind directly to the ACKR2 3'-UTR. **p 208**

Figure 5.15 ACKR2 in ACKR2 transfected HEK293 can be visualised through fluorescent antibody staining. **p 209**

Figure 5.16 Isotype control antibody staining of primary human keratinocyte monolayers. **p 210**

Figure 5.17 Reduced cytoplasmic ACKR2 following miR-146b transfection of KC, as visualised by immunofluorescent antibody staining. **p 211**

Figure 5.18 Reduced cytoplasmic ACKR2 levels following miR-10b transfection of LEC, as visualised through immunofluorescent antibody staining. **p 212**

Figure 5.19 Cytoplasmic ACKR2 following scrambled miR control transfection of LEC, as visualised by immunofluorescent antibody staining. **p 213**

Figure 5.20 Reduced cytoplasmic ACKR2 following miR-10b transfection of LEC, as visualised through immunofluorescent antibody staining. **p 214**

Figure 5.21 ACKR2 protein bands can be visualised using Western blotting. **p 215**

Figure 5.22 Reduced ACKR2 protein following transfection of KC with miR-146b. **p 216**

Figure 5.23 Reduced ACKR2 protein following transfection of KC with miR-146b as quantified through band densitometry. **p 217**

Figure 5.24 Reduced ACKR2 protein following transfection of LEC with miR-10b. **p 218**

Figure 5.25 Reduced ACKR2 protein following transfection of LEC with miR-10b, and increased ACKR2 protein following treatment with IFNγ. **p 219**

Figure 5.26 Reduced ACKR2 protein following transfection of LEC with miR-10b as quantified through band densitometry. **p 220**

Supplementary Figure 5.1 Summary of miRNA biosynthesis **p 221**

CHAPTER 6

Figure 6.1 Schematic diagram of the cell flexing system used in this study. **p 233**

Figure 6.2 Diagrammatic representation of the waveform used for the application of tensile stress. **p 234**

Figure 6.3 Representative bright field microscope images of primary human lymphatic endothelial cells (LEC) grown on different substrates. **p 235**

Figure 6.4 Effect of cell growth on Collagen 1 and Fibronectin on ACKR2 expression. **p 236**

Figure 6.5 Effect of tensile stress on ACKR2 expression by primary human keratinocytes (KC). **p 237**

Figure 6.6 Effect of tensile stress on miR-146 expression in inflamed keratinocytes. **p 238**

Figure 6.7 Cytokine treatment of healthy human primary keratinocytes and lymphatic endothelial cells. **p 239**

Figure 6.8 Effect of tensile stress on ACKR2 expression by lymphatic endothelial cells. **p 240**

Figure 6.9. Effect of incisional skin trauma *in vivo* on ACKR2 expression. **p 241**

CHAPTER 6

Figure 7.1 Schematic summary of main findings. **p 257**

Acknowledgements

I would like to thank my supervisor Prof Gerry Graham, for his guidance, support and encouragement throughout this project. Prof Graham has provided a welcoming and happy learning environment, and I am privileged to have been part of his laboratory team. I am grateful for the input, encouragement and advice, on matters both scientific and clinical/dermatological, of my co-supervisor Prof David Burden. I would also like to thank my devoted partner Dr Clive McKimmie, for his supportive nature, patience and help both within and outwith the lab.

My friends and colleagues have been an indispensable part of this project. I am particularly indebted to Dr Michelle Le Brocq, Dr Gillian Wilson, and Dr Fabian Schütte, Dr Laura Medina, Dr Mark Williams, Dr Marieke Pingen, Dr Mark Singh, Dr Kay Hewit and Dr Kenny Pallas. I am the grateful recipient of the encouragement, interest and support of family and friends, both near and far, who are too numerous to list.

It has been a privilege to collaborate with colleagues from further afield, notably Dr Ellen van den Bogaard and Prof Joost Schalkwijk in the Netherlands. I am also thankful for the input of Ms Lynn Stevenson, Dr Mariola Kurowska-Stolarska and Dr Stefan Siebert.

Lastly, I would like to thank my funding body the Wellcome Trust and the Scottish Translational Medicine and Therapeutics Initiative, who made the realisation of this work possible.

Author's declaration

The work presented in this thesis represents original work carried out by the author. This thesis has not been submitted in any form to any other University.

List of abbreviations

ACKR: atypical chemokine receptor
AMP: anti-microbial peptide
ANOVA: Analysis of variance
APC: antigen-presenting cell
bp: base pair
CCL: chemokine ligand (CC-type)
CD: cluster of differentiation
cDNA: complementary DNA
CLA: cutaneous lymphocyte associated antigen
CO_2: carbon dioxide
COPD: chronic obstructive pulmonary disease
CXCL: chemokine ligand (CXC type)
DAMP: danger-associated molecular patters
DAPI: 4',6-diamidino-2-phenylindole
DARC: Duffy antigen chemokine receptor
DC: dendritic cell
DNA: deoxyribonucleic acid
ERAP1: endoplasmic reticulum aminopeptidase 1
FBS: Foetal bovine serum
FCS: foetal calf serum
FOV: field of view
GAG: glucosaminoglycan
GmbH: [Gesellschaft mit beschränkter Haftung] (German: limited company)
GPCR: G-protein coupled receptors
GWAS: Genome Wide Association Studies
h: hours
H&E: haematoxylin and eoson
hBD: human beta-defensin
HEK: human embryonic kidney cell
i.p intraperitoneally
ICAM: Intercellular adhesion molecule
iDC: immature dendritic cell
IFN: interferon
IgG: immunoglobulin G
IL: interleukin
IMQ: imiquimod
InsP3: inositol-1,4,5-triphosphate
JAK: janus kinase
K[X]: keratin[number denoting type]
KC: keratinocyte
kDa: kilodalton

LC: Langerhans cells
LCE: late cornified envelope
LEC: lymphatic endothelial cell
M: molar mass
MAPK: mitogen-activated protein kinases
mDC: myeloid DV
mDC: myeloid dendritic cell
MHC: major histocompatibility complex
min: minutes
miR: microRNA
miRNA: microRNA
mm: millimetre
mRNA: messenger RNA
NK: natural killer cell
OR: odds ratio
PBST: PBS with added 0.05% Tween
pDC: plasmacytoid dendritic cell
PDE: phosphodiesterase
PI3K: phosphatidylinositol 3-kinase
PIP3: phosphatidylinositol 3,4,5-triphophate
PKC: protein kinase C
RBC: red blood cell
RNA; ribonucleic acid
rRNA: ribosomal RNA
s.c subcutaneously
SALT: skin-associated lymphoid tissue
sec: seconds
SEM: standard error of the mean
SNP: single nucleotide polymorphism
TBP: TATA-binding protein
TGF: transforming growth factor
Th: T helper cell
TLR: toll-like receptor
TNF: tumour necrosis factor
TPA: 12-O-tetradecanoylphorbol-13-acetate
T_{reg}: regulatory T-cell
T_{RM}: resident memory T-cell
tRNA: transport RNA
U: unit
UTR: untranslated region
UV: ultraviolet
VEGF: vascular endothelial growth factor
WT: wilt-type
XMP: xenotransplantation models of psoriasis

CHAPTER 1

1 Introduction

1.1 Chemokines

1.1.1 Chemokines and chemokine receptors: evolution, nomenclature and classification

Chemokines are the principal regulators of leukocyte migration, and key regulators of inflammation (Sokol & Luster 2015). Psoriasis is considered to be a predominantly T-cell driven inflammatory disease and, unsurprisingly, chemokines play a critical role in its pathogenesis with several chemokines and chemokine receptors implicated (Singh et al. 2013; Di Meglio et al. 2011).

Chemokines are evolutionarily ancient, having first emerged over 650 million years ago and appear to be exclusive to vertebrates (DeVries et al. 2005). The name *chemokine* is derived from *chemo*tactic *cyto*kine, and comprises a family of over 50 small ~8-10kDa proteins, displaying significant sequence homology (Luster 1998; Nomiyama & Yoshie 2015). Chemokines are grouped into four subfamilies (summarised in Table 1.1), based on a conserved cysteine residue arrangement within their N-terminal; namely CC, CXC, XC, and CX3C, that forms the basis for the internationally approved nomenclature for this receptor family (DeVries et al. 2005; Zlotnik & Yoshie 2000; Nomiyama et al. 2013; Murphy et al. 2000). CC and CXC chemokines are the most numerous sub-families, functioning as both regulators of inflammation as well as homeostasis (Griffith, Sokol & Luster 2014). For instance, CCL19/21 play a critical role in T-cell LN homing, whilst CCL2-5 play a role in recruiting inflammatory cells (including T-cells, and DCs) into tissues such as the skin (Griffith, Sokol & Luster 2014). CXCL9/10/11 can be produced by inflamed keratinocytes and recruit T-cells into tissues, whereas CXCL1-3/5-8 regulate neutrophil trafficking (Flier et al. 2001; Sokol & Luster 2015) (Table 1.1).

Chemokine	Receptor	Main function(s)	Suggested role in psoriasis
CXCL1	CXCR2	Neutrophil trafficking	Keratinocyte hyperproliferation
CXCL2	CXCR2		
CXCL3	CXCR2		
CXCL4	?	Procoagulant	
CXCL5	CXCR2	Neutrophil trafficking	
CXCL6	CXCR1, CXCR2		
CXCL7	CXCR2		
CXCL8	CXCR1, CXCR2		Keratinocyte hyperproliferation
CXCL9	CXCR3	Th1 response; TH1, CD8+, NK trafficking	Th1/pDC trafficking
CXCL10	CXCR3		
CXCL11	CXCR3		
CXCL12	CXCR4	Bone marrow homing	
CXCL13	CXCR5	B cell positioning in LN	
CXCL14	?	Human macrophage skin homing	
CXCL15	?	? (mouse only)	
CXCL16	CXCR6	NKT/ILC migration and survival	Keratinocyte hyperproliferation, leukocyte trafficking
CCL1	CCR8	Th2 and Treg migration/survival	
CCL2	CCR2	Monocyte trafficking	Monocyte/ Macrophage/DC/Th1 cell trafficking
CCL3	CCR1, CCR5	Macrophage, NK cell, T-cell migration, T-cell-DC interactions	Th1 cell chemotaxis/Monocyte /DC chemotaxis
CCL4	CCR5		
CCL5	CCR1, CCR3, CCR5		Th1 cell chemotaxis/Monocyte /DC chemotaxis
CCL6	?	? (mouse only)	
CCL7	CCR2, CCR3	Monocyte mobilisation	
CCL8	CCR1, CCR2, CCR3, CCR5, (CCR8 mouse)	Th2 response (skin homing in mice)	
CCL9/10	?	?	
CCL11	CCR3	Eosinophil and basophil migration	
CCL12	CCR2	Inflammatory monocyte migration (mouse only)	
CCL13	CCR2, CCR3, CCR5	Th2 responses	
CCL14	CCR1	?	
CCL15	CCR1, CCR3	?	
CCL16	CCR1, CCR2, CCR5	?	
CCL17	CCR4	Th2 responses, Treg, lung and skin homing	Th1 and Th17 cell trafficking
CCL18	CCR8	Th2 responses, skin homing	
CCL19	CCR7	T cell and DC homing to lymph nodes	
CCL20	CCR6	Th17 responses	Th17 trafficking
CCL21	CCR6, CCR7	T-cell and DC homing to lymph nodes	
CCL22	CCR4	Th2 response, Th2 migration, Treg migration	Th1 and Th17 cell trafficking
CCL23	?	?	
CCL24	CCR3	Eosinophil/Basophil migration	
CCL25	CCR9	T-cell homing to gut, thymocyte migration	
CCL26	CCR3, CX3CR1	Eosinophil/Basophil migration	
CCL27	CCR10	T-cell homing to skin	CD4+/CD8+ trafficking
CCL28	CCR3, CCR10	T-cell and plasma cell homing to mucosa	
XCL1	XCR1	CD8+ presentation to DCs	
XCL2	XCR1		
CX3CL1	CX3CR1	NK, monocyte and T-cell migration	Th1 cell polarisation

Table 1.1 Table of chemokine-receptor interactions.

Generated with data from (Griffith, Sokol & Luster 2014; Mabuchi et al. 2012). Green; CXC-chemokines, Orange; CC-chemokines, Blue; XC-chemokines, Red; XC3C-chemokines.

Chemokines signal through binding to a family of 7-transmembrane spanning G-protein coupled receptors (GPCR). The chemokine receptors share a conserved (DRYLAIV) amino acid motif between the third transmembrane domain and the second intracellular loop, that appears to be important for classical intracellular signalling (Neote et al. 1994; Nibbs & Graham 2013). There are currently ten CC- (CCR1-10), eight CXC- (CXCR1-8), one XC- (XCR1), and one CX3C- (CX3CR1) known chemokine receptors, and like their ligands, they play a role in both inflammation and homeostasis depending on the context (Nibbs & Graham 2013). Both chemokine ligand- and receptor genes form clusters within the genome, which is in keeping with evolution through (at least in part) rapid gene duplications (Zlotnik & Yoshie 2012).

With a few exceptions (e.g. CCL20 binding only CCR6), there is considerable chemokine ligand-receptor binding promiscuity notably amongst inflammatory chemokines/receptors (Zlotnik & Yoshie 2012), although binding only occurs within one chemokine-receptor subfamily (e.g. CC-receptors only bind CC-ligands). Typically, one inflammatory chemokine binds multiple receptors, and one receptor typically binds several different chemokines ligands (Nibbs & Graham 2013). This receptor-ligand binding promiscuity allows for a sophisticated and fine-tuned system by which leukocyte migration is regulated. Functionally, chemokines are broadly either inflammatory (the most numerous grouping) or homeostatic (Luster 1998; Zlotnik & Yoshie 2012). Chemokines play diverse roles in e.g. development, homeostasis, and inflammation (Nomiyama & Yoshie 2015) though they are, in the main, collectively considered to be principally regulators of leukocyte migration (Thelen 2001). Chemokines and chemokine receptors have evolved in parallel (e.g. CXCL12/CXCR4 pair is highly conserved and also found in fish). But, the evolution of ligands has been more rapid, leading to greater discrepancies in the number of chemokines between species as compared to receptors. This difference is particularly apparent in lower vertebrates (Bajoghli 2013). Nonetheless, the orthologous relationship of chemokines between species have in many cases been determined, thus enabling the study of specific chemokine networks in animal models (Nomiyama et al. 2013).

1.1.2 Chemokines-chemokine receptor interactions: intracellular signalling events; PI3K pathways

Chemokines act on receptors expressed on a range of immune and non-immune cells, and thereby influence cell migration and a range of other processes including development, angiogenesis, and oncogenesis (Rossi & Zlotnik 2000). Chemokine receptor activation on leukocytes may have several possible effects on the cell, the most typical of which (in the case of chemokines acting on immune cells) is induction of cell migration, which is also the focus of this thesis section (Rot & Andrian 2004). The typical chemokine receptors signal through trimeric $G\alpha_i$-type G-proteins (Sokol & Luster 2015; Kuang et al. 1996), whilst receptors associated with $G\alpha_q$ and $G\alpha_s$ G-proteins do not appear to induce migration (Arai et al. 1997). GPCR activation is followed by dissociation of the trimeric G-protein into α and $\beta\gamma$ subunits in a GTP-dependent manner, and typically the production of second messengers (Dohlman 2015). Whilst chemokine induced chemotaxis is dependent on the $G\beta\gamma$ rather than the $G\alpha$i subunit of Gi-proteins, there is also evidence for $G\beta\gamma/G\alpha_i$-independent chemotaxis-inducing signals triggered by activation of the Gi-protein (Neptune et al. 1999; Arai et al. 1997). The $G\beta\gamma$ subunit activates phosphatidylinositol 3-kinase (PI3K), that plays a critical role in cell polarisation and chemotaxis (Funamoto et al. 2002). There are several known PI3K isoforms that are expressed in leukocytes, and the specific isotype that mediates chemotaxis depends on the cell type. For instance, PI3Kγ and PI3Kδ isoforms are essential in macrophage and neutrophil migration respectively (Hirsch et al. 2000; Sadhu et al. 2003). PI3K plays a role in chemotaxis mainly (but not exclusively) through the generation of the second messenger phosphatidylinositol 3,4,5-triphophate (PIP3), that induces leukocyte polarisation, F-actin accumulation and cell migration (Niggli 2000; So & Fruman 2012). Both PI3K and PIP3 co-localise in the leukocyte pseudopod together with Rac, where PIP3 and Rac induce actin polymerisation through direct and indirect mechanisms (Rot & Andrian 2004). Additional pathways exist downstream from PI3K following chemokine-receptor activation, including 1) protein kinase B (Thelen 2001) and 2) activation of mitogen-activated protein kinases (MAPK), the latter of which appears to be dependent on PIPKγ (Bondeva 1998).

1.1.3 Intracellular signalling events; non-PI3K pathways

The Gβγ subunit activates further pathways beyond PI3K upon chemokine receptor activation. Specifically, the Gβγ subunit plays a role in the activation of phospholipase C isoforms, leading to a raise in inositol-1,4,5-triphosphate (InsP3), intracellular Ca^{2+} and subsequent protein kinase C (PKC) activation, all of which play a role in cell migration and other leukocyte functions (Thelen 2001). Yet further complexity is added as activated GPCRs do not solely act through G-proteins (e.g. interact with β-arrestins) and as GPCR oligomerisation modulates the biological activity of the chemokine receptors (Dohlman 2015). Together, and as reviewed in detail elsewhere (Thelen 2001), chemokine-receptor binding leads to signalling mediated by G-protein dependent and independent mechanisms, leading to the activation of complex intracellular signalling cascades, thereby affecting migration and a broad range of other cellular processes.

1.1.4 Chemokine haptotactic gradient formation

The sequence of events leading to leukocytes entering tissues from the blood, involves a series of complex interactions between the leukocyte, the vessel wall and tissues, as reviewed elsewhere (Ley et al. 2007). The steps include rolling (which involves selectins), leukocyte adhesion (involves chemokines) and cell arrest (involves integrins and chemokines), which is then followed by paracellular or transcellular migration into tissue (Ley et al. 2007). Such migratory cells generally interact not with free soluble chemokines, but instead with chemokines that are bound to e.g. long sulphated polysaccharides known as glycosaminoglycans (GAGs) (Johnson et al. 2005; Rot & Andrian 2004). Chemokines that regulate cell migration may originate from within the vessel lumen, or directly from within tissues, and appear on the luminal side of endothelial cells through active internalisation/transport, or through diffusion through intercellular junctions(Rot & Andrian 2004). Interactions between GAGs and the bound chemokine can influence the function of the chemokine, thus playing a role in controlling leukocyte migration and inflammation (Johnson et al. 2005). GAG binding can also protect the chemokine against proteolytic cleavage

(Ley et al. 2007), or may functionally neutralise (by sequestration) chemokines released by e.g. degranulating T-cells (Wagner et al. 1998).

Chemokine solubility allows chemokine diffusion from their site of origin, whilst GAG binding limits the spread (Rot & Andrian 2004). However, chemokine-GAG binding is not random; certain chemokines bind only certain GAGs, which in turn constitutes a sophisticated manner in which the bound chemokine gradients can be spatially organised (Witt & Lander 1994). Chemokine-GAG binding is influenced by factors such as pH and also the degree to which the GAG is sulphated, which has implications for how migration studies are interpreted if not performed in (near)-physiological conditions (Singh et al. 2015).

Chemokine binding to GAGs has been exploited therapeutically in experiments where non-heparan sulphate binding CXCL12 failed to promote migration, but instead reduced leukocyte CXCR4 expression through desensitisation, and thereby limited chemotaxis (O'Boyle et al. 2009). Bound chemokines are sensed by leukocytes (in a manner that has been likened to 'fingers reading braille'), and are thus believed to migrate through 'haptotaxis' (Rot & Andrian 2004; Rot 1993). These gradients can be replicated *in vitro*, through e.g. high-resolution printing of immobilised chemotactic gradients, that are then sensed and followed by leukocytes *in vitro* (Rink et al. 2015). Importantly, the strength of leukocyte-tissue adhesion in situations of e.g. high shear forces is not directly due to chemokine-chemokine receptor 'anchoring'. Instead, adhesion is mainly achieved through chemokine-induced integrin activation, that allows leukocyte adhesion to tissues (Laudanna et al. 2002).

1.1.5 Homeostatic chemokines in skin

Chemokines are expressed in the skin, both in inflammation and under homeostatic conditions. Chemokines can be produced by stromal cells, infiltrating leukocytes and tissue-resident immune cells. Some chemokines are homeostatic and are expressed in healthy skin, and play a role in leukocyte positioning and trafficking in health. Similarly, chemokine receptors, expressed in non-inflammatory contexts, govern homeostatic leukocyte trafficking. CCL19/21 for instance bind to CCR7 and control DC/T-

cell trafficking to tissue draining lymphoid tissue (Braun et al. 2011). In addition, CXCL14 is prominently expressed by non-inflamed skin vessels in the superficial dermal plexus and in basal keratinocytes (KC), and has a role in the recruitment of DC precursors that mature into APCs(Nibbs et al. 2007). Similarly, CCL1 is constitutively expressed in the skin microvasculature, and plays a role in the localisation of CCR8+ T-cells, that when activated can produce both IFNγ and TNFα (Nibbs et al. 2007). Interestingly, CCR8 (which binds CCL1) can be induced by skin-specific soluble factors, expressed by keratinocytes. This represents an additional mechanism by which T-cell positioning within the skin is regulated (McCully et al. 2012). Although the induction of CCR10 on T-cells has been associated with recruitment to the skin, this does not appear to be the case in mice where skin T-cells lack CCR10 expression (Homey et al. 2002). Thus, both CCR10 and CCR8 co-ordinate the homeostatic recruitment and tissue localisation of T-cells.CXCL12 meanwhile is produced by dermal DC in healthy skin, and may play a role in recruiting naive non-activated T-cells that are CXCR4+ (Pablos et al. 1999). CCL27 is expressed within the healthy epidermal KCs, and is thought to mediate homeostatic T-cell trafficking (notably CLA+ memory T-cells), and thus promote immune surveillance (Morales et al. 1999).

1.1.6 Chemokines in inflamed skin and psoriasis

Whilst several chemokines/chemokine receptors are expressed in healthy skin, the chemokine/chemokine receptors expression profile of stromal and infiltrating cells can differ markedly in the context of inflammation. Regulation of chemokine production/removal and chemokine receptor expression represent a sophisticated system by which leukocyte migration and tissue positioning is controlled (Rot & Andrian 2004). Only very small amounts of inflammatory chemokines are produced under homeostatic conditions. However, and as reviewed elsewhere, KCs have the capacity to express high levels of an array of chemokines, depending on the context, including e.g. CCL2/5/17/20/22/27 and CXCL1/8/9/10/11/16 (Singh et al. 2013; Flier et al. 2001; Harper et al. 2009). Cytokines can activate the expression of many chemokines by KC, for instance IFNγ leads to a marked

upregulation of CXCL9/10/11 in KCs (which attracts CXCR3 expressing cells such as Th1 T cells). In comparison IL-17 leads to an upregulation of several chemokines that are not significantly upregulated by IFNγ, such as CXCL1/3/5/6/8 (attracts neutrophils) and CCL20, (attracts CCR6 expressing Th17 T-cells, and some DCs) (Graham & McKimmie 2006). Other cells can produce T-cell attracting chemokines (Sokol & Luster 2015), including DCs and neutrophils, thus enabling orchestration amongst several classes of stromal cells and leukocytes.

In psoriasis, IL-17A, TNFα and IL-22 lead to the upregulation of CCL20 when injected into skin *in vivo*. CCL20 in turn, is a chemoattractant for CCR6 expressing Th17 cells, which provides one mechanism whereby Th17 cells can amplify accumulation of further T-cells through the induction of chemokine production by KC (Graham & Locati 2013)(Harper et al. 2009). Psoriatic KCs also produce CCL5, which is believed to account for the accumulation of activated T-cells and memory T-cells, that eventually migrate from the dermis into the epidermis in psoriasis (Raychaudhuri et al. 1999). The localisation of T-cells in the epidermis, as opposed to the dermis, is in turn essential to see a full psoriasiform phenotype (Conrad et al. 2007). Thus, the chemokine/receptor expression profile of stromal cells (e.g. KC) and infiltrating cells (e.g. T-cells) is dynamic, and depends on the context. It should however also be noted, that whilst chemokines are considered the principal regulators of leukocyte migration, other classes of molecules can act as chemoattractants, including bacterial fragments and lipids (Sokol & Luster 2015).

1.2 Immune cells and chemokines

1.2.1 Dendritic Cells: chemokines and DC entry into and localisation in skin

DCs play a central role in skin immunity and immune surveillance, and are found in healthy as well as inflamed skin. Numerous DC subsets have been described, and they play a critical role in the initiation and establishment of

psoriatic plaques (as illustrated in Figure 1.1). DCs in skin express a broad range of chemokine receptors, and are therefore able to respond to a wide range of chemotactic stimuli in the event of inflammation (Sokol & Luster 2015). For instance, studies have shown that CCR2 and CCR6 are both involved in DC migration into inflamed dermal and epidermal skin (Bogunovic et al. 2006; Merad et al. 2002). Resident DCs in healthy skin may originate principally from two sources; 1) DC precursor migrating into the skin, where they mature into DCs (Griffith, Sokol & Luster 2014) and 2) DCs proliferating *in situ* (Bogunovic et al. 2006) (McKimmie et al. 2013). Immature APCs are localised in both the epidermis (where they are also referred to as Langerhans cells (LC) and express Langerin (Valladeau et al. 2000) and in the dermis (Bogunovic et al. 2006). Homeostatic turnover of the epidermal LCs is very slow compared to DCs localised elsewhere (Miller et al. 1976). However, the chemokines that govern this homeostatic turnover in non-inflamed skin are poorly understood (Sokol & Luster 2015).

1.2.2 Dendritic Cells: chemokines and trafficking to draining lymph nodes (LN); a CCR7-dependent process

Chemokines regulate not only DC entry into the skin, but also their egress from the skin. DCs are efficient antigen-presenting cells, that can take up antigen in peripheral tissues, but require migration to secondary lymphoid tissue in order to optimally elicit an immune response (Randolph et al. 2008). It therefore follows that to function adequately; they need to possess the capacity to migrate both to and from peripheral tissues. DC maturation can be triggered by pro-inflammatory factors e.g., TNFα and LPS, both *in vivo* and *in vitro*. This leads to a down-regulation of skin homing molecules in KCs such as E-cadherin, and a change in chemokine responsiveness in CD103+ DCs; whilst immature DCs are responsive to e.g. CCL3, CCL5 and CCL20, mature DCs down-regulate e.g. CCR6 whilst upregulating CCR7 (Forster et al. 1999).

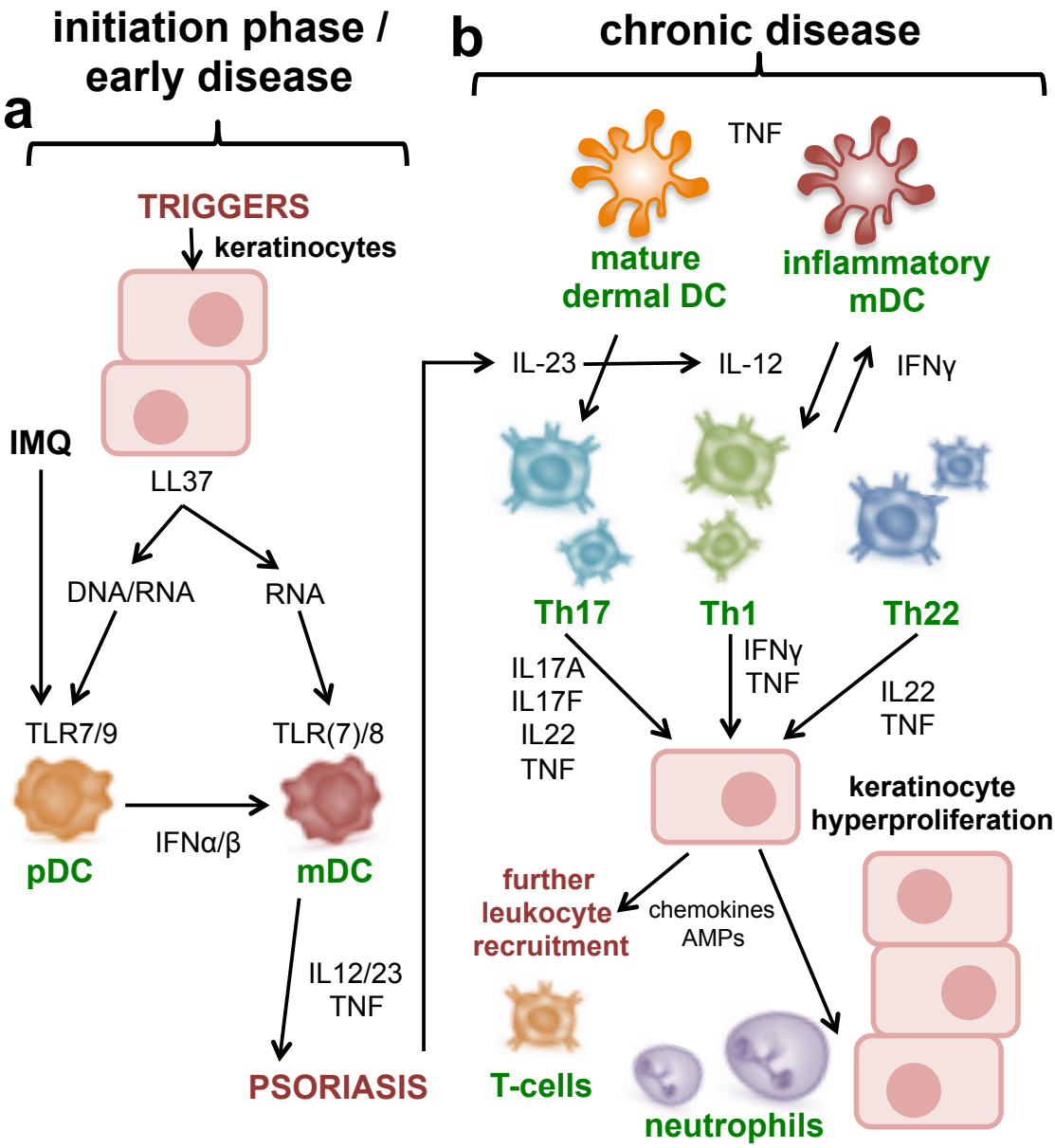

Figure 1.1 Key pathways in psoriatic plaque initiation and maintenance
Adapted from (Lowes et al. 2014). Psoriasis pathogenesis has an early initiation phase, where triggers such as trauma, lead to dendritic cell (DC) activation. DCs, as well as T-cells and neutrophils play a key role in the chronic phase, that is then characterised by keratinocyte hyperproliferation, and the development of characteristic psoriatic plaques. Note: Leukocyte images from Adobe Stock Photos.

CCR7 is indispensable for DC migration to LN; whereas contact sensitisation of skin using FITC causes DC maturation and migration to lymphoid organs in wild type mice, DCs in FITC skin-treated CCR7-/- mice fail to migrate to lymph nodes (Nibbs & Graham 2013). Mature DCs respond to CCL21 gradients and migrate to lymphatic vessels in the tissue. CCL21 in dermis is bound to sulphated sugars through its C-terminus, which allows chemokine immobilisation and retention and it has been suggested that this enables DCs to follow gradient through 'haptotaxis' (Weber et al. 2013). Subsequent to lymphatic entry, DCs follow gradients of both CCL21/CCL19 to migrate into the lymph nodes (LN) (Sokol & Luster 2015). Chemokines produced by the T-cell zones of both the spleen and LN are critical for both appropriate DC localisation within secondary lymphoid organs, and in order to mount an adequate immune response to e.g. infection (Sokol & Luster 2015; Marsland et al. 2005). Once in the LN, DCs pass through the subcapsular sinus, from where they migrate into the LN parenchyma and then into the T-cell zone, in a CCR7 dependent manner (Braun et al. 2011)(Sokol & Luster 2015).

1.2.3 T-cell migration: the role of chemokines

T-cell trafficking is a highly regulated and complex process. Naïve T-cells utilise CCR7 to re-circulate between the blood and lymphoid tissue, where they interact with DCs (Braun et al. 2011). Naïve T-cells express CCR7 and CXCR4, that interact with CCL21/CCL19 and CXCL12 respectively, both of which are presented on the luminal endothelium of the lymph node high endothelial venules (Griffith, Sokol & Luster 2014). Once in the LN, T-cells co-localise with DC in the T-cell area of the LN (Masopust & Schenkel 2013). T-cells can follow bound (haptotactic) chemokine gradients in the LN, rather than soluble gradients (Woolf et al. 2007). T-cells exit the LN through cortical lymphatic sinuses as effector cells if antigen presentation has taken place by APCs, and T-cell differentiation has taken place (Benechet et al. 2014). Whilst CCR7 is required for homing to lymphoid tissues, T-cells typically downregulate CCR7 once activated and upregulate inflammatory chemokine receptors, allowing them to egress from the lymphoid tissue and migrate to inflamed peripheral tissues. In addition to CCR7, different T-cell

subtypes express different chemokine receptor repertoires. For instance, Th1 cells express CCR5, CXCR3 and CXCR6, Th17 cells express CCR4 and CCR6, Th2 cells CCR2, CCR8, CX3CR1 and Th22 CCR4, CCR6 and CCR10 (Griffith, Sokol & Luster 2014). These differences highlight the dynamic nature of chemokine receptor expression that depends on the context and function of the cell (Schulz et al. 2016). For instance, CCR5 (which binds CCL5, that in turn is produced by a range of tissues) is expressed on Th1 cells, and plays a role in Th1 migration into peripheral tissues (Suffee et al. 2011). CXCL9/10/11, which bind CXCR3, are particularly important chemokines in regulating T-cell migration in peripheral inflamed tissues, and are expressed in a broad range of diseases (including rheumatoid arthritis, inflammatory skin disorders, cardiovascular disease), with chemokine levels correlating with the number of infiltrating CXCR3+ T-cells in the tissue (Storelli et al. 2007). In addition to regulating migration, chemokines/chemokine receptors aid differentiation of T-cells. For instance, CXCR3 is implicated in Th1 differentiation, whilst CCL3/4 are required for formation of pre-memory CD8+ T-cells (Schulz et al. 2016).

Advances in *in vivo* imaging techniques have enabled considerable insights to be gained in T-cell migration (Benechet et al. 2014). Concurrently, advances in techniques in printing haptotactic/chemotactic gradients have enabled the study of cell migration *in vitro* in a reductionist and targeted manner (Rink et al. 2015). T-cells move rapidly (5-10μm/min) in an amoeboid pattern following extravasation and entry into the interstitial space (Germain et al. 2012).

The pattern of T-cell movement in the interstitial space can be apparently random (Brownian motion) or random, but with intermittent rapid directional motion (Lévy walk). The latter pattern is proposed to cover a larger surface area more quickly, and possibly enables finding the specific T-cell target more efficiently, and is believed to be supported by CXCL10 (Weninger et al. 2014). This serves to illustrate how chemokines not only govern direction of leukocyte migration, but also the finer nuances of the type and pattern of migration, adding yet further sophistication to an already complex system.

T-cell TCR binding to the target, generally leads to cessation of migration (Weninger et al. 2014). It is noteworthy, that in the context of *Leishmania major* infection, T-cells that are interacting with the antigen-presenting cell, are capable of generating an IFNγ gradient, that extends 80μm beyond the site of T-cell-Antigen interaction, believed to aid amplifying anti-parasitic responses (Müller et al. 2012; Weninger et al. 2014). The retention signals leading to the arrest of CD3+ cells in the epidermis are thus unknown. Indeed, relatively little detail is known about the chemotactic signals that govern interstitial T-cell migration, compared to e.g. neutrophils (Weninger et al. 2014).

1.3 The atypical chemokine receptors

1.3.1 Atypical Chemokine Receptor family: nomenclature and overview

In addition to the signalling GPCR chemokine receptors described above, there exists a family of 7-transmemebrane spanning (7TM) chemokine receptors that do not signal in a classical G-protein dependent manner upon chemokine binding. Common to this family is, instead, an ability to internalise chemokines (Nibbs & Graham 2013) and a role in regulating chemokine function (Graham et al. 2012). These are thus termed Atypical Chemokine Receptors (ACKR) of which there are four, and which have recently been re-named according to a new nomenclature; ACKR1 (formerly DARC), ACKR2 (formerly D6 or CCBP2), ACKR3 (formerly CXCR7) and ACKR4 (formerly CCRL1) (Nibbs & Graham 2013). Additionally, two possible ACKRs are still undergoing functional characterisation but have reserved names, with one of these (ACKR6) apparently lacking a 7TM structure (Bachelerie et al. 2015).

Unlike the classical chemokine receptors that signal through G-proteins upon ligand binding, ACKRs are unable to elicit and sustain such signalling pathways, despite sharing many structural similarities with conventional chemokine receptors (Graham et al. 2012). Although the reason for this apparent inability to signal is not completely understood, structural

differences between classical and atypical receptors (notably in the DRYLAIV amino-acid motif) may account for their inability to signal through G-proteins. Conventional chemokine receptors possess a conserved DRYLAIV amino-acid motif between the second intracellular loop and the third receptor transmembrane domain (Nibbs & Graham 2013). Specific mutations (substitution of ARG-126 with Asn) in the DRYLAIV motif in a classical chemokine receptor was shown to prevent interactions with G-proteins (and thus impede signalling) but enhanced interactions with β-arrestin (and thus internalisation) (Lagane et al. 2005). The DRYLAIV motif is entirely absent in ACKR1 and modified in ACKR2-4, which is in keeping with the atypical properties of the ACKRs being at least in part due to an absence (or modification) of this motif (Nibbs & Graham 2013). Although these data highlight a role for an intact DRYLAIV motif for adequate chemokine receptor signalling function, other experiments where a signalling DRYLAIV motif has been reinstated in ACKR2, have yielded conflicting results (Graham et al. 2012). Indeed, notwithstanding similarities between ACKR2 and classical chemokine receptors, there are also significant structural differences outside the DRYLAIV motif in the ACKRs, that could account for differences in signalling upon ligand binding (Nibbs & Graham 2013).

Importantly, whilst classic chemokine receptors are predominantly expressed by leukocytes and mediate cell-autonomous leukocyte migration; ACKRs are predominantly expressed by stromal cells, and regulate leukocyte positioning by scavenging chemokines from the distinct tissue microenvironments in which they are expressed. Indeed, although ACKRs are not directly involved in leukocyte migration, they all have the capacity to internalise chemokines in a G-protein independent manner, and are believed to 'fine-tune' chemokine gradient formation (Bachelerie et al. 2000). Through this internalisation, ACKRs collectively play important roles in development, homeostasis and inflammation (Lee et al. 2014; Townson & Nibbs 2002; Lee et al. 2011; Nibbs & Graham 2013). Whilst this capability to internalise chemokines has led to these ACKRs sometimes simplistically being termed 'chemokine decoys' the precise mechanism/context of chemokine internalisation, as well as the fate of the chemokine internalised, is highly variable and subject to complex regulatory processes (discussed below).

Furthermore, although the ACKRs do not appear to signal through G-proteins, most do have some capacity to interact with some cytoplasmic proteins e.g. β-arrestin, which in turn plays a role in receptor internalisation and scavenging (Galliera, Jala, et al. 2004). Ligand binding characteristics of the atypical chemokine receptors is summarised in Table 1.2.

1.3.2 ACKR2: molecular mechanism of chemokine scavenging

ACKR2 (formerly D6) is highly promiscuous and binds almost all pro-inflammatory (but not homeostatic (Graham & Locati 2013)) CC-chemokines (Bonecchi et al. 2004). The first demonstration that ACKR2 binds inflammatory chemokines in humans (Nibbs, Wylie, Yang, et al. 1997), and in mice (Nibbs, Wylie, Pragnell, et al. 1997), was carried out at the University of Glasgow, in the Graham laboratory. However, considerable insight into the ability of ACKR2 to function as a putative decoy receptor, was first suggested by an Italian group based in Milan (Fra et al. 2003). This paper is the first to report chemokine scavenging by ACKR2, and thereby suggested a key concept in atypical-chemokine receptor biology. The mechanism that regulate the expression and function of ACKR2, remained undescribed for several years. More recent work has begun to identify inflammatory factors that mediate its upregulation in both stromal (Singh et al. 2012) and leukocyte subsets (McKimmie et al. 2008). Whilst binding occurs with high-affinity (like other atypical chemokine receptors) ACKR2 does not signal in a conventional manner upon ligand binding (Nibbs, Wylie, Yang, et al. 1997; Borroni et al. 2013). Instead, ACKR2 functions as a scavenger of pro-inflammatory CC-chemokines, through binding, internalising and aiding in the degradation of chemokines (Weber et al 2004) (summarised in Figure 1.2). ACKR2 is localised on recycling endosomes, and is thus constitutively cycled between the cell surface and intracellular compartment (Weber et al 2004). It has been shown that over 80% of ACKR2 is localised in intracellular vesicles at rest (Blackburn et al. 2004), whilst maintaining constant expression of ACKR2 on the cell surface (Galliera, Galliera, et al. 2004). Indeed, ligand binding of ACKR2 enhances ACKR2 mediated scavenging in a Rab11 dependent manner, thus providing one mechanism by which its activity is regulated at the post-transcriptional level (Bonecchi et al. 2008).

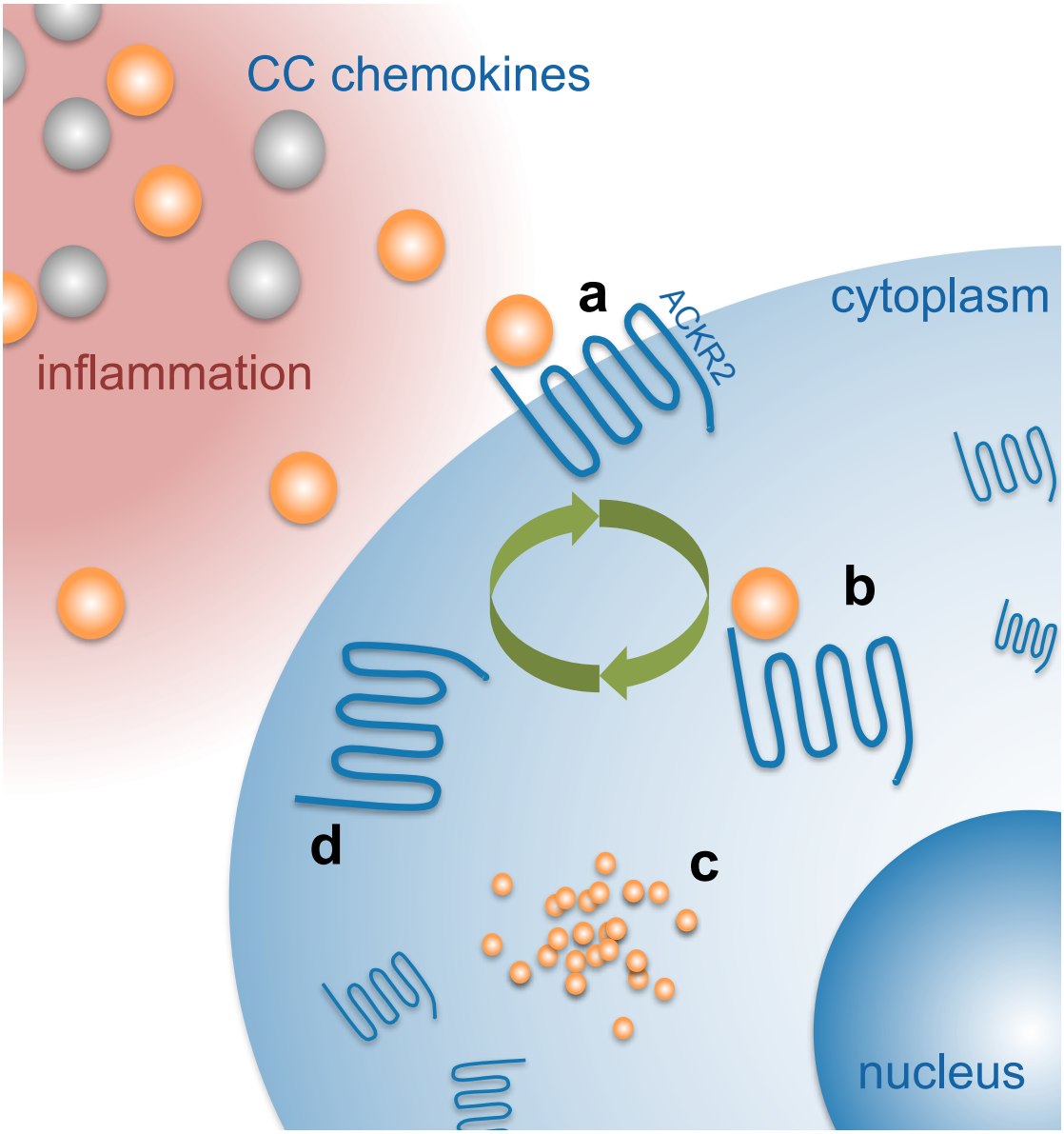

Figure 1.2 Summary of ACKR2 function.

a) ACKR2 binds most inflammatory CC-chemokines, after which b) the receptor-ligand is internalised, and c) the chemokine degraded. ACKR2 then continues to cycle back to the cell surface, and the process repeated. Adapted from (Graham & McKimmie 2006)

RECEPTOR	LIGANDS	REFERENCES
ACKR1	*CCL2, CCL5, CCL7, CCL11, CCL13, CCL14, CCL17, CXCL1, CXCL2, CXCL3, CXCL5, CXCL8, CXCL11*	(Gardner et al. 2004; Szabo et al. 1995; Chaudhuri et al. 1994; Mei et al. 2010; Neote et al. 1994)
ACKR2	*CCL2, CCL3, CCL3L1, CCL4, CCL5, CCL7*, CCL8*, CCL11, CCL12, CCL13, CCL14**, CCL17, CCL22*	(Nibbs, Wylie, Yang, et al. 1997; Hansell, Schiering, et al. 2011; Nibbs, Wylie, Pragnell, et al. 1997; Bonini & Steiner 1997; Bonecchi et al. 2004; Savino et al. 2009; Nibbs et al. 1999; Fra et al. 2003)
ACKR3	*CXCL11, CXCL12*	(Burns et al. 2006)
ACKR4	*CCL19, CCL21, CCL25, CXCL13****	(Townson & Nibbs 2002; Gosling et al. 2000; Watts et al. 2013)

Table 1.2 Chemokine binding profiles of atypical chemokine receptors.

Chemokine binding profiles of atypical chemokine receptors (ACKRs), adapted from (Nibbs & Graham 2013). This table lists all the chemokines that bind mouse and/or human ACKR2, for which affinity measurements are known, e.g. binding affinity (K_i) or dissociation constant (K_d) (defined as being less than 100nM). Some of the chemokines listed are expressed in humans but not in mice, including CCL3L1 (has high affinity for both human and mouse ACKR2), CCL13, CCL14, CCL16, CCL18, CXCL6 and CXCL8 (Zlotnik & Yoshie 2012). It should also be noted that CCL12 is fund in mice, but not humans (Zlotnik & Yoshie 2012). In addition to binding profiles listed, human ACKR1 also weakly binds to the following ligands, CCL1, CCL8, CCL16, CCL18, CXCL4, CXCL9, CXCL10 and CXCL13 (K_i between 100nm and 1μM) (Gardner et al. 2004; Szabo et al. 1995; Chaudhuri et al. 1994). Unpublished observations by Prof Robert Nibbs (referred to in Nature Review Immunology article), indicate human ACKR2 also weakly interacts with CCL24 and CCL26, but their affinities are not known (Nibbs & Graham 2013). Although ACKR2 binding affinities to all known chemokines have been investigated, interactions between ACKR2 and the following chemokines appear to not have been studied; CCL3L1, CCL24, CCL28, CXCL7, CXCL14, CXCL16 (Nibbs & Graham 2013).

* Human ACKR2 binds to human CCL7 and CCL8, but mouse ACKR2 does not bind to mouse CCL7 and CCL8 (Nibbs, Wylie, Yang, et al. 1997; Hansell, Schiering, et al. 2011).

** CCL14 is a homeostatic chemokine present at high concentrations in the serum, which in inflammatory conditions is cleaved at the N-terminal to a biologically active truncated version that also is a high affinity ligand for ACKR2 (Savino et al. 2009).

*** Binding of CXCL13 by ACKR4 has been reported in humans, but not in mice (Townson & Nibbs 2002; Gosling et al. 2000).

The mechanisms underpinning ACKR2 cycling have proven controversial. In some studies, ACKR2 cycling has been shown to be dependent on the receptor's C-terminus interacting with β-arrestin (Galliera, Galliera, et al. 2004), which is a receptor associated protein that has a role in regulating internalisation of a range of receptors (Ferguson et al. 1996). In contrast, others have suggested that internalisation is not dependent on β-arrestins (McCulloch et al. 2008).

Through the use of sophisticated immunohistochemistry to label both cell-surface ACKR2 in live cells, and labelling of endosomal compartments post-fixation, the localisation of ACKR2 within the cell, and its ability to continuously recycle from the cell surface to the cytoplasm and back again, was characterised (Weber et al Nibbs 2004). Ligand binding is followed by rapid internalisation of the ACKR2-ligand complex. Subsequently, the chemokine dissociates from ACKR2 following vesicle acidification and is degraded, whilst the ACKR2 remains intact and continues to cycle to the cell surface where it can bind and internalise more chemokine. Thus, ACKR2 can act in a semi-catalytic manner to remove inflammatory CC chemokine from the extracellular environment (Weber et al 2004). ACKR2 cycling requires both Rab4 (fast cycling) and Rab11 (slow cycling) activity, whilst constant levels of cell surface ACKR2 are maintained (in proportion to chemokine binding) through a Rab11-dependent mechanism (Bonecchi et al. 2008). ACKR2 function is not dependent on N-terminal glycosylation nor its state of phosphorylation (Galliera, Galliera, et al. 2004), nor does ligand binding alter the state of phosphorylation of ACKR2 (Blackburn et al. 2004). However, ACKR2 function (including ligand binding, internalisation, scavenging) is highly dependent on a conserved tyrosine motif within its N-terminus (Hewit et al. 2014). Additionally, the ACKR2 C-terminus has been shown to be critical for chemokine scavenging, as removing a portion of the C-terminus, whilst allowing internalisation of CC-chemokines, prevents continued cycling and scavenging (McCulloch et al. 2008).

1.3.3 ACKR2: expression patterns and disease associations

ACKR2 is predominantly expressed in barrier tissues, with high expression by lymphatic endothelial cells (LEC), both in peripheral tissue (such as gut, skin and lungs) secondary lymphatic tissues (Nibbs et al. 2001), healthy keratinocytes (Singh et al. 2012), placental tissue (where some of the highest expression levels of ACKR2 are found) (Nibbs, Wylie, Yang, et al. 1997; Bonini et al. 1997) hepatocytes (Berres et al. 2009; Wiederholt et al. 2008), but also some leukocytes such as DCs (McKimmie & Graham 2006) and innate B-cells (Graham & Locati 2013). Inflammatory cytokines have been shown to be able to upregulate the expression of ACKR2. In particular, IL-6 and TGFβ can upregulate expression of ACKR2 in cultured primary human lymphatic endothelial cells (McKimmie et al. 2013), whilst IFNγ can potently upregulate ACKR2 expression in primary cultures of keratinocytes (Singh et al. 2012).

ACKR2 binds at least 12 pro-inflammatory chemokines (Nibbs & Graham 2013), with slightly fewer ligands in mice (Graham & Locati 2013). Unchallenged ACKR2-/- mice are relatively indistinguishable from WT mice, apart from some differences in B-cell and monocyte numbers/function (Graham & Locati 2013). But, differences rapidly become apparent in response to injury and infection. ACKR2 is differentially expressed in a range of pathological processes, with increased expression in clinically unaffected skin of patients with psoriasis (Singh et al. 2012), in pulmonary macrophages of patients with chronic obstructive pulmonary disease (COPD) (Bazzan et al. 2013) and in peripheral leukocytes of patients with systemic sclerosis (Codullo et al. 2011). Studies have also implicated ACKR2 as playing a role in limiting overwhelming sepsis, as in ACKR2-/- mice, pulmonary inoculation of Mycobacterium tuberculosis led to overwhelming systemic inflammation and death, in contrast to WT mice where the disease followed a considerably milder and more localised course (Di Liberto et al. 2008).

ACKR2 has been shown to have a role in the development of both gastrointestinal and cutaneous tumour (Nibbs et al. 2007). In ACKR2 null mice, exaggerated pro-tumorigenic inflammation and the associated inflammatory cell infiltration drives the generation of papillomas in response to application of a carcinogen (Nibbs et al. 2007). Thus ACKR2 plays an important, if indirect, role as a tumour suppressor by preventing cutaneous

inflammation from promoting tumorigenesis (Nibbs et al. 2007). Furthermore, studies have shown that certain single nucleotide polymorphisms in the ACKR2 are associated with a more severe inflammatory phenotype, in hepatitis C virus associated liver inflammation (Wiederholt et al. 2008). ACKR2 also has a key role in in the control of lymphatic branching morphogenesis during embryogenesis. In this case, ACKR2 regulates macrophage positioning relative to developing lymphatic vessels in the embryo and so controls the amount of pro-angiogenic factors delivered to lymphatic vessels as they develop (Lee et al. 2014). ACKR2 expression patterns are summarised in Table 1.3.

Tissue / cells	Reference	Comments
Keratinocyte	(Singh et al. 2012)	*Expressed both in non-inflamed skin, and in psoriatic skin. ACKR2 expression upregulated by IFNγ.*
Lymphatic endothelial cells (primary cultures and *in situ* staining)	(McKimmie et al. 2013) (Nibbs et al. 2001)	*ACKR2 expresson upregulated by IL-6, IFN-γ, IFN-β, VEGF-D and TGF-β in vitro. In the Nibbs et al study, vascular tumours also stained positive for ACKR2.*
Placental tissue, trophoblasts	(Madigan et al. 2010; Bonini et al. 1997)	*ACKR2 expression is very high and constitutive. ACKR2 on primary human trophoblasts plays role in development and also during inflammation-induced abortion* (Teoh et al. 2014).
Haematopoietic stem cells	(Nibbs, Wylie, Pragnell, et al. 1997)	*These cells , alongside placental tissue, were the site from which ACKR2 was originally cloned*
Hepatocyte	(Berres et al. 2009)	*Role in context of hepatitis C associated liver inflammation.* (Wiederholt et al. 2008)
Innate B-cells (peritoneal, mouse)	(Hansell, Schiering, et al. 2011)	*Innate B cells are the only leukocyte subset in which ACKR2 demonstrates functional uptake of CCL2.*
Mouse bone marrow-derived dendritic cells, mast cells and human circulating DCs	(McKimmie et al. 2008)	*Expression determined by qPCR, flow cytometry and IHC. This paper also identifies putative TGF-β responsive Smad3-binding sites in the mouse ACKR2 promoter.*
Secondary lymphatic tissue	(Bonini et al. 1997)	
Lung (alveolar macrophages)	(Bazzan et al. 2013)	*Expression correlates with degree of inflammation*
Human peripheral blood mononuclear cells (from patients with systemic sclerosis)	(Codullo et al. 2011)	
THP-1 monocytic cell line	(McKimmie et al. 2008)	*ACKR2 downregulated by lipopolysaccharide and upregulated by TGFβ.*
Gastrointestinal tract (lymphatic endothelial cells and leukocytes)	(Vetrano et al. 2010; Nibbs et al. 2001)	*ACKR2 expressed in resting tissue and during inflammation. Data suggest reduced ACKR2 expression in context of colonic adenocarcinoma, with low levels correlating with enhanced invasiveness* (Langenes et al. 2013).

Table 1.3 Overview of ACKR2 expression.

Overview of cells and tissues where ACKR2 expression has been demonstrated, including in health, in the context of inflammation and cancer, and in which contexts ACKR2 expression can be induced.

1.3.4 ACKR2: *in vivo* function: lymphatic endothelial cells

ACKR2 is highly expressed in lymphatic endothelial cells (LECs) in dermal and mucosal tissues (Nibbs et al. 2001). Its prominent expression on LECs and its chemokine scavenging capacity would support a role in clearing pro-inflammatory chemokines from inflamed tissues by scavenging chemokines throughout the lymphatic network (Graham & McKimmie 2006). However ACKR2 is not found on all lymphatic vessels, suggestive of thus far unidentified mechanism whereby ACKR2 expression in lymphatics is regulated under homeostatic conditions (Graham & Locati 2013). In ACKR2-/- mice, pro-inflammatory chemokines accumulate in lymphatics and are bound onto LECs, thereby impairing APC (and subsequently fluid) flow from inflamed tissues and into lymphatics. Thus, it is possible that ACKR2 enables the LEC surface to be kept free from bound chemokines, thus enabling efficient interactions between CCR7+ APCs and the CCR7 ligands expressed on LECs, and free flow of both cells and fluid from inflamed sites (Lee et al. 2011). In this context, ACKR2 functions as a facilitator of leukocyte movement into lymphatics and the draining lymph nodes. In addition, ACKR2 chemokine scavenging in lymphatic vessels prevents inappropriate clustering of cutaneous CCR2+ inflammatory myeloid cells at lymphatic vessels during inflammation, thus limiting egress of leukocytes from tissues into lymphatic vessels. Furthermore, using cell culture systems it has been shown that ACKR2 may control immature DC position within tissues by enabling LECs to discriminate between immature DCs (iDC) and mature DCs (mDC) (McKimmie et al. 2013). Together these data suggest that ACKR2 helps compartmentalise chemokine function during inflammation, enabling interactions between lymphatics and CCR7+ DC, whilst simultaneously preventing interactions with leukocytes that express inflammatory chemokine receptors such as CCR2.

1.3.5 ACKR2: *in vivo* function: skin and keratinocytes

An early study of ACKR2 *in vivo* function demonstrated that repeated skin application of the phorbol ester 12-O-tetradecanoylphorbol-13-acetate (TPA) to ACKR2-/- mice, led to more skin inflammation as compared to wild type

mice. In particular, a TNF-dependent increase of CCL3 and CXCL2 (a mouse homolog of CXCL8) was demonstrated, as well as an inflammatory infiltrate of mast cells, macrophages and T-lymphocytes that was more marked in ACKR2-/- mice following TPA induced skin inflammation (Jamieson et al. 2005). Since the initial experiments, it has also been suggested that ACKR2 may play a role in human skin disease, specifically systemic sclerosis and psoriasis. One study of patients with systemic sclerosis demonstrated an association between ACKR2 expression and skin/systemic inflammation, where peripheral blood leukocyte ACKR2 expression (transcript and protein) was found to be high, whilst circulating chemokines such as CCL2/3/4 and CXCL8 were also elevated (Codullo et al. 2011). Expression of ACKR2 in sclerotic skin is however undetermined.

As histopathological changes observed in the above outlined TPA experiments bore some resemblance to those seen in human psoriasis, it was hypothesised that ACKR2 may be involved in the pathogenesis of psoriasis. Interestingly, a subsequent study showed that ACKR2 transcript expression is higher in unaffected skin of patients with psoriasis, compared to the psoriatic plaque. ACKR2 expression is however unaffected in eczema, which suggests that high ACKR2 expression seen in psoriasis is not a generalizable feature seen in all forms of inflammation. ACKR2 in psoriasis is expressed throughout the epidermal keratinocytes in unaffected skin where it is closely associated with ACKR2 ligands such as CCL2 and CCL5, but is predominantly expressed in the basal keratinocytes in healthy control skin. Furthermore, mild trauma to unaffected skin of patients with psoriasis, (in the form of tape stripping, that induces a degree of epidermal damage and tensile stretch of skin), led to a rapid down-regulation of ACKR2 transcript (Singh et al. 2012). In keeping with a potential role in the pathogenesis of psoriasis, it has been shown that ACKR2 plays a key role in the regulation of type 1 IFN-mediated inflammatory processes (Baldwin et al. 2013), that are recognised as important events in early psoriasis. Furthermore, a key role for ACKR2 in suppressing excessive inflammation was demonstrated by studies in which ACKR2 was transgenically expressed in keratinocytes of mice. This led to less inflammation (and reduced tumorigenesis) upon TPA stimulation of skin *in vivo* (Nibbs et al. 2007).

1.3.6 ACKR2: *in vivo* function: leukocytes

ACKR2 is expressed on a range of leukocytes, in addition to being found on PBLs of patients with systemic sclerosis as discussed above (Codullo et al. 2011). ACKR2 is expressed at variable levels by monocytes, DCs, mast cells, myeloid progenitor cells, on megakaryocytes (McKimmie et al. 2008), as well as being found in platelets in systemic inflammatory disease (Codullo et al. 2011). ACKR2 is expressed by murine plasmacytoid DCs, where it internalises e.g. CCL2 (Ford et al. 2014) and also by innate-like B-cells in mice, where it has been shown that ACKR2 can interact with, and inhibit, CXCR5 function. ACKR2 expression can further be utilised to distinguish between innate-like B-cells and other B-cell subtypes (Hansell, Schiering, et al. 2011). However, whilst being expressed on leukocytes the function of ACKR2 in this context is not understood. It has however been suggested that ACKR2-mediated scavenging by leukocytes in inflamed tissue, may play a role in the resolution phase of inflammation (McKimmie et al. 2008). Additionally, neutrophil expression of ACKR2 may modulate neutrophil migration in a cell autonomous manner (Rot et al. 2013).

The anti-inflammatory role of ACKR2 is also apparent in solid organs, including the liver, where ACKR2 is expressed by hepatocytes. ACKR2-/- mice were more susceptible to carbon tetrachloride in an *in vivo* model of acute liver injury, with liver damage being associated with elevated expression of the ACKR2 ligands CCL2 and CCL5 (Berres et al. 2009). In contrast, in experimental colitis, lack of ACKR2 was not associated with measurable differences in levels of CC chemokines, but was associated an unexplained increase in IL-17 production by γδ T-cells (Bordon et al. 2009).

1.3.7 ACKR2: regulators of expression

Relatively little is thus far known about the molecular mechanisms that underpin the differential regulation of ACKR2 expression and function. ACKR2 expression by LECs is strongly induced by both IL-6 and IFNγ (McKimmie et al. 2013) and is also upregulated, albeit to a lesser degree, by IL-1α and IFNβ (Singh et al. 2012). Simple skin trauma in the form of tape stripping of clinically clear skin of patients with psoriasis (where ACKR2

expression is relatively high), has been shown to rapidly down-regulate ACKR2, though the mechanism for this is thus far unknown (Singh et al. 2012). In myeloid cells, it has been shown that ACKR2 expression is downregulated by some pro-inflammatory molecules such as lipopolysaccharide (LPS), but upregulated by the anti-inflammatory cytokine TGFβ (McKimmie et al. 2008). Overall however, our understanding of how ACKR2 expression is regulated *in vivo* and *in vitro* remains limited.

1.3.8 The Atypical Chemokine Receptor 1

Though the Duffy blood group antigen had been known for some times and was known to be important for *Plasmodium vivax* entry into red blood cells (Miller et al. 1976), it is only in the past two decades that it has been identified as a 7-transmemberane receptor that binds both CC- and CXC chemokines (Neote et al. 1994; Horuk et al. 1993). Thus, it subsequently became known as Duffy antigen/Chemokine Receptor (DARC) and more recently it was again renamed ACKR1 (Nibbs & Graham 2013). ACKR1 binds numerous, albeit not all, pro-inflammatory CC and CXC chemokines (Hansell, Hurson, et al. 2011), and has a particularly high affinity for CXCL2 (e.g. compared to CXCL11 (Nibbs & Graham 2013). Indeed, ACKR1 binds a variety of CC-chemokines (CCL2, 5, 7, 11, 13, 14 and 17) and CXC-chemokines (CXCL1, 2, 3, 5, 6, 8, 11), as reviewed elsewhere (Nibbs & Graham 2013). As such, ACKR1 is unique among the atypical chemokine receptors, in being able to effectively bind both CC and CXC chemokines. The capacity of RBC-expressed ACKR1 for binding chemokines released from tissues is considerable, and is believed to play a role in buffering and regulating bioavailability of circulating chemokines. In this manner, it is believed that ACKR1 buffering acts to ensure that leukocyte interactions with chemokines are at vessel endothelial cells, rather than freely in the circulation (Nibbs & Graham 2013).

1.3.9 The Atypical Chemokine Receptor 3

ACKR3 (formerly CXCR7) was identified as a new non-Ca^{2+} mobilising receptor that binds (with high affinity) both CXCL12 and CXCL11 and is expressed on a range of cell types, including endothelial cells, hepatic cells

(Burns et al. 2006) and heart valves (Naumann et al. 2010). From its discovery, it has been implicated in oncogenesis, where antagonism of ACKR3 was found to inhibit tumour growth in several model systems (Burns et al. 2006). ACKR3 acts as a scavenger for both CXCL11 and CXCL12 (Naumann et al. 2010). Constitutive β-arrestin-dependent cycling of ACKR3 from the surface to the intracellular compartment has been demonstrated in breast cancer cells, where ACKR3 was shown to facilitate the degradation and extracellular depletion of CXCL12 (Luker et al. 2010). ACKR3 cycling can however also take place without ligand binding (Naumann et al. 2010). Chemokine scavenging by ACKR3 has shown to be, dependent on receptor C-terminus (Hoffmann et al. 2012), with ubiquitination being important for correct receptor cycling (Canals et al. 2012). Further complexity into the regulation of ACKR3 function is added by receptor dimerisation. ACKR3/CXCR4 dimerisation result in activation of β-arrestin linked signalling in preference over CXCR4-linked G—protein pathways (Decaillot et al. 2011). Although ACKR3 does not signal through classical G-protein pathways, there is evidence for MAP kinase pathways in a β-arrestin dependent manner (Rajagopal et al. 2010).

1.3.10 The Atypical Chemokine Receptor 4

ACKR4 (formerly CCX-CKR, CCR11 or CCRL1) binds to the homeostatic CC-chemokines CCL19/21 (CCR7 ligands), and CCL25 (CCR9 ligand) (Townson & Nibbs 2002) and to a lesser degree to CXCL13(Gosling et al. 2000). ACKR4 is believed to play a role in adaptive immune processes and inflammation (Comerford et al. 2006; Nibbs & Graham 2013). ACKR4 is expressed in certain LECs in secondary lymphoid tissues (Astarita et al. 2012), and it has been shown that it is involved in regulating homeostatic trafficking of skin DCs to skin draining LNs (Heinzel et al. 2007). In the EAE model of multiple sclerosis, using ACKR4-/- mice it has additionally been shown that absence of ACKR4 is associated with a Th17 skewing (from Th1) in T-cell responses, and increased expression of IL-23 (Comerford et al. 2010). In keeping with a key role in adaptive immunity, ACKR4-/- mice also display aberrant self-tolerance, develop a Sjögren's-like pathology and display abnormalities in thymic leukocyte development (Bunting et al. 2013). There is a role for

ACKR4 in the formation of functional CCL21 gradients in lymph nodes, that facilitate DC migration (Ulvmar et al. 2014). Recent studies have also demonstrated ACKR4 in the the thymus, but any functional significance in terms of thymic development and function remains unclear (Lucas et al. 2015).

1.3.11 Chemokines as therapeutic targets

Due to their prominent role in the regulation of leukocyte migration, it is perhaps surprising that there are so few approved therapies that specifically target chemokines/chemokine receptors. The two best examples of chemokine-based therapies are CCR5 blockade (Maraviroc™) for the treatment of HIV infection (Tan et al. 2013), and CXCR4 blockade (Plerixafor™) for bone marrow mobilisation (Devi et al. 2013). There have been no drugs licenced for use that target inflammatory chemokine pathways to date. This is due to a number of reasons and ultimately reflects our relative lack of understanding of the chemokine system in health and disease. Despite the two successes above, progress in therapeutic targeting of chemokines has been slow. Significant receptor-ligand binding promiscuity has led to suggestions that the chemokine system is redundant, where blocking one chemokine/receptor will merely be compensated by another chemokine/receptor. There is however evidence that true redundancy appears relatively uncommon; for instance CCL5 binds CCR1/3/5 but induces different receptor recycling in each case. Furthermore, knockout studies of different CCRs (with apparently 'redundant roles') yield specific phenotypes (Schall & Proudfoot 2011), and indeed, clinical trials have also shown efficacy when using CXCR2 blockade in COPD (Durham et al. 2016). Thus, rather than being merely a function of redundancy, it has been argued the lack of progress in translation of advances made in chemokine biology to novel therapies lies in 1) inappropriate target selection in past trials (e.g. CCR2 as a target in rheumatoid arthritis, where it has a questionable role) and 2) inappropriate dosing (existing pharmacological approaches tend to overestimate *in vivo* lead compound potencies) (Schall & Proudfoot 2011).

There exist several further potential chemokine drug targets, some of which show considerable promise. In the case of psoriasis, due to the high

expression of CCL20, targeting CCL20/CCR6 has been proposed as a therapeutic strategy (Mabuchi et al. 2012). Whilst there are chemokine targeting drugs in current development, no skin-targeting chemokine-based therapies have yet been licenced. It has been suggested that previous shortcoming in this area of drug development can be overcome in several different ways, including through improved target selection (by means of more judicious and critical use of animal models of disease), and through improved methodology for performing potency assays/improved dosing in trials (Schall & Proudfoot 2011).

1.4 Clinical aspects of psoriasis

1.4.1 Overview

Psoriasis is a common, systemic inflammatory disorder that profoundly impacts those affected (Eberle et al. 2016; Di Meglio et al. 2014). It is typically characterised by red plaques with adherent white scale on the skin (Figure 1.3-4), but increasingly it is recognised as a systemic disorder associated with significant co-morbidities. Management of psoriasis remains complex and challenging. However, significant advances having been made in recent years in our understanding of its pathogenesis, with an increasing availability of therapeutic options (Di Meglio et al. 2011).

1.4.2 Structure and function of skin in health and psoriasis

There are three main compartments of skin; the outermost stratum corneum, the intermediary epidermis and the dermis (Figure 1.5). Keratinocytes (KC) are the principal cell type in the epidermis, which proliferate at the basal layer (superior to the basement membrane that separates the epidermis from the dermis). KC gene and protein expression changes progressively upon maturation, and as they mature different protein/lipid expression patterns lead to the characteristic appearance of the spinous and subsequently granular layer of the epidermis. KCs normally lose their nuclei as they continue to mature, eventually forming the outermost stratum corneum (composed of lipids and proteins) that protects

against infection, dehydration and additionally provides tensile strength. The stratum corneum is continually shed in health, and is replaced by proliferating KCs from beneath; this orderly maturation process takes some 28 days in health. Additional cells in the epidermis include melanocytes (that produce melanin and account for pigmentation) as well as a range of immune cells (both transient and resident populations) (Clark 2015). Normally, there is a degree of undulation forming shallow broad based 'waves' parallel to the skin surface at the dermo-epidermal junction (known as rete ridges), thought to confer additional structural integrity. The dermis that lies beneath the epidermis in turn, is predominantly composed of extracellular-matrix-producing fibroblasts, and is the compartment in which the majority of skin appendages are found, including sweat glands, sebaceous glands, hair follicles, loops of blood vessels and lymphatic vessels. Whilst KC proliferation/maturation is a relatively ordered process in health, in psoriasis, KC proliferation is much more rapid. The maturation is accelerated many-fold to approximately 4 days (compared to 28 healthy skin) (Lowes et al. 2014). Through this accelerated turnover (summarised in Figure 1.5), the epidermis is thickened (*acanthosis*; accounts for the thickening of skin and thus plaque formation), nuclei are retained high in the epidermis (*parakeratosis*), the stratum corneum is thickened with the haphazard cross linking of keratin (*hyperkeratosis*, which accounts for the scaling that characterised psoriasis, and a reduced barrier function), the rete ridges are elongated/deeper, and blood vessels dilated and more numerous (accounting for the redness of plaques) (Nestle, Kaplan, et al. 2009). Additionally, Munro's microabscesses (neutrophil filled cavities in the stratum corneum) and Kogoj Pustules (neutrophil filled cavities in the epidermis) are seen, as is a lymphocyte infiltrate, notably in the epidermis (Lowes et al. 2014).

Figure 1.3 Typical psoriatic plaques

Typical psoriatic lesions at elbows, demonstrating raised, well-demarcated erythematous plaques, with characteristic silver scale. Photograph from Adobe Stock Photos.

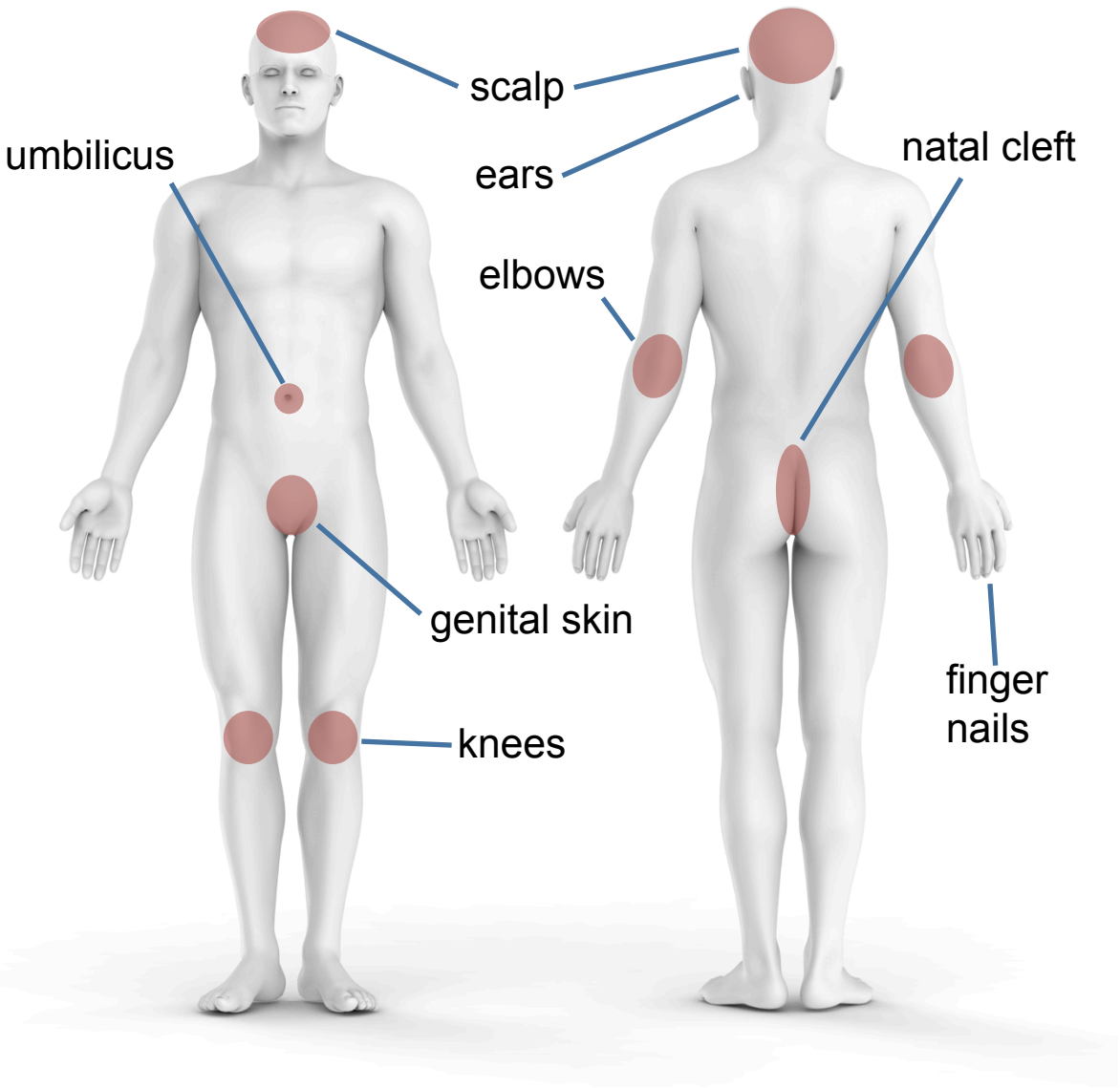

Figure 1.4 Anatomical sites typically involved with psoriasis.
Image indicated sites frequently involved in psoriasis, which tend to be more common in skin flexures (e.g. natal cleft), and at sites of repeated tensile trauma (e.g. elbows and knees). Human figure from Adobe Stock Photos.

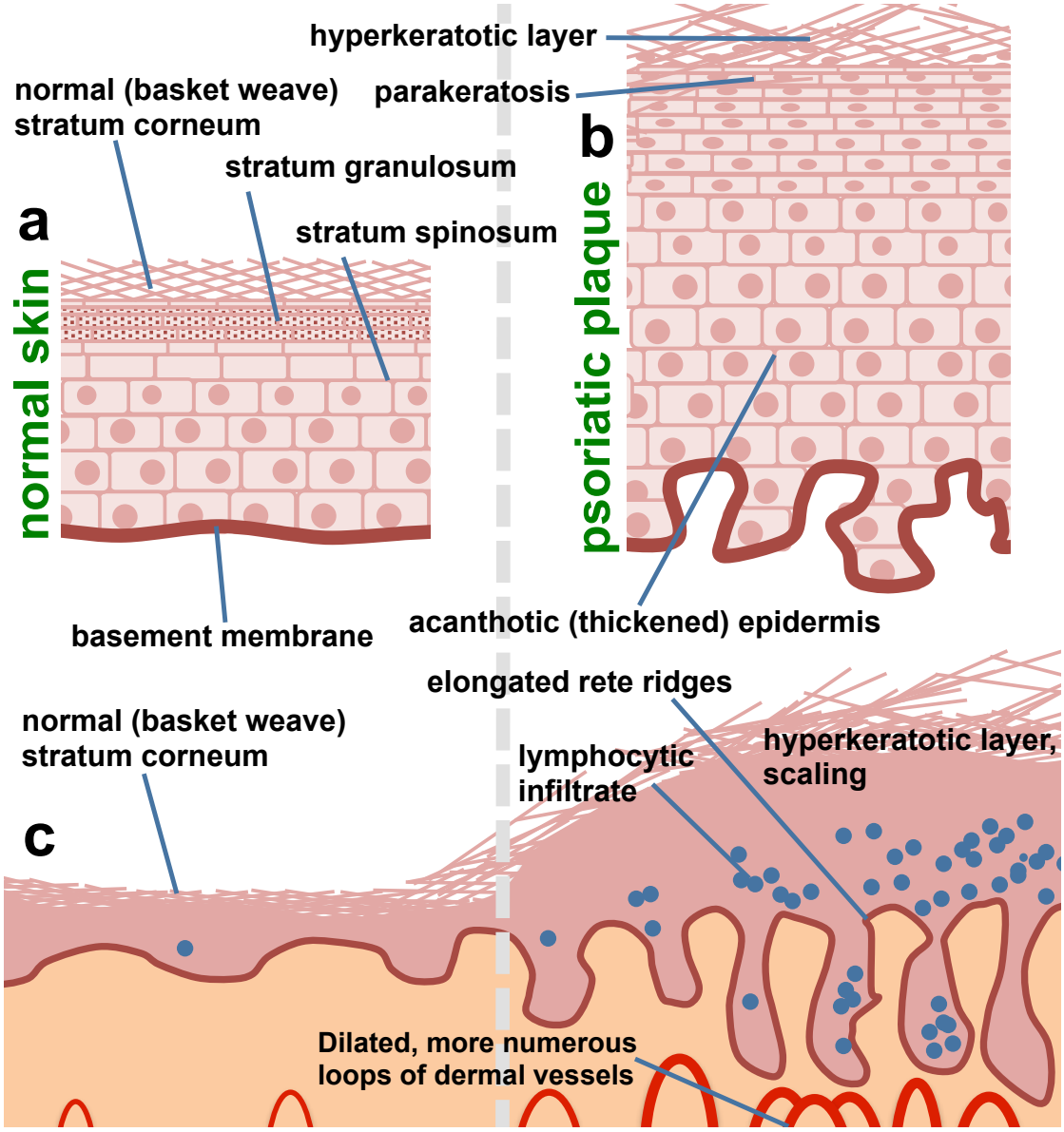

Figure 1.5 Schematic representation of psoriatic plaque development.

a) normal skin, displaying keratinocyte maturation into distinct epidermal layers, with an ordered basket weave stratum corneum b) psoriatic skin, with epidermal thickening, retention of nuclei is stratum corneum (parakeratosis), and elongation of rete ridges c) comparison of whole skin including dermis, in normal and psoriatic skin.

1.4.3 Diagnosing psoriasis

The clinical history and clinical appearance of psoriasis is usually sufficiently typical, that a clinical diagnosis can be made in most patients (Lebwohl 2003). A diagnostic skin biopsy is required only in exceptional cases, where the appearance is atypical and significant doubt persists over the underlying diagnosis. The first accurate clinical description of psoriasis is attributed to Robert Willan in 1808 (Griffiths & Barker 2007), although it took another three decades before a firm distinction was made between psoriasis and leprosy (Nestle, Kaplan, et al. 2009). Despite refinements in our understanding of psoriasis in modern times, the physical manifestations of psoriasis remain a source of misconceptions among the public, which can cause a profound degree of social stigmatisation and suffering for patients with psoriasis (Halioua et al. 2015).

Despite the clinical appearance of psoriasis being well characterised for over two centuries, it is only in recent years that significant advances have been made in our understanding of the molecular and cellular basis of psoriasis pathogenesis, and how genetic and environmental factors interact in the establishment of psoriatic lesions (Di Meglio et al. 2014). Several clinical subtypes of psoriasis have been described, the most common of which include psoriasis vulgaris (80% of cases), guttate psoriasis (10% of cases), pustular psoriasis, erythrodermic psoriasis (each under 3% of cases) and palmo-plantar pustulosis (Biondi Oriente et al. 1989). Sub-classification can be clinically meaningful, as prognosis and treatment responses do vary between many of these subtypes (Di Meglio et al. 2014). The current classification system is based on physical appearance, though molecular insights gained in recent years suggest there are important differences in pathogenesis subtypes (Di Meglio et al. 2014). With an increasing understanding of the molecular mechanisms that underpin psoriasis, it is likely that the way we classify psoriatic sub-types, and choose treatments, may change in the future. Transcriptomic analysis of psoriatic subtypes already suggest there are distinct gene expression patterns for different subtypes, although the clinical and therapeutic significance of these differences remain to be fully elucidated (Ainali et al. 2012). For example, a

specific mutation in IL36RN, a member of the IL-1 family, has been recently identified as being causative in certain familial forms of generalised pustular psoriasis, which has highlighted IL-1 blockade as a potential therapeutic strategy in that patient cohort (Onoufriadis et al. 2011).

Whilst psoriasis is typically diagnosed on clinical grounds, several co-morbidities (e.g. metabolic syndrome, hypertension, arthritis) are associated with psoriasis and must also be considered. Therefore, guidelines suggest screening for diabetes, arthritis and determining the body-mass index in all patients diagnosed with psoriasis, with further screening being warranted depending on the individual's risk factors and other co-morbidities (Paul et al. 2010).

1.4.4 Features of clinical variants of psoriasis

The most common variant of psoriasis is psoriasis vulgaris (some 80-90% of cases), that is characterised by scaly, erythematous, sharply demarcated plaques, that have a particular predilection for extensor surfaces (e.g. elbows, knees), the scalp, buttocks, genital skin and umbilicus (Griffiths & Barker 2007) (Figure 1.4). Plaques are typically symmetrically distributed and affect certain body sites more frequently, though they can affect any site (Di Meglio et al. 2014) (Figure 1.4). Though the clinical manifestations of psoriasis are generally dynamic over time, individual established plaques tend to remain static, and are often persistent unless treated (Ayala 2007).

Guttate psoriasis is a relatively common psoriasis variant (10% of cases (Biondi Oriente et al. 1989) that typically occurs in children, adolescents and young adults. It is characterised by small (typically around 5mm in diameter) drop-like psoriatic plaques (*Latin; gutta* = droplet), which often appear acutely and occurring some 2-4 weeks following a Strepcotococcal infection (Griffiths & Barker 2007). T-cell clones have been identified in both the tonsils and skin in this variant that are homologous, in keeping with cross reactivity (Diluvio et al. 2006). Guttate psoriasis is often self-limiting, and responds particularly well to e.g. UV therapy and/or topical treatments, though it can on rare occasions progress to a chronic form of psoriasis (Lebwohl 2003; Di Meglio et al. 2014).

Erythrodermic psoriasis is characterised by widespread erythema (typically affecting >75% of the body surface area), can lead to haemodynamic collapse and death (Lebwohl 2003). Generalised pustular psoriasis (GPP) too is a potentially fatal variant (also known as von Zumbush psoriasis in older literature), that is characterised by sterile, neutrophil predominant pustules and severe systemic features (e.g. fever) (Di Meglio et al. 2014). It is relatively rare, accounting for less than 3% of psoriasis cases (Biondi Oriente et al. 1989). Both erythrodermic psoriasis and GPP are most commonly triggered by withdrawal of systemic corticosteroids, which are therefore generally avoided in psoriasis management (Lebwohl 2003), but flares can also occur in response to triggers such as pregnancy, drugs and infection (Ayala 2007). There is mounting evidence for GPP being significantly different from other types of psoriasis. Mutations have been identified in the IL36RN gene in a minority of affected families (Onoufriadis et al. 2011; Marrakchi et al. 2011), though there is likely also significant contribution by other, hitherto undetermined genes (Di Meglio et al. 2014). Such genetic differences may explain, at least in part, long-standing clinical observations that GPP patients respond poorly to anti-psoriatic therapies such as TNF-blocking monoclonal antibodies (Di Meglio et al. 2014).

There are also other subtypes that are frequently described, which include; palmo-plantar pustulosis, nail psoriasis, seborrhoeic psoriasis and flexural psoriasis (Ayala 2007). Some have features suggestive of them being distinct disease entities (e.g. palmo-plantar pustulosis), whilst others likely represent a specific focal manifestation of a psoriatic variant (e.g. nail psoriasis).

1.4.5 Quantification of disease severity

Psoriasis is a complex multi-factorial disease, thus making quantification of its severity challenging. Presently, the Psoriasis Area Severity Index (PASI) is the most common and well-established means of quantification used in the clinic and gives a score between 0=no disease to 72=severe disease (Fredriksson & Pettersson 1978). This is a widely used and well validated scoring system, that quantifies the severity of the physical manifestation of psoriasis, and takes into account 1) the percentage of body covered, 2) the

degree of erythema (redness), 3) skin thickening and 4) scaling. However, as the impact of psoriasis on the psycho-social well-being of the patient can be profound, the PASI score on its own would give an incomplete picture of the severity of disease. Hence, it is also common to quantify the psycho-social impact of psoriasis using quality-of-life questionnaires, in particular the well-established Dermatology Life Quality Index (DLQI), that is frequently performed alongside the PASI (Paul et al. 2010). These quantitative scores are frequently used both in a research and clinical setting, to determine whether patients are eligible for certain categories of treatment, and to quantify/assess treatment response over time. Indeed, national treatment guidelines (such as the British Association of Dermatologists guidelines for the treatment of psoriasis) have set criteria for both PASI and DLQI scores, before biological agents should be considered (Smith et al. 2009). In the research setting, the gold-standard marker of improvement in clinical trials is the PASI75 that is defined as the percentage of trial participants that display a 75% improvement in their PASI score (Papp et al. 2005). With increasing efficacy of modern therapies however, some advocate that higher response categories, such as the PASI90 would be more appropriate (percentage of participants that display a 90% improvement in their PASI score) (Puig 2015).

1.5 Treatment of psoriasis

1.5.1 Principles of treating psoriasis

There are no curative therapies for psoriasis. Treatments aim to 1) lessen the appearance of skin manifestations 2) improve psycho-social well-being and more recently 3) prevent/manage co-morbidities. Psoriasis pathogenesis is complex, and it follows that its management is similarly multi-faceted. The precise choice of treatment needs to be personalised to the individual circumstances of the patient, the type of psoriasis and the severity of disease. As a T-cell driven (notably Th17/Th1) disorder, as expected, the most efficacious treatments alter T-cell associated immune processes. Milder disease is frequently controlled with topical treatment, whilst phototherapy

and systemic agents are required for more severe/refractory disease (Di Meglio et al. 2014) (treatment options summarised in Table 1.4).

Frequently, it becomes necessary to combine different treatment modalities for optimal effect, e.g. using topical coal tar plus UVB (the Goeckerman regimen) (Lebwohl 2003; Bailey et al. 2012; Gustafson et al. 2012), and retinoids combined with UV (Almutawa et al. 2013). Furthermore, the precise choice of therapy will also depend on co-existing co-morbidities. For instance some systemic anti-TNFα directed biologicals and PDE4 antagonists would also treat any co-existing psoriatic arthritis, whilst e.g. topical treatments/phototherapy do not have any effect on co-morbidities. For limited or localised disease, it is common for topical treatments to be the first line choice (Leonardi et al. 2015; Lebwohl 2003). In contrast, more severe and/or widespread disease (especially where topical agents have failed) warrant the use of phototherapy and/or systemic agents to achieve disease control (Di Meglio et al. 2014). The individual patients' needs are also dynamic over time, and the treatment choice must reflect these changes (e.g. spontaneous regression with old age), and the life events applicable to the patients (e.g. avoidance of teratogenic retinoids in women of childbearing age).

1.5.2 Biological agents

Numerous biological agents are used in psoriasis (Table 1.4), with a meta-analysis showing some of the most efficacious ones for induction of remission as being infliximab, adalimumab and ustekinumab (Menter et al. 2008; Papp et al. 2005; Baerveldt et al. 2013; Schmitt et al. 2014). Infliximab is a chimeric human-mouse IgG1 monoclonal antibody that binds and neutralises both soluble and membrane bound TNFα (A. B. Gottlieb et al. 2003), and was initially licenced for inflammatory bowel disease. Early case-reports indicated patients who received infliximab for inflammatory bowel disease, unexpectedly noted a rapid improvement in their concurrent psoriasis (Oh et al. 2000). Subsequent studies in patients with psoriasis demonstrated a rapid normalisation in skin histology, with normalisation of skin thickness and a significant reduction in epidermal CD3+ T-cells, 2 weeks after administration of infliximab (A. B. Gottlieb et al. 2003).

Category	Agent	Comments/target
Topical therapies	**Corticosteroids**	*Intracellular receptors; multiple anti-inflammatory effects*
	Calcipotriol	*Keratinocyte proliferation*
	Tazarotene	*Intranuclear retinoid receptor, keratinocyte proliferation*
	Tacrolimus	*Calcineurin inhibitor/immune modulation*
	Tar	*mode of action unclear*
	Dithranol	*mode of action unclear*
Systemic therapies	**Acitretin**	*Intranuclear retinoid receptor, keratinocyte proliferation*
	Methotrexate	*Folic acid reductase*
	Ciclosporin	*Calcineurin inhibitor/immune modulation*
	Fumaric acid esters	*Dimethylfumarate: mode of action unclear*
Light based therapies	**UVB (narrow band, 311nm)**	*LC depletion*
	PUVA (UVA plus methoxypsoralen)	*LC depletion (deeper skin penetration vs UVB)*
Systemic small molecules	**Apremilast**	*PDE4 inhibitos; cAMP/PKC signalling in DCs/macrophages*
	Tofaticinib	*JAK1/JAK3*
Anti-cytokine/receptor monoclonal antibodies and fusion proteins	**Infliximab**	*TNF (murine-human chimaeric IgG1)*
	Etanercept	*TNF (human IgG1)*
	Adalimumab	*TNF (Human IgG1)*
	Ustekinumab	*IL12/23 shared p40 subunit (human IgG1)*
	Secukinumab	*IL-17A (Human IgG1)*
	Ixekizumab	*IL-17A (Human IgG4)*
	Brodalumab	*IL-17RA (human IgG2)*

Table 1.4 Common anti-psoriasis therapies currently used.

Information collated from (Eberle et al. 2016; Di Meglio et al. 2014). The most common treatment modalities for the treatment of psoriasis summarised

A mean 50% improvement in PASI score was noted at both 5mg/kg and 10mg/kg doses of infliximab. Treatment with the TNF-targeting etanercept (an IgG1 Fc portion/TNF-receptor (CD120b) fusion protein (Scallon et al. 2002), similarly, shows a significant reduction in epidermal thickening and T-cells, and a reduction in the expression of IFNγ, IL12/23 and the chemokines CXCL8, CCL20 and CXCL10 (A. B. Gottlieb et al. 2005). Adalimumab is a fully human IgG_1 antibody that also targets TNFα (Menter et al. 2008). Despite targeting the same cytokine-receptor pair, differences in binding characteristics leads to difference in therapeutic activity between the different TNF-blocking drugs (Scallon et al. 2002). More recently, biologicals have become available that target cytokines other than TNFα. One of these is ustekinumab, which targets the p40 subunit that is shared by both IL-12 and IL-23 (Sivamani et al. 2012). Ustekinumab has the added advantage of needing to be injected only every 3 months, thereby aiding patient compliance.

The efficacy of the above first generation anti-TNF biologicals highlights Th1 T-cell pathways as being important in the pathogenesis of psoriasis. However, our understanding of psoriasis has since become more refined, and psoriasis is believed to be mediated by both Th1 and Th17 cells (Zaba et al. 2008). Etanercept for instance, is known to have an early effect on Th17 inducing DCs, Th17 products, but in the later stages of resolution also Th1 products including IFNγ (Zaba et al. 2007).

More recently, biological agents have become available that specifically target Th17 T-cell cytokines. The IL-17A directed monoclonal antibody secukinumab has been approved for use in psoriasis and has been shown to act, at least in part, through normalising keratinocyte-neutrophil interactions (Reich et al. 2015). Meanwhile, another IL17A targeting antibody ixekizumab has shown favourable efficacy in trials (Griffiths et al. 2015), and now has marketing approval (Markham 2016). Furthermore, given the central role of T-cells and IFNγ in the pathogenesis of psoriasis, it is perhaps surprising that recombinant IFNγ injections have been used successfully to treat psoriasis with the improvement appearing to be dose-dependent (Morhenn 1987). The results is not as striking as TNFα inhibitors

at the doses used in studies, but it is noteworthy that the degree of improvement appeared to be dose-dependent (Morhenn 1987). This, coupled with the potential adverse effects of IFNγ suggests that greater improvements may have been achievable (at least in theory) had higher doses been tolerated/safe.

The use of biologicals, though often efficacious, is not without challenges. Whilst the above biologicals remain in use today (e.g. etanercept, adalimumab, ustekunumab), two other early biologicals, alefacept and efalizumab, have been withdrawn, due to unspecified reasons and due to cases of progressive multifocal leukoencephalopathy on treatment, respectively (Tan & Koralnik 2010). All biologicals are associated with a risk of serious infections and re-activation of latent infection with e.g. *Mycobacterium tuberculosis*, with the use of biological treatments (Sivamani et al. 2012; Cantini et al. 2015). Favourable long-term safety data for biologicals is progressively becoming available (Leonardi et al. 2011), and results suggest that serious adverse events are generally rare, with a discontinuation rate due to serious infection of 0.7% for ustekinumab over a 5-year period (Papp et al. 2013).

However, as reviewed elsewhere (Di Meglio et al. 2014), 1/3 of patients will not respond to biologicals, or progressively respond less well over time (e.g. due to formation of anti-drug antibodies), and additionally they remain very costly. Critically also, many patients on biologicals will still require topical/other treatments to achieve adequate disease control, which underlines the continued need for further therapies to be developed in the future (Warren et al. 2015).

1.5.3 Small molecule antagonists

Advances have also been made in small molecule drugs in the treatment of psoriasis, which unlike current biologicals, can be delivered topically, and are less costly to manufacture. The Janus kinase (JAK) inhibitor tofacitinib has shown efficacy in trials, both as an oral and topical preparation (Papp, Menter, et al. 2012), and acts through suppression of Th1/Th17 cell differentiation (Ghoreschi et al. 2011). Another is a small molecule drug that inhibits PDE_4 (Schafer et al. 2009), and has shown promise in clinical trials,

albeit to a lesser degree than e.g. TNFα blockade (PASI75 achieved in 41% on highest dose in a small trial) (Papp, Cather, et al. 2012). Apremilast inhibits production of TNFα and IL-12/23 (Schafer et al. 2009), and is now in clinical use both for psoriasis and psoriatic arthritis (Schafer et al. 2009). Despite initial studies suggesting the clinical benefit is not comparable to biological agents, favourable adverse event profile and reports of their use in combination regimes for psoriasis (Rothstein et al. 2016), underlines an important niche for these small molecule drugs.

1.6 Genetics of psoriasis

Psoriasis pathogenesis is complex, with numerous overlapping pathways and disease mechanisms at play. Further complexity is introduced due to increasing recognition of heterogeneity between psoriasis sub-types that were previously, possibly simplistically, placed under the same umbrella term of 'psoriasis' on grounds of appearance. Unless otherwise specified, this chapter refers to chronic plaque psoriasis/psoriasis vulgaris.

1.6.1 Heritability of psoriasis

Familiar clustering of psoriasis is well described. However, a clear Mendelian patter of inheritance is not apparent, even though many of those affected have a positive family history of psoriasis (Di Lernia et al. 2014). Twin studies have demonstrated higher concordance rate in monozygotic as compared to dizygotic twins (33 versus 17%), and that genetic factors account for 60-75% of psoriasis risk (Lønnberg et al. 2013). Additionally, in concordant twins the clinical course of psoriasis (e.g. age of onset) tends to be similar in both individuals (Oka et al. 2012). It has been suggested that some of the global variation in prevalence of psoriasis (e.g. higher in Caucasians than patients of African heritage (Gelfand et al. 2005)) may relate to heritability, rather than merely ambient UV levels (Enamandram & Kimball 2013). Further evidence for this notion is provided by high rates of psoriasis in Australia, despite relatively high UV levels, which is likely accounted for by the predominantly European genetic heritage of the

Australian population (Parisi et al. 2012). Significant advances have been made in our understanding of individual gene variants that confer psoriasis susceptibility, but all the identified disease associated loci alone do not explain psoriasis risk entirely (Tsoi et al. 2012; Zuo et al. 2015). Together, this underpins the complex heritability of psoriasis, and the importance of genetic as well as environmental factors in determining the absolute psoriasis risk (and disease characteristics) of individuals.

1.6.2 Genetic determinants of psoriasis: PSORS1 and HLA-C

A correlation between psoriasis and the MHC class I molecule HLA-C (and specifically HLA-Cw6) has been known for several decades, with a high carrier rate among patients with psoriasis (Tiilikainen et al. 1980). Advances in genomic technologies e.g. genome-wide association studies (GWAS), have since enabled the genetic basis of psoriasis to be studied in increasing detail (Baurecht et al. 2015). Studies have shown that nearly half of the susceptibility in genetic variables in psoriasis is likely conferred by the 250kb PSORS1 locus, which spans the MHC complex on chromosome 6p21.3 (Di Meglio et al. 2014). GWAS studies have enabled this risk-conferring region to be further refined, and it is now believed that the human leukocyte antigen-A (HLA-C) is the most likely gene candidate in the PSORS1 locus. Specifically, the gene with the overall highest association with psoriasis is *HLA-Cw*0602* that encodes HLA-Cw6, which is in keeping with serologic typing studies from the 1970s and 1980s (Tiilikainen et al. 1980). Whilst abnormal HLA-Cw6 protein function/expression has not been demonstrated in psoriasis (Nair et al. 2006; Duffin et al. 2009; Clop et al. 2013), *HLA-Cw*0602* carriers tend to develop psoriasis at an earlier age, have skin disease that is more extensive and are more likely to have guttate psoriasis compared to controls (Gudjonsson et al. 2006). The important role that HLA-C plays in both adaptive and innate immune processes, further underlines the plausibility of its association with psoriasis, although the mechanism(s) by which HLA-Cw*0602 affects phenotype remain elusive. One study aimed to characterise the functional implications of psoriasis associated SNPs, and demonstrated that 144 variants of PSORS1 are associated with *HLA-Cw*0602*, and that some of these SNPs may constitute new binding sites for transcription factors that

are involved in immune regulation (Clop et al. 2013). Other studies have however failed to show HLA-C responsiveness to psoriasis associated interferons and TNF (Hundhausen et al. 2011). There is also evidence for epistasis between HLA-C and endoplasmic reticulum aminopeptidase 1 (*ERAP1)*, which plays a role in class I processing/antigen presentation (Strange et al. 2010), as well as between HLAC-C and the late cornified envelope genes LCE3B and LCE3C (which play a role in barrier function) (Riveira-Munoz et al. 2010), thus demonstrating the complexity of psoriasis genetics.

1.6.3 Genetic determinants beyond HLA-C

In recent years, genome-wide association studies (GWAS) have collectively enabled the identification of over 40 susceptibility loci for psoriasis (Tang et al. 2013). Although HLA-C SNPs are associated with the greatest increase in psoriasis risk (odd ratio 3.07) (Chen et al. 2011), GWAS studies have highlighted numerous other genes and pathways involved in diverse biological processes, including antigen-presentation, skin-barrier function, Th1/Th17 function and NFκB signalling (Hébert et al. 2015; Duffin et al. 2009; Strange et al. 2010). Many of the identified genetic variants are in fact shared between psoriasis and other conditions that have an immune basis, such as rheumatoid arthritis, multiple sclerosis and Crohn's disease, thus meaning that one SNP can confer risk to psoriasis, but also a range of other conditions with an immune basis (Cotsapas et al. 2011).

1.7 Environmental triggers of psoriasis

Numerous exogenous factors can trigger psoriasis/psoriasis-like lesions, including trauma (so called koebnerisation), medicines (such as beta-blockers, imiquimod and lithium), stress and infections (O'Brien & Koo 2006; Hampton et al. 2012; Di Meglio et al. 2014; Lowes et al. 2014), illustrating the heterogeneity of possible causative agents. Current estimates from twin studies suggest approximately one third of psoriasis risk is due to environmental triggers (Lønnberg et al. 2013), though these triggers are

often technically difficult to study and remain poorly characterised. It is also noteworthy, that there is evidence for interaction between risk conferring single-nucleotide polymorphisms (SNPs) and body mass index (BMI) (Li et al. 2013). The relative contribution of genetic factors and environmental factors, and how such factors interact in the pathogenesis of psoriasis are currently unknown.

Several drugs have been implicated as acting as triggers of psoriasis, including beta-blockers (S. Wu et al. 2014), lithium (O'Brien & Koo 2006), and even paradoxical flares induced by anti-TNFα blockers (Osório et al. 2012). The mechanism underlying these are largely unknown, but there is evidence for e.g. lithium possessing pro-inflammatory properties (Hampton et al. 2012; Petersein et al. 2014).

1.8 Immunopathogenesis of psoriasis

Psoriasis pathogenesis is complex, incompletely understood and involves innate and adaptive immune pathways. A particular importance has been assigned to Th1/Th17 pathways (Nograles et al. 2008; Ortega et al. 2009; Lowes et al. 2014) (Figure 1.1 and 1.6). In its briefest form, psoriasis pathogenesis has been described as a cascade of events starting with activation of DCs that release IL-12/23, subsequently leading to activation of Th17/Th1 and Th22 T cells, that express high levels of IL-17, IFNγ, TNF and IL-22. These cytokines drive keratinocyte hyperproliferation and further immune activation (Lowes et al. 2014). The development of a psoriatic plaque is not simply a linear chain of events. Instead, there is an increasing recognition that the immunopathogenesis of psoriasis is driven by a combination of stromal cells, immune cells and mediators acting together in complex, often concurrent pathways that are in turn activated/driven/perpetuated by both genetic and environmental factors (Lowes et al. 2013; Swindell et al. 2014). There is much debate in the literature surrounding attempts to organise various cell types in a hierarchy according to ‘importance’.

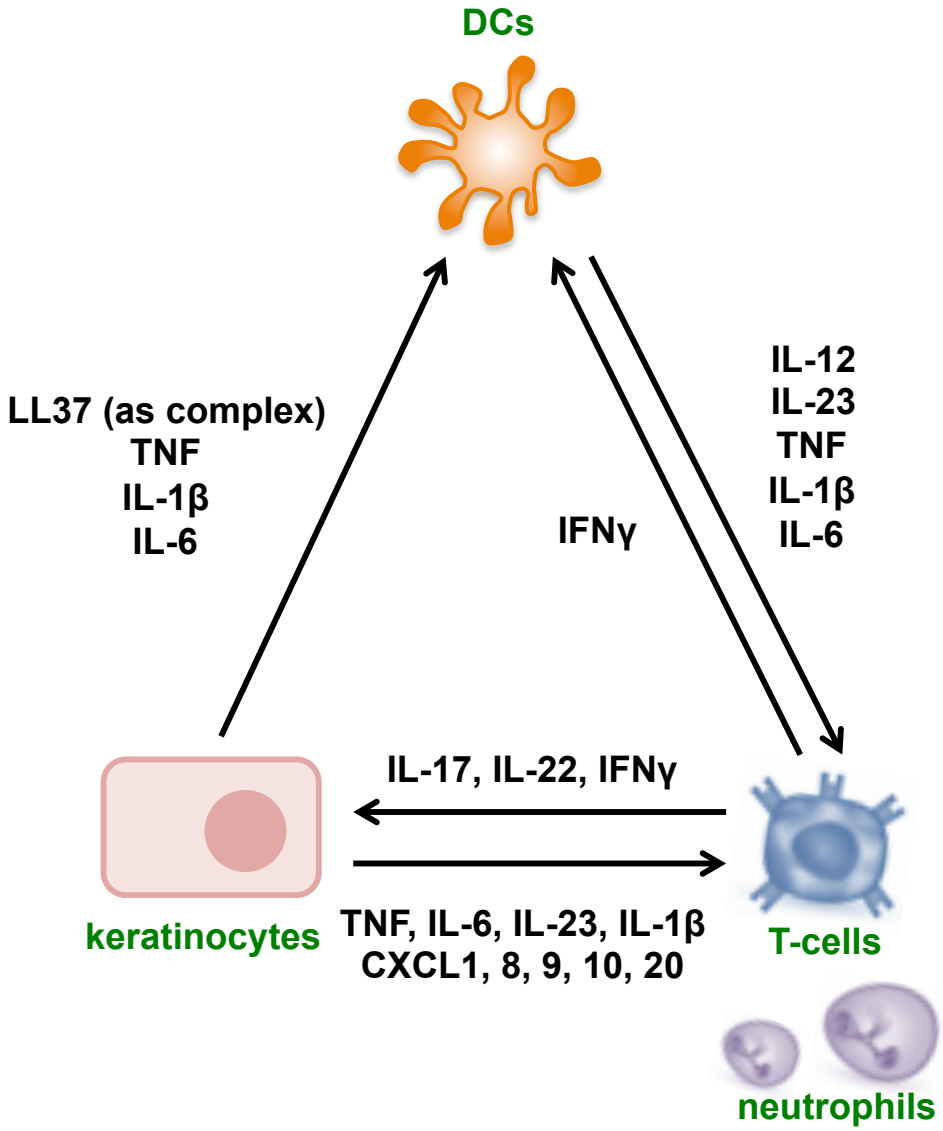

Figure 1.6 Summary of interactions between somatic cells and leukocytes in psoriasis.

Adapted from (Di Meglio et al. 2014). Key interactive pathways between the principal cells in psoriasis pathogenesis summarised.

The comparable clinical efficacy of biologicals despite them targeting different cytokines/receptors (e.g. TNF, IL-17, IL-12/23), highlights difficulty in ranking components of a complex interconnected system in order of relevance. This caveat notwithstanding, psoriasis is broadly considered to be a predominantly T-cell driven disorder, notably driven by Th1 and Th17 T-cell pathways (Lowes et al. 2014).

Psoriasis was, in the past, considered a condition caused principally by abnormal keratinocyte proliferation and differentiation. Though this model is now believed to be too simplistic (Lebwohl 2003; Di Meglio et al. 2014), undoubtedly keratinocytes (the main cell type in the epidermis) play a critical role in psoriasis pathogenesis. Over the past two decades, there has been an increasing emphasis on the role of immune cells, notably in light of the success of drugs that specifically target immune mediators/pathways (Papp et al. 2008; Ohtsuki et al. 2014; Swindell et al. 2014). The importance of leukocytes is illustrated by experiments in which psoriatic leukocytes induce psoriasis-like lesions upon injection into dermal skin (Wrone-Smith & Nickoloff 1996). Furthermore, bone marrow transplantation from patients with psoriasis to non-affected donors, has been known to lead to the development of psoriasis in the recipient (Snowden & Heaton 1997). It is notable that psoriasis risk is associated with HLA-genes, and that autoreactive T-cells have been identified in psoriatic skin (Eberle et al. 2016), again underlining the importance of the immune system. For instance, CD8+ cells have been identified that display reactivity to ADAMTSL5 expressing skin cells, suggesting that this is a putative antigen in psoriasis (Arakawa et al. 2015).

Importantly, even grossly normal skin contains a large number of immune cells, leading to the skin compartment often being considered an immune organ (Di Meglio et al. 2011), with the immune component being termed skin-associated lymphoid tissue (SALT) (Lowes et al. 2014). Xenotransplantation models, whereby unaffected skin from patients with psoriasis are transplanted onto mice, demonstrate that the psoriatic skin has inherent factors that can drive lesion development (Boyman et al. 2004), and it is likely that resident leukocytes also play a critical role.

1.8.1 T-cells in psoriasis: overview

T-cells play a central role in adaptive immune responses, of which there are several subtypes, the majority of which express the αβ T-cell receptor heterodimer, most of which are either CD4+ T-cells (that binds MHCII, and include T helper Th1 cells, Th2 cells, T regulatory (T_{reg}) cells, Th17 cells), and CD8+ T-cells (that bind MHCI) (Singh et al. 2013). In general, T-cells are classified according to the cytokines which they produce (Lowes et al. 2014). It has been known for decades that there are large number of T-cells in psoriatic lesions (Bos et al. 1983), but psoriasis was nonetheless initially considered to be driven by abnormal keratinocyte (KC) proliferation. This notion was supported by the dramatic, rapid turnover of epidermal KCs, and the apparent efficacy of retinoids that are known to inhibit KC hyperproliferation (Marcelo & Tomich 1983; Di Meglio et al. 2014). From the late 1980s, with the emergence of lymphocyte targeting drugs such as ciclosporin (first mainly used to prevent rejection of organ transplants), it became apparent that leukocytes appeared to play a key role in psoriasis pathogenesis (Ellis et al. 1991; Elder et al. 1993). The emergence of denileukin-diftitox, that induces apoptosis of IL-2 receptor expressing active T-cells, confirmed further that specific targeting of T-cells could indeed aid resolution of psoriatic lesions (S. L. Gottlieb et al. 1995) Additionally, there was a direct correlation between epidermal thickening in psoriatic plaques, and the number of infiltrating T-cells (S. L. Gottlieb et al. 1995). In more recent times, the therapeutic approach to T-cells has been refined yet further. The clinical efficacy in psoriasis of biological agents specifically targeting T-cell pathways, have further underlined how such T-cells play a central role in psoriasis pathogenesis. Psoriasis was initially considered a Th1 mediated disease, based on the presence of Th1 cytokines, such as IFNγ and TNFα, and a relative deficiency of Th2 cytokines (e.g. IL-4/5/10) (Schlaak et al. 1994; Di Cesare et al. 2009). Whilst Th1 cytokines are still believed to be important, there is an increasing appreciation for a central role of Th17 cytokines; in particular for IL17 and for γδT-cells in psoriasis pathogenesis. Th1 and Th17 mechanisms are not mutually exclusive, and some have suggested that that immune activation in psoriasis has two interconnected

phases; initiation of the lesion being predominantly Th17 driven, and perpetuation being Th1 driven (Christophers et al. 2014). Though other cell types, beyond Th1/Th17 have also been implicated in psoriasis (e.g. Th22 cells and $T_{reg)}$, comparatively little is known about their role in psoriasis pathogenesis (Van Belle et al. 2012; Lowes et al. 2014).

It is also noteworthy that whilst psoriasis is not generally considered an autoimmune disorder *per se*, CD8+ cells have recently been identified that display reactivity to ADAMTSL5 expressing skin cells, suggesting this is a putative antigen in psoriasis (Arakawa et al. 2015).

1.8.2 T-cells subsets in healthy skin

Most epidermal CD3+ T-cells in normal healthy human skin are CD8+ memory cells, which bear $\alpha\beta$ T-cell receptors (TCR), which is in contrast to murine skin where the majority of epidermal T cells bear $\gamma\delta$ TCRs. The ratio of CD8+/CD4+ cells in human healthy epidermis has however been shown to be very variable in health, depending on the body site investigated. Human epidermal T-cells tend to be localised in the basal layer, whilst dermal T-cells tend to be preferentially localised just below the dermo-epidermal junction (Foster et al. 1990). Effector-memory T-cells that are imprinted to localise into the skin, express the skin-homing chemokine receptors (CCR) CCR4 and CCR10, as well as ligands for E- and P-selectin. This skin targeting of T-cells occurs in skin draining lymph node where skin-derived DC present antigen to T cells, and appears to be dynamic; the tissue tropism of CD8+ T-cells is reversible, and their migratory potential can be altered (Mora 2005). In addition to CD8+ T-cells, several types of CD4+ T-cells can also be found in inflamed skin, and express cytokine profiles that identify them as either Th1, Th17, or Th2 cells (Nestle, Di Meglio, et al. 2009).

1.8.3 Cytotoxic CD8+ T-cells in psoriasis; early arrivals in the epidermis

Xenotransplantation models (using AGR129 mice) have shown that development of psoriasiform inflammation is dependent on the migration of CD8+ T-cells from the dermis to the epidermis. Blockade of this migration through targeting $\alpha 1\beta 1$ integrin effectively prevents psoriasiform lesion

development in an experimental model (Conrad et al. 2007). Animal studies have shown a central role for such cytotoxic CD8+ cells in 1) CD4+ activation, 2) neutrophil recruitment/microabscess formation, 3) recruitment of γδT- and Th17-cells. Furthermore, skin inflammation induced in this model (through H-RAS^{V12G} expression in suprabasal KCs in AGR129 mice) was not reduced by depletion of CD4+ T-cells, emphasising the particular importance of CD8+ T-cells in this context (Gunderson et al. 2012). CD8+ cells are increased in the psoriatic epidermis, and are a source of key psoriasis-associated cytokines, including IL-17A, TNF, IL-22 and IFNγ (Di Meglio & Duarte 2013; Di Meglio et al. 2014).

1.8.4 Th17 cells in psoriasis; the IL-23/Th17 axis

Whilst animal models suggest that resident skin T-cells may be sufficient for initiating psoriasiform inflammation, it is also clear that several subtypes of circulating T-cells infiltrate human plaques, and that they play a role in both plaque initiation and maintenance. As introduced above, there is an increasing recognition that Th17 cells play a pivotal role in psoriasis pathogenesis, a discovery that was largely made through studies into IL-23. High levels of IL-23 are detected in psoriatic skin (Lee et al. 2004), the main sources of which are myeloid inflammatory DCs, Langerhans cells as well as macrophages (Di Meglio et al. 2014; Piskin et al. 2006). IL-23 is a heterodimeric cytokine that is composed of a p19 and p40 subunit (p40 subunit shared with IL-12), and can bind both IL-23R and IL-12Rβ1 (Suzuki et al. 2014; Oppmann et al. 2000). IL-23 is known to be central in the pathogenesis of psoriasis due to a number of findings; firstly, the p40 subunit (common to both IL-12 and IL-23) is targeted by ustekinumab, which has been shown to be one of the most efficacious biologicals available in the treatment of psoriasis. Secondly, it is now known that variation in the IL-23R genes modulate psoriasis risk (Capon et al. 2007). Upon its discovery, IL-23 was found to induce proliferation of both murine and human memory T-cells (Oppmann et al. 2000) and was subsequently shown to particularly induce IL-17 production by a new IL-17 producing T-cell subtype (Aggarwal et al. 2003). It is now known that IL-23 induces IL-17 production by CD4+ T-cells

(i.e. Th17) but also by cytotoxic CD8+ T-cells (Tc17), which frequently co-produce IFNγ and TNFα concurrently with IL-17 (Ortega et al. 2009).

Beyond its role regulating Th17 cells/IL-17 production, IL-23 also plays a role in inducing IFNγ production by tissue-resident memory T-cells (T_{RM}) cells (Piskin et al. 2006). Although KC produce very low levels of IL-23, KC derived IL-23 has been shown to be sufficient to induce IFNγ production by T_{RM} cells, even in the absence of APC derived IL-23 (Piskin et al. 2006). Nonetheless, the principal role of IL-23 in psoriasis pathogenesis, appears to be the maintenance of the IL-23/Th17 axis (Suzuki et al. 2014). Indeed, polymorphisms in IL-23A, IL-23R, STAT2, RUNX3 and TYK2 have been implicated in psoriasis, all of which are associated with Th17 pathways (Eberle et al. 2016). It should however be noted, that several cell types (apart from Th17 cells) are now recognised as producers of IL-17, including γδT-cells, pDCs, innate lymphoid cells, mast cells and neutrophils (Lowes et al. 2014; Eberle et al. 2016). Th17 T cells in turn are also capable of producing cytokines other than IL-17A, including IL-9, IL-10, IL-17F, IL-21 and IL-22 (Eberle et al. 2016). Interestingly, TNFα blockade limits IL-17 production by T-cells (Ortega et al. 2009), which further illustrates that key psoriasis–associated immune pathways are intimately interconnected, and do not operate in isolation from each other.

1.8.5 γδT-cells in psoriasis: innate-like pro-inflammatory cells

Not all IL-17 producing T-cells express the αβ T-cell receptor. The γδT-cell receptor expressing T-cell subtype has also been shown to express this cytokine in psoriasis. These γδT-cells are skin homing, require no priming in lymphoid tissues, can therefore respond quickly and thus are sometimes referred to as 'innate-like' cells (Nestle, Di Meglio, et al. 2009). In humans γδT-cells only make up <10% of total T-cell numbers in dermis/epidermis, but the murine γδT-cell equivalent (Vγ5+ Dendritic Epidermal T-cells; DETC) constitutes the majority of epidermal T-cells in mice (Nestle, Di Meglio, et al. 2009). In humans, γδT-cells become more abundant in traumatised skin (induced by e.g. suction blisters) and are also found in large numbers in psoriatic plaques. In psoriasis, high numbers of γδT-cells are also localised in

unaffected skin of patients with psoriasis, and may play a role in the 'priming' of clinically normal skin that allows for rapid plaque development, if appropriate triggers are encountered (Laggner et al. 2011). γδT-cells produce (constitutively) high amounts of CCL5, but also CCL3/4 and CXCL8 upon activation and can activate KCs through the production of pro-inflammatory cytokines such as TNFα and IFNγ (Laggner et al. 2011), and thereby can perpetuate leukocyte infiltration and inflammation.

1.8.6 Regulatory T-cells

Regulatory T-cells (T_{reg}) are a heterogeneous group of CD4+ cells that play important roles in regulating immune processes, notably in preventing autoimmunity. Their effect is exerted through the modulation of IL-2 production (Oberle et al. 2007), induction of apoptosis and production of other cytokines that regulate immune cells (Shevach 2009; Goodman et al. 2012). In this manner, T_{regs} target a broad range of immune cells, including CD4+/CD8+ T-cells, DCs, B-cells, macrophages, mast cells, NK and NKT cells (Shevach 2009). FoxP3 is a marker for murine T_{regs}, but other CD4+ cells can also express FoxP3 (Fontenot et al. 2003). T_{reg} function has been shown to be abnormal in psoriasis, with a suppressed regulatory function, thus possibly contributing to unrestricted inflammation that characterises psoriasis (Sugiyama et al. 2005).

1.8.7 Resident memory T-cells; initiators of psoriasiform inflammation

A large number (an estimated 20 billion) of T-cells are present in skin and outnumber circulating T-cells (Clark 2015). Recent data suggest that there are two distinct populations of resident memory T cells; and two populations of recirculating memory T-cells, all of which are functionally distinct (Watanabe et al. 2015). Tissue resident cell populations, most of which are CD103+, provide a pool of rapid responders to injury. Tissue resident memory T-cells (T_{RM}) likely have a key role in the early phases of plaque induction, but our understanding of their role in disease is only beginning to emerge (Di Meglio et al. 2014). For instance, T_{RM} in psoriasis express higher levels of both IL-17A and IL-22 compared to cells in healthy controls (Eberle

et al. 2016). Most cutaneous T-cells express the cutaneous lymphocyte-associated antigen (CLA) (Clark 2009), and it has been shown that the chemotactic chemokine CCL27 produced by KC plays a role in recruiting CLA+ T_{RM} to skin (Morales et al. 1999). Skin homing circulating T-cells (CCR4/6/10) positive) play a role in skin immune surveillance, are found in the circulation and periodically enter tissues in response to e.g. danger signals (Boyman et al. 2007). However, it has been shown that significantly more T-cells reside in the skin than exist in the circulation (ratio 2:1), with most of the skin resident T-cells being Th1 effector memory cells (Clark 2015). Most CLA+ effector memory T-cells are localised in skin, and display a very diverse T-cell repertoire. T-cell responses in the skin can be initiated very rapidly, even before additional T-cells are recruited from the circulation (Clark et al. 2006). The capability of resident immune cells to promote psoriasiform inflammation in the absence of circulating B/T-cells or NK cells, is confirmed by studies where psoriasiform inflammation is rapidly established in unaffected human skin that is transplanted onto AGR129 mice. In this particular model, T_{RM} already in the human graft, migrate from the dermis into the epidermis, and cause psoriasiform inflammation without the need for circulating T-cells (Boyman et al. 2004). Resident T-cell populations may also account for why certain body sites in the same patient may develop plaques recurrently; studies have shown that both CD8+ and CD4+ T-cells can remain in skin even after apparent clinical normalisation of the skin upon treatment, and retain their ability to produce psoriasis-inducing cytokines (Cheuk et al. 2014).

1.8.8 Keratinocytes in health and disease: overview

Keratinocytes (KC) make up >90% of the epidermal layer (Nestle, Di Meglio, et al. 2009), and provide a crucial barrier function, as well as playing a role in innate and adaptive immune processes (Perera et al. 2012). In health, generally only basal KCs proliferate, whilst differentiation is the predominant process in the higher epidermal layers (Perera et al. 2012). Both KC proliferation and differentiation are grossly abnormal in psoriasis (Di Meglio et al. 2014). The clinical efficacy of retinoids that primarily target KC differentiation and proliferation, suggested the notion that KCs were the

main culprits in psoriasis in early studies. Though KCs are now not considered the sole drivers of psoriasis immunopathogenesis, there is again an increasing appreciation for their central role in this disease. Indeed, KCs play a role in all stages of plaque initiation, development, maintenance, and even in response to therapies (Barker et al. 1991; Lowes et al. 2013). KCs are e.g. capable of regulating recruitment and function of T-cells in the skin (Lowes et al. 2014), and there are extensive interactions between keratinocytes and immune cells, mediated by a range of cytokines and chemokines, many of which are in fact produced by KCs themselves (Figure 1.6).

1.8.9 Keratinocytes in psoriasis; environmental and immune sensors

Inflamed/damaged KCs display a different phenotype compared to normal cells. There is an upregulation of keratins 6, 16 and 17, cytoskeletal components and cell surface receptors (Perera et al. 2012), and cytokines including IL-1, IL-6, TNFα and chemokines (Vinter et al. 2014). Traumatised KCs are also a key source of anti-microbial peptides or AMPs (including LL37) and self-nucleic acids (RNA and DNA) that play a role in breaching self-tolerance through activating TLR-receptors (Lande et al. 2015). Specifically, LL37-DNA complexes act on TLR9, thereby activating pDCs leading to production of IFNα (Lande et al. 2007). In addition, LL37-RNA complexes activate mDCs by acting on TLR8, leading to production of TNFα and IL-6 (Ganguly et al. 2009) (Figure 1.1). The TNFα produced in this process enhances KC proliferation and is a key driver of psoriasiform inflammation as evidenced by the efficacy of TNFα targeting therapies (Sweeney et al. 2011). Meanwhile, IL-6 expression is thought to aid the differentiation of Th17 cells (Sweeney et al. 2011).

In addition to DCs, KCs play a role in immune surveillance, by expressing a range of TLRs (1-6 and 9) (Sweeney et al. 2011). In addition to KC expressed TLRs, there is a recently characterised family of proteins capable of sensing danger-associated molecular patters (DAMPs) which can lead to activation of pro-inflammatory cascades (Nestle, Di Meglio, et al. 2009).

1.8.10 Keratinocytes in psoriasis; amplifiers of immune signals and recruiters of leukocytes

Inflamed KCs produce a variety of chemokines, including CXCL8, CXCL20 (Sweeney et al. 2011), CCL20, CXCL9, CXCL10 and CXCL11 (Nestle, Di Meglio, et al. 2009), that together can recruit a range of inflammatory leukocytes. Some of these chemokines can be induced in KC by T-cell sourced cytokines. In this manner, KCs act as amplifiers of T-cell signals; Th1 cells produce IFNγ, which induces the expression of CXCL9/10/11 (CXCR3 ligands) by KC, and thereby promote the further recruitment of CXCR3-expressing Th1 cells. In addition, Th17 T-cells release IL-17, leading to KC expression of CXCL1/2/8 and CCL20, which promotes recruitment of neutrophils and more CCR6-expressing Th17 T-cells (Nograles et al. 2008; Lowes et al. 2014). Th22 derived IL-22 in turn leads to enhanced KC proliferation, disordered KC maturation, and thereby contributes to the characteristic histological appearance of psoriatic plaques (Eyerich et al. 2009).Additionally, KC derived AMPs LL37 and β-defensin, together, act as chemoattractants for a range of psoriasis-associated leukocytes including T-cells, monocytes, neutrophils, DCs and mast cells (Oppenheim & Yang 2005). Inflamed keratinocytes furthermore produce pro-angiogenic factors, including VEGF, which lead to the formation of the tortuous abnormal vasculature that characterises psoriasis. These vessels are 'leaky' and permissive to enhanced leukocyte transmigration, thus further facilitating leukocyte recruitment (Costa et al. 2007). Psoriasis-associated IFNγ increases expression of intercellular adhesion molcecule-1 (ICAM-1) and thereby enhances T-cell adhesion to the vasculature (Dustin et al. 1988).

KCs are the main IL-17R expressing cells in psoriasis, and respond to IL-17 and other key psoriasis-associated cytokines (including TNF, IFNγ, IFNα and IL-22), leading to keratinocyte hyperproliferation, production of further pro-inflammatory cytokines and chemokines and further leukocyte recruitment, thereby are at the core of a self-amplifying pro-inflammatory loop (Lowes et al. 2014). It has been argued that the profound clinical effect observed with the blockage of IL-17 is rather unexpected (by virtue of IL-17 being a cytokine relatively far down the inflammatory cascade, and regulates a relatively low number of genes in KC). It has been suggested however, as

reviewed elsewhere, that this may in part be to IL-17 stabilising chemokine mRNA and synergising with TNF (Lowes et al. 2014).

1.8.11 Dendritic cells in psoriasis; bridging adaptive and innate immune systems

Dendritic cells (DCs) are a heterogeneous group of cells, that bridge the innate and adaptive immune systems, recognise external signals through Toll-like receptors and migrate to lymph nodes where they present antigens and activate T-cells (Ganguly et al. 2013). They are believed to play a critical role in psoriasis pathogenesis, and their numbers are reduced by several anti-psoriatic therapies, including ultraviolet B (UVB) and anti-TNF antibodies (Lowes et al. 2014). Though DC numbers are increased in inflammatory skin disorders, their source, origin and function remains an area of controversy (Haniffa et al. 2015). DCs are abundantly present in psoriasis where they tend to be localised in the dermis (Nestle et al. 1994; Lowes et al. 2005), and are capable of producing several key psoriasis-associated cytokines. pDCs and mDCs dominate in psoriatic lesional skin, whilst Langerhans cell numbers are less variable in lesional as compared to unaffected skin. Early studies showed that DCs are present in psoriatic lesions, and mediate T-cell production of Th1 cytokines such as IFNγ and IL-2 upon stimulation (Nestle et al. 1994). It has furthermore been demonstrated that psoriatic plaques express high levels of chemerin, and it has been proposed that the so called chemerin/ChemR23 axis is important for pDC recruitment to skin in the initiation stages of psoriasis (Albanesi et al. 2009). Indeed pDC numbers are increased in psoriatic plaques, but comparatively rare in unaffected skin of patients (Glitzner et al. 2014). Psoriatic pDCs have been shown to produce IFNα, and play a key role in the initiation of T-cell driven psoriatic lesion development (Nestle et al. 2005). Recently, it has been suggested that pDC (rather than Th17 T-cells) may be the principal producers of IL-17.

1.8.12 DC activation in psoriasis by antimicrobial peptides

Keratinocyte-DC interactions appear to be central to psoriasis pathogenesis (Figure 1.6). A range of antimicrobial peptides (AMP) are produced by KCs

(and some other skin cells) in response to damage and injury. These AMPs exert an antibacterial effect principally by e.g. disrupting microbial membranes, and thereby play a role in innate skin defences (Borkowski & Gallo 2011; Nakatsuji & Gallo 2011; Wimley 2010). The AMP LL37 is a mediator in the initiation stages of psoriasis, is highly expressed in psoriatic lesions and is released principally by keratinocytes. It has been shown that LL37 forms aggregates with self-DNA that have been shown to act on Toll-like receptors (TLR) 9 and 10, that are expressed by plasmacytoid dendritic cells (pDCs) (Lande et al. 2007). LL37 also forms complexes with self-RNA and thereafter activates pDCs by acting on TLR7 and 8 (Ganguly et al. 2009). LL37 been shown to act as an autoantigen in psoriasis, that induces proliferation of skin-homing LL37-reactive T-cells, that produce e.g. IFNγ, IL-17 and IL-22 (Lande et al. 2014). KCs in psoriasis thus help produce the AMP LL37 that complexes with self-nucleic acids, and thereby enables the immune system to overcome self-tolerance, in the context of trauma. This leads to the production of psoriasis-associated cytokines and inflammation. TLR9, in addition to being expressed on pDCs, is also expressed by KC (that are themselves also producers of LL37). Stimulation of KC with first LL37 and then subsequently genomic DNA has been shown to lead to enhanced KC production of type I IFN, in a non-LL37-DNA complex dependent manner (Morizane & Gallo 2012).

The ability to activate pDCs via TLR9 is not a feature unique to LL37. A recent study has shown that other AMPs that are overexpressed in psoriasis can exert similar effects as LL37. Specifically, human beta-defensin (hBD) hBD2 and hBD3 are also capable of forming pDC activating aggregates together with self-DNA (Lande et al. 2015). Studies have shown a significant (albeit weak) association between the risk of psoriasis and the copy number of beta-defensin genes (odd ratio OR=1.1-1.3) which would be in keeping with it playing a role in psoriasis pathogenesis (Stuart et al. 2012).

1.8.13 Neutrophils in psoriasis

Neutrophils are abundantly present from a very early stage in psoriatic lesions where they accumulate in particularly large numbers to form the so called Munro's microabscesses (Sweeney et al. 2011). Expression of

neutrophil chemoattractants is enriched in psoriasis, with the degree of enrichment correlating with the number of infiltrating neutrophils (Choy et al. 2012), with neutrophils tending to accumulate particularly in the epidermis (Lowes et al. 2014). Though neutrophils are present in psoriasis, and it is known that they are capable of producing a range of psoriasis-associated mediators (including IL-6, IL-17 and TNFα) (Sweeney et al. 2011), it is only relatively recently that the mechanistic role of neutrophils in psoriasis pathogenesis has become apparent. Recent trials of the IL-17 neutralising monoclonal antibody secukinumab demonstrated that neutrophil clearance, and a reduction in IL-17 inducible neutrophil attracting CXCL1/8, were some of the earliest events in lesion clearance following treatment. This would be in keeping with the efficacy of secukinumab in clearing psoriatic plaques being, in part, due to an effect on neutrophils (Reich et al. 2015). Additionally, neutrophils are producers of IL-17 (Lin et al. 2011). Despite recent advances, the precise role and function of neutrophils in psoriasis pathogenesis remain to be determined.

It has been suggested that 'unevenness', in terms of the degree of inflammation within a psoriatic lesion, coincides with localised clustering of neutrophils, and that such neutrophils can induce localised acute inflammatory flares within already inflamed tissues. The resulting damage in turn leads to the release of pro-inflammatory and neutrophil attracting complement (C3a and C5a) and CXCL8 (formerly IL-8) (Terui et al. 2000). It is hence possible, that whilst psoriasis is predominantly T-cell driven, neutrophils play a role in perpetuating and potentiating T-cell mediated inflammation.

1.8.14 Macrophages in psoriasis

Previous experiments have identified the monocyte attracting chemokine CCL2 in psoriasis (Deleuran et al. 1996), though its role was originally undefined. Further studies demonstrated that IFNγ stimulation of keratinocytes led to an increased expression of CCL2, and furthermore that CCR2 (the receptor for CCL2) was expressed on the majority (though not all) of peripheral monocytes in patients with psoriasis (Vestergaard et al. 2004).

Subsequently, studies have shown that specific CD163+ macrophage populations are activated in psoriasis, and that they produce pro-inflammatory mediators, thereby perpetuating Th1/Th17 responses (Fuentes-Duculan et al. 2010). However, the precise role of monocytes/macrophages in psoriasis remains relatively unexplored.

1.9 Laboratory models of psoriasis

1.9.1 Animal models of psoriasiform inflammation

The complexity of psoriasis pathogenesis, coupled with psoriasis being found almost exclusively in humans (with the exception of rare isolated reports of psoriasiform inflammation in primates) (Jayo et al. 1988; Lowe et al. 1981), makes modelling and studying psoriasis *in vivo* challenging. For this reason, the term *'model of psoriasiform skin inflammation'* is a more accurate description than *'model of psoriasis'* when referring to non-human disease models of psoriasis as such models though helpful, never perfectly mimic human disease (Swindell et al. 2014). The lack of adequate animal models had for some time hampered research into psoriasis pathogenesis (Gudjonsson et al 2007). Research into psoriasiform inflammation in primates is generally not undertaken for practical and ethical reasons. There have also been some attempts to induce psoriasis-like inflammation in animals such as guinea pigs, but with relatively poor results (Wolf et al. 1994). Over recent years however, a large number of mouse models of psoriasiform skin inflammation has become available. There are proposed criteria for what is required of a good model of psoriasis; 1) typical epidermal changes; e.g. thickening (acanthosis), retained nuclei in the stratum corneum (parakeratosis) 2) elongation of rete ridges (papillomatosis) 3) presence of cells including T-cells, monocytes/ macrophages, DCs and neutrophils 4) T-cells playing a role in the pathogenesis 5) altered vascularity/tortuous capillaries and 6) response to typical anti-psoriatic drugs (e.g. retinoids, ciclosporin, anti-TNFα antibodies) (Nestle & Nickoloff 2006). Existing mouse models fulfil these criteria to a greater or lesser extend. Although a perfect model of psoriasis does not exist and each of the available mouse models has

specific inherent limitations, the murine models have, collectively, provided important insights into not only psoriasis, but also psoriasis-associated conditions (Weitz & Ritchlin 2013). Such mechanistic insights into psoriasis immunopathogenesis have already been translated into many novel therapies as reviewed elsewhere (Nickoloff & Nestle 2004).

1.9.2 Imiquimod mouse model: the conception of the IMQ model

Imiquimod 5% cream (Aldara™, IMQ) is mainly used for the treatment of anogenital warts (Grillo-Ardila et al. 1996), actinic keratoses (Szeimies et al. 2004), superficial basal cell carcinomas (Geisse et al. 2004), likely mediated by pDC recruitment. Imiquimod (IMQ) acts on toll-like receptor (TLR) 7 and 8, and when applied to skin, induces a strong immune response (Schön & Schön 2007), that is characterised by activation of pDCs, Langerhans cells, neutrophils, T-cells, γδT-cells and RORγt+ innate lymphocytes. It should be noted that whilst IMQ acts as an agonist of TLR7 and TLR8 in humans, it acts on TLR7 in mice (Flutter & Nestle 2013; Walter et al. 2013; Urosevic et al. 2005; Pantelyushin et al. 2012).

Cytokines including IL-17, IL-22, and IL-23, as well as pro-inflammatory chemokines are found in skin of Aldara treated mice and humans (Walter et al. 2013; Ueyama et al. 2014) with IL-17A, IL-17F and IL-22 being essential for the formation of plaques in mice (Pantelyushin et al. 2012). Additionally, it has been demonstrated that Aldara cream induces inflammation through TLR-*in*dependent mechanisms, and that the vehicle alone (and specifically the excipient isostearic acid used to aid solubility (Chollet et al. 1999), is capable of inducing inflammasome activation in the absence of the active agent imiquimod (Walter et al. 2013). For consistence and convenience, IMQ in this thesis refers to *Aldara* cream rather than pure imiquimod (in line with published literature), unless otherwise stated. There have been reports of topical IMQ application causing enlargement of pre-existing psoriatic plaques (Gilliet et al. 2004), inducing widespread psoriatic lesions where the patient has a history of (previously) stable psoriasis (Fanti et al. 2006; J. K. Wu et al. 2004), and triggering development of *de novo* psoriasis (absence of a personal, or family history) (Patel et al. 2011). The widespread nature of

new psoriatic lesions induced by localised topical IMQ in such reports, suggests that lesions did not occur simply due to e.g. koebnerisation and focal irritation (Rajan & Langtry 2006).

1.9.3 Imiquimod mouse model: characteristics

Skin changes in the IMQ model closely resemble human psoriasis macroscopically (erythema, scaling, thickening), microscopically (acanthosis, parakeratosis, angiogenesis), in terms of infiltrating immune cells (that include CD4+/CD8+ T-cells, macrophages, DCs and γδT-cells) and broadly also in terms of cytokine pathways involved (van der Fits et al. 2009). Given the key similarities with human psoriasis, it is likely that understanding the precise mechanisms, by which IMQ induces psoriasiform skin changes in mice, will help provide insights into psoriasis pathogenesis in humans. For instance, there is an increasing appreciation for IMQ activating several concurrent pathways, both TLR-dependent and independent, which leads to inflammation (Walter et al. 2013).

pDCs express TLR-7 receptors (Kadowaki et al. 2001), and it has been shown that IMQ is an inducer of pDC type-1 IFN production through TLRs, and also enhances pDC viability *in vitro* (Gibson et al. 2002). *In vivo* skin studies have confirmed that IMQ acts on pDC TLR7, leading to pDC production of e.g. IL-23, IL-6 and TNFα (Ueyama et al. 2014). Data from a melanoma model in mice have demonstrated that IMQ leads to an upregulation of CCL2 by mast cells (and thereby recruitment of pDCs to the skin), and that the CCL2 upregulation was dependent on IFNα/β-receptor 1. This suggests that IMQ not only stimulates pDC cytokine production and pDC viability, but potentially may play a role in regulating pDC numbers in skin (Drobits et al. 2012).

IMQ-induced increases in expression of IL-23p19 by pDCs occur after 48h in the IMQ model, and is subsequently followed by an increased expression of IL-17A, IL-17F and IL-22 after 72h (van der Fits et al. 2009). Application of IMQ to IL-17RA-/- mice, and IL-23p19-/- mice, shows that psoriasiform inflammation is significantly suppressed, thereby suggesting that psoriasiform inflammation in the IMQ mouse model is not only associated with, but is dependent on the human psoriasis-associated IL-17/IL-23

pathway (van der Fits et al. 2009). The main producers of IL-17 in the IMQ model are IL-23 responsive γδT-cells (Cai et al. 2011). γδT-cells have been found to be the key producer of IL-17 in response to IL-23 stimulation, in an IL-1β dependent manner (Cai et al. 2011). Dermal γδT-cells, whilst appearing skewed towards IL-17 production, also produce TNFα and IL-22 whereas γδT-cells in the lymph nodes also produce IFNγ in response to IL-23 (in addition to IL-17/IL-22/TNFα). Furthermore, IL-23 was found to drive γδT-cell expansion *in vitro*, and likely plays a role in γδT-cell homeostasis and maintenance. Thus, there appears to be a central role for IL-17 production by γδT-cells in the IMQ model (Cai et al. 2011), and indeed also in humans there is an increasing recognition that IL-17 is produced by a range of immune cells, and not only Th17 cells.

Beyond IL-17, the phenotype of the IMQ model is also dependent on IL-22, as studies have shown that IL-22 knockout mice (and mice treated with neutralising IL-22 antibodies), are relatively protected against IMQ induced psoriasiform inflammation (Van Belle et al. 2012). The principal producers of IL-22 were again γδT-cells, although one-third of IL-22+ cells in one study were αβTCR+ T-cells. However, as IL-22 production was preserved in Rag2-/- mice treated with IMQ, this suggests that αβT-cells are not essential for IL-22 production, and that in addition to the adaptive system, innate cells play a role in IL-22 production (and therefore psoriasiform skin changes) (Van Belle et al. 2012). Importantly, although it has been suggested that innate immune processes alone are sufficient for promoting the *key* features of psoriasiform skin inflammation (Pantelyushin et al. 2012), the overall T-cell dependence of the IMQ model, underlined by CD3+ depletion greatly attenuating IMQ induced psoriasiform skin inflammation, suggests that T-cells do play a key role in the IMQ mouse model, as they do in human psoriasis (van der Fits et al. 2009). It is also noteworthy, that data from other model systems (e.g. EAE) suggest that IL-23/IL-1β activated γδT-cells can act on CD4+ Th17 cells to stimulate IL-17 production, thus serving as an amplification loop (Sutton et al. 2009). However, it remains unclear to what extent this mechanism may apply in psoriasiform inflammation.

1.9.4 Spontaneous mouse models

Numerous spontaneously occurring mouse models have been described, some of which display some key features of human psoriasis (Sundberg & King 1996). Specifically, this includes homozygous mouse models for flaky skin (fsn), asebia and chronic proliferative dermatitis (cpd) (Boehncke & Schön 2007). The 'flaky skin' (Ttc^{fsn}/Ttc^{fsn}) mouse model displays hyperkeratotic plaques and some histological similarities with human psoriasis, and is possibly the best characterised of the spontaneous models. Interestingly the Ttc^{fsn}/Ttc^{fsn} mouse model also demonstrates koebnerisation in response to tape stripping, which few other models have been reported to do (Sundberg et al. 1990). The flaky skin mice also have some severe haematological abnormalities (Sundberg & King 1996). Despite histological similarities, in general, these spontaneous models are rarely used due to important differences compared to human disease, including differing skin vascular changes (Mizutani et al. 2003), and a relative absence of T-cells, which as discussed above are central in human psoriasis (Gudjonsson et al 2007).

1.9.5 Xenotransplantation mouse model

Xenotransplantation models are technically challenging compared to many other mouse models of psoriasis, require unaffected human donor skin from patients with psoriasis and are also very costly (Gudjonsson et al 2007). Some of the earliest studies of xenotransplantation models of psoriasis (XMP) suggested that unaffected psoriatic skin grafted onto nude mice develop certain features of psoriasis: these early findings were initially interpreted as meaning that (undefined) features inherent to the skin were the sole drivers of psoriasis, independently of other (non-skin) host factors such as immune cells (Fraki et al. 1982). This is now considered too simplistic. The generation of modern XMP involve either one of 1) psoriatic plaque skin from human patients, that will contain high numbers of leukocytes, to be grafted onto the back of immunodeficient mice (Villadsen et al. 2003; Kvist et al. 2009), or 2) unaffected (clear) skin from human patients with psoriasis treated with superantigen, grafted onto the back of immunodeficient mice, plus the addition of psoriatic donor leukocytes, pre-treated with bacterial superantigen, injected systemically (Boehncke et al. 1996) or alternatively directly into the lesion (Wrone-Smith & Nickoloff 1996), 3) unaffected skin

from patients with psoriasis grafted onto AGR129 mice, that are deficient in B-/T-cells and type I and II IFN receptors (Boyman et al. 2004), or 4) bioengineered skin equivalents grafted onto immunodeficient mice (Guerrero-Aspizua et al. 2010). Histologically, the psoriasiform skin that results following successful grafting, bears a close resemblance to human plaque psoriasis, with e.g. increased epidermal thickening and elongated rete ridges being apparent (Villadsen et al. 2003). In models using unaffected psoriatic skin plus injected epidermotropic T-cell injections, CD3+ T-cells were found to localise in the epidermis, and most of these were found to be CD8+ rather than CD4+ (Wrone-Smith & Nickoloff 1996). The XMP is often used to assess potential responses to novel therapies, and to assess the effect of therapies *in vivo* and in the development of biomarkers (Kvist et al. 2009). Indeed, and as expected, the use of anti-psoriatic therapies such as ciclosporin and etanercept effectively reverse the psoriasiform changes seen in the plaque transplant XMP (Villadsen et al. 2003). The current methods of generating XMP are in broadly in keeping with current thinking of psoriasis pathogenesis, where both skin cells (e.g. keratinocytes) and immune cells (e.g. T-cells) play critical roles in pathogenesis, though the XMP model often depends on T-cells already resident in the skin, rather than those present in the circulation. Critically however, both the skin cells and T-cells are derived from the donor in current XMP, as the host mouse (SCID, $RAG^{-/-}$, AGR129 mice) generally lacks both T- and B-cells (and have deficient NK cells), which is necessary for successful engraftment of the human donor skin (Boyman et al. 2004). The absence of host B-/T-cells/other cell mediators in XMP is in some respects a weakness of this model, in that the systemic host immune responses to the cutaneous inflammation are inherently limited. The lack of host immunity can however also be experimentally very useful; for instance, the development of psoriasiform lesions in unaffected psoriatic transplanted skin using the AGR129 mouse (Boyman et al. 2004), 1) demonstrates the importance of T-cells resident in the skin in pathogenesis and 2) suggests that systemic factors in the human donor may prevent plaque formation whilst in the human; once this 'systemic suppression' is removed through grafting, skin inflammation develops rapidly. Furthermore, early work in this AGR129 XMP has also

implicated TNFα as an essential driver of resident T-cell mediated psoriasiform plaque development (Boyman et al. 2004).

1.9.6 Transgenic mouse models

Several mouse transgenic mouse models have been developed, that e.g. target the Stat3 pathways, TGFβ, the AP-1 transcription factor family, cell adhesion molecules, growth factors and the NFKB pathways, as reviewed in detail elsewhere (Gudjonsson et al 2007). Most of these models bear significant similarities to human psoriasis, as assessed by genome-wide expression profiling (Swindell et al. 2011). In one model Tie2 (an angiopoietin receptor) is overexpressed in keratinocytes and endothelial cells (KC-Tie2), leading to infiltration of epidermal CD8+ cells, dermal CD4+ cells, and the expression of psoriasis-associated cytokines, including IFNγ, IL-6, IL-17 and TNFα (Wolfram et al. 2009). Comparisons between these models are difficult to make due to the sheer number of transgenic models available, but also due to inconsistencies in terms of e.g. the strain in which the model is generated, which in turn can affect the resulting phenotype (Gudjonsson 2007). Furthermore, inflammation cannot be easily induced at specific sites in most of these models, as in e.g. the IMQ- and xenotransplantion models. There are however some examples of transgenic psoriasis models where lesions may be partially inducible; transgenic skin overexpression of vascular endothelial growth factor VEGF (K14-VEGF) leads to spontaneously occurring psoriasiform lesions, but that can also be induced in response to cutaneous trauma (so called koebnerisation) (Xia & Zhang 2014).

1.9.7 Exogenous IL-23 induced mouse model

A role for IL-23 in psoriasis pathogenesis is suggested by its overexpression in plaques (Lee et al. 2004), and further underlined by one of the most clinically efficacious drugs on the market (ustekinumab) that targets the common p40 subunit of IL-12 and IL-23 (Papp et al. 2008). It has been shown that intradermal injections of IL-23 recapitulate many aspects of psoriasis pathogenesis. The psoriasiform inflammation in this model is dependent on TNFα and IL-20R2, but apparently independent of IL-17A (Chan et al. 2006).

This model has since been used to demonstrate a possible role for CXCR4 to counteract some of the pro-inflammatory effects of Th17 cytokines (Takekoshi et al. 2013), and has further highlighted a role for the CCL20 receptor CCR6 (that is expressed on IL-17A producing T-cells) (Hedrick et al. 2009). Whilst the IL-23 injection model has been useful in some regards, it has some deficiencies, such as an absence of typical structural changes (e.g. elongated rete ridges). Perhaps more critically, it is also not associated with recruitment of psoriasis-associated (CD8+) T-cells into the epidermis (Chan et al. 2006).

1.10 Overview of thesis

Psoriasis is a common, systemic inflammatory disorder that affects approximately 2% of the adult and 0.5-1% of the paediatric population. It profoundly impacts on those who are affected both in terms of morbidity and mortality, notably in severe disease (Eberle et al. 2016; Di Meglio et al. 2014). Several clinical subtypes of psoriasis exist, the most common of which (and that is the focus of this thesis) is psoriasis vulgaris. Psoriasis vulgaris is characterised by thick, erythematous (red) plaques on the skin, with silver-white scaling (Figure 1.2). Such plaques have a particular predilection for extensor surfaces, such as the elbows and knees, as well as skin folds (Lebwohl 2003) (Figure 1.3). The cause for psoriasis is multifactorial and complex, with interactions between genetic and environmental factors. Recent genome-wide association studies (GWAS) studies have identified multiple gene susceptibility loci, and several environmental triggers are known, including skin trauma (Lowes et al. 2014). Though significant advances have been made, important gaps remain in our understanding of psoriasis.

Histopathologically, the psoriatic plaques are characterised by epidermal hyperproliferation and thickening, elongation of the rete ridges, hyperkeratosis, and an infiltration of inflammatory cells. Psoriasis is considered predominantly a Th17 and Th1 driven condition, though numerous other cells have been implicated including Th22 cells, CD8+ cytotoxic cells, neutrophils, mast cells and dendritic cells (myeloid dendritic cells (mDCs)

plasmacytoid dendritic cells (pDC), Langerhans cells). Additionally, keratinocytes play a central role in disease pathogenesis (Lowes et al. 2014; Di Meglio et al. 2011; Diani et al. 2015). Numerous inflammatory mediators play a role in psoriasis, particularly Interleukin-17 (IL-17), IL-23, IL-22, Tumour Necrosis Factor (TNF), Interferon α (IFNα) and IFNγ being central to pathogenesis (Di Meglio et al. 2014). T-cell entry into the epidermis itself does appear to be critical for the development of psoriatic plaques (Conrad et al. 2007). A great deal of insight into psoriasis pathogenesis has been gained through studying the effect of an ever-increasing armamentarium of effective anti-psoriatic therapies. These include newer biological agents (monoclonal antibodies) targeting TNF, IL-12/23, IL-17, small molecule inhibitors targeting PDE4 and the JAK/STAT pathways, as well as older therapeutic strategies, such as UV-based therapies, ciclosporin, fumaric acid esters, methotrexate and retinoids. The mode of action of the majority of these drugs confirm that T-cells are key players in psoriasis (Di Meglio et al. 2014).

Critically, psoriasis is no longer considered merely a disease confined to the skin, but one that is systemic. This is perhaps best illustrated by psoriasis being associated with several comorbidities (e.g. cardiovascular, musculoskeletal and metabolic diseases) as well as increased mortality (Di Meglio et al. 2014). However, despite such recent insights, little has been known about how focal skin inflammation interacts, on a molecular level, with remote skin and other tissues. Furthermore, though epidermal T-cell entry appears to be critical for the pathogenesis of psoriasis, little is known about how T-cell positioning within skin is controlled, and how such regulation may influence the disease course.

Chemokines are the principal regulators of leukocyte migration, and play a key role in the pathogenesis of psoriasis (Lowes et al. 2014). The atypical chemokine receptor ACKR2 is a scavenger for pro-inflammatory CC-chemokines, and is believed to play a role in regulating chemotactic chemokine gradients *in vivo*. Recently, it has been shown that ACKR2 is differentially expressed in human psoriatic skin, where there is an upregulation in unaffected skin, and a relative downregulation in inflammatory plaques. ACKR2 is mainly expressed in basal epidermal

keratinocytes, and also in lymphatic endothelial cells, in human psoriatic skin (Singh et al. 2012). However, the functional relevance of this observation is not understood, nor do we understand the molecular basis for differential regulation of ACKR2 expression. Here, it is hypothesised that differential regulation of ACKR2 in skin is critical for the development of psoriatic plaques, and that modulation of ACKR2 expression can regulate the disease through its ability to remove inflammatory chemokines and so control leukocyte positioning within the skin. Specifically, it is hypothesised that high expression of ACKR2 protects against psoriatic plaques (by chemokine scavenging and regulation of T-cell migration), whilst focally reduced ACKR2 levels leads to dysfunctional chemokine gradient formation (as a result of inadequate scavenging by ACKR2), and thereby uncontrolled inflammation.

This thesis is organised across 4 main results chapters, that explore;

1) the role of ACKR2 in psoriasiform inflammation and its effect on T-cell migration and tissue positioning
2) regulation of ACKR2 in skin remote from the lesion, and the effect of ACKR2 modulation on disease pathogenesis
3) the role of microRNAs as epigenetic regulators of ACKR2 in human cells
4) the role of tensile trauma in regulating ACKR2 expression

CHAPTER 2

2 Methods and materials

2.1 Animal work

2.1.1 General principles of experiments involving mice

All animal work was conducted following approval from the University of Glasgow Ethical Review Committee, and carried out under the authority of a UK Home Office Licence, in accordance with all applicable regulations. All mice were housed in environmentally enriched boxes in maximum groups of 6, had access to food and water *ad libitum*, and received additional calorie supplementation with fruit puree during treatment. All mice were given a 7-day acclimatisation period following any transfers prior to the commencement of experimental work. Mice were weighed daily, with weight loss >20% of the baseline being the cut-off for a cull as per the applicable Home Office regulations; no mice reached this threshold in any of the experiments in this thesis. The sole exclusion criterion for mice from data analysis was if the individual mouse was in a hair re-growth cycle, as this would preclude clinical assessment of skin inflammation.

2.1.2 Imiquimod mouse model

The imiquimod mouse model was based on previously published work (van der Fits et al. 2009), and modified as indicated in the results section. 6-8 week female C57BL/6J wild-type (WT) mice (Charles River, UK) and ACKR2 deficient mice (Jamieson et al. 2005), on a pure C57BL/6J background (backcrossed >12 generations) were used in the studies. 62.5mg of Aldara™ IMQ cream (Aldara™ cream, Meda, UK) or 10% Vaseline Lanette cream as negative control (Fagron, Netherlands), was applied to shaved mouse flank or to ear skin on a daily basis. Details of the treatment area are given in Chapter 3, whilst specific treatment application schedules are indicated in the results and relevant figures. Hair bearing skin was shaved using electric clippers (WAHL, USA) 24 hours prior to the first application of cream. *In vivo* experiments included a minimum of 6 mice per treatment group.

2.1.3 Cytokine treatment of mice

IFNγ treated mice were treated with 10,000U or 20,000U recombinant murine IFNγ (R&D systems) either intraperitoneally (i.p.) or subcutaneously (s.c.) twice daily (as indicated in figure legends). IFNγ was reconstituted in 0.01% sterile BSA in PBS (Sigma, UK), whilst 0.01% sterile BSA in PBS acted as negative vehicle control. Boluses of IFNγ/vehicle control for injection were standardised to 100ul across experiments, and were allowed to reach room temperature prior to injection. All injectable treatments were prepared aseptically, using sterile equipment in a tissue culture hood.

2.1.4 Assessment of skin inflammation *in vivo*

Mice were fully assessed individually at least once daily throughout all experiments, and severity of any psoriasiform skin inflammation quantified daily using a newly developed severity score (detailed in Chapter 3), taking into account the degree of skin thickening, erythema (redness) and skin scaling. Ear thickness was assessed using calipers (accurate to 0.01mm). Ear thickness was measured post-cull across three different sites on the mouse ear, and mean values used for analysis. Additionally, mice were weighed and the weight charted on a daily basis.

2.1.5 Infection of mouse skin with Bunyamwera virus

Mouse skin was injected with 4×10^4 plaque-forming units of Bunyamwera virus (BUNV) intradermally, kindly donated by Dr Clive McKimmie, University of Leeds. Injected skin and internal organs were harvested following cull 24h post injection, as detailed below.

2.1.6 Processing of tissues post cull

Mice were culled by means of a rising concentration of carbon dioxide (CO_2), following which the thoracic cavity was immediately opened and the ventricles cut along the coronal plane, and blood removed by means of a 5ml syringe (BD, Germany). Treated and control skin (as indicated in figures), the heart, liver, spleen, and lymph nodes draining flank skin were dissected out. Tissues were immediately placed in RNAlater (Sigma, UK), and stored overnight at 4°C prior to further processing as detailed below. Where long-

term term storage was necessary, RNAlater treated samples were stored at -80°C prior to RNA extraction. Where samples were also to be used for microscopy in addition to RNA extraction, half the tissue was placed in 10% neutral buffered formaldehyde (Sigma, UK). All tissue processing took place in a tissue culture hood.

2.2 Protein quantification in murine skin

Secreted cytokines/chemokines in murine skin were quantified through the removal of skin upon cull. 20×2mm diameter circles (dermis and epidermis) of skin were obtained per treated site, by means of a 2mm diameter punch biopsy (Stiefel, UK). Skin was maintained at 4°C during all processing, to reduce the risk of protein degradation. Skin samples were placed in 0.1ml PBS (Sigma, UK) in the presence of Pierce protease inhibitor (Thermo Fisher, UK), and gently agitated (4 rotations per minute) at 4°C for 4 hours. Skin sections were subsequently removed, and any residual cell debris removed by means of centrifugation at 1000×g for 10 minutes at 4°C. The PBS containing the secreted protein was immediately frozen at -80°C until needed. Secreted protein was quantified by means of ELISA; CCL5 (R&D Systems), CCL20 (R&D Systems), IFNγ (BD Bioscience and IL-17 (BD Bioscience), as per manufacturer's instructions.

2.2.1 Dermal-epidermal skin splitting

The dermis and epidermis were separated where it was necessary to determine differences in gene expression between the dermis and epidermis. Full thickness murine skin was fully submerged in 0.025mM EDTA (LifeTechnologies, UK) and incubated at 4°C for 12 hours. This enabled the epidermal layer to be easily curetted off the dermal layer using a number 15 surgical blade (Swann-Morton, UK). Both the epidermal and dermal components were immediately lysed in Qiazol (Qiagen, UK) and processed as detailed below. The level of split was further confirmed by QPCR for the epidermal/keratinocyte marker involucrin (not expressed in the dermis), thereby enabling confirmation that the dermal compartment was relatively KC free (details of QPCR below).

2.3 Immunohistochemistry

2.3.1 Immunohistochemistry of tissues

Tissue sections intended for histological sections were maintained in 10% neutral buffered formaldehyde (Sigma, UK) for 24 hours prior to further processing. Tissue sections were processed overnight in an automated tissue processing workstation (Thermo Fisher, UK). Briefly, individual tissue samples were placed in a cassette and submerged sequentially as follows;

1. 70% ethanol; 1h
2. 90% ethanol; 1h
3. 95% ethanol; 1h
4. 100% ethanol; 1h, 2h and 2.5h
5. 100% Xylene; 1h, 1h and 1.5h
6. 100% Xylene; 1h and 1.5h
7. Heated paraffin; 4h and 5h

Processed tissues were thereafter embedded in solid paraffin. Immunohistochemistry was performed by technical staff at the University of Glasgow Veterinary School. Briefly, for H&E, Ki67 and CD3+ staining, paraffin embedded fixed skin was cut to 2 micron thickness. Heat-induced antigen retrieval was performed in pH 6 sodium citrate buffer for 100 seconds at 125°C under pressure. Polyclonal rabbit anti-human CD3 was used at 1:100 dilution and Polyclonal rabbit anti-Ki67 used at 1:400 (both Dako, UK), or negative controls, and counterstained with haematoxylin.

2.3.2 Fluorescent immunocytochemistry

Cells for fluorescent immunocytochemistry were cultured in 4-well plastic chamber slides (ThermoFisher Nunc, or BD Falcon, UK). Cells were washed gently at room temperature in PBS without Ca^{2+} (Sigma, UK), fixed in 100% methanol for 20 min and allowed to air dry. Slides were washed (twice, with 0.05% PBST, Sigma, UK), and subsequently blocked with 20% horse serum in 0.05% PBST (Sigma, UK), and thereafter Avidin/Biotin block. Slides were subsequently washed, and blocked with 30% normal horse serum (Dako, UK) in 0.05% PBST for 40 min. Cells were washed as per above, and stained

(overnight at 4°C) for ACKR2 using anti-human ACKR2 IgG antibody (Sigma Prestige Antibody, UK) at 0.5µg/ml in 0.05% PBST with 2.5% of each of horse and human serum. DAKO Negative Control Rabbit Immunoglobulin Fraction was used (0.5µg/ml) was used as isotype control. Next, biotinylated anti-rabbit IgG raised in goat was used as the secondary antibody, in 0.05% PBST with 5% human serum, and incubated for 30 min at room temperature. Slides were washed in 0.05% PBST, incubated with Avidin-D fluorochrome conjugated with FITC (Vector Laboratories, UK). Slides were incubated in a lightproof humidified box. Slides were fixed with DAPI-containing Vectamount®, and visualized through confocal microscopy (LSM510, Zeiss, Germany)

2.4 Cell culture

Cell culture was performed aseptically in laminar flow hoods at all times. All experimental work was conducted at Passage 3-4, at 70% confluence (averaged across the entire vessel). All cells were maintained at 37°C in a humidified tissue culture incubator with 5% CO_2. Cells were grown in the presence of 1% Penicillin/Streptomycin (Sigma, UK) and 0.1% Gentamicin solution (50mg/ml, Sigma, UK). Experiments were generally repeated using cells from at least 2 separate cell donors.

2.4.1 Primary cell cultures: keratinocytes (KC)

Healthy primary human skin keratinocytes (KC) from adult truncal skin were purchased from (Promocell, Germany), and were in passage 2 (P2) upon thawing and culturing (see below). KC were grown in KCGM2 medium with added $CaCl_2$ (as per manufacturer's instructions).

2.4.2 Primary cell cultures: lymphatic endothelial cells (LEC)

Healthy primary skin lymphatic endothelial cells (LEC) from neonatal foreskin, were purchased from (Promocell, Germany), and were in passage 2 (P2) upon thawing and culturing (see below). LEC were grown in ECMV2 medium (as per manufacturer's instructions).

2.4.3 Cell line culture; HEK293 and HEK293 ACKR2 transfectants

HEK293 cell lines were kindly donated by Dr Kay Hewit, and were grown in DMEM (Sigma, UK) to which was added 50ml Foetal Calf Serum and 5ml L-glutamine per 500mls (Sigma, UK). HEK293 transfectants were grown in the presence of G418 (plasmid expresses a neomycin resistance gene), at 0.8mg/ml (Promega, UK).

2.4.4 Freezing of cells

Where long-term storage was necessary, primary cells and cell lines were frozen in CryoSFM (a serum free, methylcellulose based cryopreservation medium PromoCell, Germany), as per the manufacturer's instructions. In brief, detached cells were frozen at a concentration of 1.5 million cells/ml CryoSFM in cryovials. Cryovials were frozen down to -80°C at a rate of 1°C per minute, and subsequently stored in liquid nitrogen.

2.4.5 Thawing of cells

All cells were thawed in accordance with the instructions of the suppliers of KC/LEC (PromoCell, Germany). Purchased primary cells (PromoCell, Germany) arrived frozen, on dry ice. Medium and all vessels were pre-warmed to 37°C. Frozen cells were stored in liquid nitrogen, and where necessary transported surrounded by dry ice. For thawing, vials were submerged in water at 37°C and gently agitated until thawed (approximately 180 sec). The vial was subsequently rinsed in 70% ethanol and wiped. Cells were transferred to the heated medium and incubated at 37°C at 5% CO_2 until adherent (approximately 16 h), after which the medium was changed.

2.4.6 Subculture protocols

Once a confluence of 90% was reached, cell cultures were split and either frozen for later use or subcultured. PromoCell DetachKit was used for all subculture of KC and LEC as per manufacturer's instructions (PromoCell, Germany). In brief, culture medium was removed, and the cells washed with 100µl HEPES BSS per cm^2 vessel surface for 15 seconds, and the HEPES BSS removed. 100µl Trypsin was added per cm^2 vessel surface at room temperature, and the vessel gently agitated until cells detached. For LEC

this took <5 min and for KC <10 min. Trypsin was neutralised by adding the same volume of Trypsin Neutralization Solution, and the cell suspension spun for 3 min at 220×g.

HEK293 cells were washed in 0.25ml fresh pre-warmed medium per cm2 culture vessel surface. Cells were detached using a sterile cell scraper into 0.33ml fresh pre-warmed medium per cm^2 culture vessel surface, prior to the cell suspension being spun for 3 min at 220×g.

The pellets obtained above were resuspended in CryoSFM (as detailed above, if cells were intended for freezing) or in fresh medium at 37°C if for subculture. Primary cells were subcultured at a ratio of 1:4, and HEK293 cells at a ratio of 1:10.

2.4.7 Cytokine treatment of cells

In order to ensure even distribution of cytokine across the cultured cells, cytokines were dissolved in the appropriate cell culture medium at the concentrations indicated in figures/results. Old medium was subsequently removed and replaced with cytokine containing medium, whilst control treated cells had their medium changed to fresh cytokine free medium. Where medium had to be treated (e.g. antibody neutralisation of cytokines using anti-human IFNγ monoclonal antibody (R&D Systems, UK), or complexing of cytokine/receptor (IL-6/IL-6R), the reaction took place in the medium prior to addition to the cells.

2.4.8 Generation of skin equivalents

All skin equivalents were prepared by collaborators (Dr Ellen van den Bogaard and Prof Joost Schalkwijk) at Radboud University Nijmegen, the Netherlands, as previously described (van den Bogaard et al. 2013). Briefly, healthy human donor dermis was enzymatically decellularised, and populated with primary healthy human keratinocytes on its upper aspect. CD4+ T-cells were added to selected skin equivalents form underneath, and were purified from healthy donors through negative selection (Koenen et al. 2008), and magnetically depleted for CD25high T_{reg} (Miltenyi-Biotec, Germany). Isolated human T-cells were activated with anti-CD3/CD28 beads (LifeTechnologies, the Netherlands) at a cell:bead ratio of 5:1 for 5h prior to

being washed and added to the skin equivalents as described above. Treatment of skin equivalents with anti-psoriatic drugs took place 48h after T-cells had been added to the skin equivalents, as follows; ciclosporin A (400ng.ml, Novartis, Netherlands) and all-trans retinoic acid (10^{-6}M, Sigma, the Netherlands)

2.4.9 Tensile stress of cells

Cells intended for tensile stress experiments were grown on BioFlex™ 6-well plate format silicon membranes (BioFlex™, Dunn, Germany). KC were grown on Collagen I pre-coated plates. For LEC, uncoated silicon plates were coated with Fibronectin as follows; each well was filled with 1.5ml of Fibronectin solution (at 10µg/ml in PBS, both Sigma, UK) at 4°C for 24 hours, after which the solution was removed prior to the plating of LEC. Cells were grown until approximately 70% confluent (confluence was generally higher at the centre of the well, and more sparse at the edges, partially due to the flexibility of the silicone membrane)

Once sufficiently confluent, the membranes were stretched using the FlexCell™ FX5000 machine. This incorporates a computer controlled base unit, and a plate with a solid stage (detailed in Figure 6.1) on which 4 separate 6 well plates can be placed. The solid stage is then placed in an incubator at 37°C for the duration of stretching (the principles of the FlexCell™ are summarised in Figure 6.1). Static control plates were also placed on the solid stage (to minimise sources of variation), but the vacuum underneath turned off. Stretching was set at 0.8Hz, 15% effective stretch, ½ Sine wave-form for 12 hours (Figure 6.2). Lubricant was applied to the solid stage against which the membrane would move for two reasons 1) to reduce friction and thus enable effective stretching and 2) to reduce heat generation due to friction. Due to the lubricant between the membrane and the stage being progressively pushed to the side, lubricant was re-applied every 30 minutes throughout the experiment. Cells were lysed directly on the silicone membrane using Qiazol, the homogenate vigorously pipetted up-down and the lysate put through Qiashredders to optimise homogenisation (as per manufacturer's instructions, Qiagen, UK) prior to RNA extraction, as detailed above.

2.4.10 Isolation and stimulation of human T-cells

T-cells were isolated from buffy coats supplied by the Scottish Blood Transfusion service. These were depleted for CD14+ cells using magnetic columns (Miltenyi, UK). Cells were grown in RPMI (ThermoFisher, UK) with 5% added fat-depleted human AB serum, gentamicin (Sigma, UK), 20U/ml human recombinant IL-2 (Peprotech, UK) and Concanavalin A (5ng/ml, Sigma, UK). Cells were incubated for 8 days at 37°C with 5% CO_2, after which the cell suspension was purified on Ficoll-Paque (GE Healthcare, Sweden), and grown as before, but in the presence of IL-2 alone for 4 days. Cells were subsequently activated using CD2/CD3/CD28 beads at a 1:2 bead:cell ratio (Miltenyi, UK, as per manufacturer's instructions). A bead:cell ratio of 1:4 was used where T-cells were to be used for migration assays. Cells were activated for 24 prior to removing the conditioned medium (tissue culture supernatant) and before T-cells were used for further downstream applications. Where T-cell supernatant was to be used to stimulate KC or LEC, T-cells were grown in serum free KC/LEC medium, as detailed above (Promocell, UK).

2.5 Cell migration

2.5.1 Preparation of migration chambers

Migration chambers were constructed using sterilized materials. A sterile 16×16mm glass cover slip was suspended 1mm above the surface of a glass microscopy slide, using a 1:5 mixture of paraffin and Vaseline, heated to 80°C. Using the paraffin/Vaseline mix, 3 edges of the slide were sealed, forming a pocket on one side. Slides were sterilized using UV light prior to use. The construction of the slides is represented diagrammatically in Figure 3.15-16).

2.5.2 Preparation of cell layers

0.5×10^6 activated T-cells were suspended in 300µl semi-solid collagen matrix, and used to fill the chamber halfway up (Figure 3.16). This was allowed to set in a humidified incubator at 36°C with 5% added CO_2. The collagen matrix was made as follows;

166.6µl bovine collagen solution, 22.2µl MEM and 11.2µl $NaHCO_3$ (all Sigma, UK) were carefully mixed. For the T-cell layer, 0.5×10^6 activated T-cells were suspended in 100µl serum free medium, and mixed with 300µl of the collagen mixture above. For KC and HEK layer, 1.05×10^6 or 3.6×10^6 HEK293 were mixed into 16.7µl of serum free culture medium, and mixed with 33.3µl of collagen solution (166.6µl bovine collagen solution, 22.2µl MEM and 11.2 µl $NaHCO_3$). Please note that these quantities were scaled up as appropriate to reduce error.

A cellular (KC or HEK293) interface was subsequently layered on top of the T-cell layer, with the cells making up 10% of the total volume of the interface. That volume of cells was shown not to inhibit the formation of a chemotactic chemokine gradient as cells could migrate towards a chemotactic stimulus beyond the cell layer. Once the interface layer was set, the chemokine layer was made up in KC medium where the interface consisted of KC, and HEK medium where the interface consisted of HEK293 cells, as detailed previously (but maintained serum free so as to not interfere with chemotaxis). This was layered on top of the other layers, and the chamber top sealed using paraffin/Vaseline. The slide was subsequently maintained flat on a heated stage (37°C) and photographs obtained every 30 sec for 3 hours.

2.5.3 Analysis of cell migration

All cells visible in the recorded field of view were tracked using ImageJ with a cell tracker plugin (see Figure 3.17-18). Entirely non-motile cells were excluded form analysis as viability could not be determined. Vector data were assessed by the Rayleigh test for vector data in chemotaxis plugin in ImageJ (http://imagej.nih.gov/ij/). $P<0.05$ was deemed significant.

2.6 microRNAs

2.6.1 microRNA *in silico* selection

MicroRNAs that were predicted to bind to the 3'-untranslated region (UTR) of ACKR2 were identified using TargetScan version 6.2 (www.targetscan.org). MicroRNAs with the highest likelihood of binding (as indicated by the total context, C_T score) the ACKR2 3'-UTR and that were concurrently identified as being upregulated in psoriatic plaques in humans were selected for further study. Further detail of the selection process is provided in Section 5.5.1, and Figures 5.1-3.

2.6.2 microRNA transfection of cells

Cells were transfected with Lipofectamine RNAiMax as per manufacturer's instructions (ThermoFisher, UK). Cell culture medium was changed to antibiotic free equivalents 24h prior to transfection, and maintained antibiotic free throughout the transfection process. Cells were transfected at 70% confluence. microRNAs, scrambled microRNA control and miR inhibitors (miRvana, ThermoFisher, UK) were aseptically reconstituted in nuclease free water so as to yield 10pmol of miR/µl. miR/control/inhibitors were transfected at the recommended 10nM, unless otherwise indicated in figures. Briefly, 6pmol of miR was dissolved in 50µl Opti-MEM (reduced serum medium, ThermoFisher, UK), and separately 1.5µl RNAiMax was mixed with 50µl Opti-MEM. The two were mixed, and allowed to complex at room temperature for 20 minutes. 100µl of this mix was added to each 24-well tissue culture plate (this was scaled up/down according to well/plate size). Transfection was allowed to occur at 37° for 24 hours before the cells were lysed (or the medium was changed for prolonged incubation, as indicated in figures). At this concentration, the microRNAs had no detectable effect on cell viability. A minimum of 3 replicates (tissue culture wells or flasks) were used for each experiment.

2.6.3 Luciferase microRNA assay

The 3'-untranslated region (UTR) of ACKR2 was amplified from genomic DNA using primers 8aNheI (tgacctagctcaaagtgctctctccagg) and 8bSalI (tgccccaacttcattatcaaagtcgactcga) and Platinum Pfx Polymerase (Invitrogen, ThermoFisher, UK). The ACKR2 UTR was subsequently cloned into the dual luciferase system containing the pmiRGLO vector (as per manufacturer's instructions, Promega, UK). Subsequently, the PCR product and pmiRGLO Vectors were digested using NheI and SalI. Fragments were run along with a 1kb ladder (Promega, UK). 10µl ladder was used with 1µl BlueJuice (ThermoFisher, UK) and run on a 0.7% agarose gel with added ethidium bromide. Fragments were cut out and extracted from the gel (ACKR2 3'-UTR 1577bp, pmirGLO 7332bp) using the QiaQuick Gel extraction kit (Qiagen, UK). Fragments were ligated (T4 ligase, Invitrogen, ThermoFisher, UK) and transformed into chemo-competent *Escherichia coli* bacteria (OneShot® TOP10 Chemically Competent *E coli*, Invitrogen, ThermoFisher, UK). The 3'-UTR region was sequenced to ensure putative microRNA binding sites were intact (Eurofins, UK, see Figure 5.11). The plasmid was transfected into HEK293 cells and stable transfectants generated through selection with 0.8mg/ml G418 (Promega, UK). Non-ACKR2 containing pmiRGLO vector was transfected as a control. HEK293 cells were cultured as outlined above (Section 2.4.3). Several clones were identified for further testing, and two of these clones were transfected with the relevant microRNAs/controls (Section 2.6.2), cells lysed and Firefly luciferase activity normalised to Renilla luciferase (as per manufacturer's instructions, Promega, UK). pmiR containing HEKS (i.e. with no ACKR2 3'-UTR) and native HEK293 cells were used as controls in the assay, that was repeated using two separate HEK293 clones.

2.7 Western Blots

2.7.1 Lysis of Cell cultures

Cell cultures were lysed in lysis buffer, made up as follows; 1µl HALT Protease and Phosphatase Inhibitor (ThermoFisher, UK) in 100µl MACS Lysis Buffer (Miltenyi, Germany), and kept on ice at all times. Cell pellets were

prepared form tissue cultures plates as described in detail above and lysed by the addition of the lysis buffer (1ml lysis buffer per 1×10^6 cells), followed by pipetting up-down multiple times to ensure even lysis, as per manufacturer's instructions. Cell debris was removed through centrifugation for 10 min at 10,000×g at 4°C, and the supernatant removed, and aliquots frozen at -80°C were kept until needed. Where lysates were to be compared, the same cell numbers were lysed for each lane of the Western Blot.

2.7.2 Preparation of Western Blot Gel

15µg protein lysate (prepared as per above) was mixed with 5µl LDS buffer, after which 2µl NuPage Sample Reducing Agent (ThermoFisher, UK) was added to each sample. 20µl of each sample (or 20µl ladder, Invitrogen, ThermoFisher,UK) added of each lane of a pre-cast NuPAGE Bis-Tris SDS gel (ThermoFisher, UK). The gel was run at 150V, 125mA, 100 Watts for 60 minutes (ThermoFisher; nuPage MES SDS running buffer 25ml into 500ml distilled water, kept at 4°C). The gel was cut out, and electrophoretically transferred to a methylcellulose membrane using the iBlot system (ThermoFisher, UK). Even protein loading was confirmed through the addition of 10ml 0.1% Ponceau S in 5% acetic acid for 10 sec (Sigma, UK). Ponceau stain was removed by 4×5 min washes with 25ml 0.05% PBST (250µl Tween into 500ml Dulbecco's PBS without Ca_2^+). The membrane was blocked overnight at 4°C under gentle agitation in 20ml 5% dried skimmed milk (Marvel, UK) in PBS.

2.7.3 Antibody staining of Western Blot (for ACKR2)

Following overnight block, the 10% milk solution was removed and replaced with 20µl anti-CCBP2 (ACKR2) antibody raised in rabbit (Sigma Prestige Antibody, UK) dissolved in 20ml 5% dried skimmed milk in PBS. Binding of the primary antibody took place at 4°C overnight under gentle agitation. The solution was washed off with 5×5min 20ml 0.05% PBST washes. 2µl anti-rabbit IgG linked to HRP (Cell Signaling Technologies, USA) was used as a secondary antibody, dissolved in 20ml 5% dried skimmed milk, and allowed to react with the blot for 1h at room temperature. The membrane again

underwent 5×5min 20ml 0.05% PBST washes. Subsequently 750µl SuperSignal® West Femto Luminal Enhancer (ThermoFisher, UK) was mixed with the same volume of SuperSignal® West Femto Stable Peroxide Buffer ThermoFisher, UK), and added to the blot, and allowed to react for 2 minutes. The blot was then placed in a transparent plastic pocket, excess liquid removed, and the edges sealed shut. The blot was kept in a dark developing box, until being developed onto photographic film (Kodak, UK). Where signal was too strong, multiple blank films were placed between the blot and the final film in order to optimize exposure.

2.7.4 Antibody staining of Western Blot (for ß-tubulin, housekeeping gene)

Following development, the membrane was washed for 10 min in 0.05% PBST, then 25ml Strip Buffer at room temperature for 15 min, and a further 3×15min washes with 0.05% PBST. The blot was then blocked with 20ml 5% BSA in PBST for 1h at room temperature, before adding 20µl anti-ß-tubulin rabbit antibody 9F3 pre-conjugated with HRP (Cell Signaling Technologies, USA) in 20ml 5% BSA in PBS, and allowed to react for 1h at room temperature. The blot was washed 3×15min washes with 0.05% PBST, and was developed with SuperSignal® West Femto, as above.

2.7.5 Western blot band densitometry

Band density was quantified using ImageJ
(http://rsb.info.nih.gov/ij/index.html), as detailed at;
http://lukemiller.org/index.php/2010/11/analyzing-gels-and-western-blots-with-image-j/
In this manner, the density of bands (as indicated in Figure 5.23a) of ACKR2 were quantified, and normalised to the house keeping ß-tubulin band.

2.8 RNA extraction

2.8.1 RNA purification from cell cultures

Total RNA from adherent and non-adherent cell cultures was extracted by using the RNeasy Micro kit (Qiagen, UK), where samples were not intended for microRNA quantification. The kit is based on a silica gel column that relatively excludes rRNA and tRNA (www.qiagen.com), and extraction was carried out as per the manufacturer's instructions. In brief, prior to lysis, tissue culture medium from confluent cell monolayers was removed, and the cell layer gently washed by once adding/removing the same volume of PBS at 37°C in order to remove any dead/non-viable cells. For non-adherent cells, cells were washed in PBS and a cell pellet obtained through centrifugation prior to lysis (300×g for 5 min). Cell lysis was subsequently achieved through the addition of RLT buffer (with 10µl ß-mercaptoethanol/ml RLT buffer, in order to denature any RNases released during the lysis process). The lysate was pipetted up-down vigorously to ensure homogenisation of the sample. Additionally, each sample was immediately vortexed for 10 seconds to ensure full homogenisation. RNA was bound to the column by means of centrifugation, and washed once with RW1 buffer. The RW1 buffer was diluted with molecular grade isopropanol rather than ethanol (Fisher, UK) as per the manufacturer's instructions, in order to enable retention of microRNAs. This was followed by an additional 15min on-column DNAse digestion step (DNAse1, Qiagen, UK), prior to two further washes with RW1 buffer and one wash with each of RPE buffer and 80% ethanol, prior to drying of the column. The purified RNA was eluted in 20µl nuclease free water, and the eluted sample put through the column twice, to ensure maximal RNA yield. The concentration and purity of the eluted RNA was determined through the use of a Nanodrop that measures optical density (Thermo, UK), as per the manufacturer's instructions. All plastics and reagents used were of molecular grade and were RNAse free.

2.8.2 RNA purification from skin and solid organs

Total RNA from skin and solid organs and cell culture (where microRNA quantification was intended) was extracted by using the miRNeasy Mini kit (Qiagen, UK). The kit is based on a silica gel column that relatively excludes rRNA and tRNA (www.qiagen.com), and extraction was carried out as per the manufacturer's instructions. Quantities of samples that were processed in

this manner were as follows; 1) skin: approximately 5×5mm; 2) heart: quarter, cut along coronal and sagittal plane so as to include both ventricles 3) liver: lateral 1/5 cut along sagittal plane 4) spleen: quarter 5) lymph nodes: whole node. Cell culture samples were lysed directly in 700µl Qiazol by means of rapid/vigorous pipetting of the cells, and the aspirate additionally vortexed for 10 sec. Solid tissue samples (previously fixed using RNA later) were placed in 700µl Qiazol in 2mm tubes (Eppendorff, UK) and were homogenized using two 5mm stainless steel beads per tube (Qiagen, UK) at 50Hz for 10 minutes at room temperature.

The homogenate was removed, and 140µl chloroform added as per the manufacturer's instructions and the sample shaken at 50Hz for 1 minute. Samples were centrifuged for 15 min at 12,000×g at 4°C, which separated the sample into three phases. The upper clear phase was removed, and 100% ethanol at 1.5 times the volume of the aspirate added, and the RNA bound to the silica column by means of centrifugation. The column was washed with buffer RWT, which was followed by an additional 15min on-column DNAse digestion step (DNAse1, Qiagen, UK) The column was washed twice with RPE buffer before drying of the column. The purified RNA was eluted in 50ul nuclease free water, and the eluted sample put through the column twice, to ensure maximal RNA yield. The concentration and purity of the eluted RNA was determined through the use of a Nanodrop. All plastics and reagents used were of molecular grade and were RNAse free.

2.8.3 Reverse transcription of RNA

500-1000ng RNA (depending on the total yield/RNA source, which was generally lower for cell culture samples grown in a 24-well format, and higher for solid organs/whole skin) was reverse transcribed to cDNA using PrimerDesign RT or RT2 kits (the former discontinued and replaced with the latter during the thesis) as per the manufacturer's instructions (PrimerDesign, UK). In brief, 500-1000ng RNA plus RT primer (a mixture of random primers and oligodT) in water to a volume of 14µl were heated to 65°C for 5min for the annealing step, and the samples immediately placed on ice. For the extension step, Nanoscript™ Buffer, dNTP, DTT and RT enzyme were added as per the manufacturer's instructions (up to a volume

of 20µl per tube), and the tubes heated as follows; 25°C for 5 min, 55°C for 20 min and heat inactivation of the reaction by heating to 75°C for 15 min. Samples were diluted 1:5 in nuclease-free water prior to being used as a template for QPCR.

For samples intended for microRNA QPCR, 440ng total RNA was reverse transcribed using miScript II RT kit as per manufacturer's instructions (Qiagen, UK). Samples were diluted 1:5 in nuclease-free water prior to being used as a template for QPCR.

All cDNA was stored at -20°C until use, and thawed on ice prior to use.

2.9 Polymerase chain reaction

2.9.1 Quantitative Polymerase Chain Reaction (PCR) primer design

For QPCR two sets of primers were designed; 1) one 'inner pair' for amplification of a specific smaller DNA sequence within the gene of interest and 2) an 'outer pair' that amplified DNA sequence that incorporates the smaller DNA sequence amplified by the 'inner' primer pair. The outer primer pair is utilized for generation of a standard, enabling the generation of a standard curve, and hence quantification of gene expression. (see also section 2.9.5). Primers were designed using Primer3 (available on http://primer3.ut.ee) to the following basic specifications, in order to minimize risk of primer dimer formation;

- 18-23 base pairs in length
- 40-65% GC content (50% deemed optimal)
- T_m of primer between 59.5-61°C
- Max 3'-self complementarity: 1
- Overall self complementarity: 2
- Amplicon size <150bp
- ≤2 G or C bases in last 5 bases at 3' end
- <4 G or C in a row in primer

If no suitable primers were identified, these parameters were gradually relaxed until a suitable primer pair was found in the following order; 1) relaxation of self-complementarity up to 3 and 2) lowering the T_m of the

primer down to 59°C (however maintaining 3' self-complementarity at 1). BLAST analysis was performed for all primers to ensure the primers were specific to the gene of interest (http://www.mcbi.nlm.gov/BLAST/). Primers were synthesized (IDT, Belgium), and were diluted down to a concentration of 1nmol/10µl in nuclease free water prior to use.

Subsequently, primer specificity was confirmed by means of PCR (see below) for each primer pair, and the PCR product visualized on a 2% agarose gel through the use of ethidium bromide. Briefly, 2g agarose were dissolved in 100ml tris-acetate EDTA buffer and heated until the agarose had dissolved, prior to the addition of ethidium bromide and pouring of the gel. The gel was run at 100V in tris-acetate EDTA buffer until a clear separation of the ladder was evident, and visualized using an Alpha Imager ultraviolet light visualization station. Only primer pairs that yielded one single distinct band of an expected size (as per Primer3 *in silico* predictions) were deemed specific (Invitrogen 0.1-2Kb ladder, ThermoFisher, UK). The gene product of the outer primer pair for the specific gene was thereafter cut out and purified (PureLink™ PCR Purification kit, ThermoFisher, as per manufacturer's instructions; experienced users' procedure), eluted in nuclease free water (Qiagen, UK) and subsequently used for the generation of a QPCR standard (see below)

2.9.2 Polymerase Chain Reaction (PCR)

For non-quantitative PCR, the following steps were undertaken; 1ul of each forward and reverse primer for the gene of interest was added to a master mix (Red PCR mastermix, Rovalab, UK), in a 100ul clear PCR tube with a domed cap, plus 2ul of the diluted cDNA template and 2ul of nuclease free water. The sample was vortexed, and spun down prior to undergoing; one cycle at 94°C for denaturation, and subsequently 35 cycles of; 1) 94°C for 15 sec (denaturation/strand separation), 2) 60°C for 15 sec (annealing) and 72°C for 30 sec (PCR product extension). This was followed by 7 min at 72°C after which the samples were kept on ice.

2.9.3 Generation of standard curve for QPCR

A standard curve was necessary for quantification of gene expression. In general the absolute copy number was not calculated, as it was the relative change in gene expression that was of principal interest in the presented experiments. The absolute quantity of gene expression can however be calculated by determining the copy number of the gene of interest within the standard using a Nanodrop that measures optical density, thereby calculating the concentration of transcript (Thermo, UK).

The purified PCR product generated using outer primer pair product for the gene of interest (detailed in section 2.9.1, and sequences given in section 2.9.5), was denoted 10^0, and was diluted to 10^{-2} (in TE buffer, that enhances stability for freeze/thawing and additionally inhibits DNAse) for long-term storage. For the generation of a standard curve of QPCR, this was serially diluted in nuclease free water to yield a range of standards from 10^{-4} down to 10^{-10} (plus a negative Non-Transcript Control, NTC). This range would enable accurate quantification of genes that are expressed both at very high and very low levels. For ACKR2 in contrast, instead of generating a standard using a PCR fragment, a plasmid containing the cDNA of interest was used for the same purpose.

2.9.4 Quantitative Polymerase Chain Reaction (PQCR) protocol

All samples (including standards) were analysed as quadruplicate technical replicates on the QPCR machine (Applied Biosystems, HT7900, Thermo Fisher, UK), in a 384-well format for all experiments. For each well/reaction, the following reagents were used;

- 5µl SYBR Green Mix (Quanta, UK)
- 4µl nuclease free water (Qiagen, UK)
- 0.15µl primer mix (at 1:1 ratio for forward and reverse primers, diluted as per above)
- 1µl cDNA (sample or standard, or nuclease free water only for NTC)

To increase accuracy, a master mix containing all the above (minus cDNA) was prepared, and contents for each 384-well prepared in a 96-well format using a multi-channel pipette. The contents were mixed and centrifuged in this format, and 9.1µl of the contents transferred to each well in a 384-well format. This approach minimized pipetting errors. Care was taken not to

touch the 384-well plate, and the plate was light-protected as far as was practically possible. The plate was spun (3 min at 300×g) prior to analysis. As all product sizes were small (<150bp) a fast run was utilized on the QPCR machine, as follows;

1. 3 min at 94°C (once only)
2. 3 sec at 94°C and 30 sec at 60°C (repeated for 40 cycles)
3. Melt curve generation (once only, see below)

In addition to primer validation (outlined above) a melt curve was always performed to ensure the presence of one single PCR product in all samples. In this process the reaction temperature is progressively increased from 65-94°C, yielding a concurrent measure of fluorescence. One single product size yields one clear peak in fluorescence, thus confirming that a product of one size only is present. NTC samples were analysed to ensure there was no background signal.

For samples intended for microRNA quantification, QPCR was performed using the miScript SYBR Green PCR kit, with primers for miR-146a and 146b normalised to RNU6B expression (all Qiagen, and as per manufacturer's instructions), and analyzed on a 384-well Applied Biosystems 7900HT (Life Technologies). Results for microRNA were analysed according to the ΔΔ-method, rather than semi-absolute methods as used for mRNA.

2.9.5 Primer sequences

Gene/ species	Reference	QPCR1	QPCR2	Standard 1	Standard 2
ACKR2 mouse	NM_001276719.1	TTCTCCCACT-GCTGCTTCAC	TGCCATCTCA-ACATCACAGA	Plasmids of cloned gene used	
ACKR2 human	NM_001296.4	AGGAAGGA-TGCAGTGGTGTC	CGGAGCAAG-ACCATGAGAAG	Plasmids of cloned gene used	
18S mouse/ human	NR_003286	gactcaacac-gggaaacctc	taaccagaca-aatcgctccac	cgtagttccga-ccataaacga	catctaagggc-atcacagacc
TBP human	M55654	aggataagag-agccacgaacc	gctggaaaac-ccaacttctg	gggcacca-ctccactgtatc	catcttctcac-aacaccacca

INVO-LUCRIN mouse	NM_008412	gcttcaagga-aacagcagct	tacttctcctg-ctgtgtccg	cagcagcaa-cagatagagcg	tgtgggatgg-ttggagagtc

2.9.6 QPCR data analysis

The median value of the four technical replicate reactions that were conducted for each biological sample was utilized for analysis. All results were normalised to a housekeeping gene, that was 18S for murine samples and TATA-binding protein (TBP) for human samples, unless otherwise indicated in figures. These were selected as previous experience in the laboratory have found that they remain stably expressed irrespective of treatments. Results are expressed as copies of the gene of interest / copies of housekeeping gene.

2.10 Statistical analyses

Student's t-test, One-way ANOVA, two-way ANOVA and correlation tests were performed in Prism Version 7.0 (GraphPad Software Inc.), with multiple comparison tests as appropriate. $P<0.05$ was deemed significant. All data are $n \geq 3$ and given as Mean ± SEM unless otherwise stated.

CHAPTER 3

3 ACKR2 determines the severity of psoriasiform cutaneous inflammation *in vivo* and T-cell positioning in skin.

3.1 Contents

3.2

Hypotheses

3.3 Aims

3.4 Introduction

3.5 Results

3.5.1 A murine model of cutaneous inflammation for studying the *in vivo* role of ACKR2.

3.5.2 ACKR2 expression levels in the IMQ mouse model of psoriasiform inflammation.

3.5.3 ACKR2 expression in remote internal organs in the IMQ mouse model of psoriasiform inflammation.

3.5.4 Absence of ACKR2 was associated with more severe psoriasiform inflammation in the IMQ mouse model.

3.5.5 Absence of ACKR2 was associated with enhanced epidermal thickening and basal keratinocyte hyperproliferation.

3.5.6 ACKR2-/- mice demonstrated enhanced CD3+ T-cell entry into epidermal skin layers in response to topical IMQ.

3.5.7 A novel *in vitro* model of T-cell migration towards a chemokine stimulus.

3.5.8 A barrier layer of cells expressing ACKR2 regulated T-cell migration towards a chemokine stimulus.

3.6 Summary Chapter 3

3.2 Hypotheses

- ACKR2 expression in IMQ treated mice will replicate the pattern seen in psoriatic patients (high in uninvolved skin; low in plaques)

- Lack of ACKR2 expression increases severity of psoriasiform inflammation *in vivo*.
- ACKR2 expression regulates T-cell positioning in the epidermis
- ACKR2 expression in human keratinocytes regulates T-cell migration towards the inflammatory chemokine CCL5

3.3 Aims

the aims of this chapter were to;

- validate a murine model of cutaneous inflammation suitable for studying the role of ACKR2 in psoriasiform pathology *in vivo*
- determine the role of ACKR2 in the development of psoriasiform pathology using the IMQ *in vivo* murine model of psoriasis
- determine whether keratinocyte ACKR2 expression influences the positioning of inflammatory T cells within the skin

3.4 Introduction

Previous studies have shown significant differences in ACKR2 expression between affected psoriatic human skin, and apparently unaffected skin of patients. Specifically, ACKR2 expression is relatively deficient in inflammatory psoriatic plaques but significantly increased in the unaffected (normal looking) skin of the same patients (Singh et al. 2012). However, the role of differential expression of ACKR2 in psoriasis has not previously been explored. Here, it is hypothesised that reduced ACKR2 expression in skin leads to deficient chemokine scavenging, thereby allowing uncontrolled skin inflammation and thus psoriasiform plaque development. In contrast, it is hypothesised that where ACKR2 expression is high, enhanced scavenging of pro-inflammatory chemokines reduces inflammatory cell influx and inflammation.

In order to optimally study psoriasiform inflammation *in vivo,* a model is required that has sufficiently high fidelity to human psoriasis, whilst also enabling the induction of psoriasiform inflammation at discrete skin sites, in an immunocompetent organism. In recent years, the imiquimod mouse model of psoriasis (*IMQ model*) has become a widely used and extensively validated research tool that bears significant similarities to human psoriasis

(van der Fits et al. n.d.; Walter et al. 2013; Ueyama et al. 2014). This model has the added benefit of being inducible in several different mouse strains thus being appropriate for our ACKR2-/- mice that are on a C57BL/6 background. Furthermore, the psoriasiform plaques in the IMQ model can be induced at specific pre-determined sites (Van Belle et al. n.d.), thereby enabling detailed analysis of differences between affected and unaffected skin.

Studies have shown that T-cell migration from the dermis (deeper skin layers) into the epidermis (outer skin layer) is critical for the development of psoriasiform inflammation *in vivo* (Conrad et al. 2007). Thus, development of psoriatic plaques appears to not only depend on the presence of T-cells in whole skin, but also on their precise positioning within skin. Chemokines play a critical role in regulating T-cell migration into skin in psoriasis, as reviewed elsewhere (Lowes et al. 2014). The capacity of ACKR2 for scavenging CC-chemokines (Galliera, Galliera, et al. 2004), would therefore be in keeping with ACKR2 playing an important role in T-cell positioning in the epidermis. Therefore, it was hypothesised that ACKR2 plays a role in determining T-cell localisation in psoriasiform skin inflammation.

ACKR2 in unaffected psoriatic skin is particularly highly expressed in the basal keratinocytes (KC) of the epidermis (Singh et al. 2012). Keratinocytes are the most abundant cells in the epidermis, and the basal KCs form a confluent layer at its base, thus forming an interface between the epidermis and dermis (Nestle, Di Meglio, et al. 2009). As discussed above, T-cell migration from the dermis into the epidermis is critical for plaque development (Conrad et al. 2007). It is also known that CC-chemokines that bind ACKR2, and which attract T-cells (CCL2 and CCL5), are expressed in the psoriatic plaque epidermis (Singh et al. 2012). Here it is hypothesised that ACKR2 expressed in a barrier layer of keratinocytes, acts as a scavenger of CC-chemokines originating in the epidermis. The absence of ACKR2 is predicted to result in enhanced chemokine gradient formation that extends its reach beyond the epidermal KC layer, enabling leukocytes to migrate towards a CC-chemokine gradient that originates in the epidermis. Thus, it is furthermore also hypothesised that ACKR2 expressed in KCs plays a direct

role in regulating T-cell migration, in addition to eventual positioning within tissue.

3.5 Results

3.5.1 A murine model of cutaneous inflammation for studying the *in vivo* role of ACKR2.

The TLR agonist imiquimod (as Aldara™ cream) is conventionally used for the treatment of cutaneous warts and non-melanoma skin cancers in humans (Grillo-Ardila et al. 1996; Geisse et al. 2004). In recent years, imiquimod has been increasingly used for the induction of psoriasiform lesions in mice, where repeat application of topical imiquimod (IMQ) gives rise to skin changes that bear key histopathological and molecular similarities to human psoriasis (Walter et al. 2013; Ueyama et al. 2014). The IMQ model has several benefits for the purposes of the experiments below; 1) it shares important features with human disease, 2) lesions can be induced at specific, pre-determined skin sites, 3) it is well characterised in the literature, 4) it is typically generated in C57BL/6 mice (the same strain into which ACKR2-/- are back-crossed) and 5) it is a model that can be induced in immunocompetent mice, in contrast to many other murine psoriasis models that make use of immunodeficient mice (Boehncke & Boehncke 2005).

In order to study the role of ACKR2 in psoriasiform inflammation *in vivo*, the IMQ model of psoriasiform inflammation (henceforth referred to as the *IMQ model*) was initially established in WT C57BL/6 mice. The methodologies used in these experiments were based on the original publication that first described this model, in which 62.5mg of 5% imiquimod cream (or a specific control cream) was applied to the central shaved back skin of C56BL/6 mice for up to 6 consecutive days (van der Fits et al. 2009). In the experiment below, the same treatment schedule was used as in (van der Fits et al. 2009), but with the treatment area being changed to one flank (detailed in Figure 3.1), unless otherwise indicated. This was in order to enable accurate like-for-like comparisons between treated inflamed skin and control treated contralateral skin.

Whilst previous studies typically rely on changes only on the day of cull in the mouse models of psoriasis (Cai et al. 2011), there was a need to more closely study the dynamics of cutaneous change also during the course of induction of skin inflammation in the experiments below. For this reason, a comprehensive clinical scoring system to quantify the severity of skin changes was developed. The scoring system developed was based, in principle, on the Psoriasis Area Severity Index (PASI), that is widely used both in the clinical and research settings in human psoriasis, to determine the severity of psoriasis and the response to treatment (Fredriksson & Pettersson 1978). The murine psoriasis severity score developed comprised points awarded over three domains; erythema, scaling and skin thickness (detailed in Figure 3.2), which is largely analogous to the human PASI score. Because inflammation in this model was induced at a discrete site, the murine score differed from the human PASI score by not including percentage of body part covered. The criteria for the murine PASI (henceforth referred to as the *modified PASI or mPASI*) were chosen such that they could be performed with relative ease in a moving, non-anaesthetised animal. The mPASI yields a total score from 0 (normal skin) to 12 (most severe inflammation).

In keeping with the work by van der Fits *et al.*, following application of IMQ to the skin, there was a rapid induction of erythema, scaling and skin thickening. Accordingly, the PASI scores in WT C57BL/6 mice treated with IMQ over a 6-day period increased, with the PASI score plateauing at day 6 (Figure 3.3). Inflammation was apparent after only 1 application of IMQ, and reached statistical significance after 2 applications of IMQ (as assessed on day 3). In order to validate the mPASI against objective histopathological changes in skin, the mPASI scores were correlated with mean epidermal thickness and the degree of basal epidermal proliferation in the mice, as assessed by Ki67 staining (*details on histopathological analysis below*). There was a positive and significant correlation between the mPASI score at the time of cull with both epidermal thickness and hyperproliferation, which are both key features of human psoriasiform skin inflammation (Figure 3.4) (Di Meglio et al. 2014).

Together, these results demonstrate that 1) psoriasiform inflammation was successfully induced in C57BL/6 mice using IMQ, 2) qualitative clinical assessment of psoriasiform skin changes could be quantified during the course of IMQ application using the mPASI and 3) the newly developed mPASI correlated significantly with key clinically relevant histopathological parameters, that typify human psoriasis (Figure 3.4c-d).

3.5.2 ACKR2 expression levels in the IMQ mouse model of psoriasiform inflammation.

ACKR2 expression in human psoriasis is high in unaffected non-lesional skin that is remote from psoriatic plaques. In contrast, ACKR2 expression in psoriatic human plaques is relatively low (Singh et al. 2012). ACKR2 expression patterns in murine psoriasiform inflammation has however not been studied previously. In order to determine whether the ACKR2 expression patterns in the IMQ mouse model parallel those of human psoriasis, IMQ (or vehicle cream) was applied for either 3 or 6 days, with mice culled on day 4 or 7 respectively. ACKR2 mRNA expression was quantified by QPCR of whole skin RNA (Figure 3.5). In keeping with data from human psoriasis, ACKR2 transcript levels were significantly lower in psoriasiform plaques as compared to (non-inflamed) control cream treated contralateral skin. The differences were apparent and statistically significant on day 4, and appeared more pronounced on day 7 in this model. It should be noted however, that whilst ACKR2 is upregulated in human remote unaffected skin, similar upregulation in mouse skin remote from the IMQ-treated site was not observed (Figures 3.5a and 3.5b).

As previously discussed, topical IMQ/Aldara™ appears to induce psoriasiform inflammation through several mechanisms. For example, the excipient isostearic acid that is used to aid solubility in Aldara™ cream, has been shown to be capable of inducing inflammation even in the absence of IMQ (Walter et al. 2013). Hence, in order to determine whether the reduction of ACKR2 observed in IMQ-treated skin was a direct effect of imiquimod and/or due to exposure of the excipients in Aldara™ cream, murine skin explants (epidermis plus dermis) were treated with *pure* imiquimod *in vitro*. Explants were chosen rather than topical application of pure imiquimod as 1) an

Aldara™ equivalent, but isostearic acid free topical preparation is not available and 2) the trauma that would follow any injected imiquimod would likely introduce a confounding variable in the form of skin trauma, that could directly affect ACKR2 expression. Results showed that imiquimod alone was sufficient to significantly reduce ACKR2 transcript expression in murine skin *in vitro*, and that this effect appeared to be dose dependent (Figure 3.6). Additionally, these *in vitro* data demonstrated that IMQ driven ACKR2 downregulation was independent of infiltrating leukocytes and circulating factors e.g. cytokines (Figure 3.6). This finding was in keeping with the effect of IMQ cream on murine skin being, at least in part, driven by imiquimod, rather than another excipient of the IMQ/Aldara™ cream.

3.5.3 ACKR2 expression in remote internal organs in the IMQ mouse model of psoriasiform inflammation.

Whilst ACKR2 expression is elevated in unaffected remote non-lesional skin in patients with psoriasis, it is not known how ACKR2 expression is altered in internal organs *in vivo*. In order to better understand the effect of focal psoriasiform skin inflammation on the expression of ACKR2 in remote tissues, ACKR2 expression levels were determined in lymph nodes, spleen, heart and liver following IMQ induction of psoriasiform inflammation in mice. QPCR data showed that IMQ treatment was associated with a significant (albeit modest) increase in ACKR2 expression in non-draining inguinal lymph nodes (contralateral to the treated flank) on day 4, but the increase on the treated side was not statistically significant (Figure 3.7a). There were no significant differences in ACKR2 transcript levels in lymph nodes on either side on day 7 (Figure 3.7b). IMQ treatment led to visible enlargement of the spleen of mice as previously described (results not quantified) (van der Fits et al. 2009). Furthermore, a significant reduction in ACKR2 mRNA expression was observed in the spleen of IMQ, as compared to control cream treated mice. This was apparent on day 4 and persisted also on day 7 (Figure 3.7). ACKR2 expression was significantly elevated in both the heart and liver of IMQ-treated mice on day 7 (Figure 3.8b), whilst no such differences were observed in on day 4 (Figure 3.8a).

Together these data demonstrated that 1) IMQ induced psoriasiform plaques displayed reduced ACKR2 transcript expression as compared to control treated skin, which mimicked ACKR2 skin expression in human psoriatic plaques, 2) reduced ACKR2 expression in murine skin explants occurred in response to imiquimod, apparently also independently of excipients in Aldara™, at least *in vitro,* 3) IMQ treatment of skin was associated with decreased ACKR expression in the spleen on day 4 and 7, and 4) an increased expression of ACKR2 was observed in the heart and liver on day 7.

3.5.4 Absence of ACKR2 was associated with more severe psoriasiform inflammation in the IMQ mouse model.

To determine the role of ACKR2 in psoriasiform inflammation, ACKR2-/- mice were initially treated with IMQ to determine the basic dynamics of inflammation induction in the absence of ACKR2 (Figure 3.9). In ACKR2-/- mice, IMQ rapidly caused erythema, scaling and skin thickening, with an apparent plateauing of the mPASI score on day 4 (Figure 3.9a). In contrast, control cream treatment of ACKR2-/- did not cause any signs of inflammation in any mice (Figure 3.9a). mPASI scores in this initial experiment were suggestive of more severe inflammation as compared to previous experiments with WT mice at comparable time points (Figure 3.3). In order to confirm whether ACKR2-/- mice develop more severe psoriasiform inflammation, the response of ACKR2-/- and WT mice to IMQ was directly compared side-by-side. To this end, age matched ACKR2-/- and WT C57BL/6 mice were treated concurrently over a 4-day period. IMQ caused significantly more inflammation than control cream in both WT and ACKR2-/- mice, which reached significance from day 3 onwards as quantified by the mPASI (Figure 3.10). Notably, ACKR2-/- mice displayed significantly higher mPASI severity scores compared to WT, which reached statistical significance from day 3 onwards (i.e. after two single applications of IMQ) (Figure 3.10b).

Importantly, the cutaneous application of IMQ is frequently associated with severe systemic features including dehydration, which has been shown to be more severe in C57BL/6 mice as compared to other strains (van der Fits et al. 2009). For this reason, the weights of all treated mice were monitored in the

above experiments. IMQ treatment caused significant weight loss following 1 single application of IMQ, which was more severe in ACKR2-/- mice as compared to WT at all time points (Figure 3.10B). Previous studies suggested mice treated with IMQ lost weight very rapidly and became moribund unless injected with saline (van der Fits et al. 2009). For this reason, mice in all the above experiments were given fruit puree and a soft diet *ad libitum*. No mice became moribund in these experiments, and weight loss was less than 20% of the baseline in all mice (mice with weight loss greater than 20% were to be culled, as per applicable Home Office licences).

In conclusion, the above experiments suggest that psoriasiform skin inflammation was significantly more severe in ACKR2-/- as compared to WT mice, both in terms of skin inflammation and in terms of systemic features as measured by weight loss. These data are in keeping with ACKR2 playing a key role in limiting psoriasiform inflammation *in vivo*. However, it is necessary to repeat these experiments, in order to ensure reproducibility, before firm conclusions can be drawn.

3.5.5 Absence of ACKR2 was associated with enhanced epidermal thickening and basal keratinocyte hyperproliferation.

Next, histological features of ACKR2-/- and WT mouse skin were analysed (both IMQ and control cream treated), to determine any histopathological differences. Previous studies have demonstrated that there are no histological differences between ACKR2-/- and WT mice at rest (Nibbs et al. 2007), and similarly, no differences were observable between ACKR2-/- and WT mice in control cream treated skin in these experiments. However, in skin treated with IMQ, there was significantly increased skin thickening in ACKR2-/- as compared to WT mice (Figure 3.11 and enlarged views in Figure 3.12). Additionally, psoriatic features such as parakeratosis (retention of nuclei in stratum corneum) and hyperkeratosis (thickened stratum corneum) were evident in IMQ treated murine skin, which is in keeping with psoriasiform histological changes having been successfully induced (Figures 3.11 and 3.12). In order to examine the effect of IMQ on basal epidermal cell hyperproliferation (a hallmark of psoriasiform skin changes (Di Meglio et al.

2014)), the skin sections were additionally stained for the proliferation marker Ki67. In ACKR2-/- mice, there was a thicker layer of cells with nuclei staining for Ki67, which is in keeping with hyperproliferation. The differences between ACKR2-/- and WT mice were quantified in terms of epidermal thickness and thickness of the Ki67 positive cell layer, and differences were found to be statistically significant both on day 4 and 7 in this model. (Figures 3.11a and 3.11b) As discussed above, there was furthermore a significant direct correlation between epidermal thickness and thickness of the Ki67 positive basal cell layer, and the mPASI (Figure 3.4).

3.5.6 ACKR2-/- mice demonstrated enhanced CD3+ T-cell positioning in epidermal skin layers in response to topical IMQ.

Psoriasis is considered to be a predominantly T-cell driven inflammatory disorder, and the localisation of T-cells in the skin has previously been shown to be important for plaque development (Conrad et al. 2007). Furthermore, studies have demonstrated a role for ACKR2 in determining tissue localisation of both dendritic cells and macrophages (McKimmie et al. 2013; Lee et al. 2014). However, the role of ACKR2 in determining T-cell localisation in a model of psoriasis, has not been previously elucidated. As the absence of ACKR2 was associated with exaggerated psoriasiform inflammation in the IMQ model above, it was hypothesised that ACKR2, in its capacity as a scavenger of pro-inflammatory chemokines, could determine T-cell localisation within the skin in psoriasiform inflammation. For these reasons, the effect of ACKR2 on CD3+ T-cell localisation was explored in the IMQ model.

There were no differences at baseline between untreated ACKR2-/- and WT mice in terms of CD3+ T-cell numbers/localisation (data not shown). IMQ application to murine skin caused epidermal T-cell entry, which appeared more marked in ACKR2-/- mice as compared to WT (Figure 3.13). The percentage of CD3+ T-cells that localised in the epidermis was quantified, and a significantly higher percentage were localised in the epidermis of ACKR2-/- mice as compared to WT, both at day 4 and day 7 (Figure 3.14a). Additionally, in IMQ treated WT mice (grey bars), the proportion of CD3+ T-cells localised in the epidermis decreased significantly between 4 and 7

days. In contrast, the proportion of CD3+ cells that localised in the epidermis of ACKR2-/- mice (black bars) were maintained between the two time points (Figure 3.14a). To convincingly demonstrate a difference, a comparison of absolute numbers of T-cells, rather than percentages would have been preferable. Accordingly, absolute numbers were recorded in subsequent experiments (Figure 4.13) and show no differences in total skin T-cells, but a clear increase in the proportion of CD3+ localising in the epidermis. This is perhaps to be expected, as previously published studies using the inflammatory phorbol ester TPA, have shown absolute numbers of T-cells in skin are similar in ACKR2-/- and WT, but their distribution within the skin is not (Jamieson et al. 2005). The proximity of CD3+ T-cells to the basement membrane was determined, but the difference between ACKR2-/- and WT was only apparent in the epidermis, rather than throughout all skin layers (Figure 3.14b).

Together, these data supported a role for ACKR2 in determining cutaneous CD3+ T-cell localisation *in vivo,* in the IMQ model of psoriasiform inflammation. Specifically, ACKR2 played a role in determining T-cell entry into the epidermis, which has previously been shown to be critical for the development of psoriatic skin lesions (Conrad et al. 2007).

3.5.7 A novel *in vitro* model of T-cell migration towards a chemokine stimulus.

Whilst the above experiments demonstrated that ACKR2 is important for determining T-cell positioning in psoriasiform skin inflammation, the mechanism by which ACKR2 mediates this effect is unknown. Previous studies have demonstrated that ACKR2 expression is particularly high in basal keratinocytes in the unaffected skin of patients with psoriasis (Singh et al. 2012). This previous observation, coupled with the known CC-chemokine scavenging capacity of ACKR2, led to the hypothesis that high ACKR2 expression in basal epidermal keratinocytes enables such cells to act as a filter for any chemokines produced/released in the epidermis. This could then limit the formation of chemotactic CC-chemokine gradients emanating in the epidermis, and thereby restrict CD3+ T-cell entry in the epidermis. To test this hypothesis in a reductionist manner, a novel migration assay was

developed (Figure 3.15) to study the effect of ACKR2 expression in a barrier layer of keratinocytes (akin to that in the skin basement membrane), on the migration of human T-cells (in the 'dermis') towards a chemotactic chemokine gradient that originates above such a layer (in the 'epidermis').

This new migration assay constituted three layers; an upper chemokine containing layer; a middle layer of ACKR2 expressing stromal cells; and a bottom layer containing activated T-cells. To determine the function of ACKR2 in this system, the middle cell barrier layer was created using cells expressing different levels of ACKR2. Thus, the system recapitulated key aspects of the skin in a cell culture system, with the ACKR2 expressing stromal cells separating an ACKR2 ligand CC-chemokine (in the 'epidermis') and the active human T-cells (in the 'dermis). In this model (summarised in Figure 3.15), human T-cells were isolated, expanded and stimulated *in vitro* from whole blood of healthy donors. T-cells were suspended in a semi-solid bovine skin collagen matrix. Primary human keratinocytes (in which ACKR2 expression could be induced) or other cell types (as indicated in figures) were suspended in a semi-solid skin collagen matrix, and placed on top of the T-cell layer. This was carried out in a manner that enabled the formation of a clear sharp interface between the cell barrier layer and the T-cell layer (Figure 3.16b-c). Once set, a chemokine could be placed on top, the chamber sealed on all sides. Subsequently, a chemotactic gradient could form through the semi-liquid layers, with the keratinocyte layer forming a barrier between the migrating T-cells and the chemotactic stimulus. Using this model system it was possible to determine if ACKR2 in the KC layer could successfully scavenge/eliminate the chemokine, and thereby diminish T-cell migration towards the chemokine. The model recapitulated, in a reductionist manner, T-cell migration from the dermis towards the epidermis.

Through tracking individuals T-cells by means of time-lapse photography, migration patterns of T-cells could be determined in detail (Figures 3.17 and 3.18). Firstly, it was necessary to determine a suitable concentration of chemokine to use that caused directional migration of T-cells towards the chemokine stimulus (Figure 3.19). Although a number of chemokines are upregulated in psoriasis, CCL5 was chosen in these experiments, as it is both

highly expressed in the psoriatic epidermis (Singh et al. 2012), and is also known to bind ACKR2 (Sokol & Luster 2015; Raychaudhuri et al. 1999; Griffith, Sokol & Luster 2014; Mabuchi et al. 2012). A concentration of 160ng CCL5 per ml was found to cause optimal directional migration of T-cells towards the CCL5 layer. The accumulated distance migrated by all analysed T-cells was highest at both 160ng and 640ng CCL5/ml, but migration was only directional at 160ng/ml (Figures 3.19-3.20), though it should be noted that this optimisation experiment was performed once.

3.5.8 A barrier layer of cells expressing ACKR2 regulated T-cell migration towards a chemokine stimulus.

Next, cells that expressed no ACKR2 (HEK293 cells) or very high levels of ACKR2 (ACKR2 transfected HEK293, kindly donated by Dr Kay Hewit) were placed at the interface between the activated ('dermal') T-cell layer and the 'epidermal' chemotactic CCL5 layer. Comparing T-cell migration towards a CCL5 stimulus in the presence of both HEK cell lines was necessary, in order to determine whether ACKR2 expression levels in the interface cell layer could measurably affect T-cell migration.

As hypothesised, where ACKR2 is absent in the barrier layer (HEK293 cells), T-cell migration was significantly directional towards the CCL5 stimulus in experiments that were conducted once (Figure 3.21a), in keeping with the chemotactic gradient forming unhindered past the cell barrier layer separating the chemokine and the T-cells. In contrast, where ACKR2 expression was high (in ACKR2 transfected HEK293 cells) T-cell migration was found to be non-directional (Figure 3.21b). This in turn is suggestive of ACKR2 scavenging of CCL5 by the barrier layer preventing the formation of a chemotactic gradient, and therefore loss of directionality in T-cells.

Next, to better model human skin, the barrier layer was established using primary human keratinocytes (KC) from healthy donors (Figure 3.22), with the total cell volume (Volume = cell number x ($[4/3]\pi r^3$) maintained the same as in experiments with HEKs. This was so as to not inadvertently prevent diffusion of chemokine by a cell layer that was too dense. Cultured healthy KCs have low expression of ACKR2 at rest, but this expression can be substantially upregulated by IFNγ treatment (Singh et al. 2012). Where

ACKR2 expression was relatively low (unstimulated KCs) significant directional migration of activated human T-cells was observed (Figure 3.22a). This would be in keeping with chemotactic CCL5 gradient appeared to have formed freely past the barrier layer of ACKR2-low KCs. However, where ACKR2 expression was high (induced in this case by stimulation with IFNγ), directional T-cell migration was lost (Figure 3.22b). Together, these findings would be in keeping with the hypothesis that a high ACKR2 expressing barrier layer of KCs (as seen at the basal epidermal layers in humans) can prevent the formation of chemokine gradients, and thereby limit T-cell migration into the epidermis. The current approach was employed as it (unlike e.g. transwell systems) enables more qualitative insights into T-cell migration, e.g. directionality. However, it is acknowledged that the above experiments need to be repeated further times, in order to ascertain reproducibility and sensitivity, and in order to provide further quantitative data on the effect that an ACKR2 high/low barrier layer may have on T-cell migration.

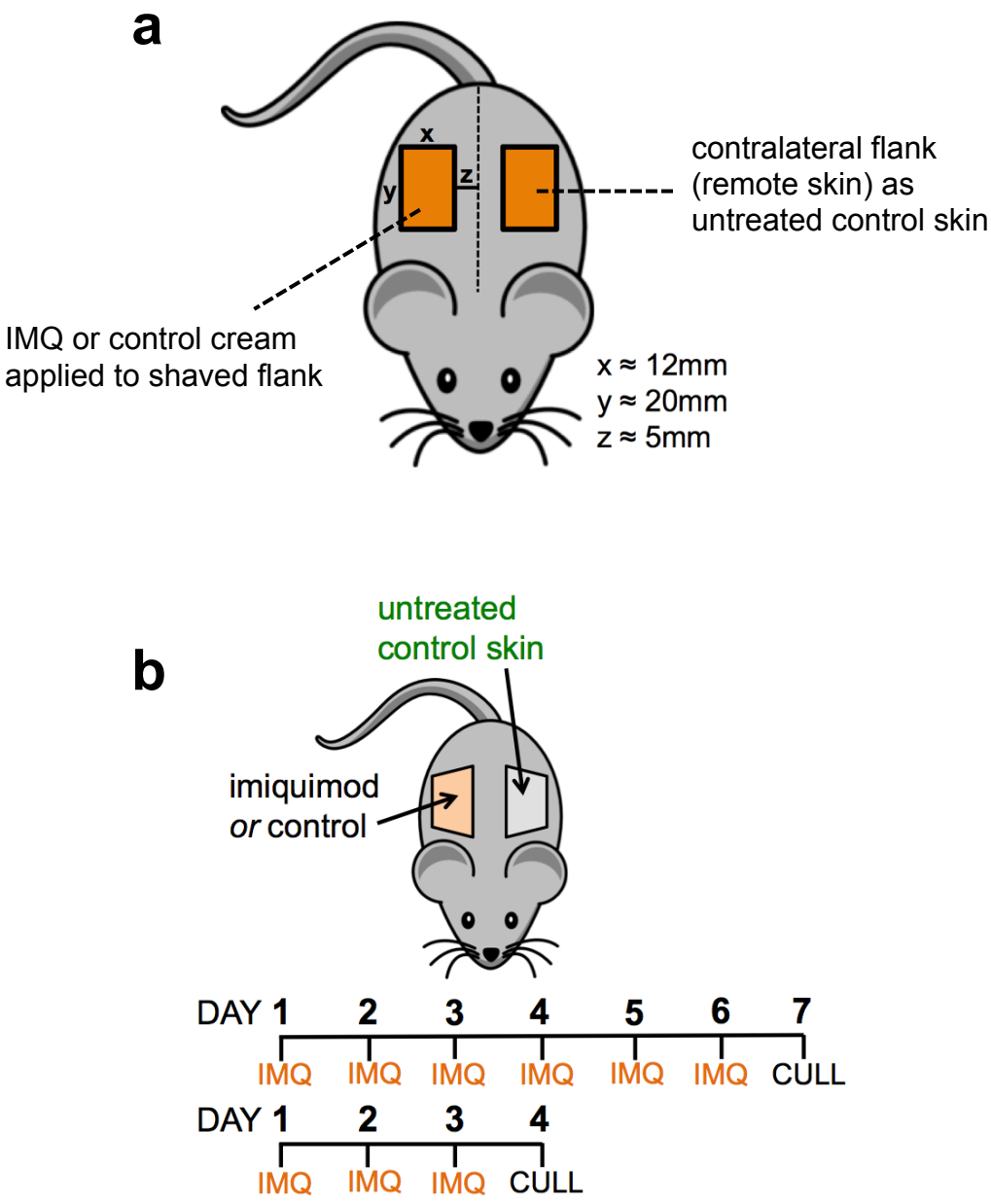

Figure 3.1 Schematic representation of the IMQ mouse model of psoriasiform inflammation.

(a) mice were shaved 1 day prior to the first application of 5% imiquimod (Aldara™) cream, or control cream (Fagron™ Lanette cream with 20% Vaseline), onto each shaved skin site as per the diagram.

(b) topical treatment was applied to one flank daily for 3 or 6 consecutive days, with cull on day 4 or 7 respectively. Contralateral flank skin acted as untreated control skin in both IMQ and control cream groups.

parameter	score	criteria	notes
erythema	0	normal	
	1	pink	
	2	red	
	3	dark red	
	4	very dark red (changing to purple)	
scaling	0	normal	
	1	fine scale covering part of the lesion	Scales <0.5mm, covering <50% of lesion
	2	fine scaling covering most of the lesion	Scales <0.5mm, covering ≥50% of lesion
	3	rough scaling covering most of the lesion	Scales ≥0.5mm, covering ≥50% of lesion
	4	very rough, thick scaling covering most of the lesion	Scales ≥1mm (or, several layers of scale), covering ≥50% of lesion
skin thickness	0	normal	
	1	some ridging of skin but dependent on posture	ridging, but not apparent when mouse walking
	2	some ridging of skin noticeable when moving	
	3	ridging is as deep as it is wide and noticeable when moving	
	4	very deep ridging noticeable when skin is stretched	ridging apparent also upon manual stretching using digits
total possible score	**12**	sum of all parameters	

Figure 3.2 Details of the modified PASI used to quantify the severity of psoriasiform pathology in murine skin.

The modified PASI was used to quantify psoriasiform inflammation on mouse skin on a daily basis. The score is carried out over 3 parameters, yielding a total score of 0 (no inflammation) to 12 (most severe inflammation), as per the criteria detailed.

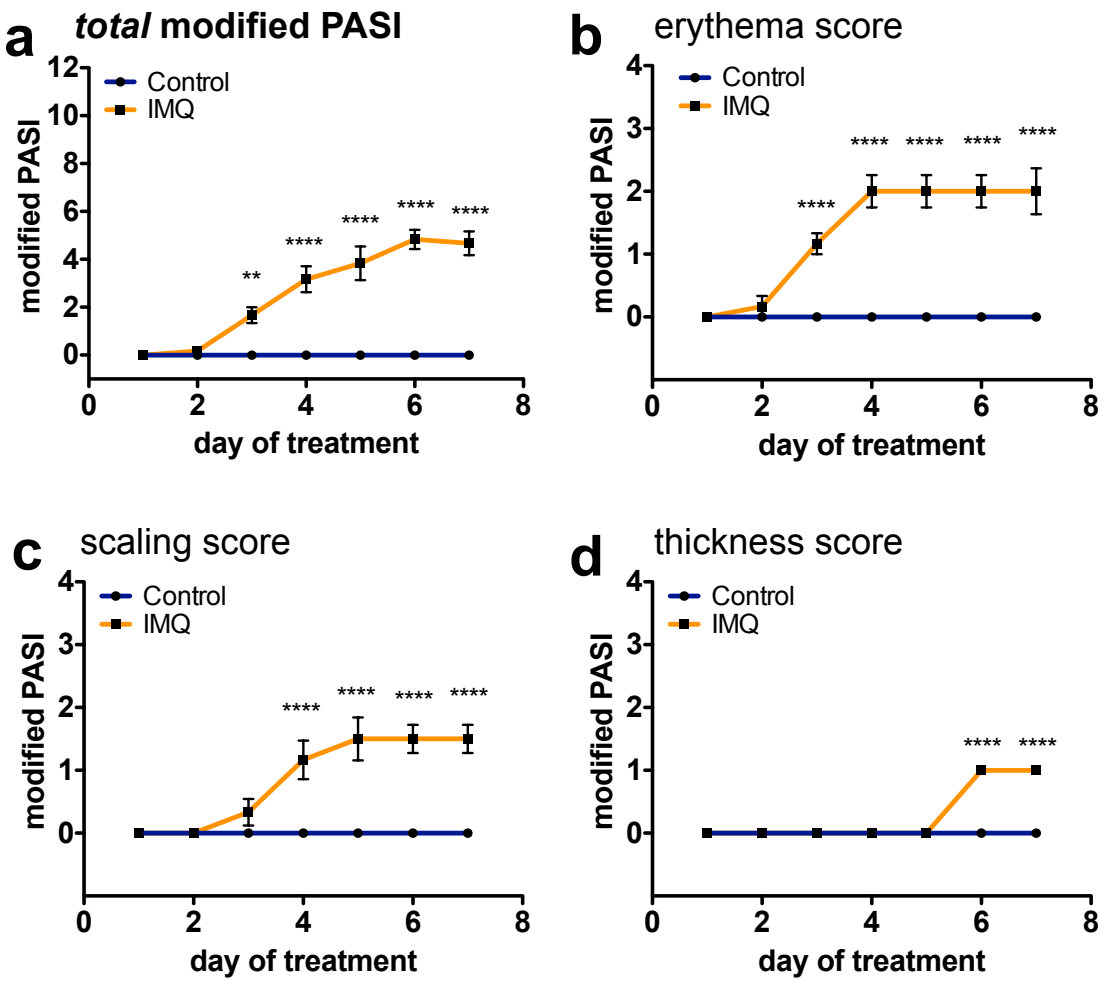

Figure 3.3 Modified PASI in wild-type mice treated with imiquimod cream.

(a) Modified total PASI, across all parameter, in wild-type C57BL/6 mice treated with IMQ (dark blue line) or control cream (orange line) on one flank. n=6 mice per group.

(b-d) modified PASI score for separate parameters the sum of which constituted the total PASI (erythema, scaling and thickness)

Data are mean±SEM, statistical analysis is two-way ANOVA with repeated measures with Bonferroni post-test. * $P<0.05$, ** $P<0.01$, *** $P<0.005$, **** $P<0.001$. Data representative of two comparable experiments.

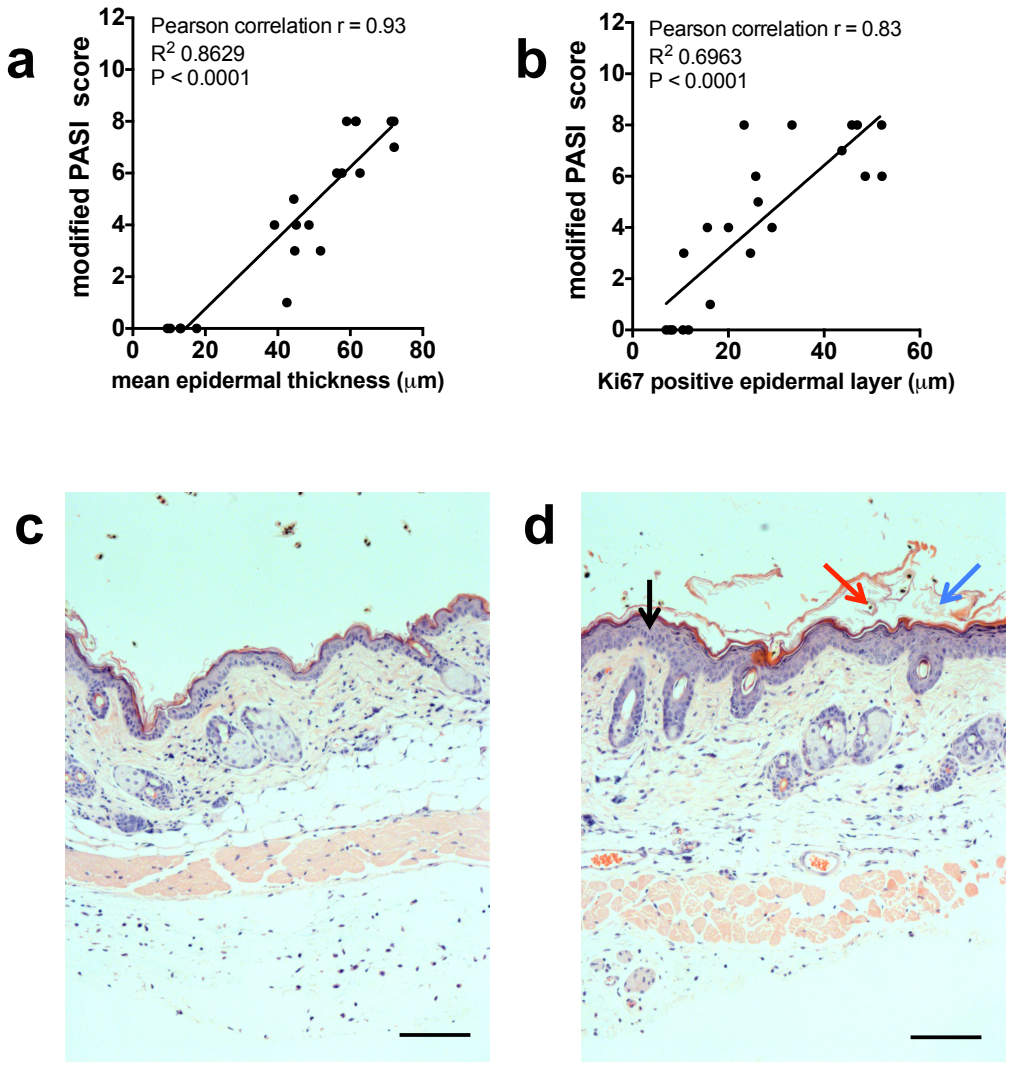

Figure 3.4 Correlation between modified PASI and histopathological changes, and psoriasiform changes in WT mice with imiquimod cream.

(a) Correlation plot between severity of skin inflammation (modified PASI) and epidermal thickness of treated skin, in IMQ treated WT mice.

(b) Correlation plot between severity of skin inflammation (modified PASI) and thickness of Ki67 positive basal keratinocyte layer (thickness between the basement membrane to uppermost Ki67 positive cell), in IMQ treated WT mice.

(c) Wild-type mouse skin treated with control cream and;

(d) Wild-type mouse skin treated with imiquimod cream for 3 days before day of cull, stained with H&E, demonstrating psoriasiform changes including; (black arrow) epidermal thickening, (red arrow) parakeratosis; retention of nuclei in stratum corneum and (blue arrow) hyperkeratosis. Scale bars 100μm.

Data for (a) and (b) are derived from separate experiments.

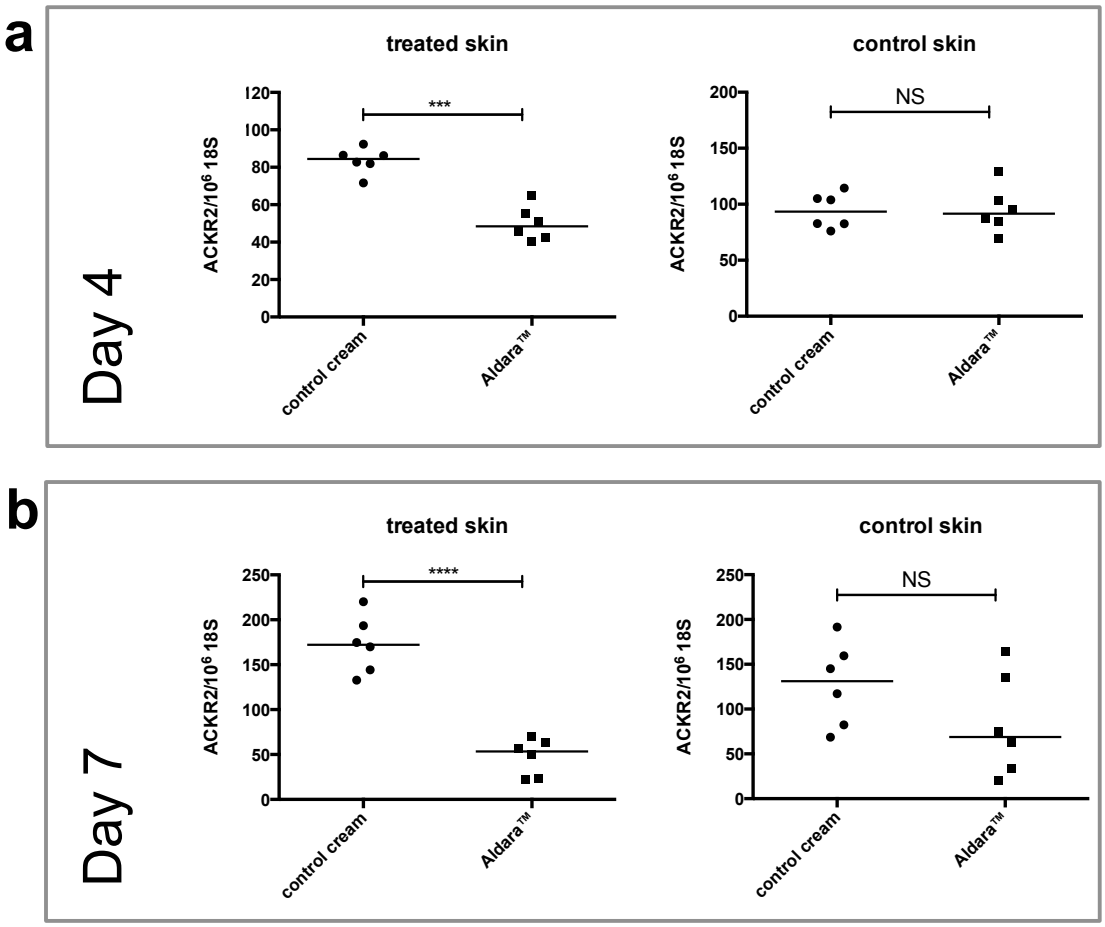

Figure 3.5 Effect of topical IMQ treatment on ACKR2 expression *in vivo*.

(a) Absolute ACKR2 mRNA expression normalised to 18S in flank skin treated with topical IMQ or control cream **(treated)** and contralateral untreated control flank skin **(control skin)**, in mice treated for 3 days and culled on day 4.

(b) Absolute ACKR2 mRNA expression normalised to 18S in flank skin treated with topical IMQ or control cream **(treated skin)** and contralateral untreated control flank skin **(control skin)**, in mice treated for 6 days and culled on day 7.

Line indicates mean, statistical analysis is Student's t-test. * $P<0.05$, ** $P<0.01$, *** $P<0.005$, **** $P<0.0001$. Each time point performed once.

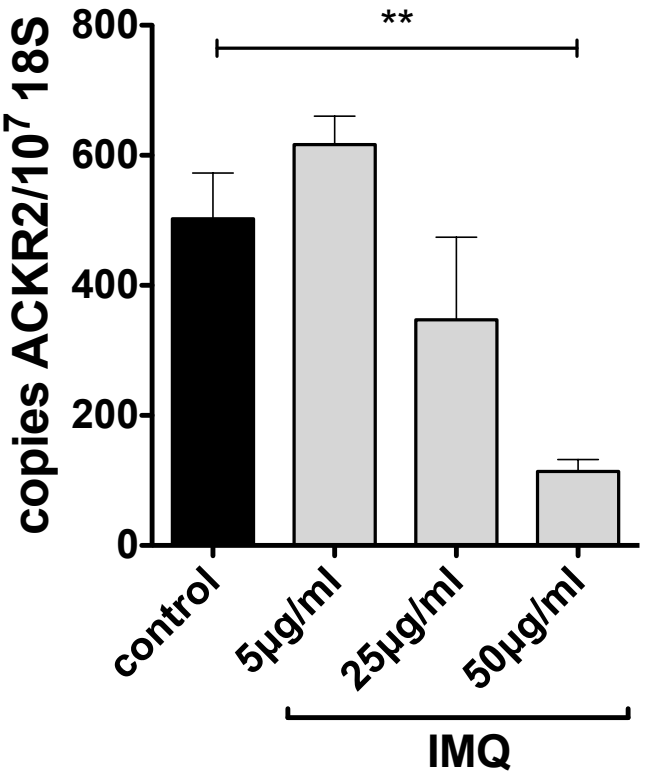

Figure 3.6 Treatment of explanted WT mouse skin with pure imiquimod *in vitro*.

Absolute ACKR2 mRNA expression normalised to 18S in murine skin incubated in the presence of increasing concentrations of imiquimod for 24 hours. Data are mean±SEM, 6 explants per group, statistical analysis is one-way ANOVA. ** $P<0.01$. Data from one experiment.

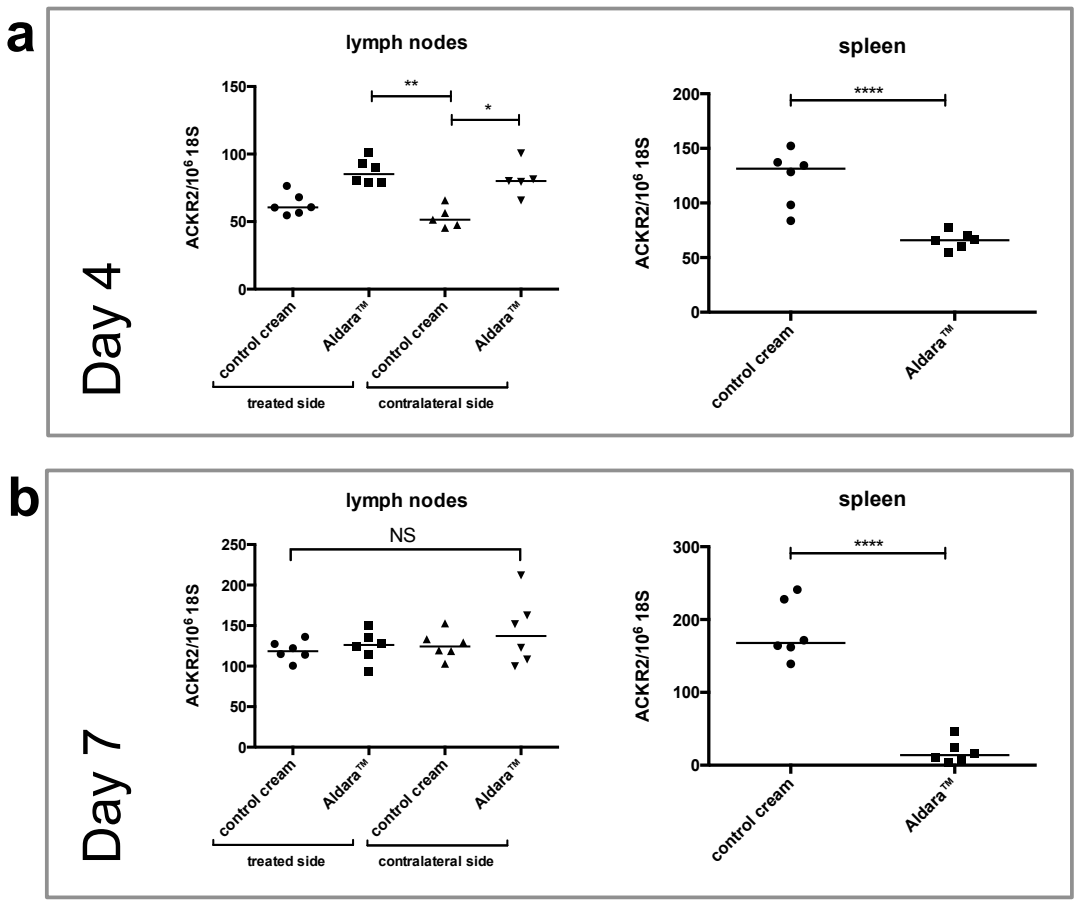

Figure 3.7 Effect of topical IMQ treatment on ACKR2 expression in inguinal lymph nodes and spleen.

(a) Absolute ACKR2 mRNA expression normalised to 18S in inguinal lymph nodes (draining/treated and contralateral nodes), where flank was treated topical IMQ or control cream and spleen. Mice treated for 3 days and culled on day 4.

(b) Absolute ACKR2 mRNA expression normalised to 18S inguinal lymph nodes (draining/treated and contralateral nodes), where flank was treated with topical IMQ or control cream and spleen. Mice treated for 6 days and culled on day 7.

Line indicates mean, statistical analysis is one-way ANOVA (left hand graphs) and Student's t-test (right hand graphs). * $P<0.05$, ** $P<0.01$, *** $P<0.005$, **** $P<0.0001$. Each time point performed once.

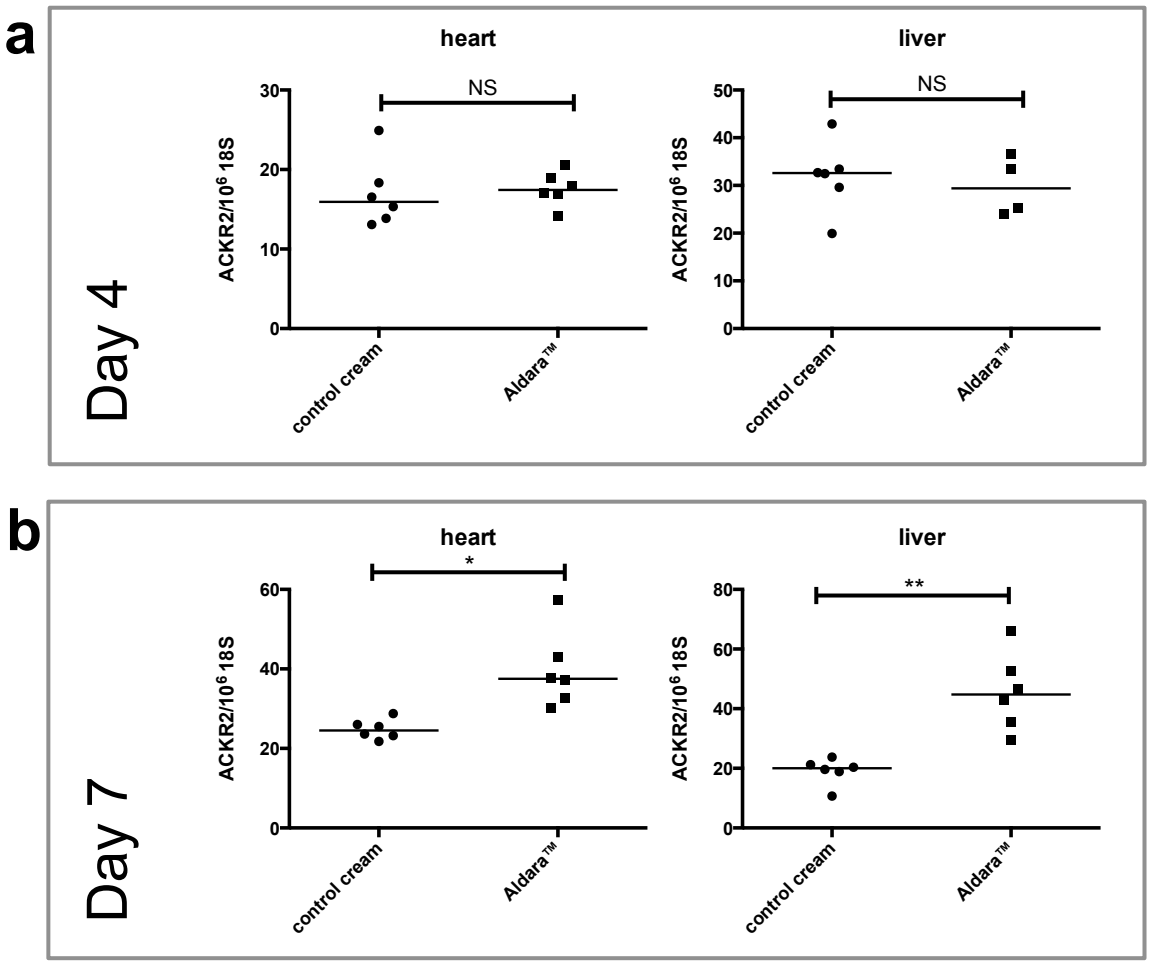

Figure 3.8 Effect of topical IMQ treatment on ACKR2 expression the heart and liver.

(a) Absolute ACKR2 mRNA expression normalised to 18S in the heart where flank was treated with topical IMQ or control cream and in liver. Mice treated for 3 days and culled on day 4.

(b) Absolute ACKR2 mRNA expression normalised to 18S in the heart where flank was treated topical IMQ or control cream and in liver. Mice treated for 6 days and culled on day 7.

Line indicates mean, statistical analysis is Student's t-test. * $P<0.05$, ** $P<0.01$, *** $P<0.005$, **** $P<0.0001$. Each time point performed once.

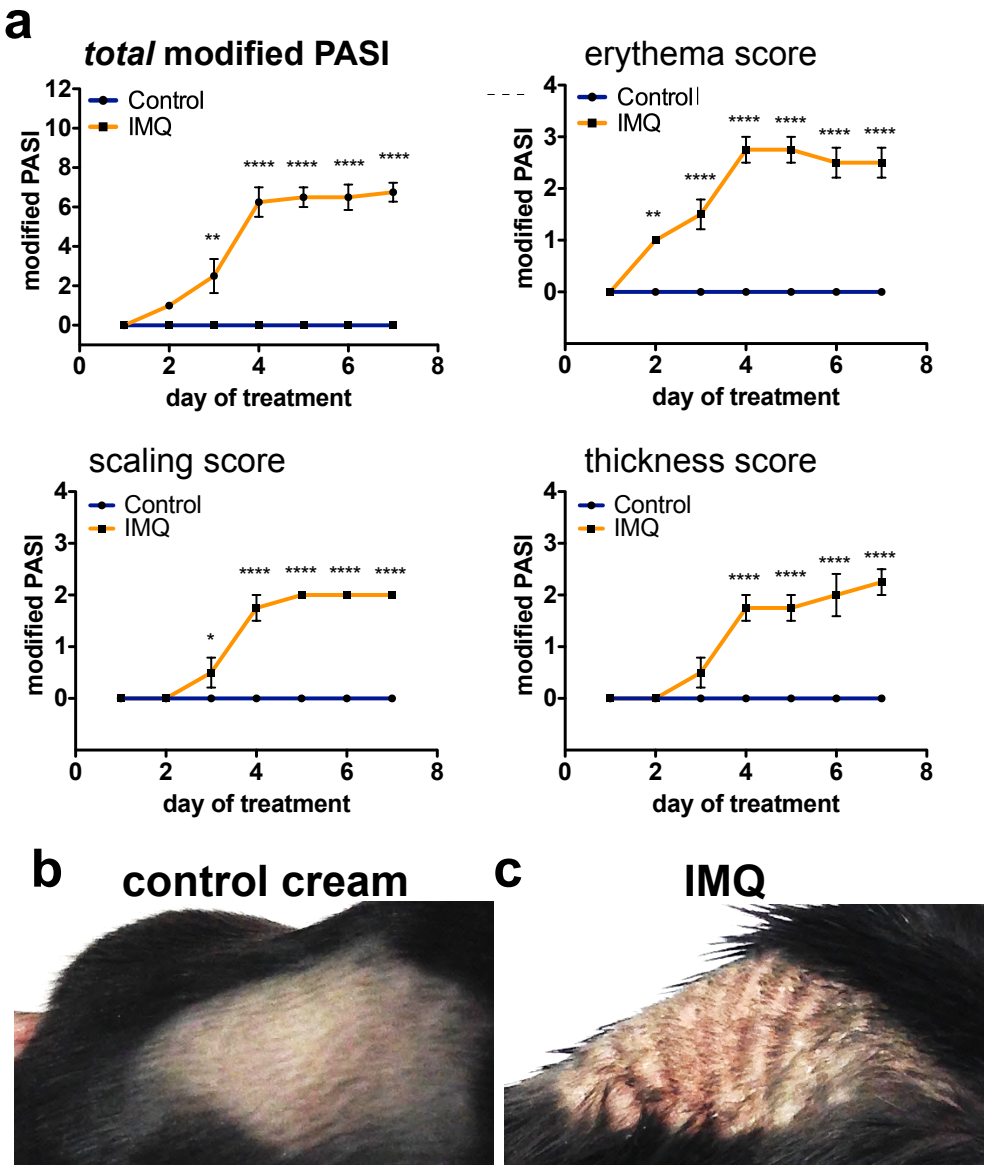

Figure 3.9 Modified PASI in ACKR2-/- mice treated with imiquimod.

(a) Modified total PASI, across all parameter, in ACKR2-/- mice treated with IMQ (orange line) or control cream (dark blue line) on one flank. n=4/3 in IMQ/control group respectively, and modified PASI score for separate parameters that constitute the total PASI (erythema, scaling and thickness)

(b) Representative images of murine flank after 6 days treatment with control cream (pre-cull on day 7).

(c) Representative image of murine flank after 6 days treatment with IMQ (pre-cull on day 7).

Data are mean±SEM, statistical analysis is two-way ANOVA with repeated measures with Bonferroni post-test. * $P<0.05$, ** $P<0.01$, *** $P<0.005$, **** $P<0.0001$. Data representative of two comparable experiments.

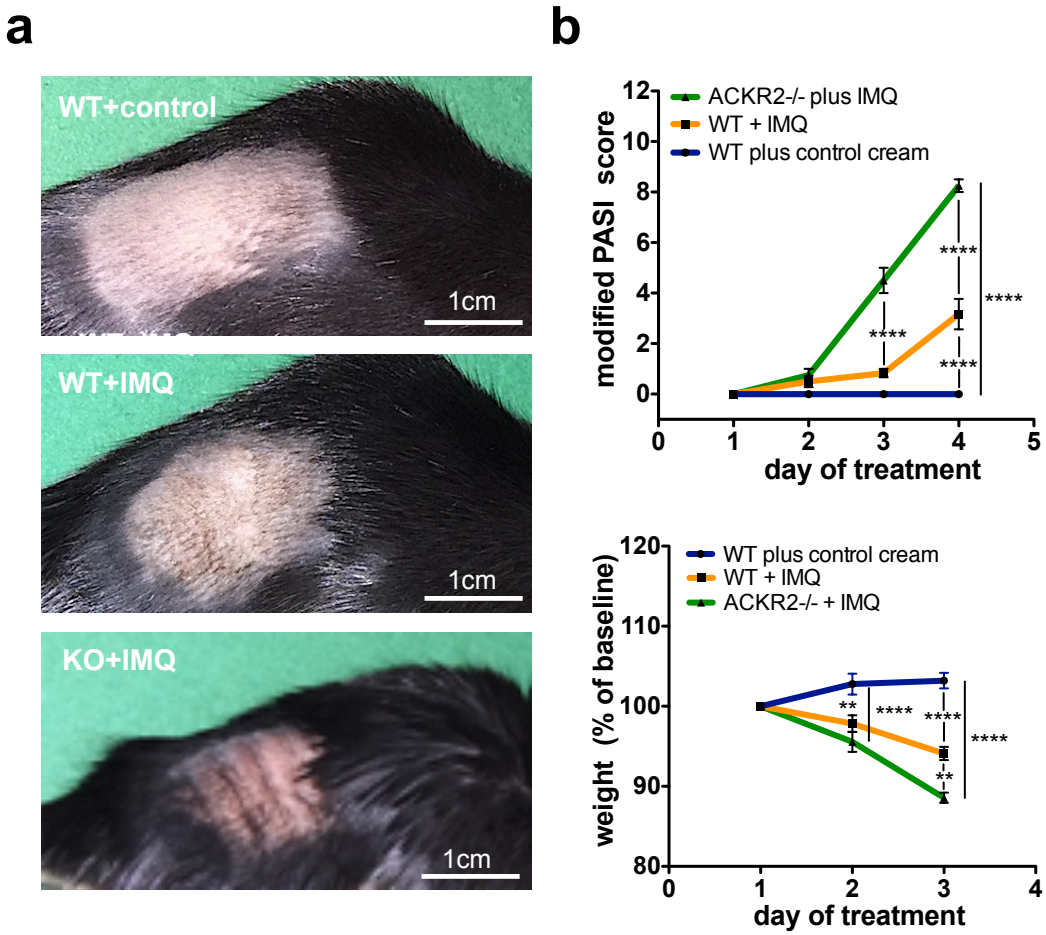

Figure 3.10 Exaggerated psoriasiform inflammation in IMQ treated ACKR2-/- mice.

(a) Images of wild-type (WT) mice treated for 3 days with control cream, IMQ and ACKR2-deficient mice similarly treated with IMQ. Mice were culled on day 4.

(b) **(top graph)** Skin inflammation severity (modified PASI) (3 groups, $n \geq 4$ in each group). **(bottom graph)** Weight change compared to baseline (100%) throughout the treatments.

Data are mean±SEM, statistical analysis is two-way ANOVA, Tukey's multiple comparisons test). Data are representative of two similar experiments. * $P<0.05$, ** $P<0.01$, *** $P<0.005$, **** $P<0.0001$. Experiment performed once.

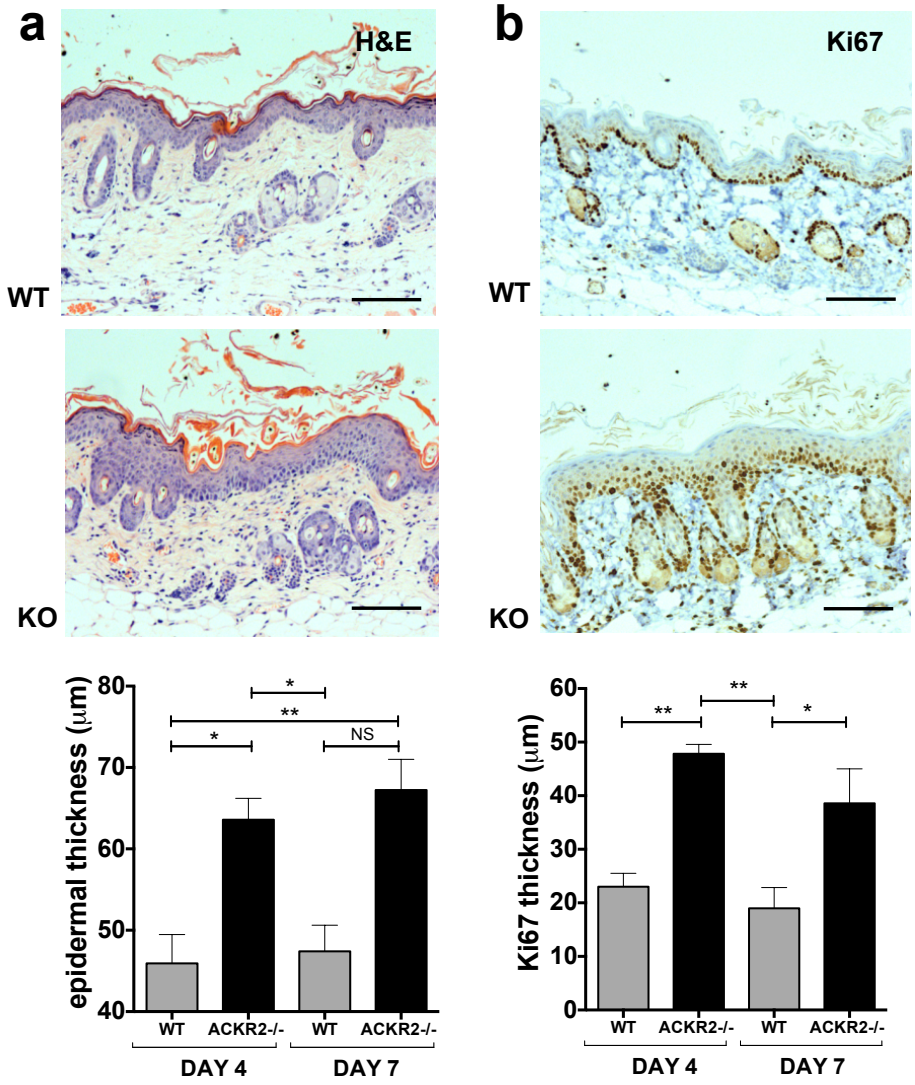

Figure 3.11 Exaggerated psoriasiform pathology in IMQ treated ACKR2-/- mice.

(a) **(histology)** H&E stains of WT and ACKR2-deficient (KO) skin after 3 days of IMQ treatment. **(graph)** Quantification of epidermal thickness on day of cull after 3 or 6 days of daily topical IMQ at x100 magnification. (all scale bars: 100μm; Statistics: one-way ANOVA).

(b) **(histology)** Ki67 stain of the epidermis of WT and ACKR2-deficient (KO) skin after 3 days of IMQ treatment. **(graph)** Quantification of the thickness of the Ki67 staining in the epidermal layer (x100 magnification). Ki67 staining is a measure of cellular proliferation and the data presented report the extent of Ki67 positivity, as demonstrated by the thickness of the Ki67 positive basal keratinocyte layer. Counter-stained with toluidine blue.

All scale bars: 100μm. For the quantitative data in B and C, thickness of 1) the epidermal layer (basement membrane up to, but not including, stratum corneum) and 2) the thickness of the Ki67 positive keratinocyte basal layer (basement membrane to uppermost cell membrane of last Ki67 positive cell) was measured across 9 sites, from 3 separate sections from each skin sample, from each mouse (n=6). Each time point performed once.

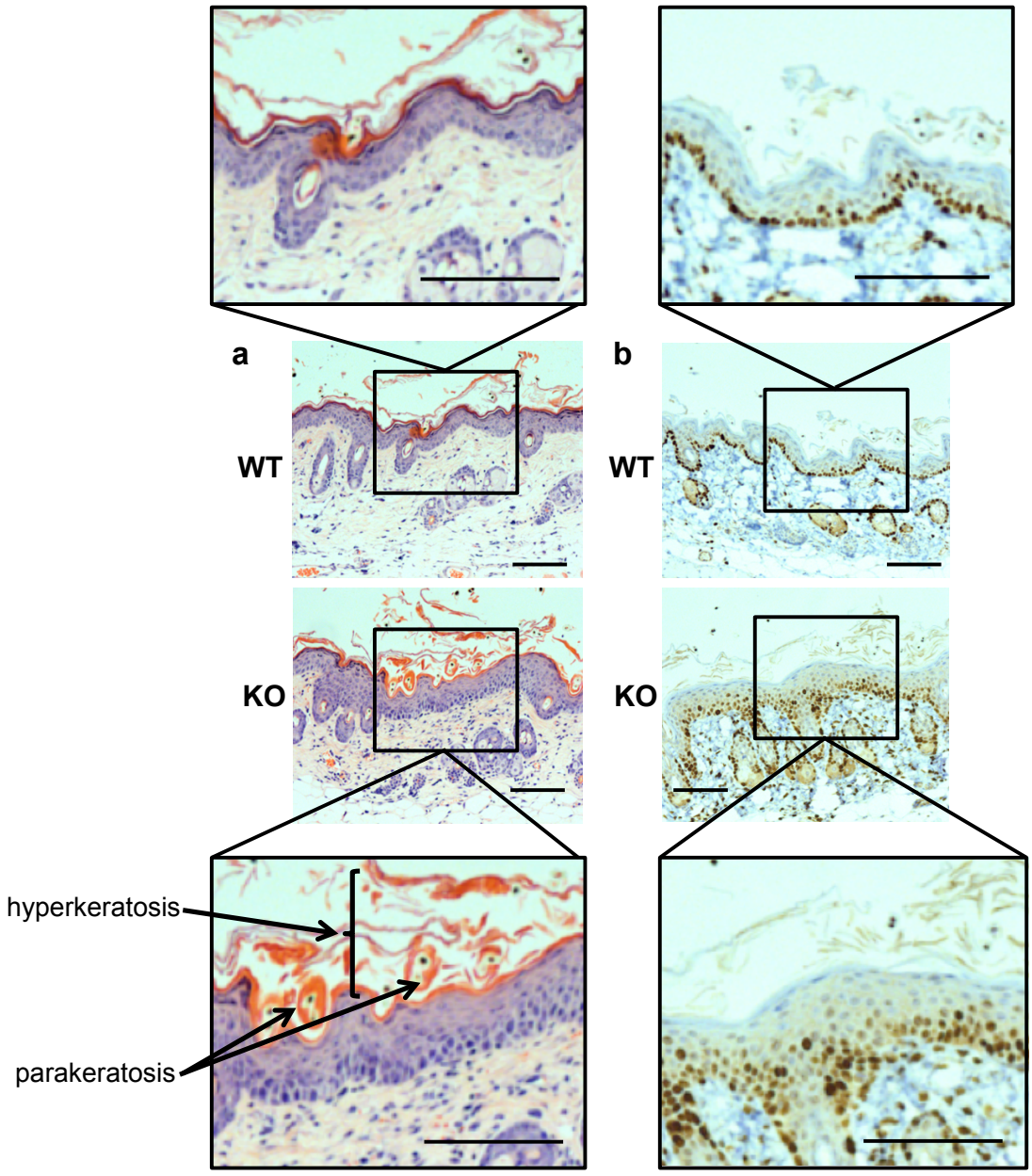

Figure 3.12 Exaggerated psoriasiform pathology in IMQ treated ACKR2-/- mice; enlarged views of representative sections.

(a) H&E stains of WT and ACKR2-deficient (KO) skin after 3 days of IMQ treatment; x100 magnification for centre images (all scale bars: 100μm). Arrows point to examples of hyperkeratosis and parakeratosis.

(b) Ki67 stain of the epidermis of WT and ACKR2-deficient (KO) skin after 3 days of IMQ treatment. Counter-stained with toluidine blue. (all scale bars: 100μm). n=6 mice, experiment performed once.

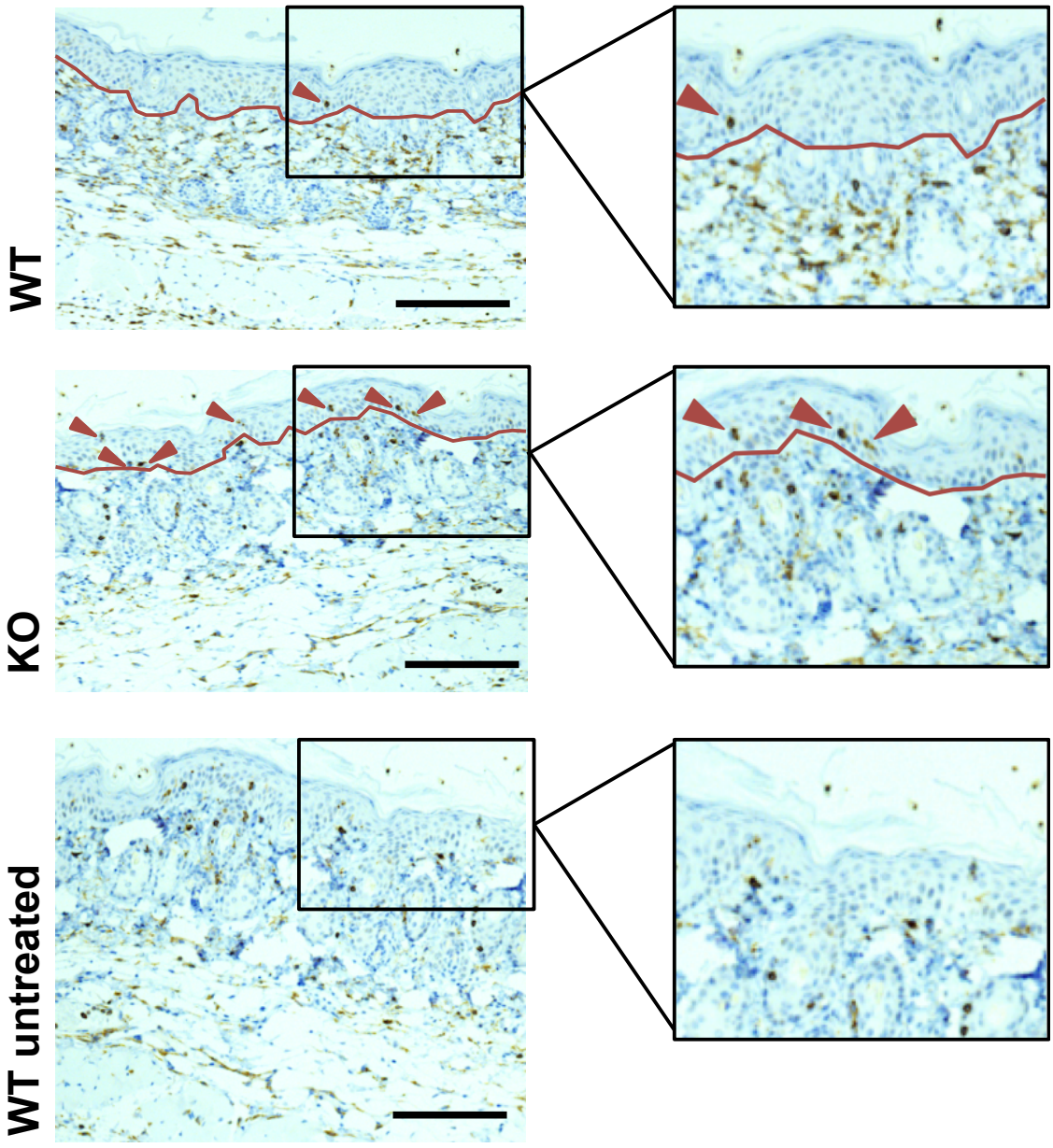

Figure 3.13 CD3+ T-cells in epidermis of ACKR2-/- mice following IMQ treatment; enlarged views of representative sections.

CD3+ staining in WT and ACKR2-deficient (KO) skin after 3 days of IMQ treatment, or control. Red arrows indicate epidermal CD3+ T-cells. The red line represents the dermal-epidermal junction (all scale bars: 100μm). Counter-stained with toluidine blue. n=6 mice, experiment performed once.

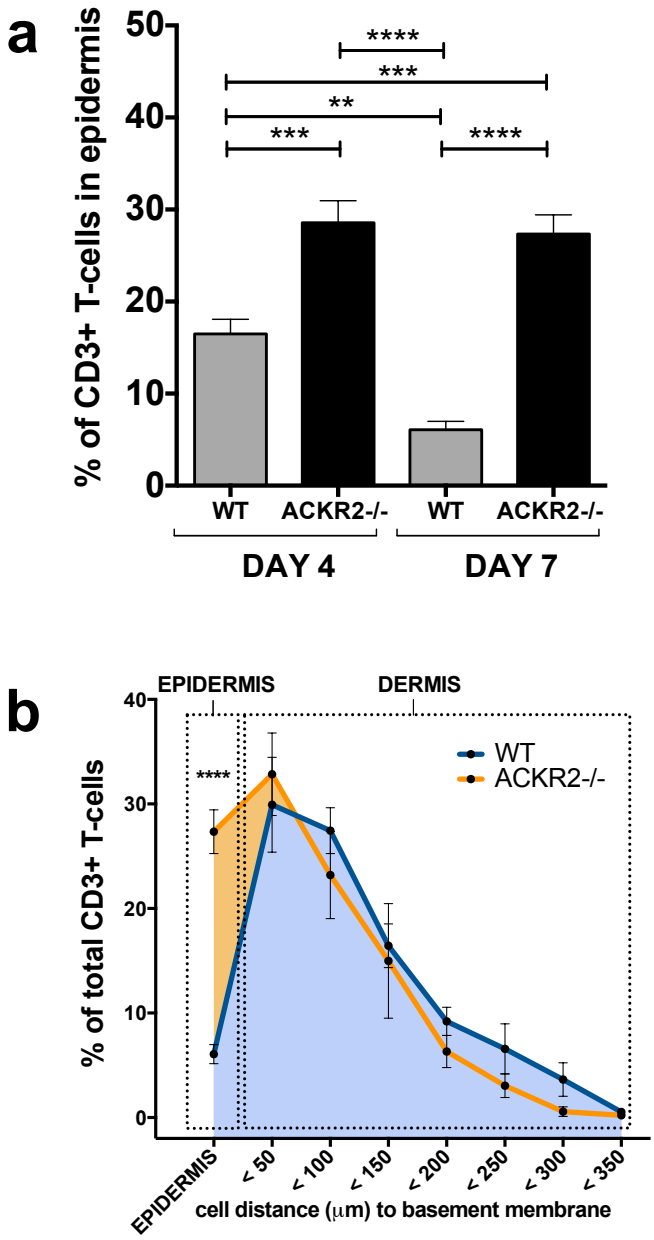

Figure 3.14 Enhanced epidermal CD3+ positioning in ACKR2-/- mice following IMQ treatment.

(a) Epidermal CD3+ T-cell numbers as a percentage of total CD3+ cells in same field-of-view (x200 magnification). Quantification conducted over 9 different sites across three separate sections from each lesion.

(b) CD3+ T-cell distance from the basement membrane (shortest distance T-cell to basement membrane) of WT and ACKR2-deficient epidermis after 3 days of IMQ treatment.

Data are mean±SEM, statistical analysis is two-way ANOVA with Tukey's multiple comparisons test. * $P<0.05$, ** $P<0.01$, *** $P<0.005$, **** $P<0.0001$. Time point performed once.

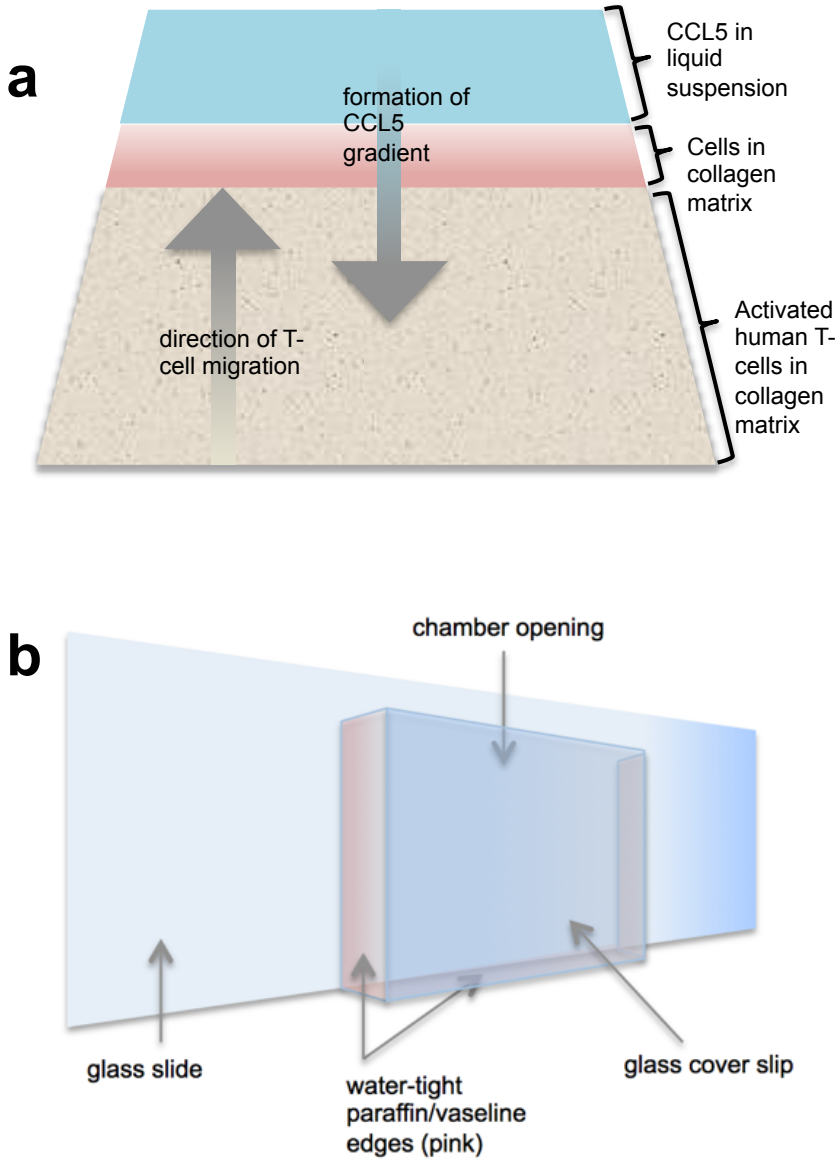

Figure 3.15 Diagram of the design of the novel T-cell migration assay.

(a) Diagram of the novel migration assay. T-cells and primary human keratinocytes (resting or activated) were added as described in the text. CCL5 was selected as a chemotactic stimulus and added to one side of the collagen gel and a gradient allowed to form through diffusion. T-cell migration towards the CCL5 gradient was imaged by time-lapse photography. Note that whilst represented in a sloping or vertical manner in this figure, the migration assays take place in slides mounted in a standard way on the microscope stage. Cellular migration therefore is in a horizontal plane in this assay.

(b) Manufactured slides holding the layers depicted in **(a)**.

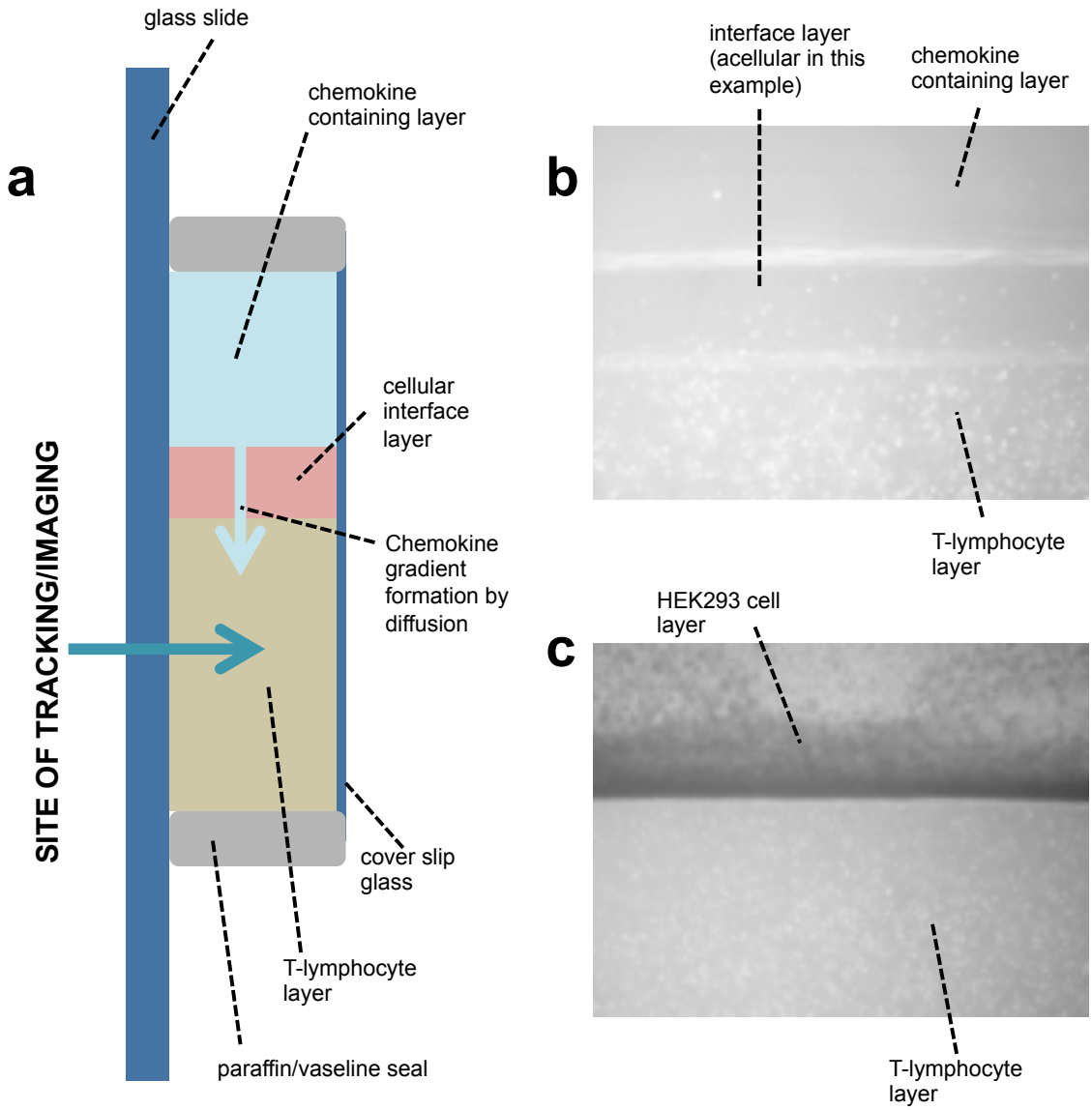

Figure 3.16 Details of the novel T-cell migration assay.

(a) Schematic side view of migration chamber. Cells and chemokines were added as indicated in the text, with the light blue representing the 'epidermis', the pink cell layer the 'basal epidermis' and the brown T-cell layer the 'dermis.

(b) Light microscopy image of completed layers, in order to illustrate that layers remained discrete and effectively separated. The interface layer is acellular in this specific example.

(c) Light microscopy image of completed layers, illustrating the interface between HEK293 cells (used in subsequent migration experiments) and T-cell layer, and the effective formation of a discrete cell barrier layer.

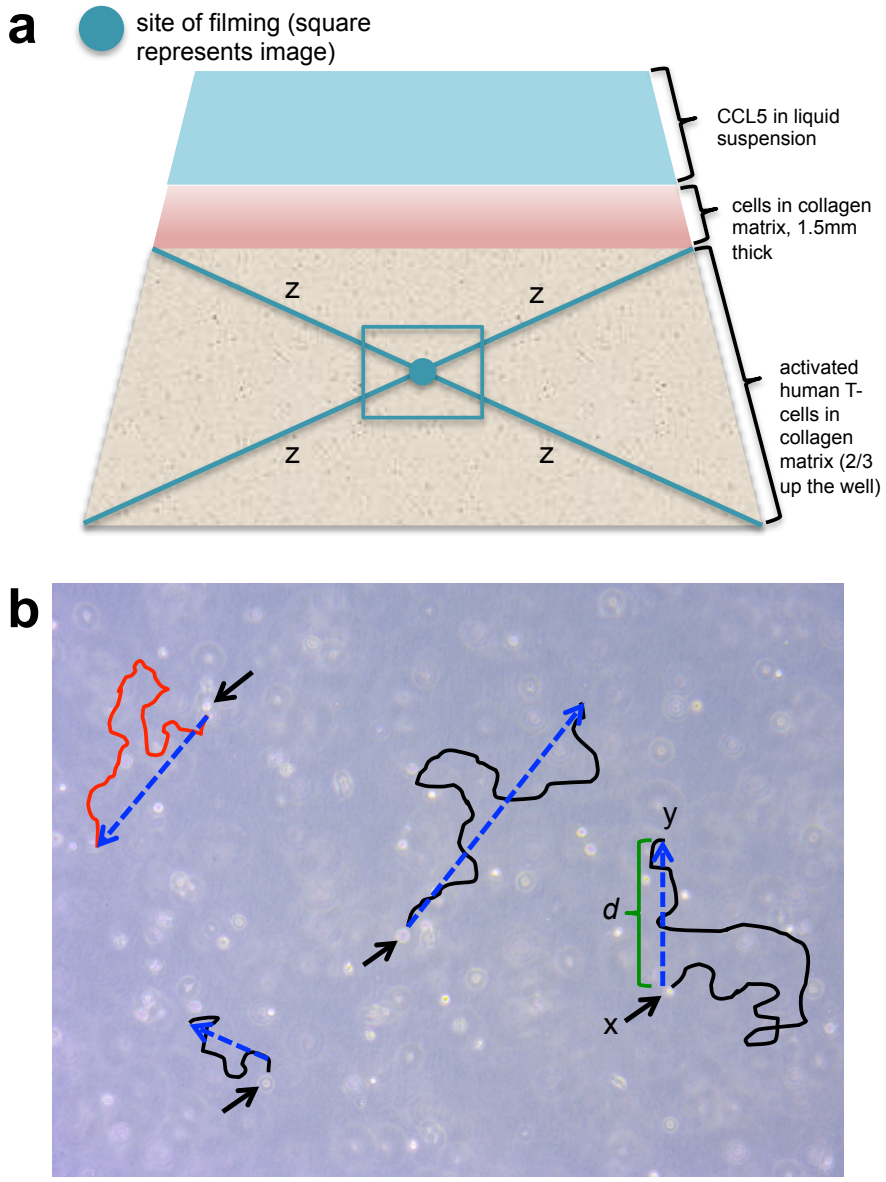

Figure 3.17 Details of the novel T-cell migration assay methodology.

(a) Illustration of the standardised site where image was obtained for time-lapse photography.

(b) In order to reduce selection bias, *all* T-cells in the first field of view were tracked, until no longer within the field of view. Completely non-motile T-cells (if encountered) were excluded, as their viability could not be determined. The tracks were plotted (see Figure 3.18) such that T-cells migrating towards the CCL5 stimulus (superior aspect of image) were marked black, and those migrating away from the stimulus were marked red. In addition to actual migration track, the data analysis software calculated 1) the direction of migration of each cell (blue arrow), 2) the Euclidian distance travelled (denoted *d*, from point x to y).

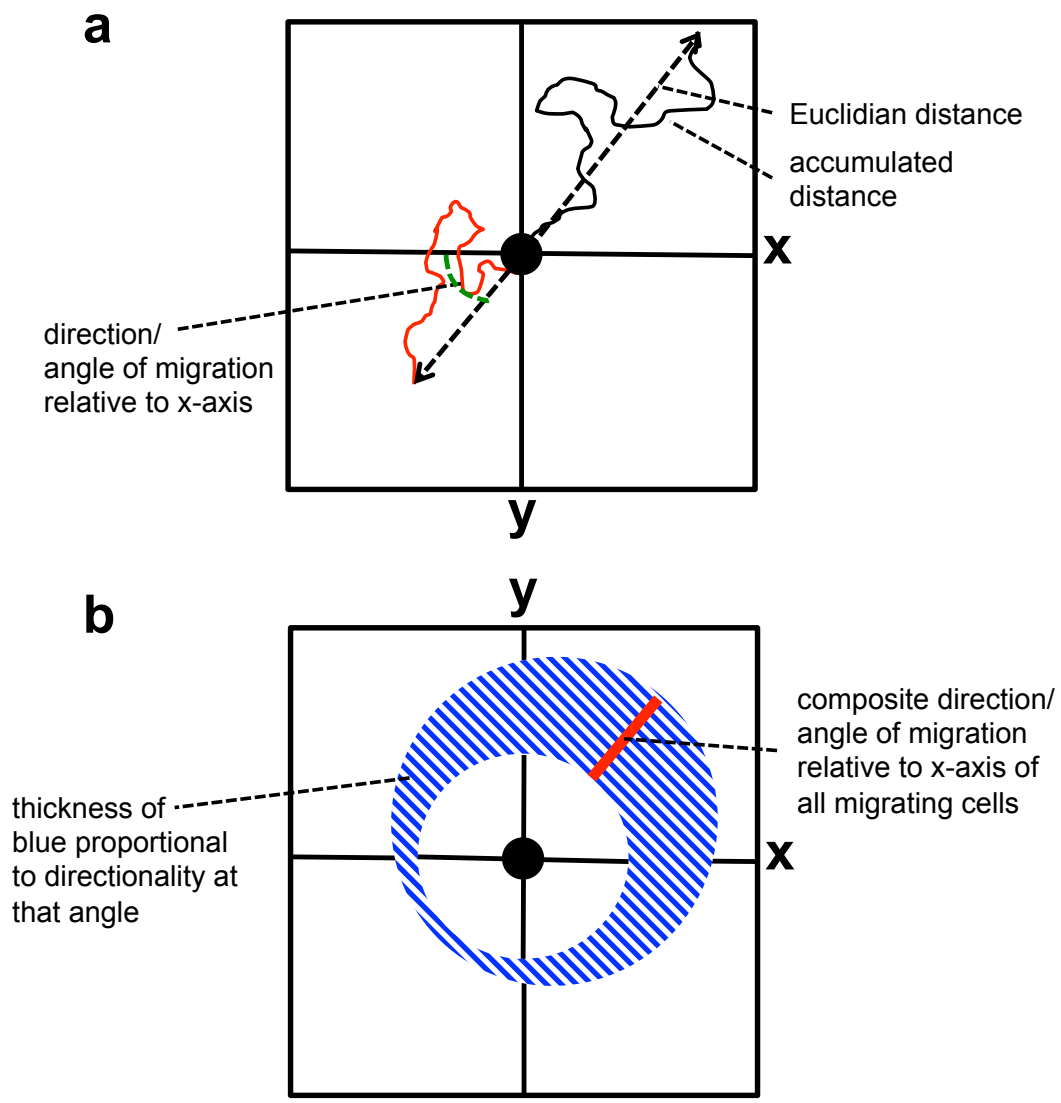

Figure 3.18 Details of the novel T-cell migration assay methodology: schematic examples of migration plots.

(a) Data are presented as a plot of all migration tracks, for each individual T-cell, with that T-cells migrating towards the CCL5 stimulus (superior aspect of image) marked black, and those migrating away from the stimulus marked red.

(b) In addition, quantitative data are also represented as a circle plot, where a red line represents the composite direction of travel of all migratory cells, and the thickness of the blue circle is indicative of the quantity of migration in each direction.

Statistical analysis of migration data is obtained through the Rayleigh test for vector data, where $P<0.05$ indicates that the cell migration is significant in the main direction of migration, as indicated by the red line in the circle plot.

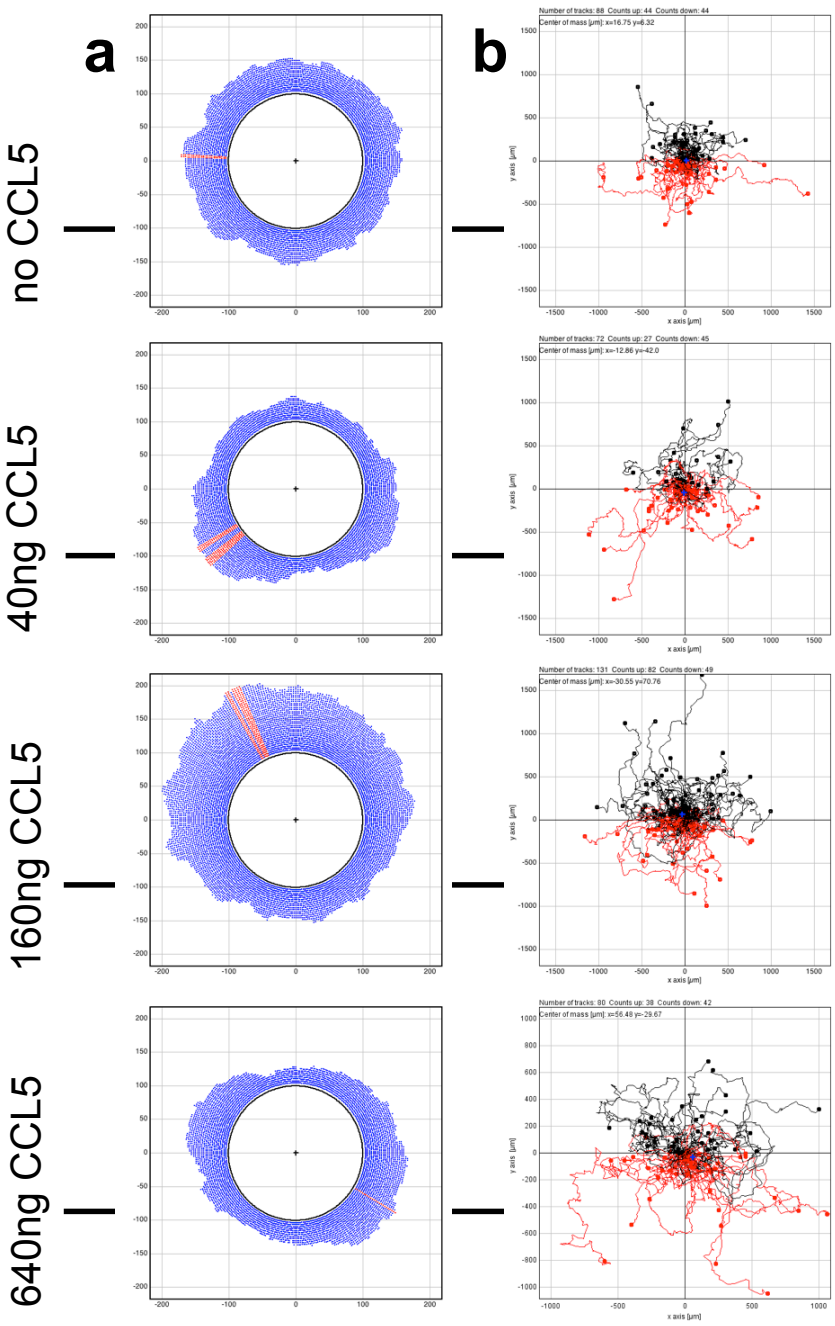

Figure 3.19 Determination of optimal CCL5 concentration for migration assay.

T-cell migration determined (no cellular interface layer) towards CCL5 layer with increasing concentrations of chemokine. Migration is presented as circle plots (column 'a') and as individual migration track plots (column 'b'). Plots on the left of each set represent a composite circle plot of cumulative migration direction. The plot on the right displays individual tracks (*black* = towards CCL5, *red* = away from CCL5). Migration was assessed over 180 minutes, and was performed once at each concentration of CCL5. Data derived from one experiment.

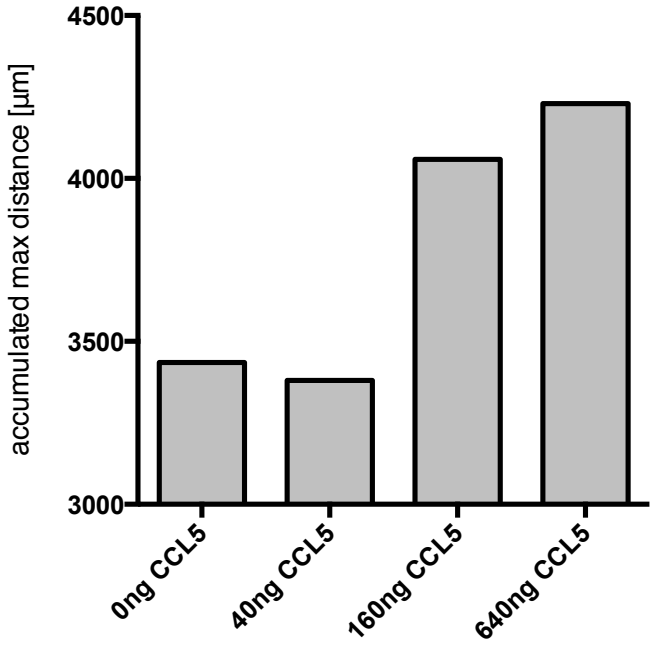

Figure 3.20 Accumulated distance travelled of all T-cells in one field-of-view.

Accumulated T-cell distance travelled (over 180 minutes) in presence of increasing concentrations of CCL5. Data derived form one experiment.

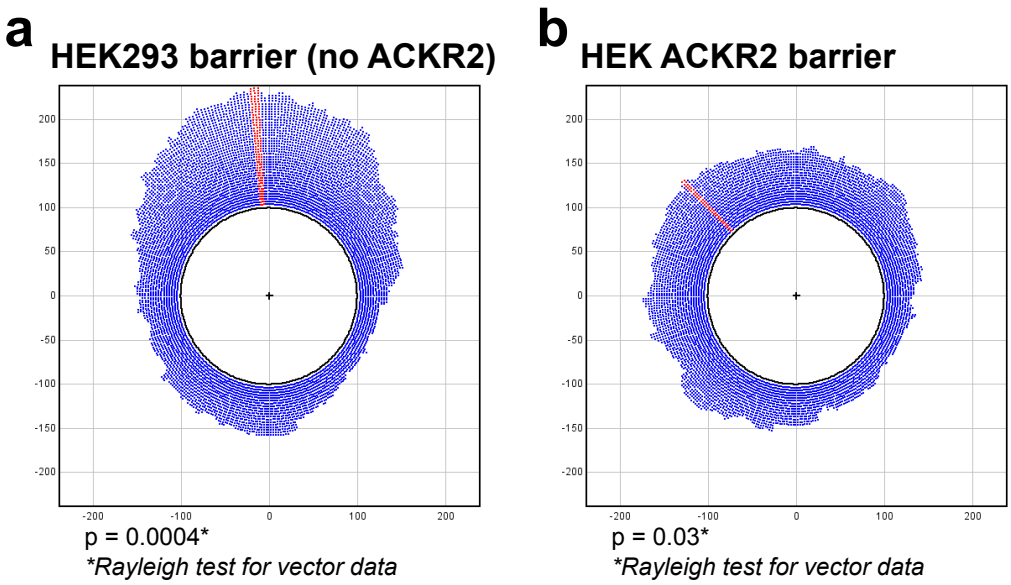

Figure 3.21 Effect of ACKR2 expression in barrier layer on T-cell migration.

(a) Circle migration plots of T-cell migration towards CCL5 chemotactic layer (160ng/ml) with interface layer composed of HEK293 cells (no ACKR2) and;

(b) HEK293 cells transfected with ACKR2 (high ACKR2 expression).

Statistical analysis was the Rayleigh test for vector data, where $P<0.05$ indicates that migration is significantly directional. Migration was assessed over 180 minutes.

Data derived from one experiment.

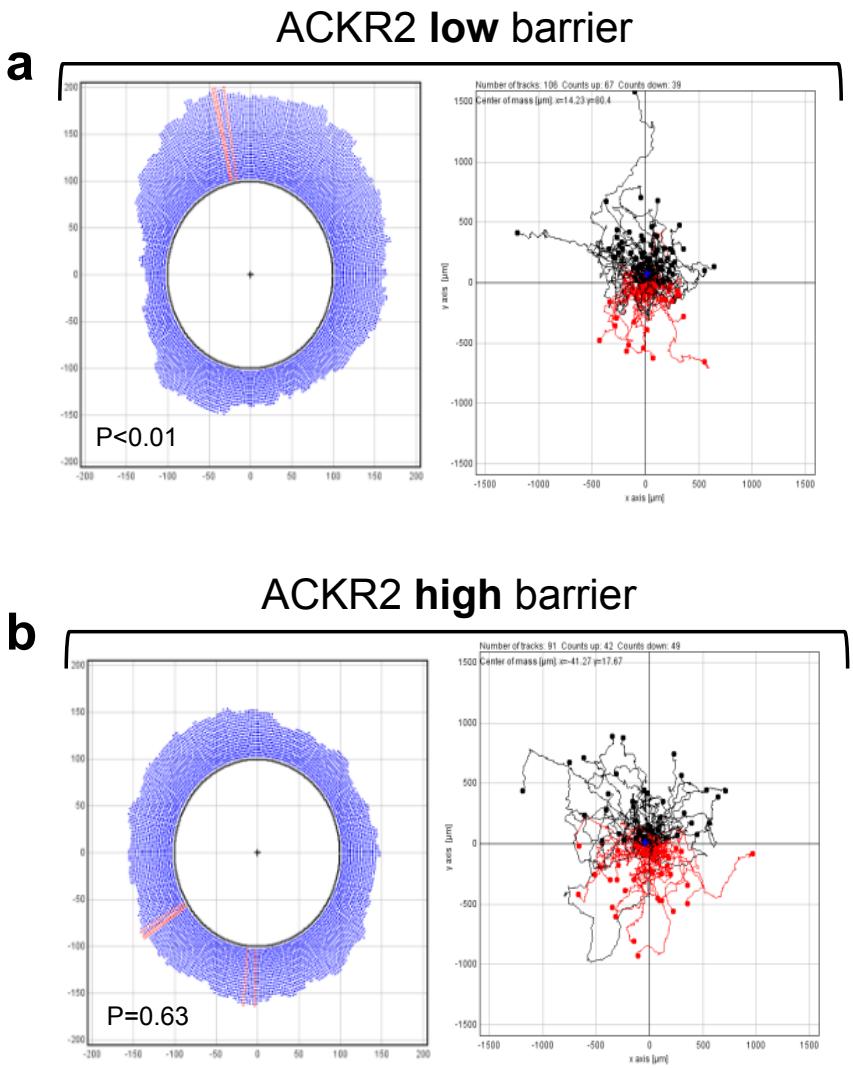

Figure 3.22 Effect of ACKR2 expression in barrier layer of primary human keratinocytes on T-cell migration.

Plots on the left of each set represent a composite circle plot of cumulative migration direction. The plot on the right displays individual tracks (*black* = towards CCL5, *red* = away from CCL5).

(a) T-cell migration towards CCL5 chemotactic layer (160ng/ml) with interface layer composed of non-inflamed low-ACKR2 expressing primary human keratinocytes. 67 cells migrating 'up' towards CCL5, 39 cells migrating 'down' away from CCL5.

(b) T-cell migration towards CCL5 chemotactic layer (160ng/ml) with interface layer composed of IFNγ stimulated high-ACKR2 expressing primary human keratinocytes. 49 cells migrating 'up' towards CCL5, 42 cells migrating 'down' away from CCL5.

Statistical analysis is the Rayleigh test for vector data, where $P<0.05$ indicates that migration is significantly directional. Migration was assessed over 180 minutes. Data derived from one experiment.

3.6 Summary Chapter 3

This chapter reports the development of a murine model of psoriasiform inflammation, which enabled the study of ACKR2 function *in vivo*, and the development and use of a novel T-cell migration assay, which enabled the study of ACKR2 function in disease-relevant cultured cutaneous cells. The well-established imiquimod (IMQ) model of psoriasiform inflammation (van der Fits et al. 2009) in C57BL/6 mice, demonstrated ACKR2 expression changes that are reminiscent of those seen in human psoriasis, with reduced expression of ACKR2 in psoriasiform plaques when compared to untreated skin. This model allowed the induction of psoriasiform lesions at discrete pre-determined sites, which in turn allowed comparisons to be made between inflamed skin and remote control tissues. However, and in contrast to human disease, induction of one psoriatic lesion through focal IMQ application alone, did not lead to an elevated ACKR2 expression in apparently unaffected remote skin. This discrepancy is addressed in detail in a later chapter in this thesis.

This chapter also reported, for the first time, that ACKR2 was essential for the limitation of IMQ-induced psoriasiform skin inflammation *in vivo*. ACKR2-/- mice displayed significantly exaggerated inflammation, increased epidermal thickening and enhanced keratinocyte (KC) proliferation at the basal epidermal layers, when compared to WT mice. These inflammatory changes observed in mice, are all features that typically characterise human psoriatic plaques (Di Meglio et al. 2014). Whether these differences were sustained is not known, due to the limited time frame of the presented experiments. It is possible that differences between ACKR2-/- and WT mice are lost over time, and that the observations are due to altered kinetics of disease induction. Longer-term comparisons between WT and ACKR2-/- mice would be required to determine whether the observed differences are sustained over time. Additionally, a novel murine clinical scoring system was developed, which was shown to significantly correlate with histological markers of psoriasiform skin change, including epidermal thickening and hyperproliferation. This scoring system (termed the modified Psoriasis Area Severity Index, mPASI) was broadly based on the principles of the Psoriasis Area Severity Index that is used in humans, both to guide therapy and in the

research setting (Fredriksson & Pettersson 1978). The mPASI was designed such that a score could be obtained rapidly in moving mice, and enabled close monitoring of the dynamics of skin inflammation, throughout the development of psoriasiform plaques. Further work is required to more comprehensively validate the mPASI in the context of typical anti-psoriatic therapies (e.g. ciclosporin and anti-TNF antibodies), and in order to quantify its sensitivity for detecting change in the degree of cutaneous inflammation in a wider range of contexts.

Psoriasis is increasingly considered to be a systemic condition, associated with excess cardiovascular and hepato-metabolic co-morbidities (Di Meglio et al. 2014; Roberts et al. 2014), whilst previous work on the IMQ model showed an enlargement of the spleen of IMQ treated mice (van der Fits et al. 2009). To determine the effect of focal psoriasiform skin inflammation on remote organs, ACKR2 mRNA expression was quantified in the heart, liver, spleen and skin draining lymph nodes in mice. Results show a significant differential regulation of ACKR2 in all the assessed organs, in response to one focal area of skin inflammation. There was an upregulation of ACKR2 mRNA in the heart and liver, and in contrast, reduced ACKR2 expression in the spleen in the IMQ model. The functional significance of these observations was not explored as part of this thesis, and future studies will need to determine whether this differential regulation in remote organs is sustained, in which cells the upregulation occurs and whether it modulates inflammatory responses in those tissues. Because the spleen mass increased so substantially following IMQ application, it is not possible to say whether this decrease in spleen ACRK2 was due to influx of non-ACKR2 expressing cells (i.e. dilution of ACKR2 signal), or if the decrease represented a decrease in cellular expression.

Psoriasis is a T-cell (notably Th1/Th17) driven condition (Di Meglio et al. 2014). To examine T-cells in this model of psoriasis, murine skin was stained for CD3+ T-cells in order to determine the effect of ACKR2 expression on T-cell positioning. Previous studies have shown that there are no significant differences in cutaneous T cells between ACKR2-/- and WT mice at rest (Jamieson et al. 2005). This chapter showed that CD3+ T-cells infiltrated skin of both ACKR2-/- and WT mice in response to topical IMQ. However, whilst

CD3+ cells were largely excluded from the epidermis in WT mice, in ACKR2-/- mice a large proportion of CD3+ T-cells localised in the epidermis. Indeed, previous studies have shown that psoriasiform inflammation is critically dependent on T-cell migration from the dermis into the epidermis *in vivo* (Conrad et al. 2007), and these new data suggest that ACKR2 plays a role in excluding CD3+ T-cells from the epidermis. This observation may explain the difference in severity of psoriasiform inflammation between ACKR2-/- and WT mice, when treated with IMQ.

The mechanism by which ACKR2 regulates T-cell migration in this context is not well defined, and a novel 3-dimensional *in vitro* model of T-cell migration in skin was thus developed to address this deficiency. By using this model, this chapter reported, that ACKR2 expressed by a primary human keratinocyte layer (as seen in the epidermis) may be capable of regulating migration of active human T-cells towards a chemotactic psoriasis-associated CC-chemokine stimulus. This could possibly be due to ACKR2 scavenging/internalisation/degradation of the CC-chemokine signal (Graham & McKimmie 2006), which could disrupt the formation of a chemotactic gradient, and further experiments are needed to test this hypothesis. The interpretation of the data is limited by the migration experiments having been performed once with HEK cells and once more with keratinocytes, and it would be important to repeat these migration experiments several times, to ensure the finding are reproducible and to provide more quantitative results, before definitive conclusions can be drawn.

Overall, the reported data demonstrated that key human psoriatic ACKR2 patterns could be replicated in mice by using the IMQ model of psoriasiform inflammation. Furthermore, ACKR2 was essential for limiting psoriasiform skin inflammation *in vivo*, and for excluding CD3+ T-cells from the epidermis that in turn are critical for psoriatic plaque development (Conrad et al. 2007). Using a novel *in vitro* T-cell migration assay, data suggest that KC expressed ACKR2 may regulate T-cell migration towards a chemotactic chemokine stimulus, though further repeat experiments are necessary in order to draw firm conclusions. These findings would place ACKR2 in a central position in the regulation of psoriasiform inflammation *in vivo*. However, more work is necessary to understand the significance of ACKR2

differential regulation away from the site of skin inflammation. Additionally, more work is required to understand how ACKR2 might influence the migration of specific leukocyte subsets that play a role in psoriasis pathogenesis.

CHAPTER 4

4 Focal psoriasiform inflammation limits the spread of inflammation to remote tissues *in vivo*, in ACKR2-dependent manner.

4.1 Contents

4.2

Hypotheses

4.3 Aims

4.4 Introduction

4.5 Results

4.5.1 Th1 and Th17 cytokines upregulate ACKR2 expression in skin

4.5.2 IFNγ is the principal T-cell derived cytokine inducer of ACKR2 expression.

4.5.3 IFNγ upregulates cutaneous ACKR2 expression when administered exogenously *in vivo*.

4.5.4 Induced ACKR2 upregulation limits psoriasiform skin inflammation *in vivo*.

4.5.5 IFNγ co-administered with topical IMQ in mice, leads to a remote upregulation of ACKR2.

4.5.6 Remotely upregulated ACKR2 protects against the spread of psoriasiform cutaneous inflammation.

4.6 **Summary Chapter 4**

4.2 Hypotheses

- Psoriasis associated T-cell-derived cytokines regulate ACKR2 expression in primary human keratinocytes
- IFNγ production is deficient in the IMQ model of psoriasiform inflammation
- The lack of remote skin ACKR2 upregulation in the IMQ model is due to a relative deficiency in circulating ACKR2-inducing cytokines.

- The lack of remote skin ACKR2 upregulation in the IMQ model of psoriasiform inflammation can be overcome by administering specific psoriasis-associated ACKR2 inducing cytokines exogenously.
- Upregulation of ACKR2 in remote unaffected skin (away from the psoriasiform plaques) limits the spread of psoriasiform inflammation *in vivo*.

4.3 Aims

the aims of this chapter were to;

- Determine the cytokines that regulate systemic ACKR2 upregulation
- Explore the effect of systemic ACKR2 induction on the skin's propensity to become inflamed
- Determine the effect of focal psoriasiform inflammation on remote ACKR2 expression, and propensity to inflammation.
- Determine the mechanism by which systemic ACKR2 upregulation modulates inflammation at sites remote from the initial site of inflammation

4.4 Introduction

Studies have shown that remote apparently unaffected human skin in psoriasis ('remote' in this context meaning in all apparently unaffected skin, away from psoriatic plaques) express high levels of ACKR2 (Singh et al. 2012). However, neither 1) the mechanism by which this remote upregulation occurs nor 2) the significance of these observations have been shown. In all but the most severe cases of psoriasis, most of the patients' skin is unaffected. Thus, high ACKR2 expression apparently occurs over very large areas of skin (Griffith, Sokol & Luster 2014), which in turn would suggest that the mechanism(s) that underpin(s) skin ACKR2 upregulation in psoriasis functions on a systemic level. Furthermore, previous work has demonstrated that the Th1 cytokine IFNγ is a potent inducer of ACKR2 expression in primary human keratinocytes (Singh et al. 2012). Soluble T-cell

derived cytokines would be plausible inducers of such widespread systemic ACKR2 upregulation (in an 'endocrine' manner), as such cytokines are expressed not only where they are produced (in local tissues into which T-cells have infiltrated), but are also detected in the systemic circulation (Lowes et al. 2014). The relative contribution of key psoriasis-associated Th1/Th17 cytokines on KC (as the principal ACKR2 expressing cell in the skin) has been relatively unexplored. Taken together, it was hypothesised that T-cell derived soluble cytokines, produced in psoriatic plaques, could mediate an upregulation of ACKR2 through their release into the circulation.

Work in our laboratory has previously identified high levels of IFNγ (a potent inducer of ACKR2 *in vitro* (Singh et al. 2012)) in the circulation of patients with psoriasis, but not in healthy controls (Supplementary Figure 4.1). Concurrently, previous work in our laboratory failed to detect IFNγ in the circulation of IMQ treated mice, which suggests that the IMQ model of psoriasiform inflammation is deficient in this particular cytokine, in comparison to human psoriatic disease. Indeed, studies that compare the IMQ model to other murine models of psoriasiform inflammation (e.g. K14-AREG and K5-Stat3C models) also demonstrate that the IMQ model is relatively deficient in IFNγ (Swindell et al. 2011). These findings in mice are in stark contrast to previously published human data, where IMQ application to human skin was associated with a significant increase in IFNγ (as well as other psoriasis-associated cytokines such as TNF, IL-16 and IL-23 (Vinter et al. 2014)). As discussed in the previous chapter, whilst topical IMQ on murine skin led to a reduction of ACKR2 expression in the psoriasiform plaque, there was no upregulation in apparently normal remote skin in the same mice. If indeed circulating IFNγ does account for remote ACKR2 upregulation in psoriasiform inflammation, the lack of IFNγ release in the IMQ mouse model may account for the apparent lack of remote ACKR2 upregulation observed previously.

The *in vivo* effect of ACKR2 is anti-inflammatory. Thus, the hypothesis that IFNγ leads to ACKR2 upregulation in apparently unaffected skin would imply that IFNγ acts as an inducer of anti-inflammatory mechanisms in this particular context. This is arguably counter-intuitive, considering that IFNγ is generally considered to be a pro-inflammatory Th1 cytokine. However, early

studies suggested that some (albeit not all) patients with psoriasis as well as psoriatic-arthritis showed a degree of improvement in their disease when given recombinant IFNγ (Morhenn 1987; Fierlbeck & Rassner 1990). IFNγ has since also been used in a trial setting for the treatment of other conditions with an immune pathogenesis, including atopic dermatitis and rheumatoid arthritis (Stevens et al. 1998; Veys et al. 1997). The mechanism by which IFNγ may have such a therapeutically beneficial effect in the context of inflammatory disorders has however not been understood. Given 1) the high capacity that ACKR2 has for pro-inflammatory chemokines, 2) the potent ACKR2 induction demonstrated with the use of IFNγ *in vivo* and 3) previous trials suggesting that IFNγ could be therapeutically beneficial in psoriasis, it was hypothesised 1) that circulating IFNγ would lead to upregulation of ACKR2 in unaffected skin and 2) that this upregulation would protect unaffected skin against the spread of psoriasiform inflammation. However, using IFNγ for the purpose of treating inflammation in the clinic is likely to be associated with unacceptable off-target effects, as well as injection site reactions (Johnson-Huang et al. 2012). Such challenges notwithstanding, IFNγ remains a useful research tool as a potent inducer of ACKR2, in experimental models exploring therapeutic ACKR2 modulation.

4.5 Results

4.5.1 Th1 and Th17 cytokines upregulate ACKR2 expression in skin.

Psoriasis is considered a predominantly Th17/Th1 driven condition (Lowes et al. 2014), but the effect and relative contribution of individual Th17/Th1 cytokines on the regulation of ACKR2 have not been explained. Determining which cytokines regulate ACKR2 expression is essential in understanding how ACKR2 is systemically upregulated in clinically unaffected skin in psoriasis. Keratinocytes are the main ACKR2 expressing cells in the skin (Singh et al. 2012), and major players in the pathogenesis of psoriasis (Nestle, Kaplan, et al. 2009). The importance of T-cells in psoriasis pathogenesis is illustrated by the efficacy of T-cell directed therapies currently in use, which target

predominantly Th17 and Th1 cytokines (Di Meglio et al. 2014). It was therefore hypothesised that Th1 and Th17 products (singly and/or in combination) were inducers of ACKR2. Thus, in order to explore the role of T-cell products on keratinocyte ACKR2 expression, T-cells were isolated from healthy human donors, grown in the presence of IL-2 and activated using CD2/CD3/CD28 beads and the tissue culture supernatant collected. The tissue culture supernatant, that contained secreted cytokines from the activated T-cells, significantly increased ACKR2 transcript expression in healthy human keratinocytes grown *in vitro*, in a dose-dependent manner (Figure 4.1a). To better understand the role of T-cells and specific T-cell cytokines in a more relevant human psoriasis disease model, a collaboration was established with colleagues in the Netherlands (E. van den Bogaard and J, Schalkwijk, Radboud University), who have developed a humanised *in vitro* skin equivalent model of psoriasis (van den Bogaard et al. 2013). In this model (summarised in Figure 4.1b, and carried out by the Radboud University team), healthy human donor skin was enzymatically decellularised, leaving a dermal connective tissue scaffold. Keratinocytes were then grown on top of this scaffold (hence constituting the epidermal equivalent), and the dermal component populated from beneath with activated T-cells. This led to changes in the skin equivalents that are similar to human psoriasis in terms of histological appearance, transcriptional changes as well as in the response to typical anti-psoriatic therapies (van den Bogaard et al. 2013). This model more closely mimics human psoriasis than keratinocyte tissue culture monolayers, and enables the study of individual cell types and cytokines in a reductionist manner. In this skin equivalent model of psoriasis, ACKR2 transcript levels were increased when activated T-cells were allowed to enter the skin equivalents (Figure 4.1c). These findings support a role for T-cells in regulating ACKR2 expression in psoriasis. The T-cell dependency of ACKR2 upregulation in this model was further confirmed through treating the skin equivalents with the anti-T-cell calcineurin inhibitor ciclosporin (Figure 4.1d). Treatment of skin equivalents with ciclosporin for 4 days significantly inhibited ACKR2 upregulation as compared to untreated skin equivalent controls, further underlining the T-cell dependency of the ACKR2 upregulation observed. In contrast, treatment

with retinoic acid (an inhibitor of keratinocyte proliferation, and a common class of drugs used in the treatment of psoriasis (Di Meglio et al. 2014)) did not significantly alter ACKR2 expression (Figure 4.1d).

4.5.2 IFNγ is the principal T-cell derived cytokine inducer of ACKR2 expression.

Next, the relative contribution of key Th1 and Th17 cytokines in the regulation of ACKR2 was determined in healthy human primary keratinocytes (both singly and in combination). Both Th1 and Th17 cytokine combination 'cocktails' (as defined in the figure legend) increased ACKR2 expression, but the effect was not additive or synergistic (Figure 4.2a). In these *in vitro* experiment, Th1 cytokines were the strongest inducers of ACKR2 expression, though Th17 cytokines also significantly upregulated ACKR2 mRNA expression (Figure 4.2a). To better understand the role of individual cytokines, healthy human primary keratinocytes were stimulated with individual key (psoriasis associated) Th1 and Th17 cytokines (Figure 4.2b). The data showed that IFNγ was the most potent single inducer of ACKR2 expression, to levels in keeping with previously published data (Singh et al. 2012). To confirm the central role of IFNγ relative to other T-cell products, primary human keratinocytes were stimulated with activated T-cell tissue culture supernatant that had been incubated with increasing concentrations of neutralising IFNγ antibodies (Figure 4.2c). Neutralisation of IFNγ in the tissue culture supernatant from activated T-cells, almost entirely eliminated the ACKR2 inducing effect on keratinocytes in a dose dependent manner. This finding is in keeping with IFNγ being the main T-cell derived inducer of ACKR2. Taken together, these data demonstrate that 1) ACKR2 upregulation in keratinocytes and in psoriasiform skin equivalents, occurs in a T-cell dependent manner, 2) Th1/Th17 cytokines are potent inducers of ACKR2 expression, and 2) IFNγ is the most potent single-agent inducer of ACKR2 transcript expression identified to date, in human primary keratinocytes *in vitro*.

4.5.3 IFNγ upregulates cutaneous ACKR2 expression when administered exogenously *in vivo*.

Given the above data showing that IFNγ is a potent inducer of ACKR2 expression, it was therefore hypothesised that circulating IFNγ could explain, at least in part, the systemic upregulation of ACKR2 observed in skin remote from the psoriatic plaques in humans (Singh et al. 2012). However, previous work in this group failed to detect circulating IFNγ in mice treated with IMQ (*unpublished data, by Dr Mark Singh*), suggesting that the IMQ model (in its basic configuration) would not recapitulate the high circulating levels of IFNγ observed in humans with psoriasis. Thus, the IMQ model apparently differs significantly from human disease in its lack of circulating IFNγ. Indeed, using the IMQ mouse model of psoriasis, QPCR data showed that treatment with IMQ did not lead to an increase in transcript levels of IFNγ in skin, draining lymph nodes or the spleen (Figure 4.3a). For these experiments, Bunyavirus infected murine skin (as a known potent inducer of IFNγ) was used as a positive control, to confirm that lack of IFNγ response was not an inherent deficiency of the mice used. Virus infection of murine skin confirmed that high levels of IFNγ could be induced (Figure 4.3a). ELISA experiments failed to show any detectable IFNγ protein in the skin of either control or IMQ treated mice (Figure 4.3b). Additionally, ELISA experiments did not detect any IFNγ protein in IFNγ-treated mice, which is likely due to the relatively short half-life of exogenously administered recombinant IFNγ *in vivo*, making it difficult to detect protein at the time of cull (the day after the last injected dose).

Next, having demonstrated that the IMQ model is deficient in IFNγ, experiments were designed to determine whether IFNγ upregulates ACKR2 *in vivo* (as had been demonstrated *in vitro* in Figure 4.2b). To this end, exogenous recombinant IFNγ was administered systemically in mice. In keeping with the above human *in vitro* cell culture data of keratinocytes, data confirmed that systemic treatment with injected recombinant IFNγ *in vivo* led to a significant increase in ACKR2 expression in murine skin (Figure 4.3c).

4.5.4 Induced ACKR2 upregulation limits psoriasiform skin inflammation *in vivo*.

ACKR2 is a scavenger of pro-inflammatory CC-chemokines that is upregulated in unaffected skin of patients with psoriasis, but relatively deficient in the psoriatic plaques themselves. It was thus hypothesised that elevated ACKR2 expression could protect against the spread of psoriasiform inflammation; high ACKR2 expression could limit inflammation through CC-chemokine scavenging, thereby limiting T-cell infiltration into skin. In contrast, it was hypothesised that focally deficient ACKR2 expression could enable unrestricted inflammation through the free formation of chemotactic CC-chemokine gradients. However, IFNγ expression appears to be deficient in the IMQ model (Figure 4.3a-b), but could be mimicked through exogenous IFNγ administration. Experiments were therefore designed to test whether induction of ACKR2 expression protects against inflammation, in the context of psoriasiform inflammation *in vivo*. Mice were initially treated with exogenous recombinant IFNγ, before and during application of IMQ, in order to upregulate ACKR2 expression, as had been shown (Figure 4.3c).

Mice were injected with IFNγ twice daily for 24 hours before the first application of IMQ in order to upregulate ACKR2 expression (the experimental model is represented schematically in Figure 4.4a). IFNγ injections continued twice daily for the duration of IMQ treatment, due to the short half-life of IFNγ *in vivo*. After the second application of IMQ, data showed that IFNγ co-treated mice (high ACKR2 expression in skin) displayed significantly less psoriasiform inflammation in response to IMQ, compared to control treated mice, as measured by the modified PASI (Figure 4.4b-c). This effect was sustained, and remained both clinically and statistically significant, until the day of cull. In this experiment, systemic IFNγ alone caused no clinically apparent skin changes in mice that were not treated with IMQ (Figure 4.4c). To further explore the role of ACKR2 in limiting the severity of psoriasiform inflammation, skin ACKR2 expression was correlated with the modified PASI score. This demonstrated a significant inverse correlation, where higher skin ACKR2 expression was associated with lower mPASI scores (Figure 4.4d).

In order to confirm that the observed effect was indeed mediated by ACKR2, experiments were additionally conducted in ACKR2-/- mice. Data showed that IFNγ in ACKR2-/- mice did not confer a protective effect against IMQ mediated psoriasiform inflammation, compared to WT (Figure 4.5). Indeed, at one time point (day 3) IFNγ appears to enhance inflammation (Figure 4.5) and it is hypothesised that in the absence of ACKR2, the pro-inflammatory effects of IFNγ could outweigh any anti-inflammatory effects. However, it would be important to repeat these experiments and continue to model for longer in order to more fully characterise the effect of IFNγ in ACKR2-/- mice. Concurrently, and in order to explore the protective effect of IFNγ on the secretion of psoriasis-associated chemokines, skin from mice was incubated in the presence of protease inhibitors, to collect secreted chemokines. The chemokine levels were quantified using ELISA, and demonstrated that IFNγ administered with topical IMQ limited not only clinical inflammation but suppressed the production of the T-cell attracting CC-chemokines CCL5 and CCL20 as well as the psoriasis associated Th17 cytokine IL-17 (Figure 4.6). Whilst CCL5 is a ligand of ACKR2, CCL20 is not. This suggests that the observed reduction in CCL5, and CCL20 in the context of IFNγ-induced ACKR2 upregulation, is not necessarily a result of ACKR2 scavenging. Instead, ACKR2 upregulation is associated with a general reduction in inflammation, as evidenced by a reduction in both ACKR2- and non-ACKR2 ligands, as well as IL-17.

4.5.5 IFNγ co-administered with topical IMQ in mice, leads to a remote upregulation of ACKR2.

As previously discussed, previous studies show that ACKR2 expression is relatively deficient in human psoriatic plaques (Singh et al. 2012). Data showed that topical application of IMQ replicates human ACKR2 expression patterns in inflammatory plaques, as demonstrated by a reduction in ACKR2 transcript in IMQ treated- as compared to control cream treated mouse skin (Figure 4.7a, orange data points). It was hypothesised that it is the focal psoriatic plaques in humans, that drive remote ACKR2 upregulation, and that this occurs through IFNγ, (that is the most potent ACKR2-inducing Th1/Th17 cytokine identified to date). However and in contrast to this hypothesis, in

the IMQ model focal IMQ failed to differentially regulate remote ACKR2 expression in skin (Figure 4.7b, orange data points). However, as previously outlined, the expression of IFNγ (both in skin and circulation) is deficient in the IMQ model. We therefore hypothesised that elevated IFNγ in the circulation was necessary for the psoriasiform inflammation to drive remote ACKR2 upregulation. For this reason, and in order to more closely model human psoriasis (where IFNγ is elevated in the circulation), mice were treated with systemically injected IFNγ (as in Figure 4.4a), and the ACKR2 expression in remote skin quantified. Data showed that IFNγ co-administered in this manner increased ACKR2 expression in control treated skin as before (Figure 4.7a, filled blue data points). Strikingly, induction of a psoriasiform plaque in skin, *with concurrent systemic IFNγ* led to a substantial increase in ACKR2 expression in remote skin (Figure 4.7b, blue data points). This stands in contrast to IMQ alone, that did not upregulate ACKR2 in remote skin (Figure 4.7b, open orange data points). Together, these experiments demonstrated that where IFNγ was administered alongside topical IMQ, the human ACKR2 skin expression patterns could be modelled in mice (high ACKR2 in remote unaffected skin, low ACKR2 expression in plaques).

4.5.6 Remotely upregulated ACKR2 protects against the spread of psoriasiform cutaneous inflammation.

The clinical significance of increased ACKR2 expression in remote apparently unaffected skin of patients with psoriasis has been unknown. Data presented previously in this thesis have demonstrated that *induced* ACKR2 expression limited psoriasiform inflammation, may have modulated T-cell migration towards a pro-inflammatory chemokine stimulus, and restricted CD3+ T-cell positioning in the epidermis (Chapter 3, Figure 3.13). For these reasons, it was hypothesised that ACKR2 upregulation in remote skin, would protect against the spread of psoriasiform inflammation to those sites. To test this hypothesis, a ‘two-hit’ IMQ model was established (summarised in Figure 4.8a), in which remote ACKR2 upregulation was achieved through treatment of the right mouse flank with IMQ together with systemic IFNγ injections. This protocol had been shown to increase ACKR2 expression in remote skin (Figure 4.7b). Having achieved remote ACKR2 upregulation in the same

manner, a second site (contralateral flank or ear) was treated with IMQ (the protocol is summarised in Figure 4.8a).

Again, and as shown in above experiments (Figure 4.4b), IFNγ limited psoriasiform inflammation at the first IMQ treated site (Figure 4.8b). Critically, and in keeping with the above hypothesis, the induction of one lesion in this model with systemic IFNγ, protected remote skin against the spread of psoriasiform inflammation (Figure 4.8c). Whilst exogenously administered IFNγ is protective against imiquimod-induced psoriasiform inflammation during and for a period after administration, data from day 8 of the model (Figure 4.8b) suggests there may be enhanced inflammation in the IFNγ-treated as opposed to the control-treated group. This does not reach statistical significance, and further experiments, where the model is maintained for longer that 8-days would be helpful in determining whether IFNγ will have pro-inflammatory effects longer-term, after an initial protective period. It is possible that whilst IFNγ-induced ACKR2-upreglation is protective in the initial stages, the pro-inflammatory pathways induced by IFNγ become more dominant at later time points, thus overcoming any early anti-inflammatory effects. Additionally, longer-term experiments with continued IFNγ injections would be required to determine whether the effect of IFNγ in terms of limiting mPASI/psoriasiform inflammation only occurs in the early stages of this model, or whether the loss of protection in terms of psoriasiform inflammation at the time of cull, is due to cessation of IFNγ injections in the presented experiments.

Whilst above experiments suggest that high ACKR2 expression is associated with reduced psoriasiform inflammation, it is important to demonstrate that any protective effect observed from IFNγ administration is indeed dependent on the presence of ACKR2. Therefore, in order to confirm that these observations were dependent on ACKR2, experiments were conducted in ACKR2-/- mice, using ear skin as a second site of inflammation. However, in ACKR2-/- no protective effect was afforded by induction of a previous psoriasiform lesion alongside systemic IFNγ (Figure 4.8d and 4.9), as had been seen in WT mice (Figure 4.7c). These data suggest that the protective effects that result from IMQ/systemic IFNγ on remote skin are ACKR2-dependent, though further work and repeat experiments are required (e.g.

also using non-ear skin as a second site in ACKR2-/- mice) to verify these findings. In addition, an elevation of ACKR2 transcript expression in the remote skin site was confirmed by QPCR (Figure 4.10a). At present, reliable staining of murine skin for ACKR2 is not possible using available antibodies. Thus, in order to confirm the location of ACKR2 upregulation in skin, skin was split into dermal and epidermal compartments and successful separation confirmed by demonstrating elevated involucrin expression (a keratinocyte differentiation marker). QPCR data confirm that ACKR2 induction predominantly occurs in the epidermal compartment, which is in keeping with previous data demonstrating epidermal keratinocytes as the main site of ACKR2 expression in human skin (Singh et al. 2012).

Histopathology showed that IFNγ limited thickening, epidermal CD3+ T-cell infiltration and epidermal hyperproliferation (as measured by Ki67 staining) of IMQ treated mouse skin both at the first flank lesions (Figure 4.11a), and also at the second lesion (Figure 4.11b). Quantification of the difference between PBS control and IFNγ treated mice (in terms of epidermal thickening, thickness of the Ki67 positive epidermal layer (a marker of proliferation) and the proportion of CD3+ T-cells in the epidermis), confirmed that these differences were significant (Figures 4.12a-b). Immunohistochemical staining for the proliferation marker Ki67 revealed a significantly thicker layer of proliferating basal keratinocytes in mice treated with IFNγ as compared to PBS control treated mice in both the first (Figure 4.12a) and second lesions (Figure 4.12b). Furthermore, proportionately fewer CD3+ T-cells were localised in the epidermis in IFNγ as compared to PBS control treated mice, both in the first lesion, and in the second induced lesion (Figures 4.12c-d). Critically, there were no significant differences between IFNγ and PBS treated mice in terms of total numbers of CD3+ cells in the skin (epidermis plus dermis), indicating that the epidermal differences are specifically a function of CD3+ exclusion from the epidermis, where ACKR2 is upregulated (Figures 4.12c-d). Immunohistochemical analyses in above experiments had been limited to CD3+ cells only. However, several cell sub-types play a role in the pathogenesis of psoriasis and in order to better understand the cell infiltrate in the skin in this model, skin sections were additionally stained for CD3+, CD4+, CD8+, CD25+ and FoxP3 positive

cells. Cells counted both in whole skin including dermis and epidermis (Figure 4.13a) and the epidermis alone (Figure 4.13b), in order to determine whether there were differences in the treatment groups in terms of leukocyte positioning in skin. Whilst no significant differences were found between the treatment groups in terms of absolute cell numbers in epidermis plus dermis (Figure 4.13a), a significantly higher proportion of CD3+ cells were found in the epidermis in imiquimod treated ACKR2-/- mice, as compared to wild-type mice. Though data did not reach statistical significance, results suggest that the relative exclusion of T-cells appear to be predominantly skewed against CD4+ cells. The significance of this finding is unclear, and whilst CD4+ and CD8+ both play an important role in psoriasis, their relative contribution and importance to pathogenesis is controversial. Further studies are required to fully understand the difference in the relative exclusion of different leukocyte sub-populations in the context of psoriasiform inflammation, and the significance this would have for the development of psoriasiform plaques. Attempts were also made to stain for RORγt cells in these experiments, given the importance of Th17 cells in psoriasis. However, despite numerous antibodies and staining methods, none of the strategies employed were successful in staining reliably for RORγt cells, which needs to be addressed in future experiments.

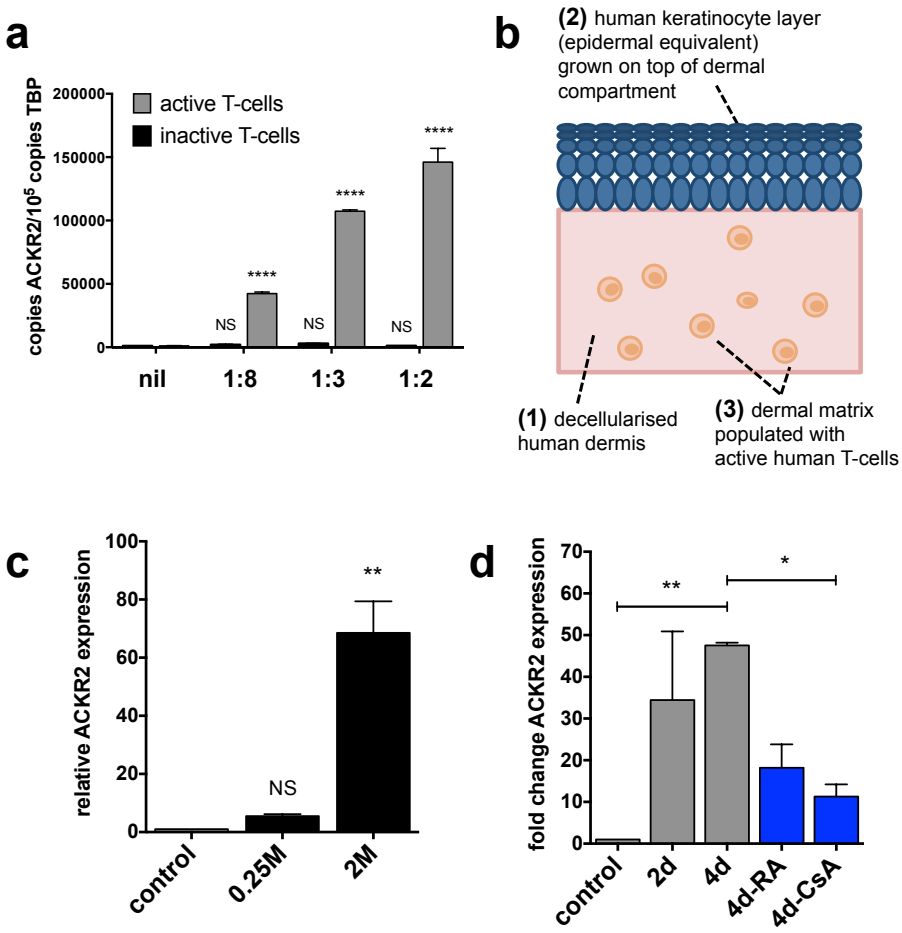

Figure 4.1 Differential expression of ACKR2 in skin is dependent on products of activated T-cells.

(a) Absolute ACKR2 mRNA expression in primary human keratinocytes treated with conditioned medium from activated or non-activated (resting) human T-cells (compared to fresh medium (*nil*), or diluted *1:8-1:2* in fresh medium).

(b) Schematic representation of the psoriasiform *in vitro* skin equivalent model set-up.

(c) Relative ACKR2 mRNA expression in *in vitro* human skin equivalents of psoriasis, with increasing numbers of infiltrating activated human CD4+ T-cells (M=million).

(d) Fold change ACKR2 mRNA expression *in vitro* human skin equivalents of psoriasis after 2-4 days of T-cell migration into the skin equivalents and following treatment with all-trans retinoic acid (*RA, 10^{-6}M*) or ciclosporin A (*CsA, 400ng/ml*).

Human skin equivalent work was carried out by our collaborators as described in section 2.4.8 (Dr Ellen van den Bogaard and Prof Joost Schalkwijk, at Radboud University Nijmegen, the Netherlands), n=3-5.

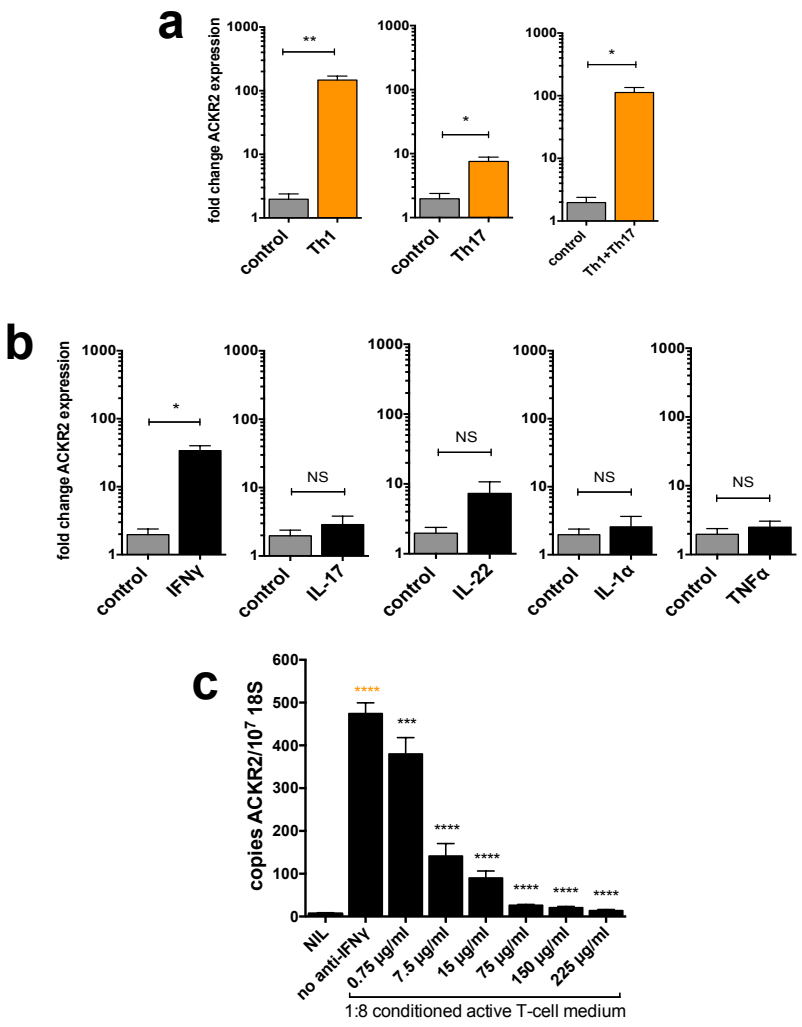

Figure 4.2 Th1/Th17 cytokines upregulate ACKR2 expression, with IFNγ being the single most potent ACKR2 inducing T-cell product.

(a) Relative ACKR2 mRNA expression in *in vitro* 'skin equivalents' treated with cytokine combinations; Th1 cytokines; IL-1α+TNFα+IFNγ: Th17 cytokines; IL-17+IL22. IL-1α 30ng/ml: IFNγ 500U/ml: TNFα 30ng/ml: IL-17 100ng/ml: IL-22 100ng/ml: Statistics is Student's t-test. * $P<0.05$, ** $P<0.01$.

(b) Relative ACKR2 mRNA expression in *in vitro* 'skin equivalents' treated with individual cytokines; IL-1α 30ng/ml: IFNγ 500U/ml: TNFα 30ng/ml: IL-17 100ng/ml: IL-22 100ng/ml: Statistics is Student's t-test. * $P<0.05$, ** $P<0.01$.

(c) Absolute ACKR2 mRNA expression in primary human keratinocytes treated with conditioned medium from activated human T-cells diluted *1:8,* with added increasing concentrations of neutralising anti-IFNγ antibodies, compared to untreated keratinocytes. Significance was assessed using two-way ANOVA with Tukey's multiple-comparisons-test. **** $P<0.0001$. Orange *; compared to NIL. Black *; compared to no anti-IFNγ, but with conditioned active T-cell medium.

Cell culture experiments in (a) and (b) was carried out by our (Dr Ellen van den Bogaard and Prof Joost Schalkwijk, at Radboud University Nijmegen, the Netherlands), n=3-5.

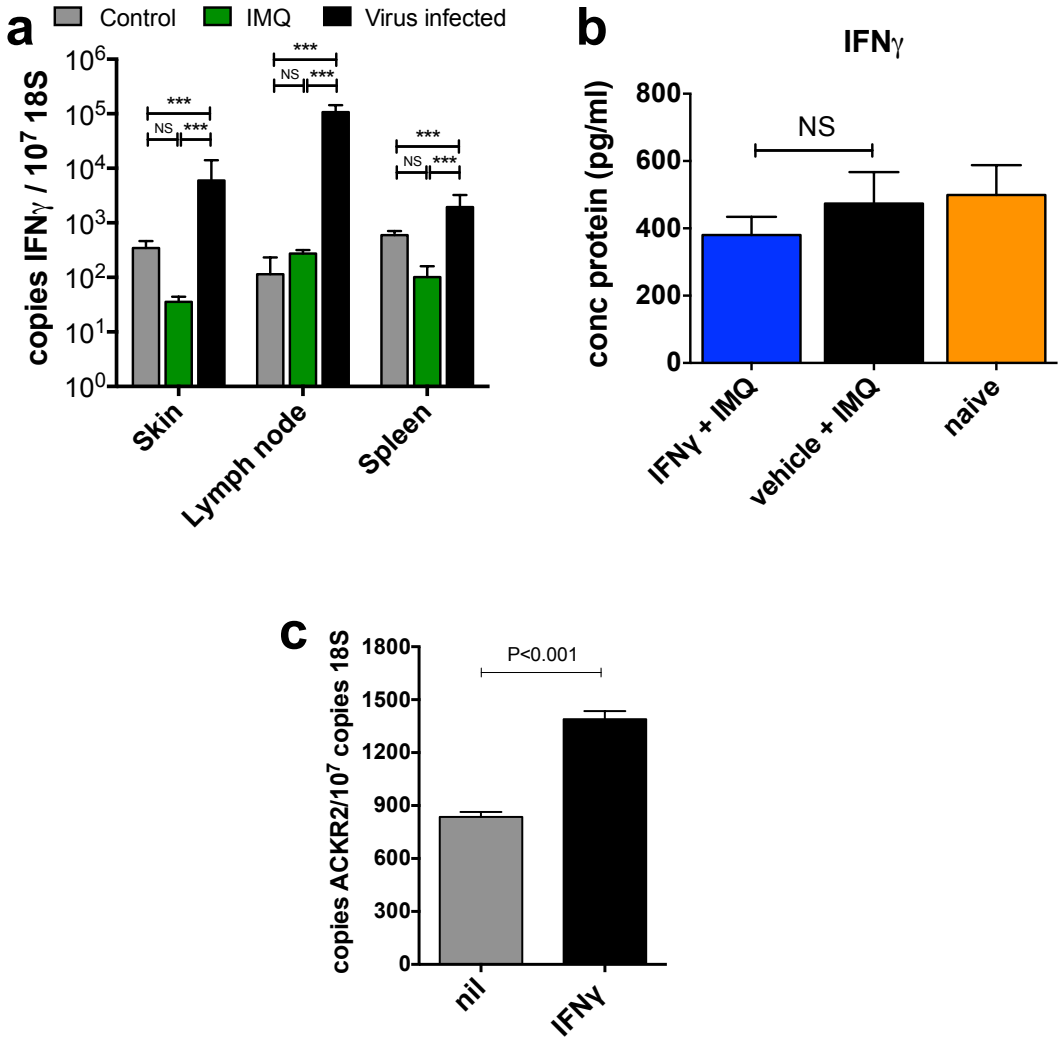

Figure 4.3 The IMQ mouse model of psoriasis is not associated with increased IFNγ transcript/protein in skin.

(a) Absolute ACKR2 mRNA expression in dorsal mouse skin, draining lymph node and spleen, 24 hours after treatment with control cream, IMQ or systemic Bunyavirus infection. *** $P<0.005$. n=6 mice per group.

(b) Concentration of IFNγ, in mouse skin on day 5 following twice daily IFNγ (20,000 U intraperitoneally [i.p.]) on days 1-4, topical control or IMQ on days 2-4, as compared to PBS vehicle control/carrier cream (naïve) mouse skin, as measured by ELISA (n=6/group). (Undertaken with the assistance of Dr G. Wilson)

(c) Absolute ACKR2 mRNA expression in dorsal skin of mice that were untreated, or treated with systemic IFNγ (20,000U i.p. per day for 4 days, *n*=6). Significance was determined using Student's t-test. Data derived from one experiment.

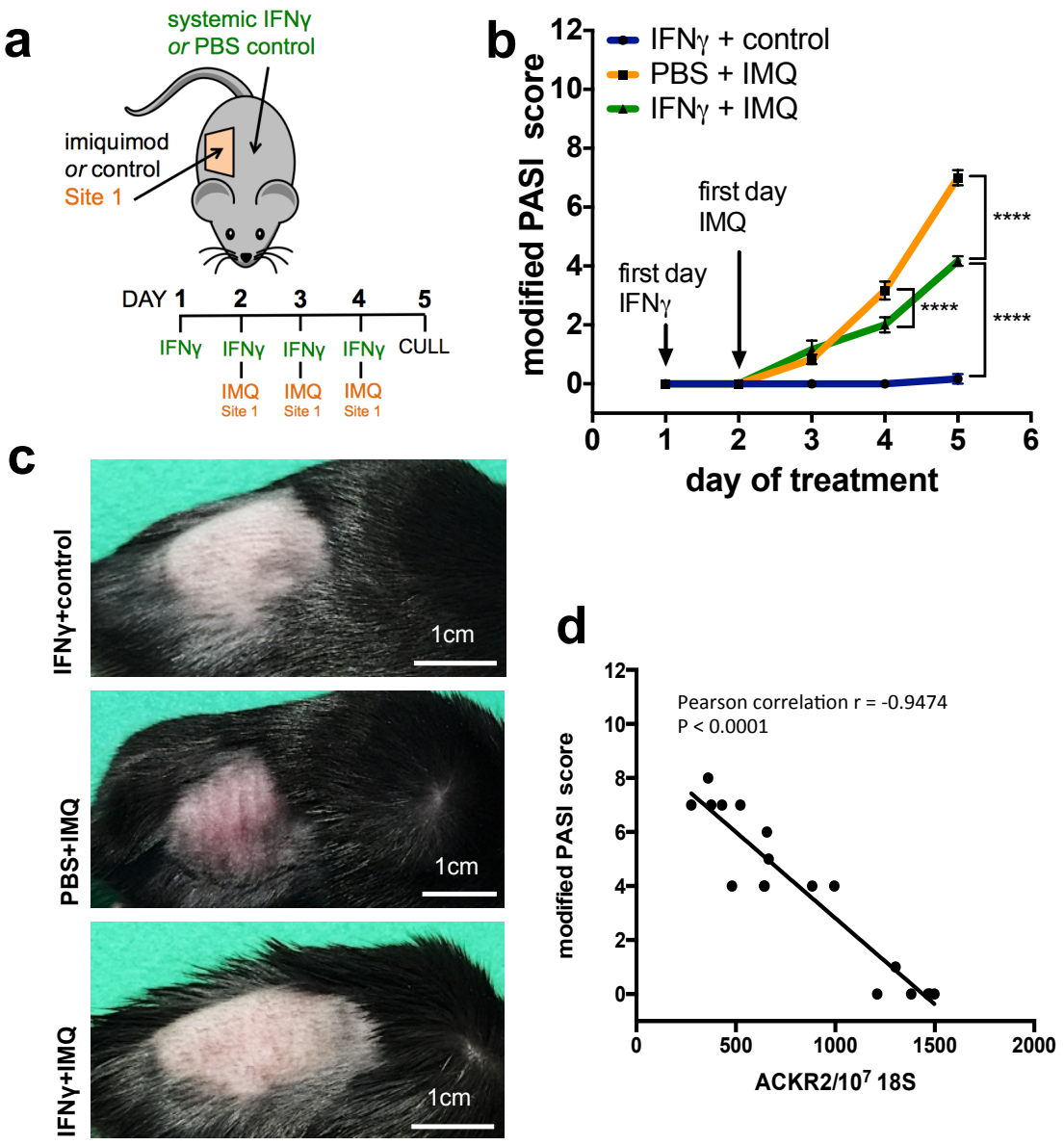

Figure 4.4 IFNγ induced ACKR2 expression in mice protects against IMQ induced psoriasiform skin inflammation.

(a) Schematic representation of the experimental model in which mice were injected with IFNγ or PBS negative control.

(b) Skin inflammation severity (3 groups of *n*=6 in each group). Arrows indicate first day of IFNγ/PBS injections and IMQ/control cream. Treatments continued until the day before cull.

(c) Representative images of wild-type (WT) mice (top) IFNγ (20,000U 2x/day) plus control cream; (middle) PBS plus IMQ and (bottom) IFNγ plus IMQ. Treatments were for 3 days and mice culled on day 4.

(d) Correlation of cutaneous ACKR2 expression and skin inflammation severity. **** *P*<0.0001. Data representative of two comparable experiments.

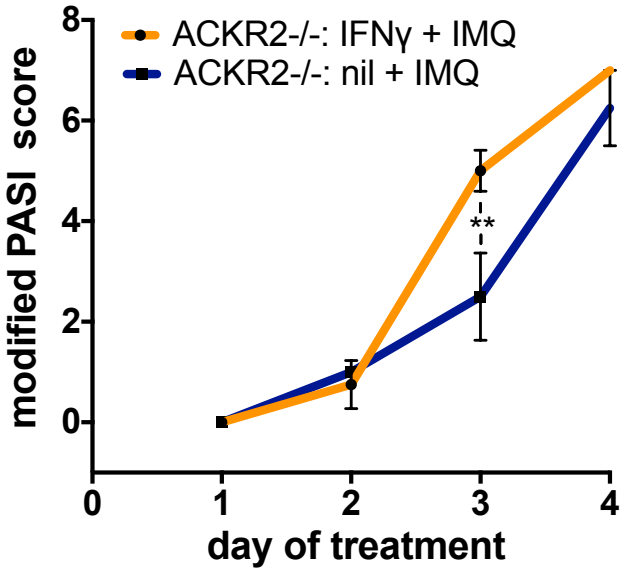

Figure 4.5 IFNγ failed to protect against IMQ induced psoriasiform skin inflammation in ACKR2-/- mice.

Modified total PASI, across all parameter, in ACKR2-/- and WT mice treated with IMQ on one flank, plus either systemic IFNγ or PBS control.

Data are mean±SEM, statistical analysis is two-way ANOVA with Tukey's multiple comparisons test. n=6, ** P<0.01. Data from one experiment.

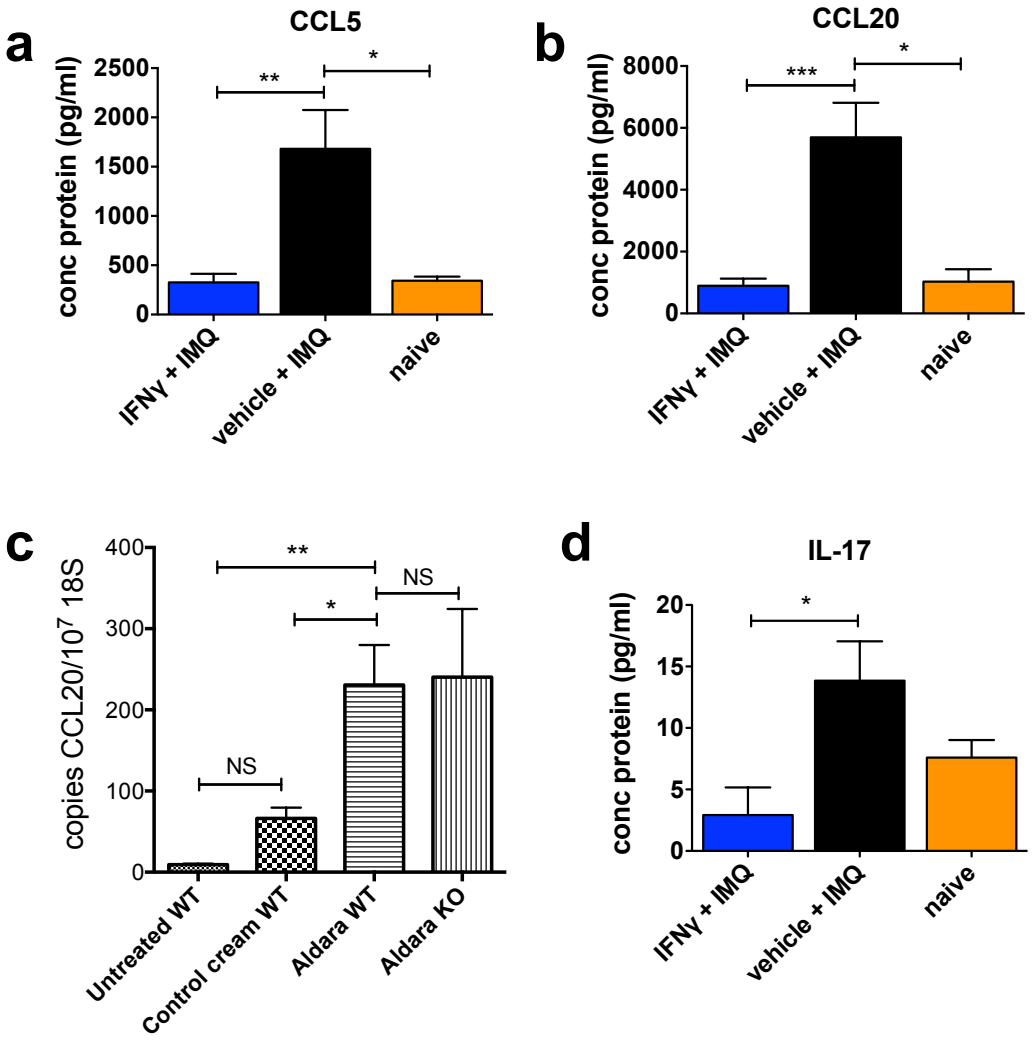

Figure 4.6 Induced ACKR2 expression in mice limits production of psoriasis-associated soluble CC-chemokines.

(a,b) Concentration of CCL5 and CCL20, in mouse skin on day 5 following twice daily IFNγ (20,000 U i.p.) on days 1-4, topical control or IMQ on days 2-4, as compared to PBS vehicle control/carrier cream (naïve) mouse skin, as measured by ELISA (n=6 mice). (Undertaken with the assistance of Dr G. Wilson)

(c) Absolute CCL20 expression, normalised to 18S, in mouse skin 3 days of control cream or IMQ in WT or ACKR2 deficient (KO) mice.

(d) Concentration of IL-17, in mouse skin. Methodology as in a-b above.
Statistics: one-way ANOVA with Tukey's post-test. **P*<0.05, ***P*<0.01, ****P*<0.005. Each experiment performed once.

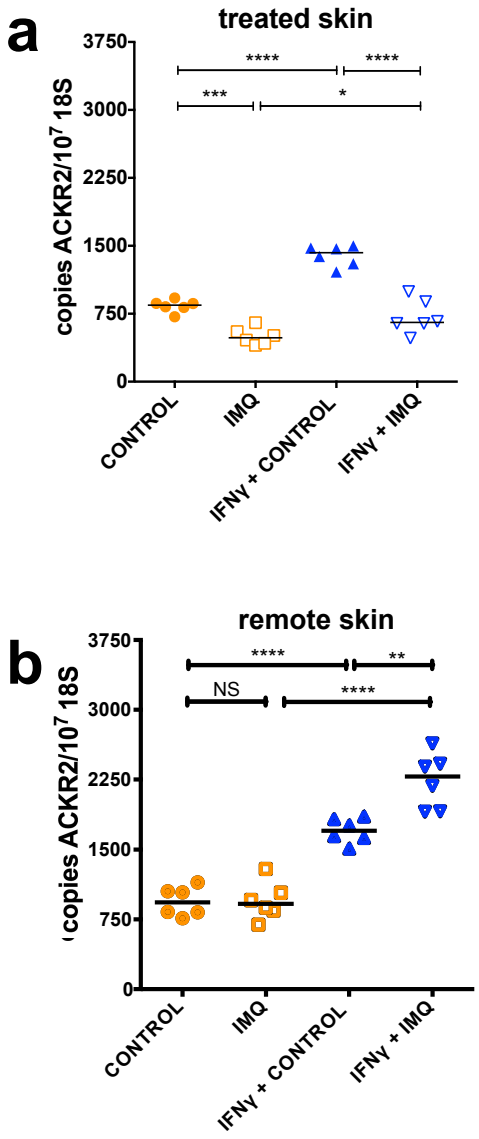

Figure 4.7 Human psoriatic ACKR2 expression patterns can be successfully modelled *in vivo* by topical IMQ at one site plus injected IFNγ in mice.

Comparison of ACKR2 expression in;

(a) topically treated skin and

(b) remote untreated control skin of IMQ treated mice in the presence or absence of subcutaneous IFNγ administration (10,000U IFNγ per day) *n*=6 in all groups. Significance was assessed using one-way ANOVA with Tukey's multiple comparisons test. * $P<0.05$, ** $P<0.01$, *** $P<0.005$, **** $P<0.0001$. Data representative of two comparable experiment.

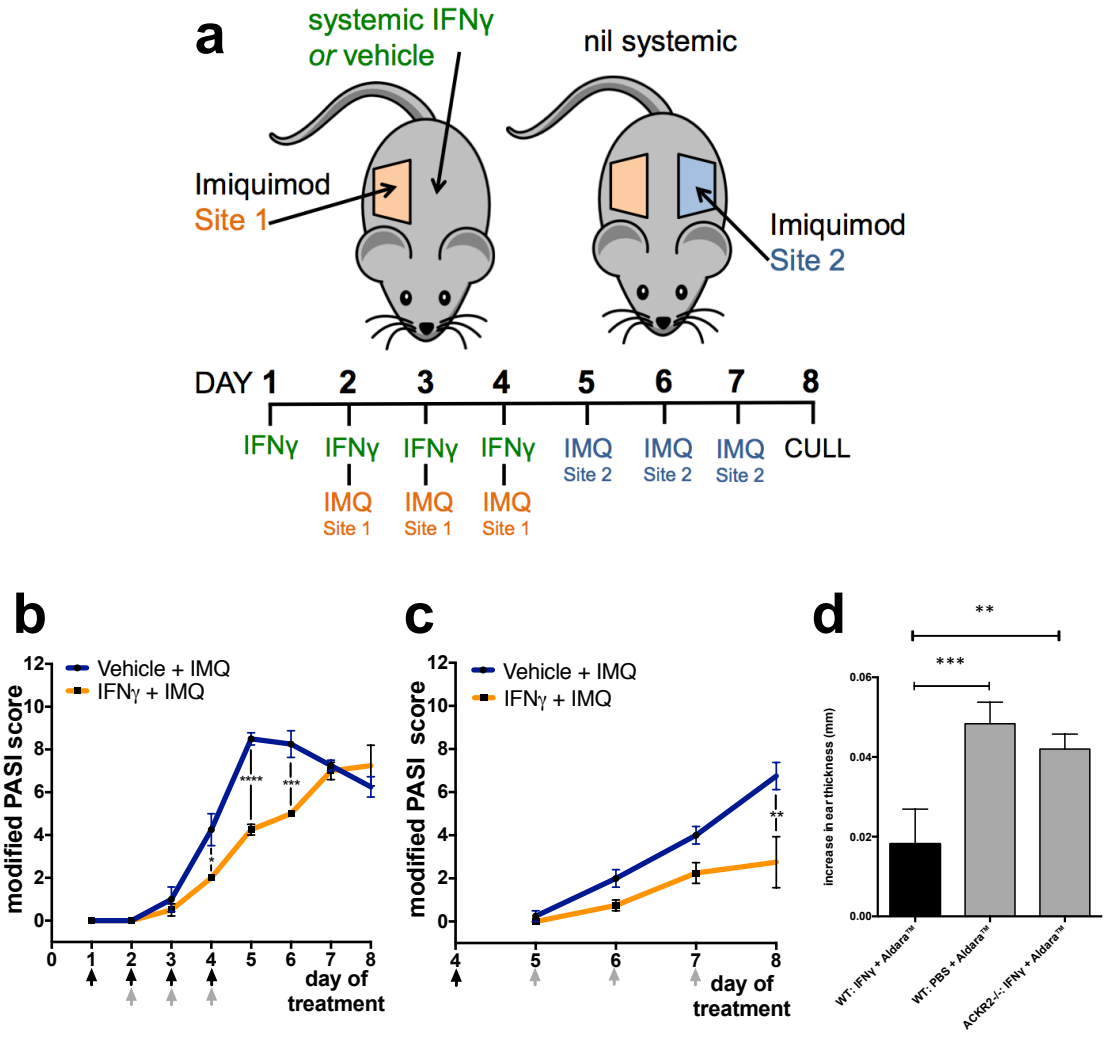

Figure 4.8 Focal psoriasiform inflammation protected remote unaffected skin from the spread of inflammation.

(a) Diagram of experimental design.

(b) Inflammation severity of initial psoriasiform lesions: Mice were treated with 20,000U IFNγ 2xdaily or vehicle (black arrows) and IMQ 1xdaily (grey arrows) to right flank. This was stopped, and;

(c) inflammation induced by daily IMQ treatment at the second site (mice were culled on day 8) was assessed. Data representative of two comparable experiments.

(d) Absolute increase in ear thickness, where ear was used as the second site for IMQ application.

Statistics: two-way ANOVA (a-c) and one-way ANOVA (d) **P*<0.05, ***P*<0.01, ****P*<0.005, *****P*<0.0001. n=6 mice. Experiment performed once.

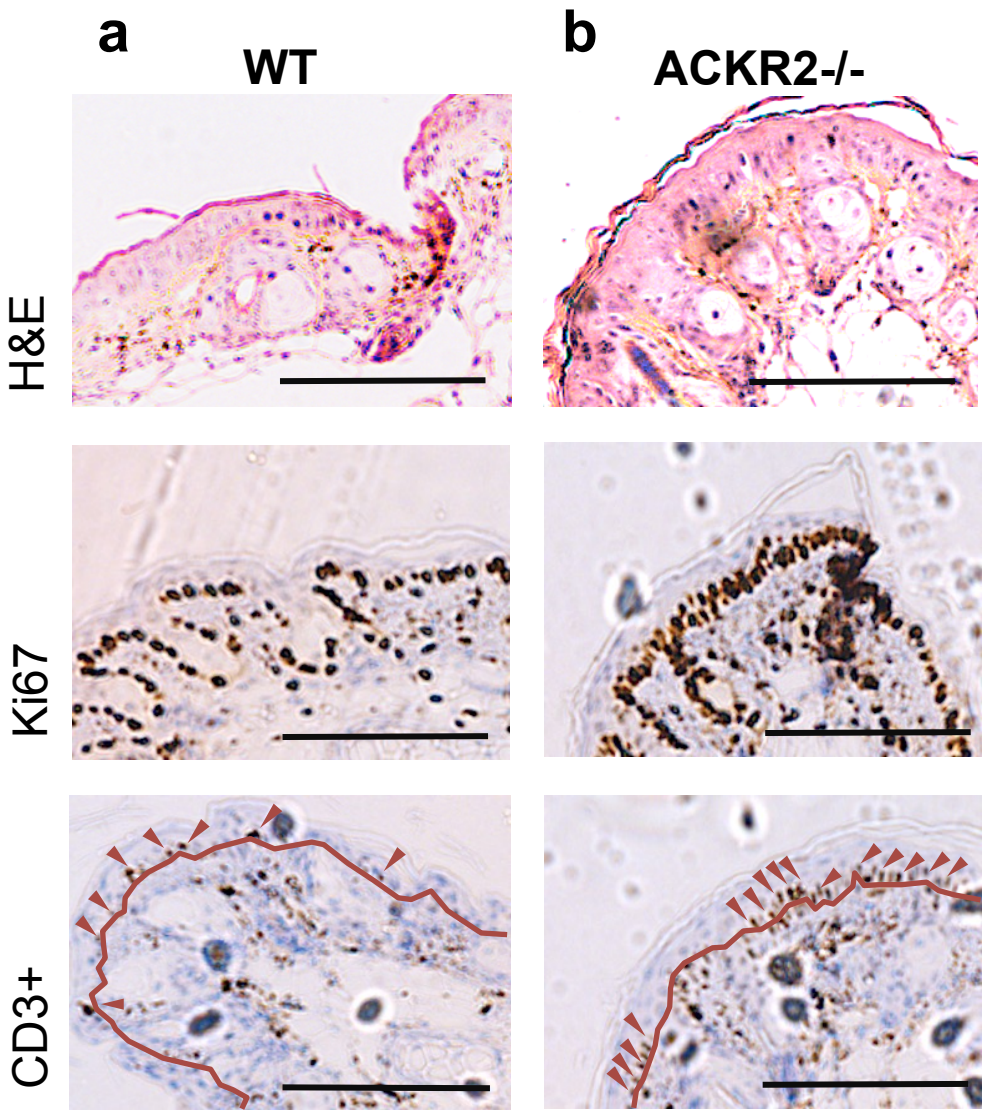

Figure 4.9 Focal psoriasiform inflammation plus IFNγ did not protect remote unaffected ear skin from the spread of inflammation in the absence of ACKR2.

Representative images of H&E, Ki67 and CD3 staining of mouse ears, in which psoriasiform lesions had been induced on flank alongside concurrent systemic IFNγ at 20,000U per day per mouse (n=6).

(a) WT mouse ear

(b) ACKR2-/- ear

The dark red arrows indicate CD3+ T-cells in epidermis, with the dark red line representing the dermal-epidermal junction. All scale bars 100μm. Experiment performed once.

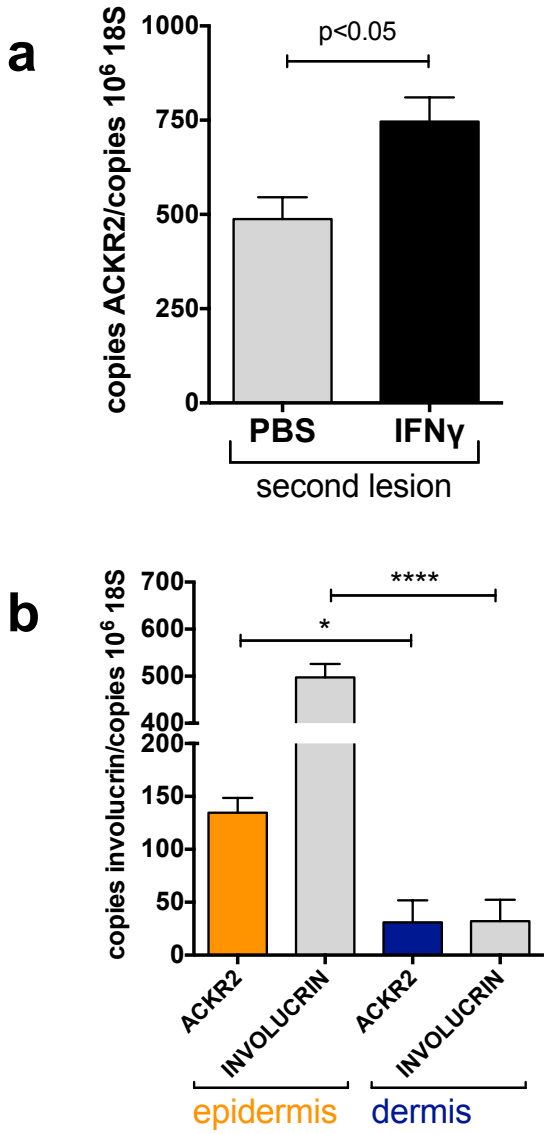

Figure 4.10 ACKR2 is essential for focal psoriasiform inflammation protecting remote unaffected skin from the spread of inflammation.

(a) ACKR2 expression (normalised to 18S) in the second IMQ-induced lesions, where the first lesion was induced with concurrent PBS (grey bar) or IFNγ (black bar). Statistics: Student's t-test. n=6 mice. Data representative of two comparable experiment.

(b) ACKR2 expression in distal epidermis (orange) and dermis (blue). Epidermal/dermal separation confirmed by QPCR for involucrin (grey bars). Statistics: Student's t-test, Tukey's multiple comparisons test. **P*<0.05, *****P*<0.0001. n=6 mice. Experiment performed once.

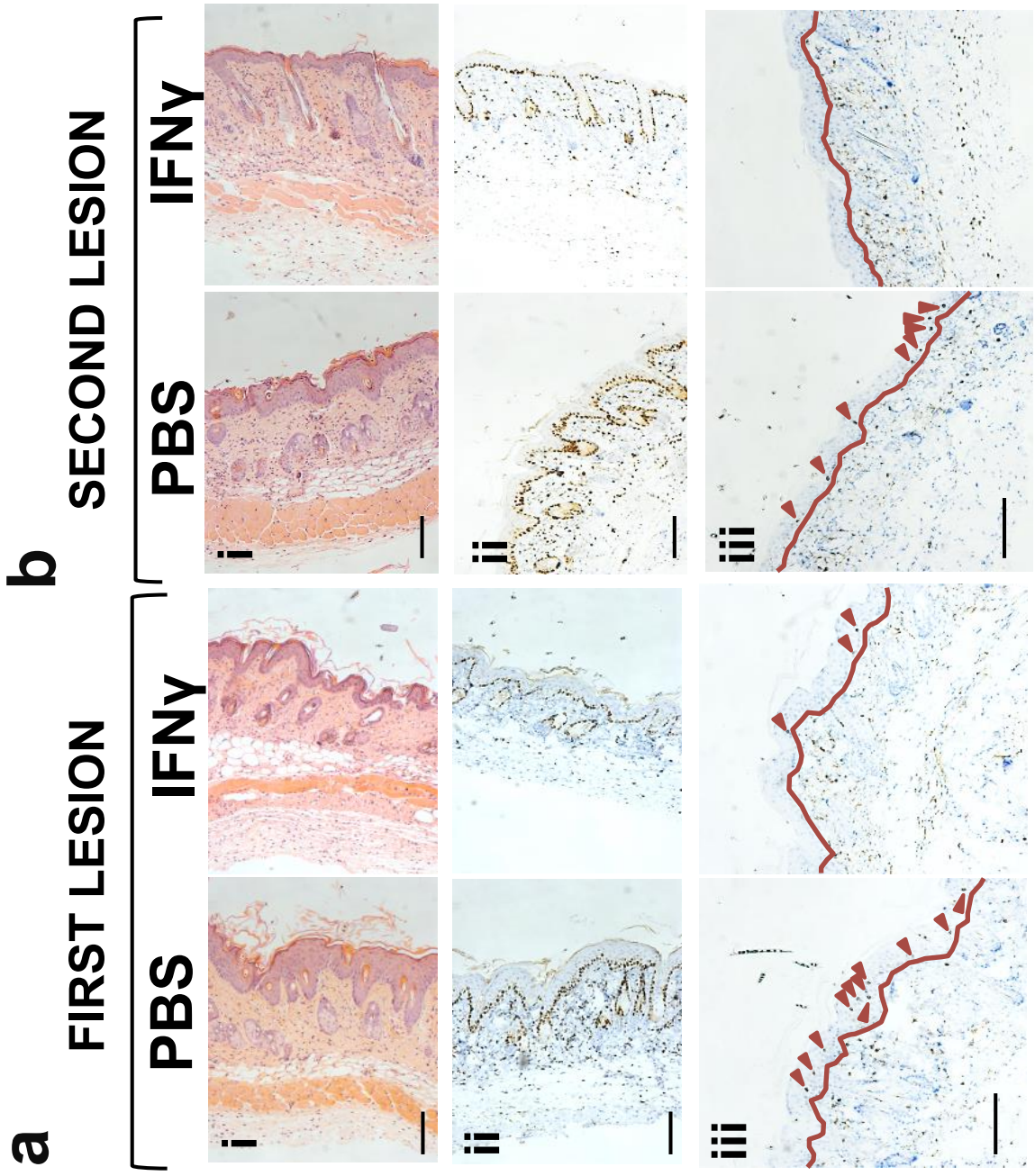

Figure 4.11 IFNγ induced ACKR2 expression limits epidermal thickening and limits epidermal CD3+ T-cell positioning.

Representative images of (i) H&E, (ii) Ki67 and (iii) CD3+ staining of:

(a) The initial IMQ-induced lesion on right mouse flank, with concurrent PBS control or systemic IFNγ at 20,000U per day per mouse and;

(b) The second IMQ-induced lesion initiated following cessation of the initial IMQ/IFNγ or PBS treatment.

In (iii) the dark red arrows indicate CD3+ T-cells in epidermis, with the dark red line representing the dermal-epidermal junction. All scale bars 100μm. Experiment performed once.

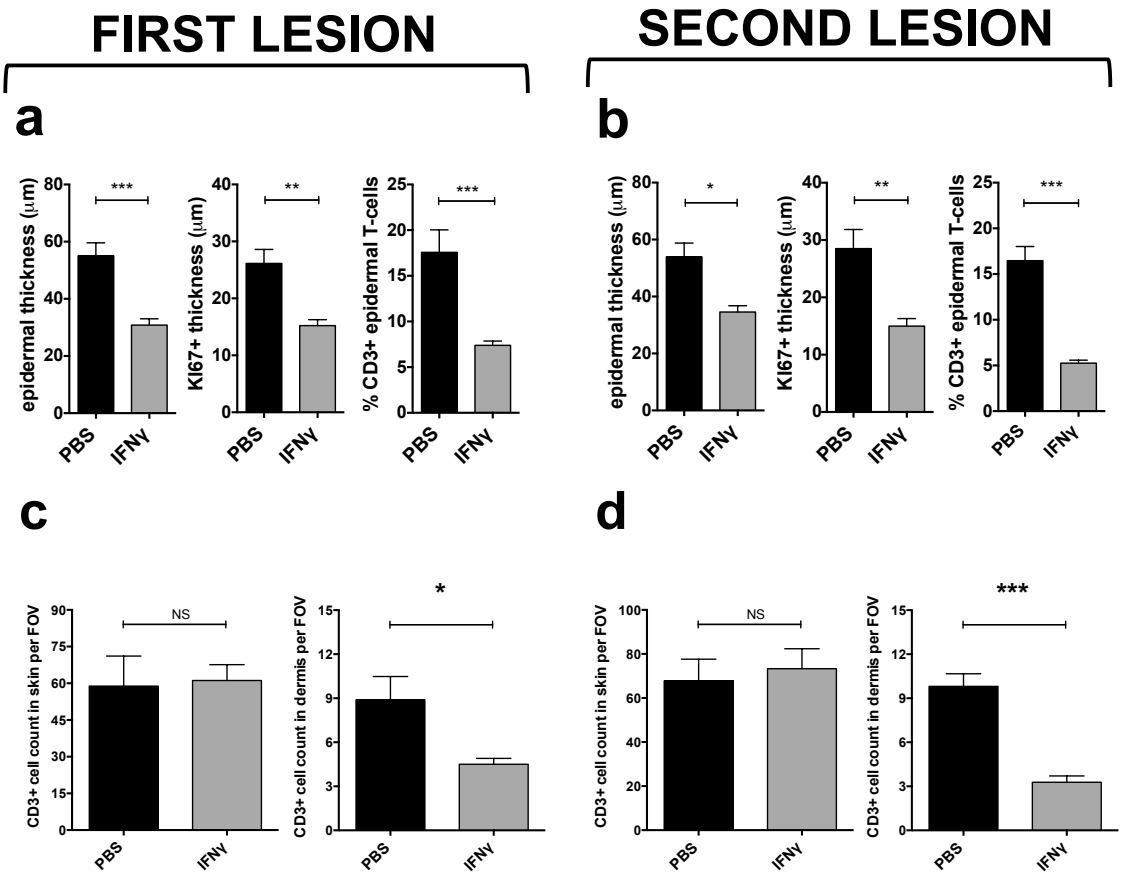

Figure 4.12 IFNγ induced ACKR2 expression is associated with limited epidermal thickening and restricted epidermal CD3+ T-cell positioning: quantitative data.
Quantification of H&E, Ki67 and CD3+ staining of:

(a) The initial IMQ-induced lesion on right mouse flank, with concurrent PBS control or systemic IFNγ at 20,000U per day per mouse and;

(b) The second IMQ-induced lesion initiated following cessation of the initial IMQ/IFNγ or PBS treatment.

(c) The first IMQ-induced lesion on right mouse flank, with concurrent PBS control or systemic IFNγ (20,000U per day per mouse).

(d) The second IMQ-induced lesion following cessation of systemic PBS or IFNγ treatment.

In **(a-b)** for the quantitative data, thickness was measured across 9 sites, from 3 separate sections from each skin sample.

Quantification of CD3+ cell numbers (mean of 3 separate fields-of-view per mouse) in **(c+d):** (left hand graphs) Total numbers of CD3+ T-cells in whole skin (dermis and epidermis) and (right hand graphs) Numbers of CD3+ T-cells specifically located in the epidermis. **P*<0.05, ***P*<0.01, ****P*<0.005. n=6 mice. Experiment performed once.

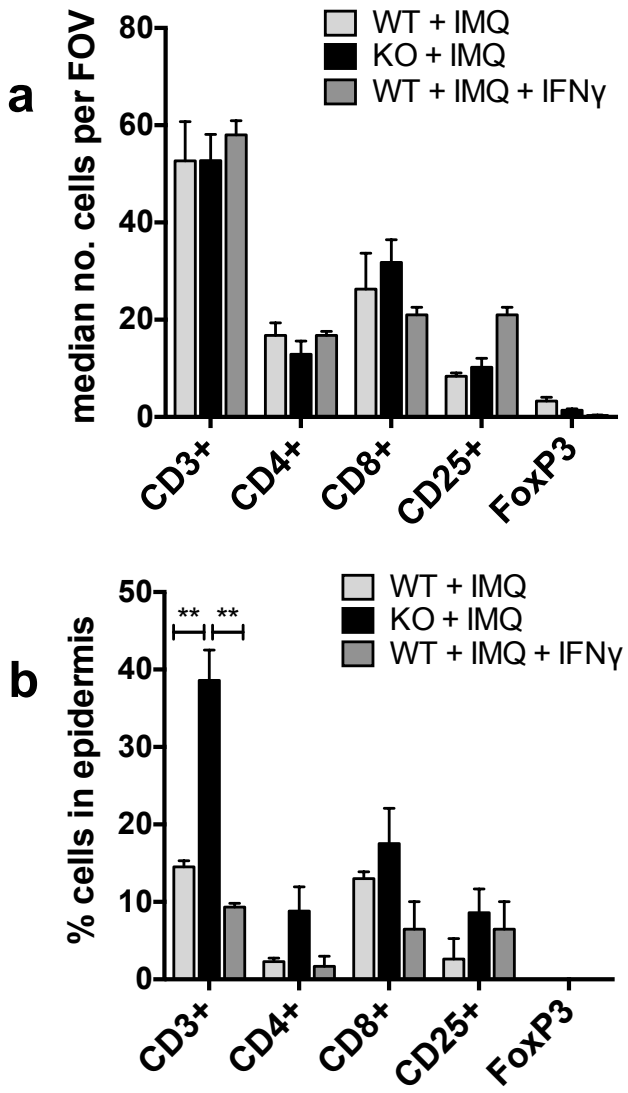

Figure 4.13 Immunohistochemical characterisation of immune cells in skin.

Markers used: CD3+ for T-cells: CD4+ for helper T-cell: CD8+ for cytotoxic T-cells: CD25+ for activated T-cells and FoxP3 for regulatory T-cells.

(a) Median cell numbers as per same field-of-view (FOV) of whole skin (x200 magnification) after 3 days of treatment with IMQ (±systemic IFNγ 20,000 U daily). (Statistics: one-way ANOVA with Tukey's multiple comparisons test). Quantifications carried out using 6 FOV per skin sample.

(b) Median cell numbers as per same field-of-view of epidermis (x200 magnification) after 3 days of treatment with IMQ (±systemic IFNγ 20,000 U daily). (Statistics: multiple t-test with Holm-Sidak multiple comparison correction. ** $P<0.01$).

Quantifications carried out using 6 FOV per skin sample. n=6 mice. Experiment performed once.

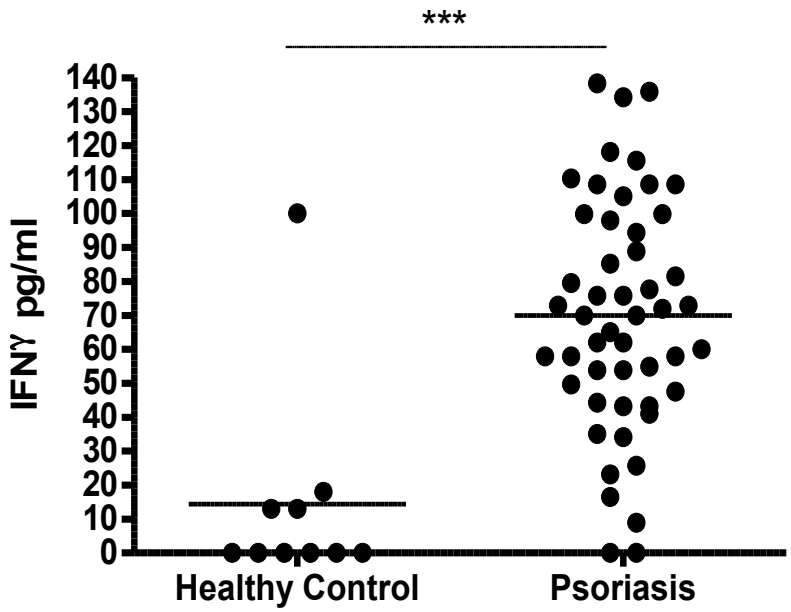

Supplementary Figure 4.1 Supplied by Dr Mark Singh. IFNγ levels were increased in patients with psoriasis as compared to healthy controls.
Plasma cytokine levels in healthy controls (*n*=10)
versus patients with psoriasis (*n*=50), assessed.
Significance was determined by Mann-Whitney U test. *** $P<0.005$. Experiment performed once.

4.6 Summary Chapter 4

This chapter reports the identification of IFNγ as an inducer of epidermal ACKR2 expression in vivo, and thus enabled the assessment of therapeutic ACKR2 induction in a murine model of psoriasiform inflammation. ACKR2 induction in vivo protected against the development of psoriasiform inflammation. Furthermore, induction of one psoriasiform skin plaque, lead to upregulation of ACKR2 in remote unaffected skin in the IMQ mouse model, and protected unaffected skin from the further spread of inflammation.

Previous studies have shown a relatively deficient expression of the CC-chemokine scavenging atypical chemokine receptor ACKR2 in psoriatic plaques. In contrast, ACKR2 expression in unaffected remote skin ('remote' from psoriatic lesions) is upregulated in patients with psoriasis (Singh et al. 2012). The mechanism and significance of this observation has not been previously understood. Psoriasis is considered a predominantly Th1/Th17 driven systemic inflammatory disorder, with elevated levels of Th1/Th17 cytokines in the circulation (Di Meglio et al. 2014). Given the apparently widespread upregulation of ACKR2 in those with psoriasis, it was thus hypothesised that T-cells and soluble Th1/Th17 cytokines could differentially regulate ACKR2 expression. To test this hypothesis, the effect of T-cell products on ACKR2 expression was assessed. Results showed that soluble T-cell products from activated human T-cells were potent inducers of ACKR2 expression in keratinocytes (KC). The T-cell dependency of ACKR2 upregulation in skin was further confirmed through the use of a novel previously validated humanised *in vitro* 3D model of psoriasis ('skin equivalents'), in collaboration with colleagues at Radboud University, Nijmegen, the Netherlands (van den Bogaard et al. 2013). In brief, this model involved culturing primary human keratinocytes on a decellularised human dermal matrix, into which active human T-cells were allowed to infiltrate. The resulting skin equivalent bears significant similarities to human psoriasis, both in phenotype and gene expression (van den Bogaard et al. 2013). Using this *in vitro* model of human psoriasis, data confirmed that T-cell infiltration of this skin model was necessary for ACKR2 upregulation in the skin equivalents. Additionally, targeting T-cells therapeutically using the calcineurin inhibitor ciclosporin, significantly limited the ACKR2 upregulation

associated with T-cell infiltration into the skin equivalents. Therapeutic targeting of KC proliferation, instead of T-cells, through the use of retinoids did not significantly reduce ACKR2 expression. Together, the data suggest a role for T-cells in the differential regulation of ACKR2 in both cultured primary human KC and in an *in vitro* model of psoriasis.

Whilst psoriasis is driven by Th1/Th17 cytokines (Di Meglio et al. 2014), the relative contribution of different Th1/Th17 cytokine products has not previously been assessed. For this reason, Th1/Th17 cytokines were tested (both singly and in combination) using healthy primary human keratinocyte monolayers. Data showed that Th1 and Th17 cytokine combinations both significantly upregulated ACKR2 expression in skin equivalents. Antibody neutralisation of IFNγ in active human T-cell supernatant obliterated the ACKR2 inducing effect of T-cell products, suggesting that the T-cell mediated ACKR2 upregulation is predominantly driven by IFNγ. Therefore, it was hypothesised that IFNγ released into the circulation from inflammatory psoriatic plaques, could upregulate ACKR2 expression *in vivo*. However, our data showed that IFNγ expression is not induced in the IMQ mouse model (transcript or protein). This is a significant deficiency of this model compared to both other murine models of psoriasis and human skin (Swindell et al. 2011; Vinter et al. 2014). This deficiency notwithstanding, the IMQ model remains a readily available model, and offers the advantage of psoriasiform lesion being inducible at specific, pre-determined skin sites. To address the lack of systemic ACKR2 upregulation in the IMQ model, next WT mice were treated with systemic recombinant IFNγ. Data demonstrated, for the first time, that cutaneous ACKR2 expression (as assessed through QPCR) could be induced on a systemic level through exogenously administered IFNγ. Having established a method by which ACKR2 expression could be induced, initial experiments were designed to determine if induction of ACKR2 could prevent the development of psoriasiform lesions. Results showed that IFNγ administered the day before IMQ (to upregulate ACKR2 prior to IMQ application) and throughout IMQ treatment, significantly limited the severity of skin inflammation in WT mice. In keeping with the reduced clinical severity of psoriasiform inflammation that was achieved with IFNγ administration, experiments also confirmed a reduction in the production of

CCL5 (a T-cell chemotactic, psoriasis-associated ACKR2 ligand), CCL20 and IL-17 in IFNγ as apposed to control treated mice, following application of IMQ. Experiments using IFNγ combined with topical IMQ were additionally performed in ACKR2-/- to assess the ACKR2-dependency of the observations. Results showed that IFNγ did not confer a protective effect against IMQ induced inflammation in ACKR2-/- as compared to WT mice. Unexpectedly, at one time point (day 3) inflammation was enhanced in IFNγ treated mice with IMQ treated skin. This would be in keeping with IFNγ having both pro- and anti-inflammatory effects *in vivo*; it is possible that where ACKR2 is absent, IFNγ cannot exert its anti-inflammatory effect through ACKR2 upregulation, which shifts the balance in favour of the pro-inflammatory effects of IFNγ. This in turn, could have been manifest as enhanced psoriasiform inflammation in these experiments. Further experiments would however be necessary, to determine the mechanism of such pro-inflammatory effects.

As previously discussed, in humans with psoriasis, there is reduced ACKR2 expression in psoriatic plaques, but elevated levels in remote unaffected skin (Singh et al. 2012). Next, experiments were conducted to determine whether the human psoriatic ACKR2 expression patterns (both in inflamed and remote skin) could be replicated in the IMQ model. As in human disease, induction of psoriatic plaques through the use of IMQ was associated with a reduction of ACKR2 mRNA expression in the plaque itself. IMQ alone did not lead to an upregulation of remote ACKR2 in mice, however as IFNγ appears to be deficient in the IMQ model and is the most potent inducer of ACKR2 identified to date, it was hypothesised that concurrent administration of recombinant injected IFNγ could overcome the lack of remote ACKR2 upregulation in the IMQ model. Data confirmed this hypothesis; systemic IFNγ plus IMQ applied to one flank, was associated with a substantial increase in ACKR2 mRNA expression in remote unaffected skin, as compared to IFNγ alone. These data imply that there are factors, possibly released by the psoriasiform plaque, that synergise with the ACKR2 induction caused by IFNγ. Furthermore, results highlight a novel mechanism by which inflammation *in vivo* could be spatially restricted; It was hypothesised that induction of one psoriasiform lesion in the context of IFNγ associated inflammation (as in

human psoriasis), leads to a remote upregulation of ACKR2. Upregulated remote ACKR2 in turn, acts to limit the spread of inflammation. This hypothesis was confirmed through experiments where a second skin site was treated with IMQ, following the establishment of a first lesion with IMQ/concurrent IFNγ in order to upregulate ACKR2 remotely; specifically, inflammation was significantly limited at the second IMQ treated site. There was significantly reduced epidermal thickening, Ki67 epidermal staining and restricted CD3+ epidermal entry at the second induced lesion where ACKR2 expression was elevated. These results were dependent on ACKR2, as repeat experiments in ACKR2-/- mice showed that, in contrast to WT mice, IMQ plus systemic IFNγ did not protect remote sites against IMQ driven inflammation in ACKR2 deficient mice.

Lastly, in order to better understand the T-cell infiltrate in IMQ treated skin, skin sections from IMQ treated WT, ACKR2-/- and WT+ IFNγ mice, were stained for CD3+, CD4+, CD8+, CD25+ and FoxP3 positive cells. Whilst there were no significant differences between the treatment groups in terms of the total number of cells positive for the above markers in *whole* skin, differences were striking when the proportion of infiltrating skin cells that localised in the epidermis were determined. Data showed that the epidermal exclusion of T-cells in WT/WT+ IFNγ is predominantly skewed against CD4+ cells, in contrast to ACKR2-/- mice.

In conclusion, data presented in this chapter highlight ACKR2 as being important not only to restrict skin inflammation at the first psoriasiform lesion, but also in limiting the further spread of inflammation beyond the first skin lesion. This provides a novel mechanism by which psoriasiform inflammation may be spatially restricted in vivo, and highlights ACKR2 induction as a novel therapeutic approach in the treatment of psoriasiform inflammation.

CHAPTER 5

5 Psoriasis associated microRNAs regulate expression of ACKR2 in human primary keratinocytes and lymphatic endothelial cells.

5.1 Contents

5.2

Hypothesis

5.3 Aims

5.4 Introduction

5.5 Results

5.5.1 Three microRNAs, predicted to bind the ACKR2 3'-UTR are differentially expressed in psoriatic lesions.

5.5.2 A microRNA transfection protocol was developed for use in primary human cells.

5.5.3 miR-146b and miR-10b reduce the expression of ACKR2 mRNA in primary human KC and LEC respectively.

5.5.4 A Dual-Glo™ Luciferase Assay was optimised to determine whether miR-10b/miR-146b modulate ACKR2 expression through directly binding the ACKR2 3'-UTR.

5.5.5 Cytoplasmic ACKR2 can be visualised in ACKR2 transfected HEK293 cells through immunofluorescent antibody staining.

5.5.6 miR-146b transfection of KC and miR-10b transfection of LEC reduce cytoplasmic ACKR2 expression.

5.5.7 miR-146b transfection of KC and miR-10b transfection of LEC reduce ACKR2 protein expression.

5.6 Summary Chapter 5

5.2 Hypothesis

- Psoriasis-associated microRNAs are negative regulators of ACKR2 expression in keratinocytes (KC) and lymphatic endothelial cells (LEC)

5.3 Aims

The aims of this chapter were to;

- Identify microRNAs capable of differentially regulating ACKR2 in primary human keratinocytes and lymphatic endothelial cells
- Determine whether identified microRNAs bind directly to the 3'-UTR of ACKR2

5.4 Introduction

ACKR2 expression is relatively deficient in psoriatic plaques. In contrast, ACKR2 expression in clinically unaffected remote skin (*remote* from inflammatory psoriatic lesions) is relatively high (Singh et al. 2012). ACKR2 acts as a scavenger of pro-inflammatory CC-chemokines, and has a role in limiting excessive/deleterious inflammation *in vivo* (Nibbs et al. 2007). It was hypothesised that the high ACKR2 expression in unaffected remote skin in psoriasis (where it is mainly expressed in the lower epidermis (Singh et al. 2012)) prevents excessive inflammation and thus psoriatic plaque development. In keeping with this hypothesis, previous chapters of this thesis demonstrated that a lack of ACKR2 enhanced CD3+ T-cell positioning in the epidermis and exaggerated psoriasiform inflammation in the IMQ mouse model (chapter 3). In contrast, where ACKR2 expression was induced *in vivo*, skin was significantly protected against psoriasiform inflammation (Chapter 4). However, the mechanism by which ACKR2 expression is relatively *de*creased in psoriatic plaques is not known. Insights into the molecular mechanism(s) by which ACKR2 downregulation is controlled, will aid in our understanding of the reasons why ACKR2 expression is focally deficient (e.g. in plaques). In addition, this could help provide a possible novel therapeutic target in limiting psoriasiform inflammation.

MicroRNAs have emerged as the most abundant class of gene regulators, and have been implicated in a range of inflammatory disease processes. They predominantly act as negative regulators of gene expression at a post-transcriptional level (Pasquinelli 2012). Specifically, microRNAs bind their

mRNA target 3'-utranslated region (3'-UTR), and lead to the degradation of their mRNA target (microRNA biosynthesis and target interactions are represented schematically in Supplementary Figure 5.1). Typically, one microRNA binds multiple mRNA targets, and the same mRNA 3'-UTR can be targeted by numerous microRNAs; this promiscuity introduces a significant degree of complexity in microRNA/target interactions and subsequent gene expression (Eulalio & Mano 2015). Recent studies have shown that a large number of microRNAs are differentially expressed in psoriasis, with many being significantly overexpressed in the psoriatic plaques (Sonkoly et al. 2007). Given their abundance as negative regulators of gene expression, microRNAs are thus plausible regulators of ACKR2 expression. There exist bioinformatics tools, that enable *in silico* predictions of which microRNAs might target any specific mRNA 3'-UTR. Such databases use microRNA-mRNA complementarity as well as microRNA conservation across species, in order to predict the likelihood of binding *in vivo* (Ekimler & Sahin 2014). It was therefore hypothesised that microRNAs capable of negatively regulating ACKR2 mRNA via binding to the 3'-UTR could be identified through studying microRNAs that are both 1) differentially expressed in psoriasis (where ACKR2 expression is diminished in plaques) and 2) are predicted to bind the ACKR2 3'-UTR *in silico*. Particular emphasis was placed on keratinocytes (KCs) and lymphatic endothelial cells (LECs), as these are the skin cells in which ACKR2 expression is particularly high and of direct relevance to skin inflammation (Griffith, Sokol & Luster 2014; McKimmie et al. 2013; Griffith, Sokol & Luster 2014).

5.5 Results

5.5.1 Three microRNAs, predicted to bind the ACKR2 3'-UTR are differentially expressed in psoriatic lesions.

Though cytokines have been identified that upregulate of ACKR2 (e.g. Th1 and Th17 cytokines, see Chapter 3), the precise molecular mechanisms whereby ACKR2 is downregulated are not known. In particular, we do not understand the molecular mechanisms by which ACKR2 expression is reduced

within psoriatic plaques, where ACKR2 expression is relatively deficient as compared to unaffected skin of patients with psoriasis (Singh et al. 2012). MicroRNAs are generally considered the largest class of regulators of gene expression, but their role in regulating ACKR2 has remained unexplored. In order to identify possible microRNA regulators of ACKR2 expression, the bioinformatics database TargetScan was used to identify possible microRNA targets. Results were filtered such that only microRNAs that are broadly conserved amongst vertebrates would be identified, in order to increase the likelihood of identified microRNA species being biologically relevant. Through this search strategy, 16 microRNAs were identified that were both 1) predicted to bind the 3'-UTR of human ACKR2, and 2) were broadly conserved amongst vertebrates (Figure 5.1). The more negative the 'total context score' becomes, the more likely that this miRNA is predicted to bind to the 3'-UTR. In Figure 5.1, the miRNAs are ranked in descending likelihood of binding the ACKR2 3'-UTR

Previously published studies have identified numerous microRNAs that are differentially expressed in psoriatic skin, though their role in psoriasis pathogenesis has remained relatively unknown (Sonkoly et al. 2007; Zibert et al. 2010). As microRNAs are predominantly negative regulators of gene expression, emphasis was placed on microRNAs that were *up*regulated in the psoriatic plaque (where ACKR2 expression is comparatively reduced). In this manner, by comparing 1) the list of microRNAs that are predicted to bind the 3'-UTR of ACKR2 *in silico* and 2) microRNAs previously shown to be differentially regulated in psoriasis, it was possible to identify 3 single microRNAs that were present in both lists; miR-10, miR-146 and miR-203. Interestingly, each of these miRNAs had a particularly high in silico likelihood of regulating ACKR2 (Figures 5.2 and 5.3). Additionally, all three microRNAs have been shown to play roles in skin homeostasis and inflammation (Xue et al. 2011; Saba et al. 2014; Primo et al. 2012), thus making them plausible candidates as ACKR2 regulators. miR-146 and 203 had been previously shown to be upregulated in psoriatic lesions (where ACKR2 expression is limited). In contrast, miR-10 is upregulated in unaffected skin, but has a particularly high predictive score for binding ACKR2. For the above reasons, these three

microRNAs were selected for further evaluation as possible regulators of ACKR2 expression.

5.5.2 A microRNA transfection protocol was developed for use in primary human cells.

In order to ensure successful transfection of cells, first the appropriate concentration of microRNA to be complexed with transfection reagent was determined. This was to ensure that the delivered concentration would be tolerated by primary cells without causing cell death, whilst also enabling efficient delivery of microRNAs to the cytoplasm. The cell types tested were those with apparently highest ACKR2 expression in skin; healthy human primary keratinocytes (KC) and lymphatic endothelial cells (LEC) (Griffith, Sokol & Luster 2014; McKimmie et al. 2013). A microRNA concentration of 10nM has been previously used in the literature with human cells, that were transfected at 70% cell confluence (Sonkoly et al. 2009). This previously used protocol was taken as the starting point in developing transfection protocols. Three concentrations of microRNAs were initially tested in pilot experiments; transfection reagent without microRNA, 10nM and 30nM;. Whilst transfection reagent (RNAiMax) alone, and microRNA at 10nM caused no cell death or discernible morphological changes in confluent cell monolayers of KC or LEC, cells were not viable/adherent after 24 hours upon treatment with 30nM microRNA (*data not quantified*). Interestingly, cells were viable if 10nM of several different microRNAs were used up to a total of 30nM (see below for details). A maximum of 10nM of *each type* of microRNA was thus used for subsequent experiments presented below.

As demonstrated in chapter 3 of this thesis, inflamed cells upregulate ACKR2 expression. In order to determine whether microRNAs are capable to reduce ACKR2 expression also in the context of upregulated ACKR2, microRNAs were transfected into both healthy and inflamed cells. In order to ensure that microRNAs were successfully transfected into both normal and inflamed cells, initially healthy KC and KC treated with IFNγ (to upregulate ACKR2) were transfected with miR-146b for 24h and the reduction of the expression of previously validated miR-146b targets (IRAK1 and TRAF6) determined by QPCR (Figure 5.4a-b). As predicted, 10nM miR-146b led to a significant

reduction in the expression of IRAK1 and TRAF6, both in untreated (Figure 5.4a) and IFNγ treated KC (Figure 5.4b) at 24 hours. IFNγ is a potent inducer of ACKR2 expression, and IFNγ treated cells were included in order to ensure that the microRNA-induced repression of gene expression would also be evident in the context of high ACKR2 expression. Next, the optimal duration of transfection was determined using KC, with cells treated with 10nM miR-146b for 8, 24 and 48h. Expression of IRAK1 (Figure 5.5a) as well as TRAF6 (Figure 5.5b) mRNA were significantly reduced at all time points with miR-146b as compared to scrambled miR control (Figure 5.5). In the case of ACKR2 however (Figure 5.6), scrambled miR control was associated with an increased ACKR2 expression at 48h as compared to 24h. This would be in keeping with the process of transfection itself being associated with an upregulation of ACKR2 at 48h. This in turn could be possible marker of confounding off target effects of the transfection process at 48h. Therefore, 24h was chosen at the duration of transfection that 1) led to the most apparent reduction in ACKR2 expression, but 2) with no apparent upregulation of ACKR2 due to the process of microRNA transfection. Together, these results demonstrated that microRNA could be successfully delivered into the cytoplasm of KC.

5.5.3 miR-146b and miR-10b reduce the expression of ACKR2 mRNA in primary human KC and LEC respectively.

Having shown, at least in principle, utilising KC and previously validated miR targets, that functional microRNAs can be delivered intracellularly, next both KC and LEC were transfected with the main microRNAs identified as potentially targeting ACKR2; miR-10a, miR-146b and miR-203. It is acknowledged that whilst viability of both KC and LEC was determined, optimisation of microRNA dose and duration of transfection was conducted in KC alone, and the protocol extrapolated to LECs. Optimisation should be conducted separately in LECs and further cell types in the future.

Primary cells from at least two separate healthy donors were used for all subsequent experiments, with 3 replicates being used per experiment (tissue culture wells or tissue culture flasks). Data showed that miR-146b significantly suppressed ACKR2 mRNA expression in KC as compared to

scrambled miR control (Figure 5.7a), with data being representative of two separate experiments. In contrast, miR-146b inhibitor (also known as antagomirs) did not influence ACKR2 expression. This is suggestive of there being low levels of miR-146b expression in KC in non-inflamed contexts (Figure 5.7a)

The above *in silico* analyses predicted that miR-146a and miR-146b both bind the ACKR2 3'-UTR with the same C_T score (Figure 5.1). However, previous studies report different results for differential expression of miR-146a and b in psoriasis, which would suggest non-redundant roles (Sonkoly et al. 2007). Thus, in order to determine whether any apparent differences exist between miR-146a and miR-146b, the two were directly compared. Results showed that both miR-146a and miR-146b reduced ACKR2 mRNA expression in KC after 24 hours compared to scrambled miR control, with no significant differences between the two variants (Figure 5.7b). Thus, miR-146a and miR-146b when transfected on their own, resulted in down-regulation of ACKR2 transcript levels.

Next, the other microRNAs identified above (miR-10b and miR-203) as well as specific miR inhibitors, were then tested for their ability to down-regulate ACKR2 in KC, both singly or in combination with each other and miR-146b (maximum concentration of any one species 10nM). Results were not statistically significant for either miR-10b or 203 or combinations in KCs, with the exception of a reduction in ACKR2 expression with miR-203 inhibitor (Figure 5.8b), and an increase with miR-146/203 in combination (Figure 5.8f). Thus, although miR-146 on its own reduced ACKR2 transcript levels, when used in combination with the other two microRNAs, there was no change in ACKR2. It noteworthy that whilst miR-146b alone reduced ACKR2 expression and miR-203 alone did not alter ACKR2 expression, together they cause a paradoxical increase in ACKR2 expression (Figure 5.8f). Complex interactions between microRNAs have been described in the literature (including synergisms and antagonism), but remain poorly understood and characterised (Vasudevan et al. 2007). It is possible that the miR-146/203 effect represents such a synergistic effect, though this particular interaction remains uncharacterised, and is based on a relatively modest effect and limited data.

Next the selected microRNAs were transfected into primary healthy human LECs, singly and in combination (Figure 5.9). Only miR-10b significantly reduced ACKR2 mRNA expression in LECs (Figure 5.9a), with data being representative of two separate experiments. Additionally, transfection of miR-203 inhibitor was associated with a significant increase in ACKR2 expression *in vitro* (Figure 5.9c), This would be in keeping with miR-203 potentially playing a role in limiting ACKR2 expression in healthy (non-inflamed) LECs.

In conclusion, the inhibition of ACKR2 mRNA expression was most substantial with miR-146a/b in KC and miR-10b in LEC. For this reason, these two microRNAs were therefore selected for further study, as detailed below, in each respective cell type.

5.5.4 A Dual-Glo™ Luciferase Assay was optimised to determine whether miR-10b/miR-146b modulate ACKR2 expression through directly binding the ACKR2 3'-UTR.

MicroRNAs exert their effect on mRNA/gene expression principally through binding the 3'-UTR of their transcript target. Thus, a dual-glo luciferase assay was optimised, in order to determine whether the microRNAs that reduce ACKR2 expression in KC and LEC, interact directly with the 3'-UTR of ACKR2 transcript. The principles of this assay, which enables quantification of microRNA to 3'-UTR transcript binding, are schematically summarised in Figure 5.10. In brief, the 3'-UTR of ACKR2 was cloned and inserted into a reporter vector containing two luciferase genes (Figure 5.10). The assay is based on the assumption that the presence of the ACKR2 3'-UTR downstream of the luciferase should enable quantification of miR interactions with the ACKR2 3'-UTR by assessing luciferase expression. To obtain this luciferase reading, cells were assayed for their ability to generate bioluminescence upon addition of Firefly luciferase bioluminescence substrate (and subsequently normalised to Renilla luciferase).

Following insertion of the ACKR2 3'-UTR into the Dual-Glo plasmid, it was sequenced, to ensure the sequence was intact and putative microRNA binding sites were unaffected (Figure 5.11a-b). Two single nucleotide

insertions and one deletion were noted, but were not located near any predicted microRNA binding sites (Figure 5.11). It was deemed that these changes were unlikely to affect binding of the miRNA to its putative RNA target. The reporter vector was transfected into HEK293 cells. Stable transfectants were selected using neomycin and clonal populations isolated as single colonies isolated in the presence of G418 (Figure 5.12). Firstly, to determine that these new luciferase-expressing clones could be transfected with microRNAs and that this led to gene expression changes, the expression of IRAK1 was determined in stable HEK transfectants. This showed that miR-146b downregulated IRAK1 in the stable transfectants (two different clones tested), thereby confirming that miR-146 could be successfully transfected into HEK cells (Figure 5.13).

Next, experiments were designed to determine whether transfection with miR-146b and miR-10a could also decrease luciferase expression, and so demonstrate that they interact directly with the ACKR2 3'-UTR transcript (Figure 5.14). These data show that these miRNAs could bind to the 3'-UTR transcript of ACKR2, as a measurable and significant decrease in bioluminescence was observed in ACKR2 3'-UTR-containing HEK293 cells, using two different stable HEK293 transfected clones. Inhibition of this signal by the presence of ACKR2 3'-UTR in the plasmid following transfection of the miR suggest that these miR do bind to the ACKR2 3'-UTR, and that this binding can inhibit the expression of the upstream ACKR2 gene (Figure 5.14). Importantly, both miR-146 and miR-10 were able to reduce the luciferase expression driven from ACKR2 3'-UTR constructs.

5.5.5 Cytoplasmic ACKR2 can be visualised in ACKR2 transfected HEK293 cells through immunofluorescent antibody staining.

Although ACKR2 scavenging entails ACKR2 cycling from the cell surface to the cytoplasm, the bulk of ACKR2 in cells at any given time is localised in the cytoplasm, specifically in recycling endosomes (Blackburn et al. 2004) Data above demonstrate that microRNA transfection (miR-146b in KC, and miR-10b in LEC) reduce ACKR2 mRNA expression (Figure 5.7 and 5.9). In order to examine the effect of miR-146 and miR-10 on ACKR2 protein expression and

localisation in cells, published ACKR2 immunofluorescent staining protocols (Singh et al. 2012), were firstly optimised. HEK293 cells that had been previously generated to stably express ACKR2 were stained for ACKR2 and compared with transfected HEK293 cells (that do not express ACKR2) as negative controls. Confocal immunofluorescent images confirmed that ACKR2 could be clearly visualised in the cytoplasm of HEK-ACKR2 cells (Figure 5.15). In contrast, non-transfected HEK293 cells that were negative for ACKR2 when similarly stained, did not stain for ACKR2. A degree of green background staining throughout the cytoplasm was noted in ACKR2 deficient cells, but this staining was faint, and diffuse compared with ACKR2 transfected HEK293 cells (Figure 5.15).

5.5.6 miR-146b transfection of KC and miR-10b transfection of LEC reduce cytoplasmic ACKR2 expression.

Next, in order to determine qualitative changes in ACKR2 subcellular localisation, a protocol was optimised to enable staining of ACKR2 in KC monolayers grown in polycarbonate chambers. KC were grown as confluent cell monolayers (Figure 5.16a), and fixed using methanol prior to immunofluorescent staining. There was a consistent degree of cytoplasmic staining even with isotype control antibodies, but again this staining was faint, evenly distributed throughout the cytoplasm, and non-punctate (Figure 5.16b). In order to determine the effect of miR-146b on ACKR2 expression and localisation, confluent KC monolayers were transfected for 24 hours. The cell medium was changed after 24 hours, but the KC incubated for a further 24 hours prior to fixing with methanol. This was due to the long half-life of ACKR2 protein; whilst a reduction in ACKR2 mRNA was observed after 8-24 hours of transfection (as previously presented), it was anticipated that a discernible reduction, or change in localisation, in cytoplasmic ACKR2 protein would take longer to be evident. Bright green punctate cytoplasmic staining was observed in KC transfected with negative scrambled miR control (Figure 5.17a). The staining was more marked in the peri-nuclear region and often in an asymmetrical fashion, which would be in keeping with higher ACKR2 levels in the endoplasmic reticulum (Figure 5.17a). In future experiments, it would be useful to perform co-stains with markers of early

and late endosomal compartments. In contrast, where KC had been transfected with miR-146b, there was a loss of ACKR2 staining throughout the cytoplasm, although the peri-nuclear staining was still evident (Figure 5.17b). These findings paralleled mRNA data presented above.

To investigate the effect of miR-10b on LECs, LECs that had been grown as confluent cell monolayers were transfected for 24 hours (Figure 5.18a). As previously, cells were incubated for a further 24 hours after the medium was changed. Similar to KC, there was a degree of faint/hazy green staining with isotype antibody control staining (Figure 5.18b). In contrast, ACKR2 staining was more pronounced and more granular where LECs had been transfected with scrambled miR control (relatively high ACKR2) as compared to miR-10b (Figure 5.18c-d). Following transfection with miR-10b, cytoplasmic green fluorescence levels were more in keeping with the fluorescent levels seen with isotope antibody background staining (Figure 5.18b). Overall, the level of fluorescence was apparently lower than KC, which is likely a reflection of lower ACKR2 expression in LEC as compared to KCs. Since images were obtained using a confocal microscope, the fact that LECs are substantially flatter/thinner than KC when grown as monolayers should not have made a substantial difference on the degree of green staining. The granular staining in LEC was again more marked to one side of the peri-nuclear cytoplasm (akin to what was observed in KC), which became especially apparent at higher magnification (Figures 5.19a-b), especially when compared to miR-10b transfected LECs (Figures 5.20a-b).

Taken together, immunofluorescent staining of cultured cell monolayers did enable staining for ACKR2, that appeared granular and more pronounced in the peri-nuclear area in the cytoplasm in both KC and LEC. Furthermore, transfection with miR-146b in KC and miR-10b in LEC lead to an apparent reduction in ACKR2 staining in both cell types, at 48 hours. This suggests that the aforementioned microRNAs not only lead to a reduction in ACKR2 mRNA expression in these cells, but possibly also a reduction in ACKR2 protein. It would also have been useful to quantify these changes, and numerical data pooled from multiple experiments would have strengthened the argument. In future experiments, the Zeiss software could be used to quantify the

fluorescence associated with ACKR2, across different experiments, and at different sites along the slide.

5.5.7 miR-146b transfection of KC and miR-10b transfection of LEC reduce ACKR2 protein expression by Western Blot.

Previous studies have demonstrated successful ACKR2 detection using Western Blotting (Blackburn et al. 2004). Western Blots enable relatively easy quantification of protein expression (through band densitometry), but also yield useful information about the ACKR2 protein (Blackburn et al. 2004). Previous studies have shown that ACKR2 does not appear as one isolated band on Western blots (Blackburn et al. 2004). Instead, several bands appear, that have been attributed to different levels of e.g. glycosylation and multimerisation state (Blackburn et al. 2004). In order to gain a better understanding of the effect of microRNAs on ACKR2 expression, cells were again grown as confluent monolayers and transfected with microRNAs for 24 hours, then incubated for a further 24 hours. To ensure that ACKR2 could be successfully identified using Western Blotting, lysates from ACKR2 transfected HEK293, and ACKR2-deficient HEK293 were studied. This revealed two darker bands (at 55kDa and 38kDa) and a stack of 3 more faint bands at 41/45/49 kDa (Figure 5.21). This appearance is in keeping with previously published data (Blackburn et al. 2004). Based on the predicted size of ACKR2 and previous studies, it is likely that the band at 49kDa represented the non-glycosylated form of ACKR2, and the darker band at 55kDa a glycosylated form, and smaller bands ACKR2 fragment(s).

Subsequently, KC were transfected with miR-146b prior to lysis. Throughout the experiments, ACKR2 transfected HEK293 and untransfected HEK293 cells were used as positive and negative controls respectively, and run on the same gel as other samples. Blots demonstrated bands in KC that are broadly similar to those observed in the positive HEK293 control (Figure 5.22). The main band at 49kDa appeared more faint where the KC has been transfected with miR-146b, which is keeping with both QPCR and the immunohistochemistry data. Though other bands appear more faint in miR-146b treated KC, the difference appeared more marked for the 49kDa band, which suggested that miR-146b induced ACKR2 reduction does not affect all

protein forms of ACKR2 equally. The functional significance of this however remains to be determined. Additionally, bands appear at approximately 100kDa (in contrast to HEK293 transfectants), and as previous studies suggest, these could represent dimerised or glycosylated variants of ACKR2.

Using ImageJ, the density of the bands were quantified, and normalised to the beta-tubulin loading control (Figure 5.23). Given the multiple bands that likely represented ACKR2, choosing one single band is challenging and might yield misleading results. To reduce the risk of this, analysis was conducted in two alternative ways; 1) densitometry of all bands likely to represent ACKR2 in KC (Figure 5.23a, bands marked in black), and 2) densitometry of the bands *most* likely to represent ACKR2 at 40-50kDa and also the dimerised form (Figure 5.23a, bands marked in red). Either approach yields a comparable reduction of band density (adjusted to the loading control) of approximately 20% (Figure 5.23b). It is acknowledged that quantification of less than three blots limits the conclusions that can be drawn, and in future experiments, it would be helpful to quantify change in band density in three or more blots, in order to yield more robust and reproducible results.

Next, LECs were transfected with miR-10b. As the amount of ACKR2 was anticipated to be less than KC, in addition to miR-10b/scrambled miR control treated LECs, LECs were included that had been treated with IFNγ (for 24h during the time of miR transfection, and then incubated for a further 24 hours), in order to upregulate ACKR2 expression. As in KCs, bands were generally more faint in miR-10b transfected LECs, which suggested that protein expression levels were reduced (Figure 5.24), although further repeat experiments are needed before drawing firm conclusions. Furthermore, the bands were more marked in IFNγ treated LECs, which suggested that ACKR2 protein expression was successfully induced in these cells (Figure 5.25). The differences between the different treatments were more apparent in the 49kDa band, and in the 38kDa band in LECs. This would be in keeping with KCs and LECs expressing ACKR2 with distinct glycosylation/fragmentation patterns.

As in KC, adjusted densitometry was employed, using two different methodologies akin to those used for KC above; 1) densitometry of all bands likely to represent ACKR2 in LEC (Figure 5.26a, bands marked in black), and

2) densitometry of the bands *most* likely to represent ACKR2 at 40-50kDa and also the dimerised form (Figure 5.26a, bands marked in red). Either method of quantification was associated with a reduction of band density adjusted for loading control, of approximately 20-25% (Figure 5.26), but further repeat experiments are required in order to draw more certain conclusions about the effect of microRNA transfection on the quantity of ACKR2 protein, notably in the context of relatively small changes in apparent band density.

TargetScanHuman
Prediction of microRNA targets
Release 6.2: June 2012

Human CCBP2 (NM_001296) 3' UTR miRNA Table

Table sorted by total context score [Sort table by aggregate P_{CT}]

miRNA families broadly conserved among vertebrates

miRNA	conserved sites				poorly conserved sites				Total Context score	Aggregate P_{CT}
	Total	8mer	7mer-m8	7mer-1A	Total	8mer	7mer-m8	7mer-1A		
miR-10abc/10a-5p	0	0	0	0	3	0	3	0	-0.57	< 0.1
miR-490-3p	0	0	0	0	2	0	1	1	-0.29	< 0.1
miR-146ac/146b-5p	1	1	0	0	0	0	0	0	-0.26	< 0.1
miR-203	0	0	0	0	1	1	0	0	-0.19	< 0.1
miR-210	0	0	0	0	1	0	1	0	-0.15	< 0.1
miR-24/24ab/24-3p	0	0	0	0	2	0	0	2	-0.15	< 0.1
miR-122/122a/1352	0	0	0	0	1	0	0	1	-0.13	< 0.1
miR-103a/107/107ab	0	0	0	0	1	0	0	1	-0.13	< 0.1
miR-145	0	0	0	0	1	0	0	1	-0.10	< 0.1
miR-375	0	0	0	0	1	0	0	1	-0.09	< 0.1
miR-217	0	0	0	0	1	0	1	0	-0.07	< 0.1
miR-219-5p/508/508-3p/4782-3p	0	0	0	0	1	0	0	1	-0.04	< 0.1
miR-139-5p	0	0	0	0	1	0	1	0	-0.03	0.13
miR-143/1721/4770	0	0	0	0	1	0	0	1	-0.01	< 0.1
miR-129-5p/129ab-5p	0	0	0	0	1	0	0	1	-0.01	0.33
miR-133abc	0	0	0	0	1	0	0	1	N/A	< 0.1

Figure 5.1 TargetScan *in silico* predictions of microRNAs potentially binding the ACKR2 3'-UTR

Table of microRNAs that are broadly conserved amongst vertebrates that are predicted (in descending order of likelihood, less negative Total Context Score) to bind the human ACKR2 3'-UTR.

miR (broadly conserved among vertebrates)	Total Context Score	regulation in psoriasis
miR-10abc/10a-5p	-0.57	miR-10b 1.32-fold up-regulated in PN[1] miR-10a 0.67-fold down-regulated in PP[2]
miR-490-3p	-0.29	n/a
miR-146ac/146b-5p	-0.26	miR-146a 3.10-fold upregulated in PP, miR-146b-59 up-regulated 2.73-fold[Q] miR-146a 3.30-fold up-regulated in PP[2] miR-146b up-regulated 3.31-fold in PP[2]
miR-203	-0.19	2.02-fold up-regulated in PP[1] 5.86-fold up-regulated in PP[2]
miR-210	-0.15	n/a
miR-24/24ab/24-3p	-0.15	1.51-fold and 1.41 up-regulated in PP and PN respectively[1]
miR-122/122a/1352	-0.13	n/a
miR-103a/107/107ab	-0.13	1.04-fold up-regulated in PP[1]
miR-145	-0.10	n/a
miR-375	-0.09	n/a

PP – psoriatic lesion (plaque) **PN** – normal (clinically unaffected) psoriatic skin

[1] Zibert J.R. *et al.* MicroRNAs and potential target interaction sin psoriasis. *J Dermatol Sci* **58(3)**, (2010)
[2] Sonkoly E. *et al*. MicroRNAs: novel regulators invovled in the pathogeneis of psoriasis? *Plos One* **2(7)**, e610 (2007)

Figure 5.2 Summary of microRNAs predicted to bind the ACKR2 3'-UTR with associated microRNA specific data from previous psoriasis publications

The 10 microRNAs most likely to target ACKR2 included in the diagram, with relevant findings in two papers given in the right hand column; miR-10, miR-146 and miR-203 were all differentially regulated in psoriasis (previous array data).

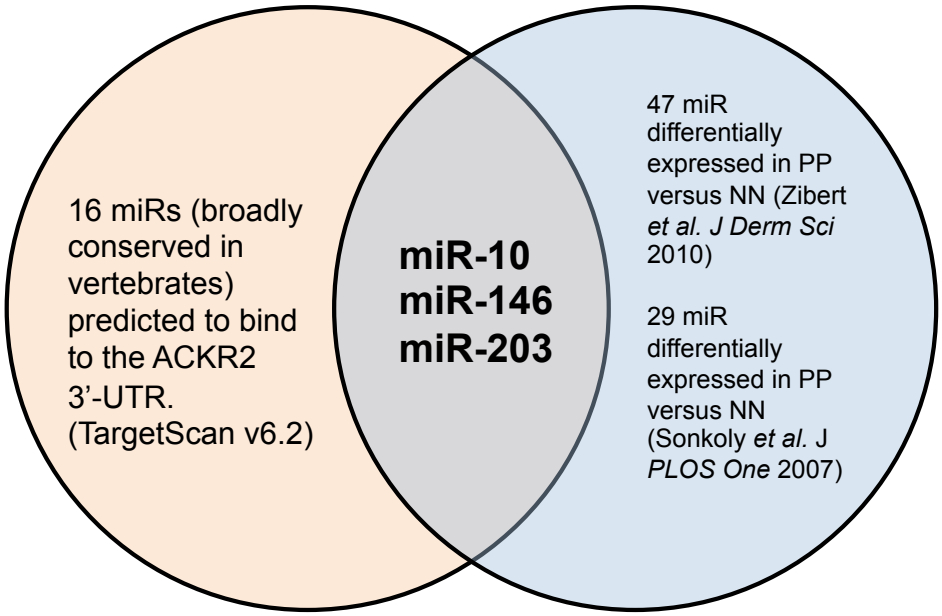

Figure 5.3 Three microRNAs (miR-10, miR-146 and miR-203) are predicted to bind the ACKR2 3'-UTR and are differentially expressed in psoriasis.

Diagrammatic representation of microRNAs that are predicted to bind the ACKR2 3'-UTR *in silico*, and that have ben shown to be differentially expressed in psoriasis in array studies.

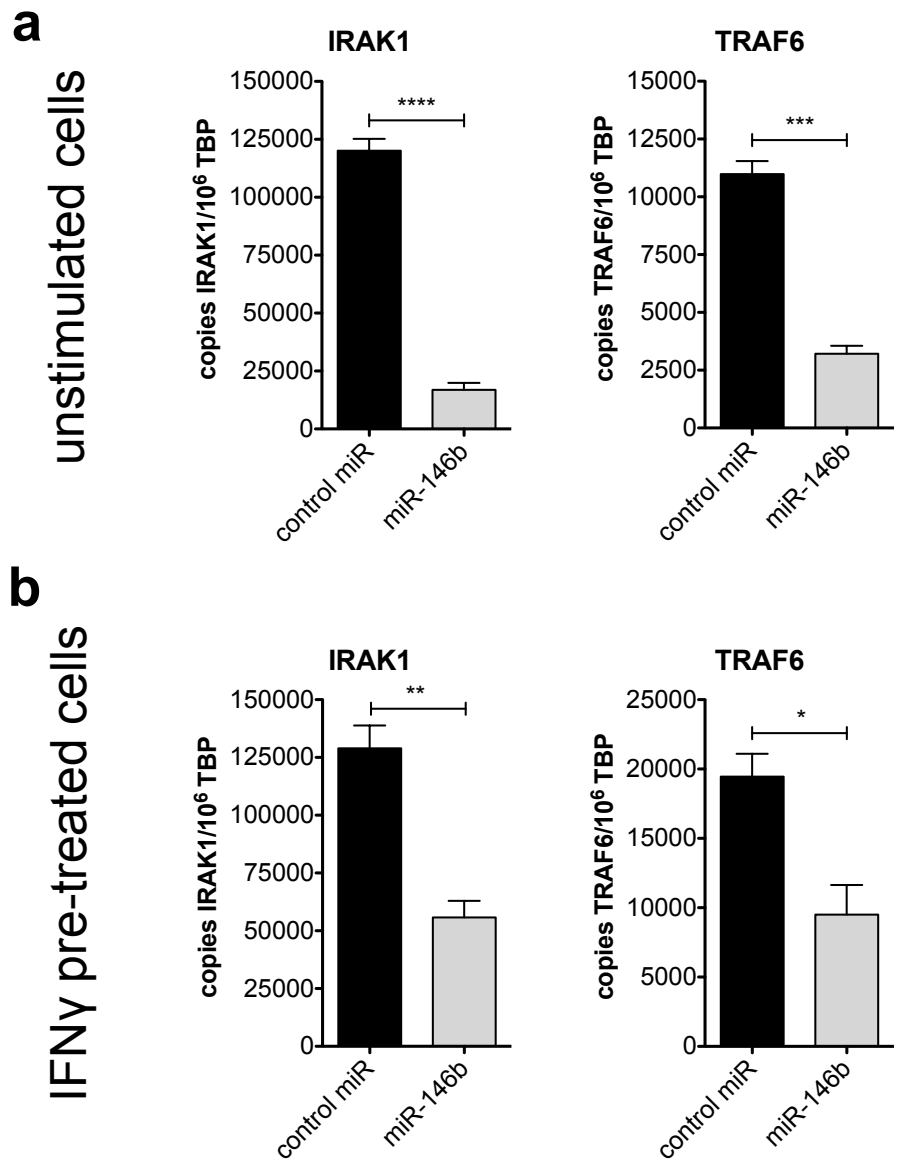

Figure 5.4 MicroRNAs can be successfully transfected into primary human keratinocytes.

Absolute quantification of IRAK/TRAF6 mRNA (previously validated miR146b targets) in primary healthy human keratinocytes that are

(a) unstimulated

(b) stimulated with 100ng/ml of human recombinant IFNγ prior to transfection

Keratinocytes were transfected for 24 hours prior to lysis and RNA extraction. All microRNAs transfected at 10nM. Significance was assessed using Student's t-test. * $P<0.05$, ** $P<0.01$, *** $P<0.005$, **** $P<0.0001$. Each validation experiment performed once.

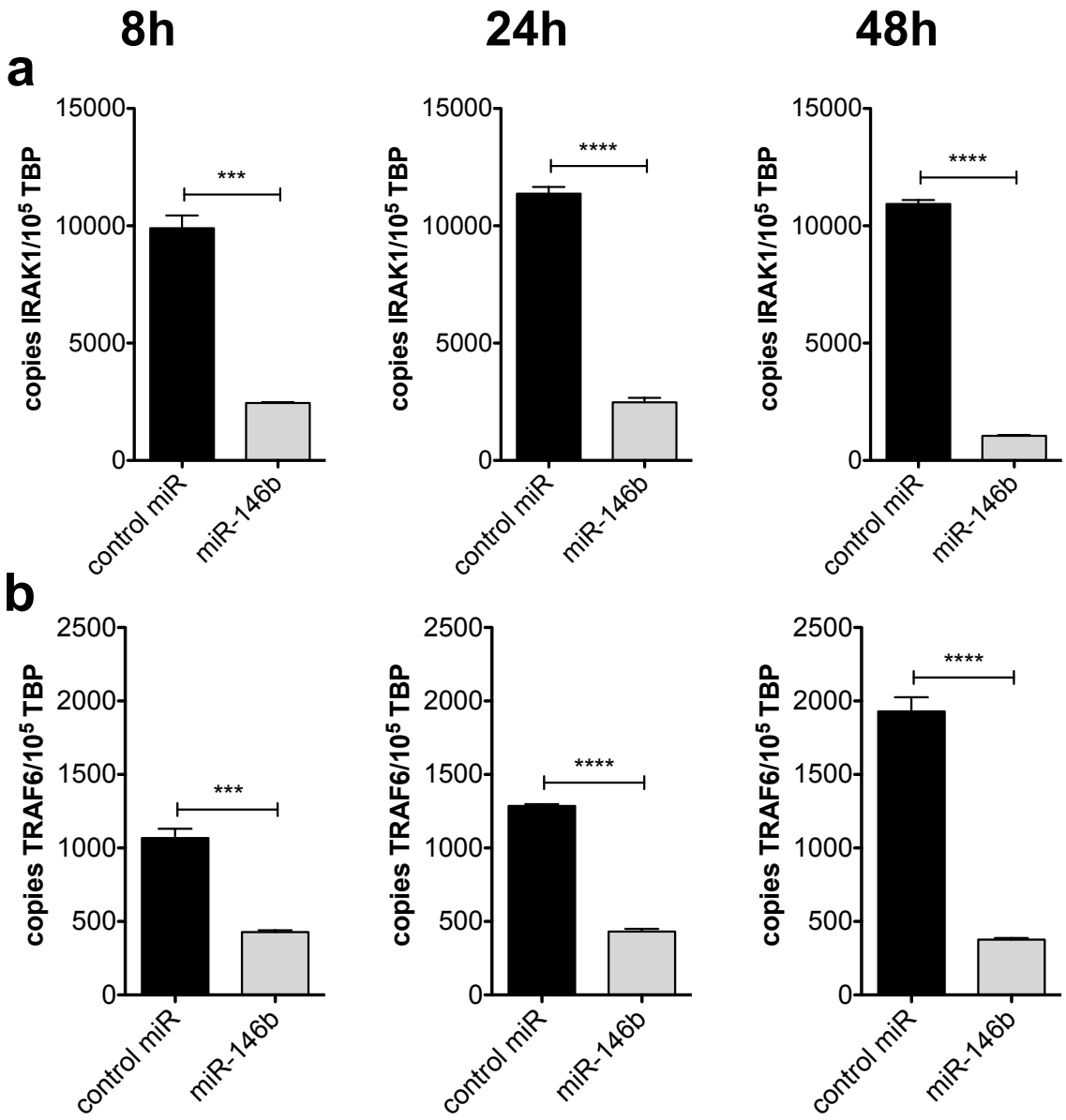

Figure 5.5 MicroRNAs can be successfully transfected into primary human keratinocytes at 8, 24 and 48-hour time points.

Absolute quantification of;

(a) IRAK1 and;

(b) TRAF 6 (both previously validated miR146b targets) in primary healthy human keratinocytes

Keratinocytes were transfected for 24-48 hours, prior to lysis and RNA extraction. All microRNAs at 10nM. Significance was assessed using Student's t-test. * $P<0.05$, ** $P<0.01$, *** $P<0.005$, **** $P<0.0001$. Each time point performed once.

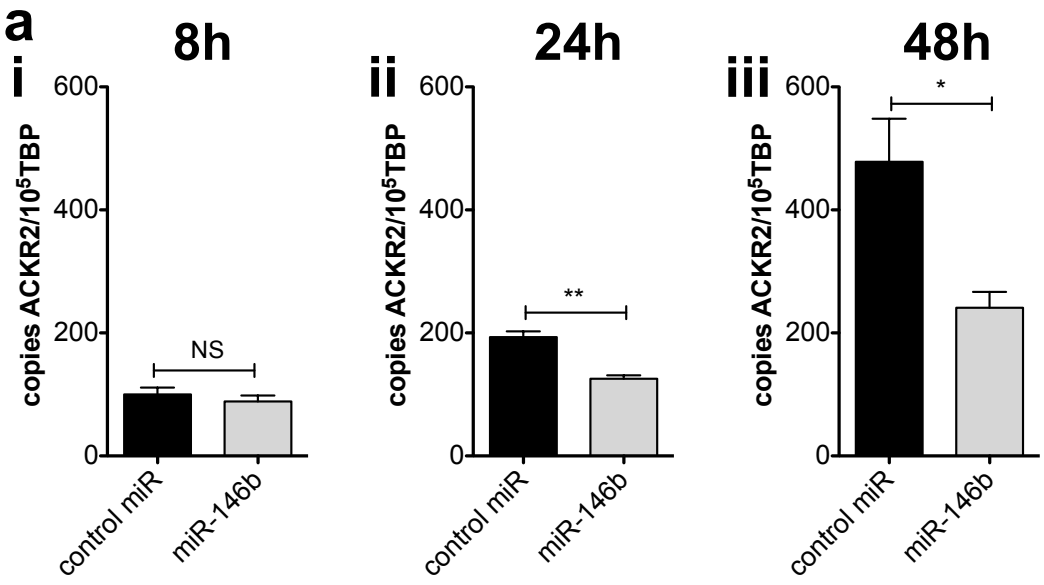

Figure 5.6 miR-146b transfection of primary human keratinocytes for 24-48 hours leads to reduction in ACKR2 mRNA, relative to control miR.

Absolute quantification of gene expression in primary human keratinocytes following transfection with miR-146b for 8, 24 or 48 hours prior to RNA extraction and QPCR for ACKR2.

Keratinocytes were transfected for 24-48 hours, prior to lysis and RNA extraction. microRNAs at 10nM, control is scrambled microRNA. Significance was assessed using Student's t-test * $P<0.05$, ** $P<0.01$. 8h and 48h time points performed once, 24h time point performed three times.

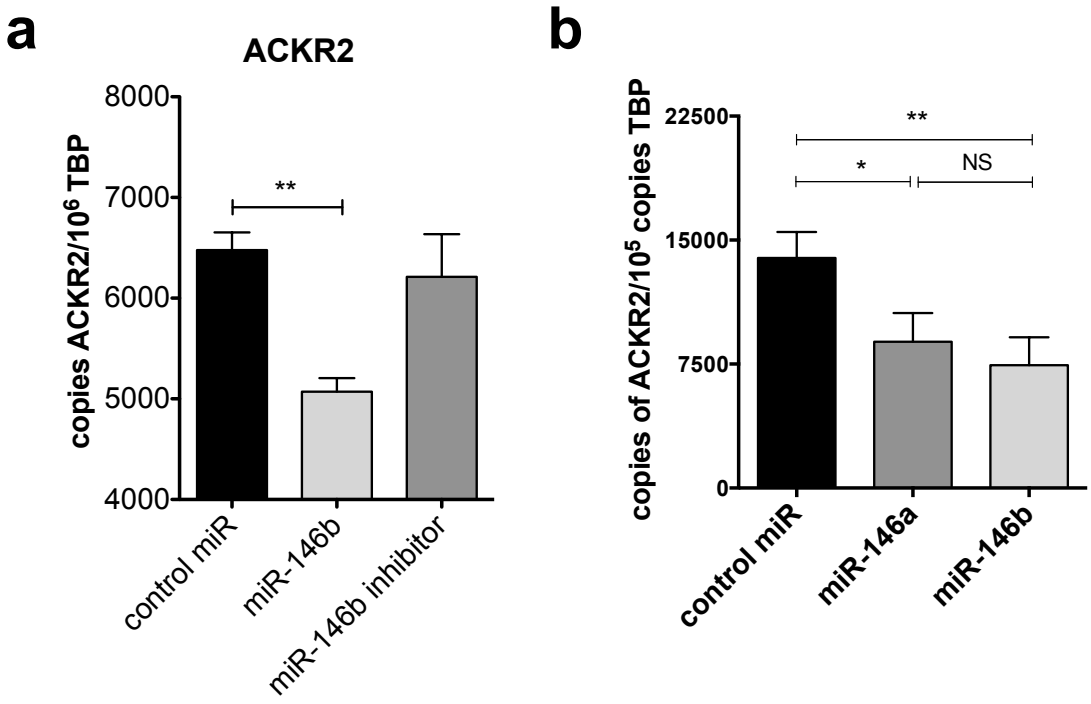

Figure 5.7 miR-146a as well as miR-146b transfection of primary human keratinocytes for 24 hours leads to reduction in ACKR2 mRNA.

Absolute quantification of;

(a) ACKR2 following transfection of KC with miR-146b or miR-146b inhibitor. Representative of three experiments.

(b) ACKR2 following transfection of KC with miR-146a and miR-146b

Keratinocytes were transfected for 24 hours, prior to lysis and RNA extraction. Data from (a) and (b) are from different experiments and cell donors. All microRNAs at 10nM. Significance was assessed by one-way ANOVA. * $P<0.05$, ** $P<0.01$. Comparison performed once.

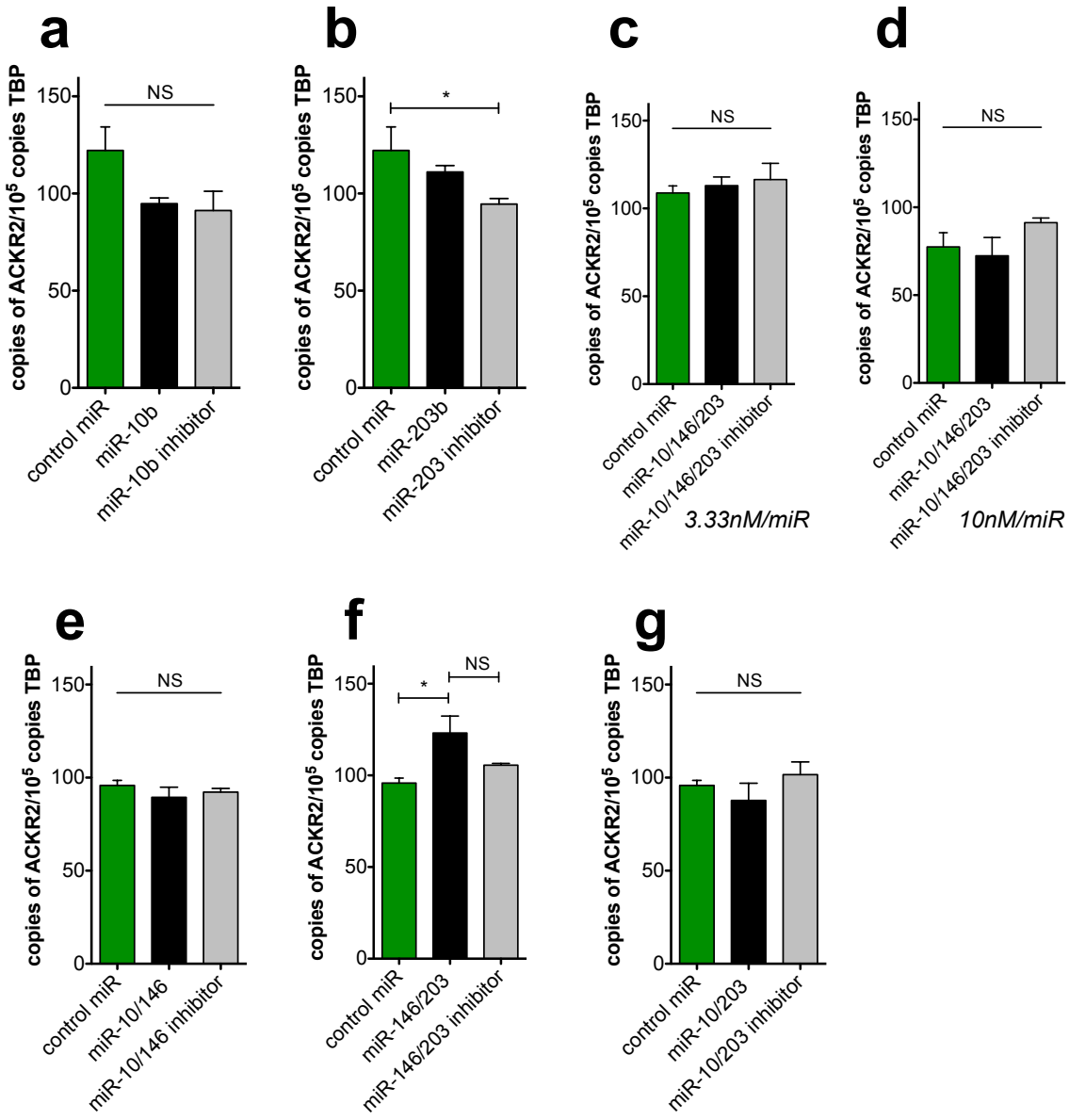

Figure 5.8 miR-10 and miR-203 do not differentially regulate ACKR2 expression in keratinocytes.

Absolute quantification of ACKR2 in primary human keratinocytes following transfection of primary human keratinocytes with various microRNAs (singly and in combination) for 24 hours. All microRNAs transfected at 10nM, unless otherwise stated. Significance was assessed using one-way ANOVA with Tukey's post-test. * $P<0.05$. Experiment performed once.

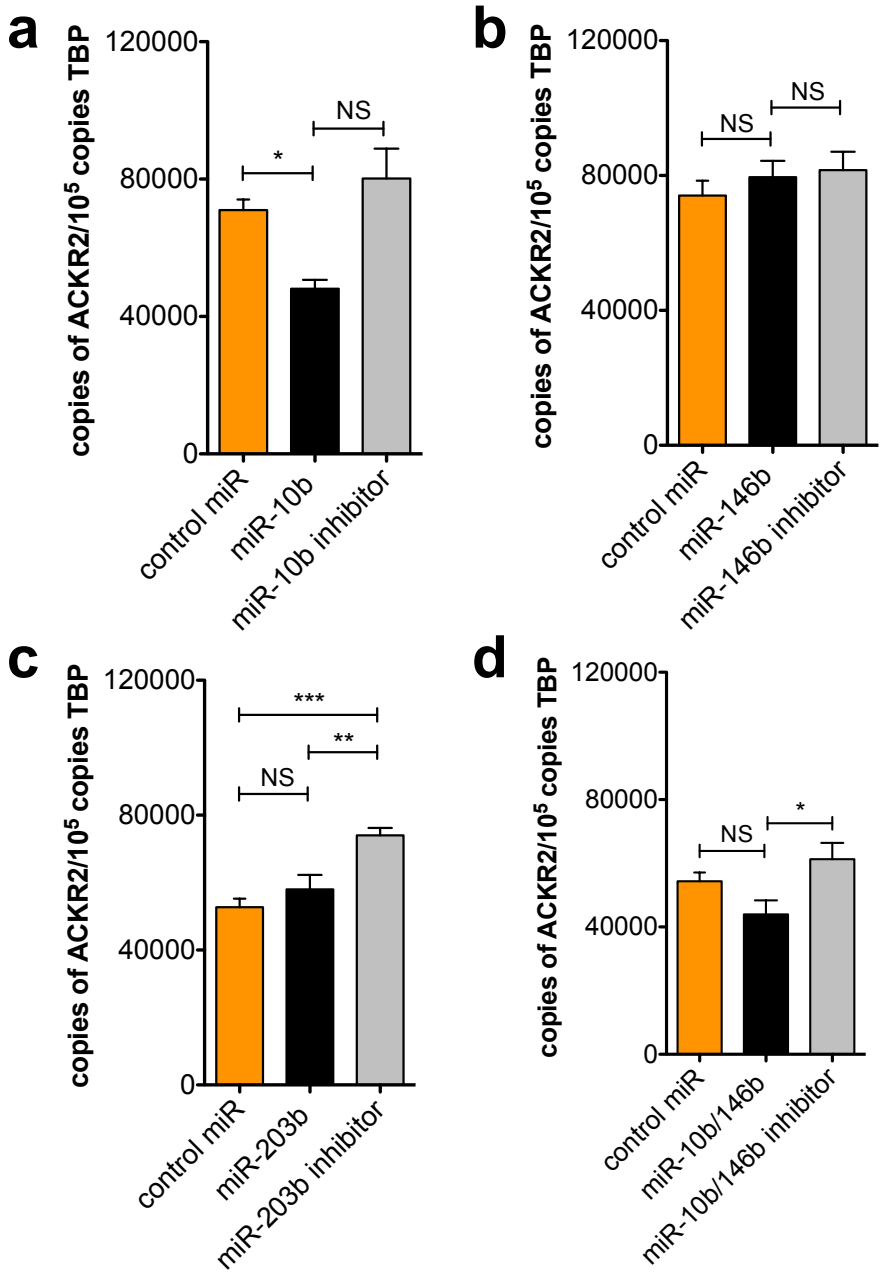

Figure 5.9 miR-10b reduces ACKR2 mRNA expression in lymphatic endothelial cells.

Absolute quantification of ACKR2 in primary human LECs following transfection with various microRNAs (singly and in combination) for 24 hours. All at 10nM. Significance was assessed using one-way ANOVA with Tukey's post-test. * $P<0.05$. Data representative of one experiment (except miR-10b, performed twice)

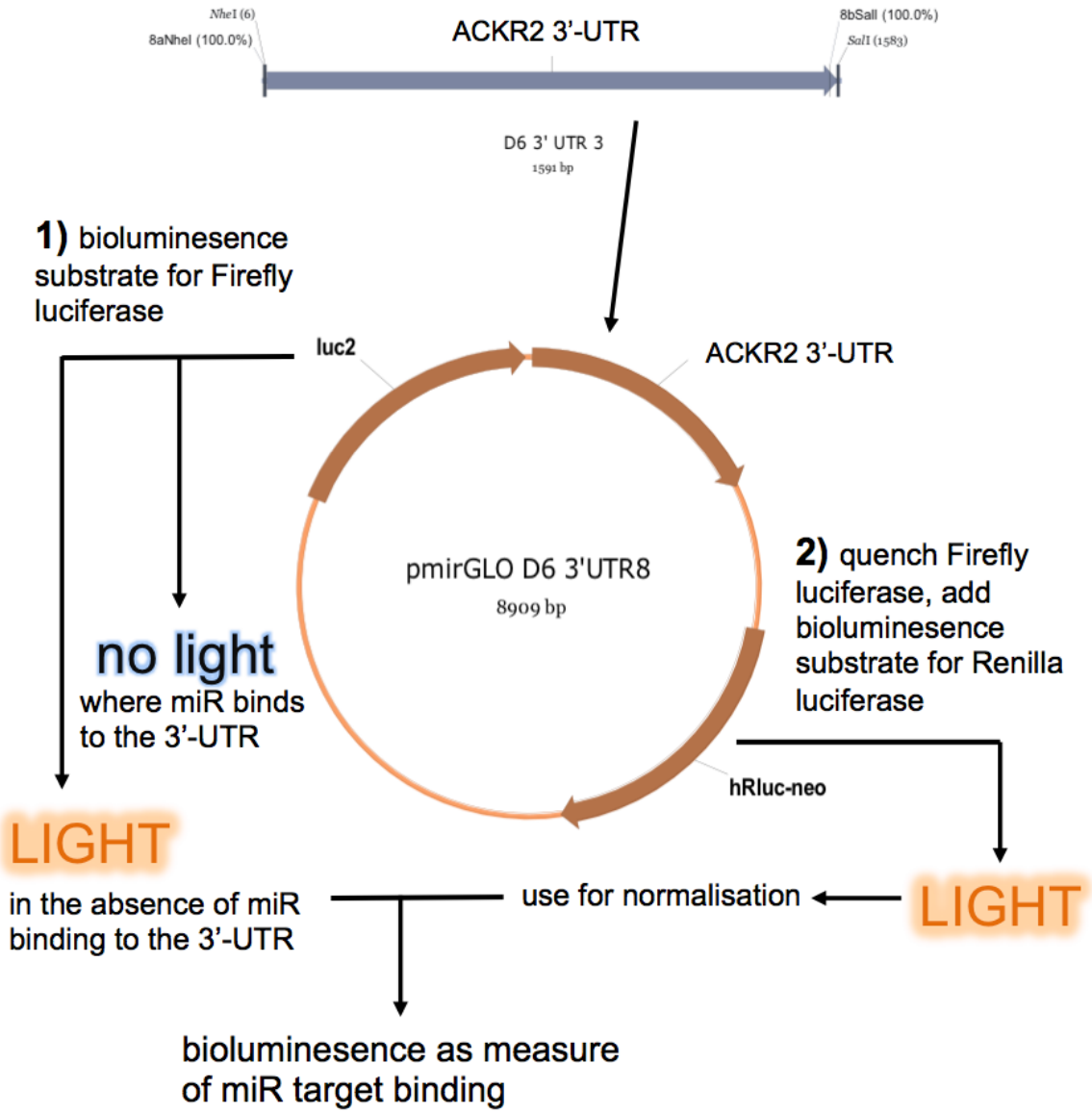

Figure 5.10 Schematic representation of Dual-Glo™ Luciferase reporter assay.

(Undertaken with the assistance of Dr F. Schütte). THe 3'-UTR of ACKR2 was cloned and inserted into a reporter vector containing two luciferase genes. This assay is works on the principle that the presence of the ACKR2 3'-UTR downstream of the luciferase enables quantification of miR interactions with the ACKR2 3'-UTR by assessing luciferase expression. To obtain this luciferase reading, cells are assayed for their ability to generate bioluminescence upon addition of Firefly luciferase bioluminescence substrate and normalised to Renilla luciferase. Note D6 is synonymous with ACKR2.

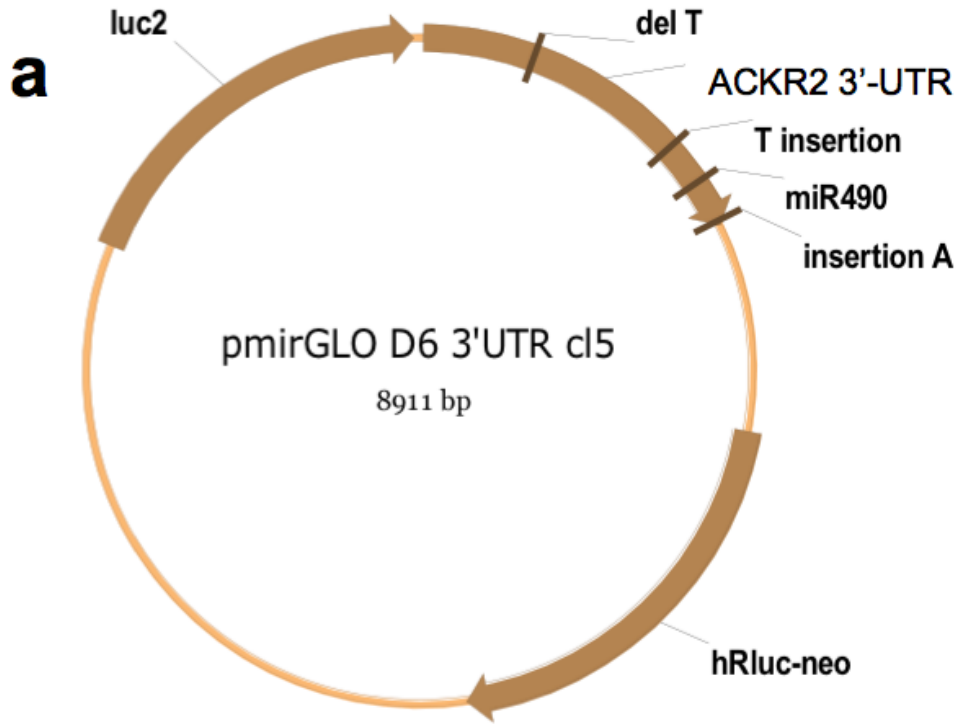

b

pmiRGlo ACKR2 3'UTR cl5 UTR sequence (as sequenced)

tcaaagtgctctctccaggggcctcagtgactgtgttgctaaacccagtggtcagttctcagttctcagccatcagcagcatttgctcgccccgcct
tcttcctccacttttcttcacttgcttccaggataccacgctttcttttctgaattgctacaatctttcttccttccttccttgcttccttccttccttccttcc
ctctctccctccctccctccctcgcttcttccctttcctccttttcctccctttcctacttttccttccttccttctgacagggtcttgctctattgctctgtcacc
caggctggaatgcagtggcgagatctccgctcactgtagcctcctccccctgggttgaagcaattctcatgcctcagcctcccaagtagccagga
ctataggcacctgccaccatgcctggctaatttttgtatttttttttctttctttctttctttttttttttttttttXgagacggagtctcactcttgttgc
ccaggctggacaacaatggcgcgatctcggctcactgcaacctccacctcccggattcaagcgattctcctgcctcagcctcctgagtagctgga
actacatgcgcgtgccaccacgcacagctaatttttataatttttagtagagatggggtttcactgcgttggccaggatgatctcgatctcttgacctt
gggatccacccgccttggcctcccaaagtgctgggattacaggtgtgagccaccatgcctggccctaatttttgtgtttttattagaaacagagttt
caccatgttggccaggctggagaattgctgtaatagttttccaactggcccctgtccttcctctctctgctctcctcccatctcatctgcacctagca
gccagagtgatcctgatactctcggcctttacttccgcctccctcagagcagcagcctgtcaaaacaccagattacaacaaatttagtttaaaggt
ctcaattagcgttattggcaattctagaatcaggcaacagactcattgaatcaggaacagattcactccataaaatacagagagtgctgcaatga
gctgggtagaagaggttagttttatagacaggaaggggctgtcaaaggcagaaagaaatgaagaacaaaaaaaaaagattgatttttttttttttT
gagacaggatctcactctgtcatccaggctgaagtccaatcccacaatcatggctcactgcagccaccacctcctgagctcaagtgatcctcccat
ctaagcccccaagtagctaggactacaggagcacaccaccacacctggctaatttttgtatttttgtggagacagggtctcagtatgttacccag
gttggactggaaaccctggctcaagcaatttgcctgcctcagcctcccaaagtgctgggattacaggcgtgagccactgcacagggccagattc
atcatttcaaagttactttctatatgcggccggaacagggtggttgacatcagttttcttcaggttacttttttaataatgattaaaacggggaacttc
attatcaaaa

X: T deletion

T: T insertion

A: A insertion

Binding site miR-10

Binding site miR-146

Figure 5.11 Schematic representation of Dual-Glo™ Luciferase reporter vector showing results of sequencing of the ACKR2 3'-UTR.

Insertion/deletion and predicted microRNA binding sites highlighted. Sequencing performed once. Note D6 is synonymous with ACKR2.

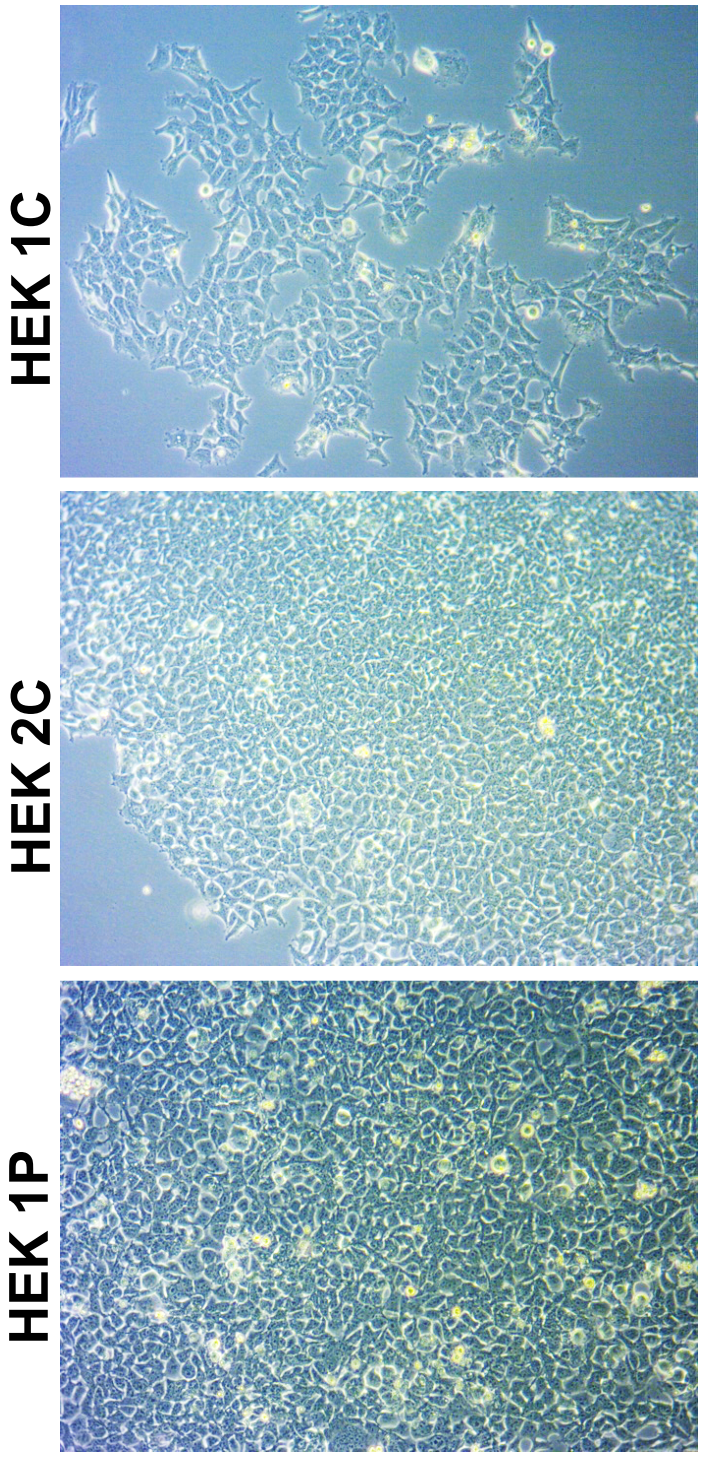

Figure 5.12 Representative images of stable transfected HEK293 clones. Stable HEK293 transfectants, expressing luciferase plasmid constructs, were selected using neomycin and clonal populations cultured from single colonies isolated in the presence of G418. Three different clones were grown.

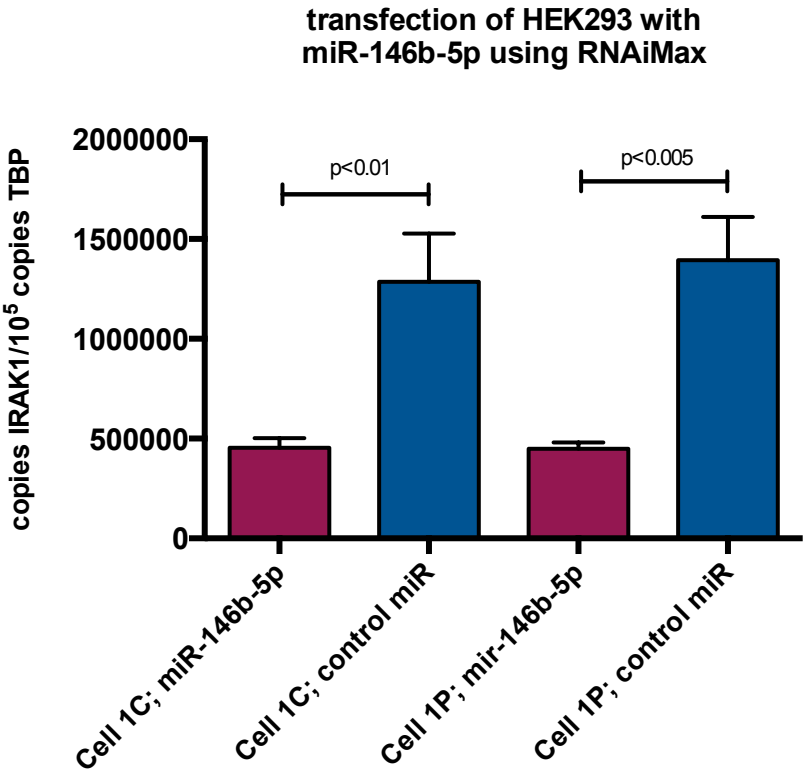

Figure 5.13 miR-146b can be successfully transfected into HEK293 cells
Absolute quantification of IRAK1 mRNA as assessed by QPCR in HEK293 cells following transfection of two different stable HEK293 populations (named '1C' and '1P') with miR-146b (purple bars) as compared to scrambled control (blue bars). Experiment performed once per HEK293 population.

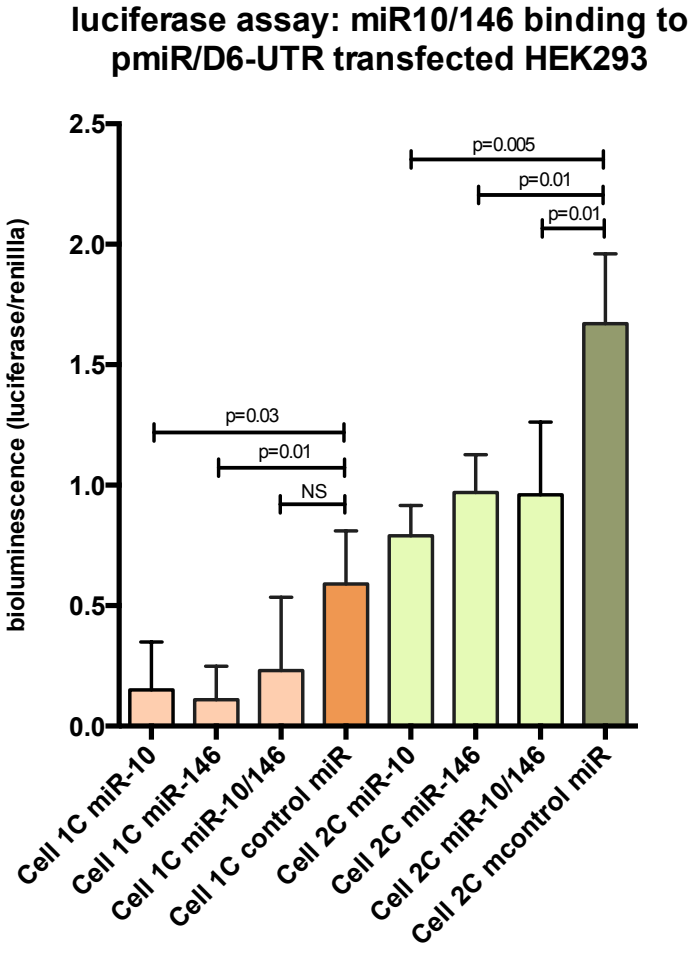

Figure 5.14 miR-146b and miR-10b bind directly to the ACKR2 3'-UTR. Results from Dual-Glo™ luciferase reporter assay, measuring bioluminescence following addition of substrate for Firefly luciferase (bioluminescence inversely proportional to microRNA 3'-UTR binding) normalised to Renilla luciferase. Results are from two different stable transfected HEK293 populations ('1C' and '1P') following transfection of HEK293 cells with miR-10b and miR-146b (singly and combination) and scrambled miR control. Statistics: one-way ANOVA, results mean±SEM. Assay performed twice.

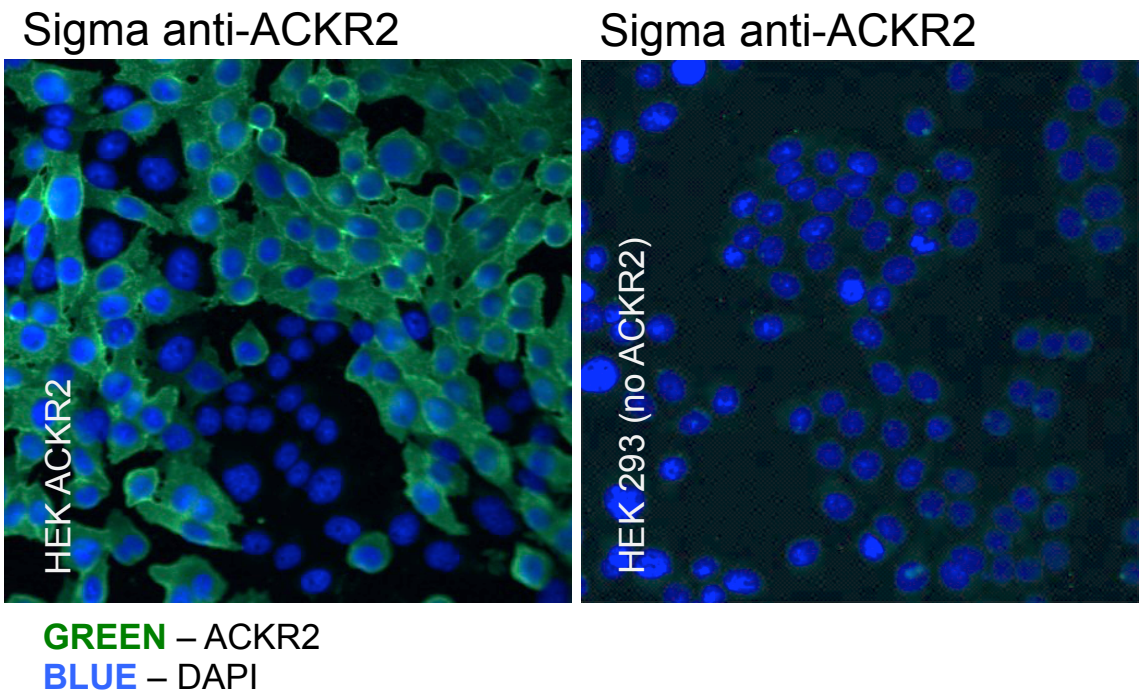

Figure 5.15 ACKR2 in ACKR2 transfected HEK293 can be visualised through fluorescent antibody staining.

Representative immunofluorescence in ACKR2 transfected HEK293 cells (high ACKR2) and HEK 293 cells (no ACKR2) grown as confluent monolayers. Experiment performed once, two wells per stain.

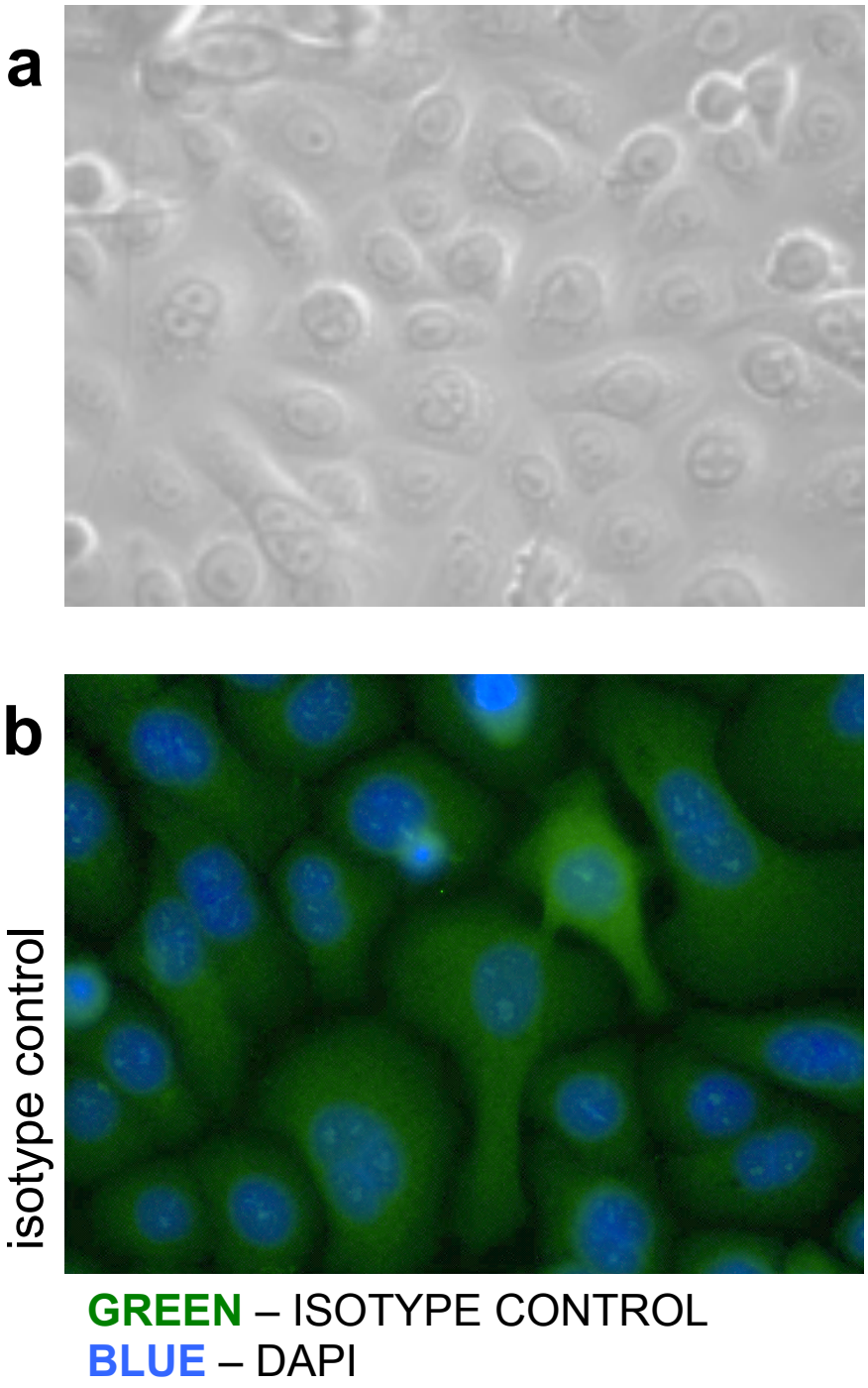

Figure 5.16 Isotype control antibody staining of primary human keratinocyte monolayers.

(a) Representative bright-field image of KC grown as confluent monolayer

(b) Representative immunofluorescence of KC grown as confluent monolayers, stained with isotype control antibody. Experiment performed once, two wells per stain.

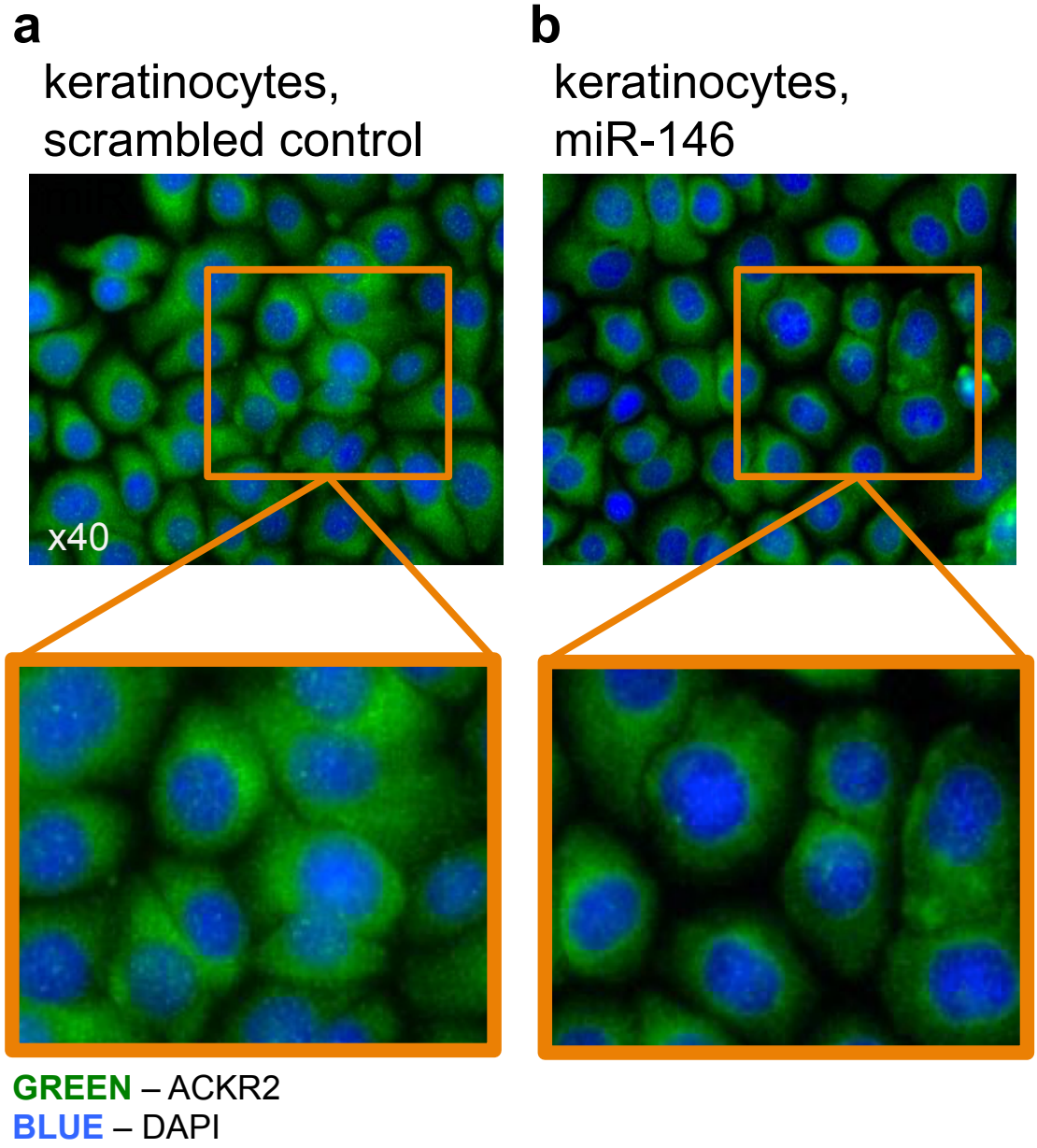

Figure 5.17 Reduced cytoplasmic ACKR2 following miR-146b transfection of KC, as visualised by immunofluorescent antibody staining.

Representative immunofluorescence microscopy images of confluent monolayers of keratinocytes 48 hours after transfection with;

(a) scrambled miR control

(b) miR-146b.

Results representative of two comparable experiments, four wells per stain/treatment.

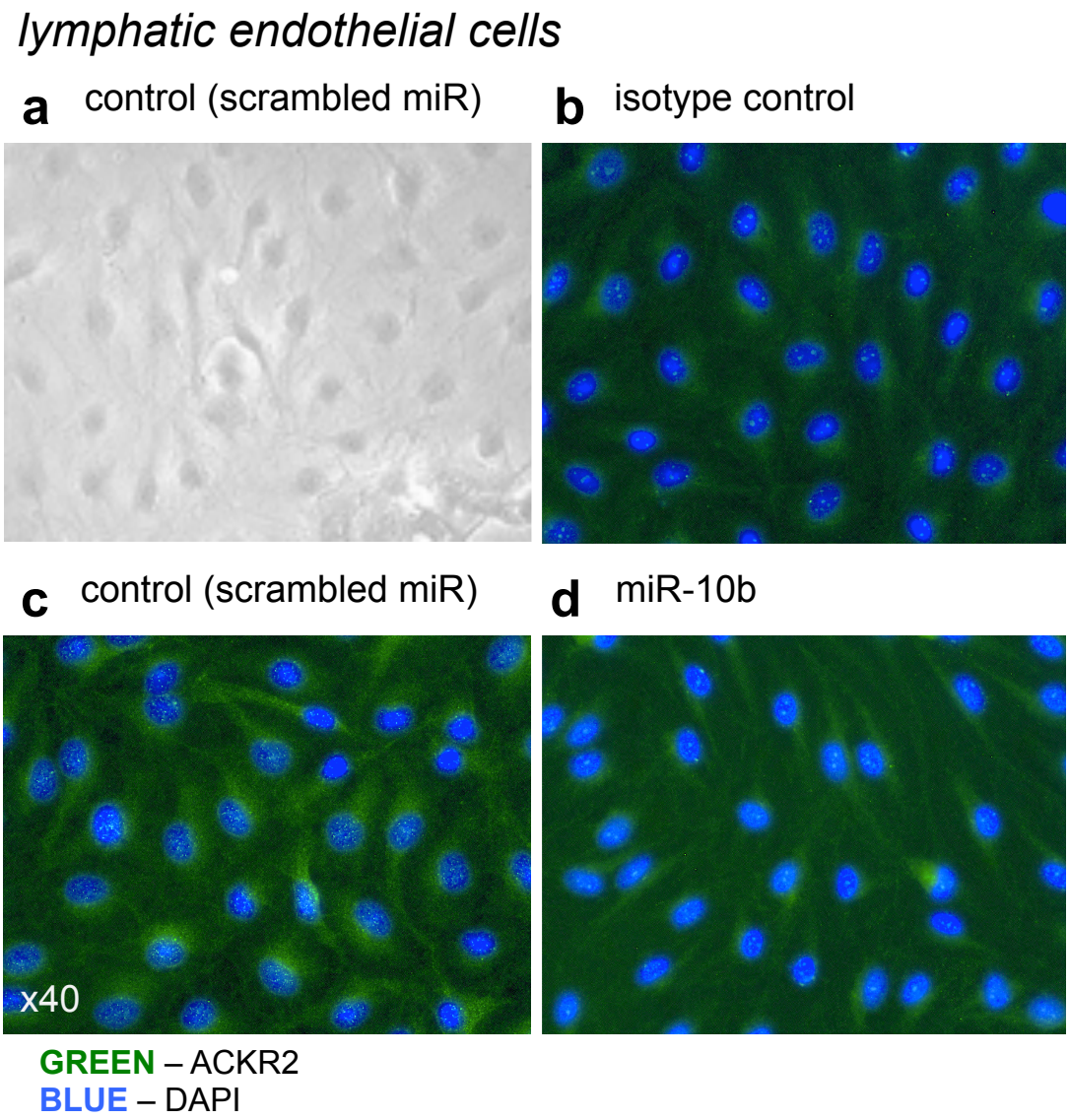

Figure 5.18 Reduced cytoplasmic ACKR2 levels following miR-10b transfection of LEC, as visualised through immunofluorescent antibody staining.

(a) Representative bright-field image of LEC grown as a confluent monolayer Representative immunofluorescence microscopy images of confluent monolayers of LECs 48 hours after transfection with;

(b) scrambled miR control, isotype antibody stain

(c) scrambled miR control, stained for ACKR2

(d) miR-10b, stained for ACKR2

Results representative of two comparable experiments, four wells per stain/treatment.

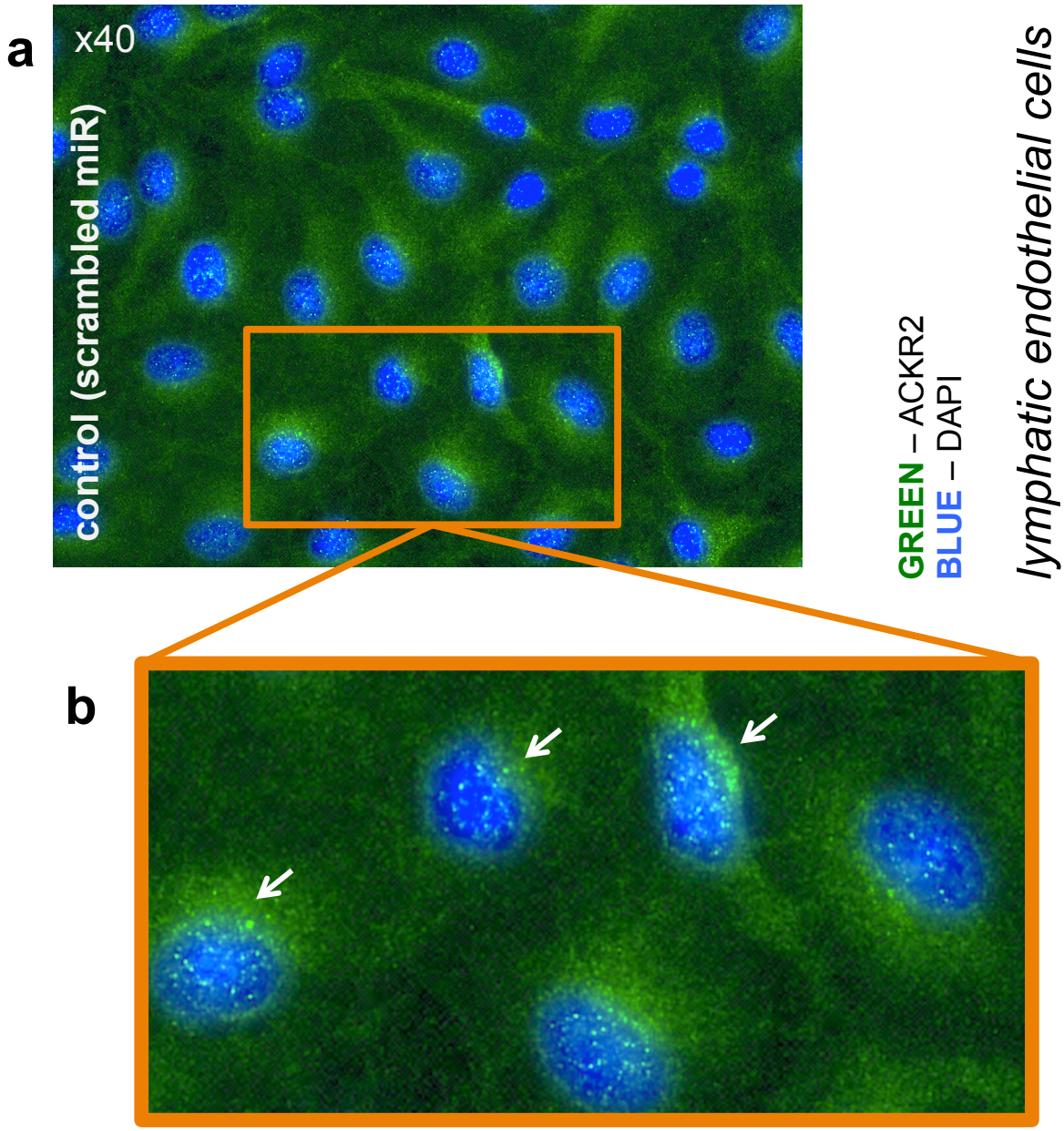

Figure 5.19 Cytoplasmic ACKR2 following scrambled miR control transfection of LEC, as visualised by immunofluorescent antibody staining.

(a) Representative image of LEC grown as confluent monolayer, stained for ACKR2.

(b) Enlarged part of above image, illustrating punctate ACKR2 staining (arrows).

Results representative of two comparable experiments, four wells per stain/treatment.

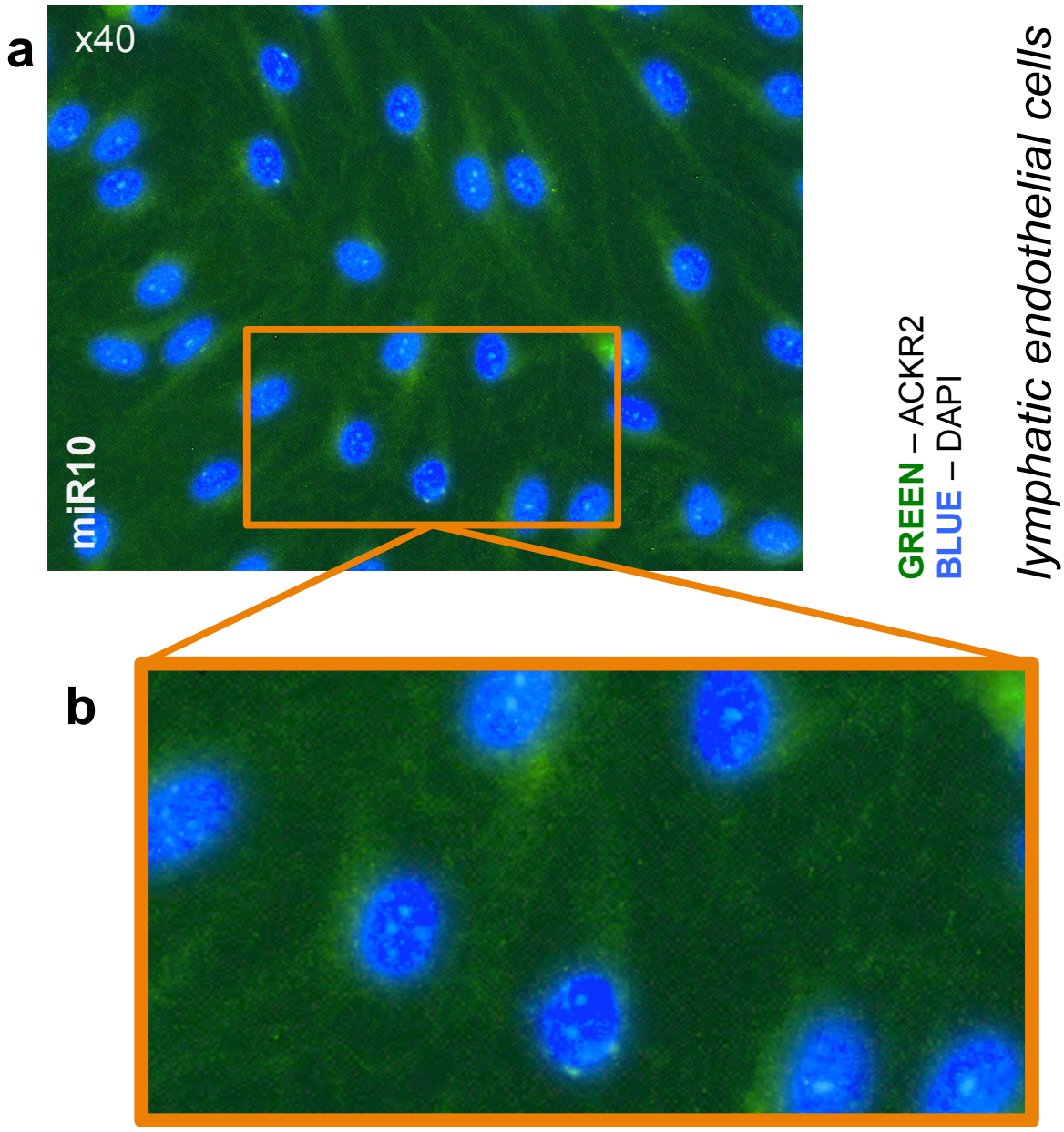

Figure 5.20 Reduced cytoplasmic ACKR2 following miR-10b transfection of LEC, as visualised through immunofluorescent antibody staining.

(a) Representative image of LEC grown as confluent monolayer, transfected with miR-10 and stained for ACKR2.

(b) Enlarged part of above image, illustrating relative absence of granular ACKR2 staining.

Results representative of two comparable experiments, four wells per stain/treatment.

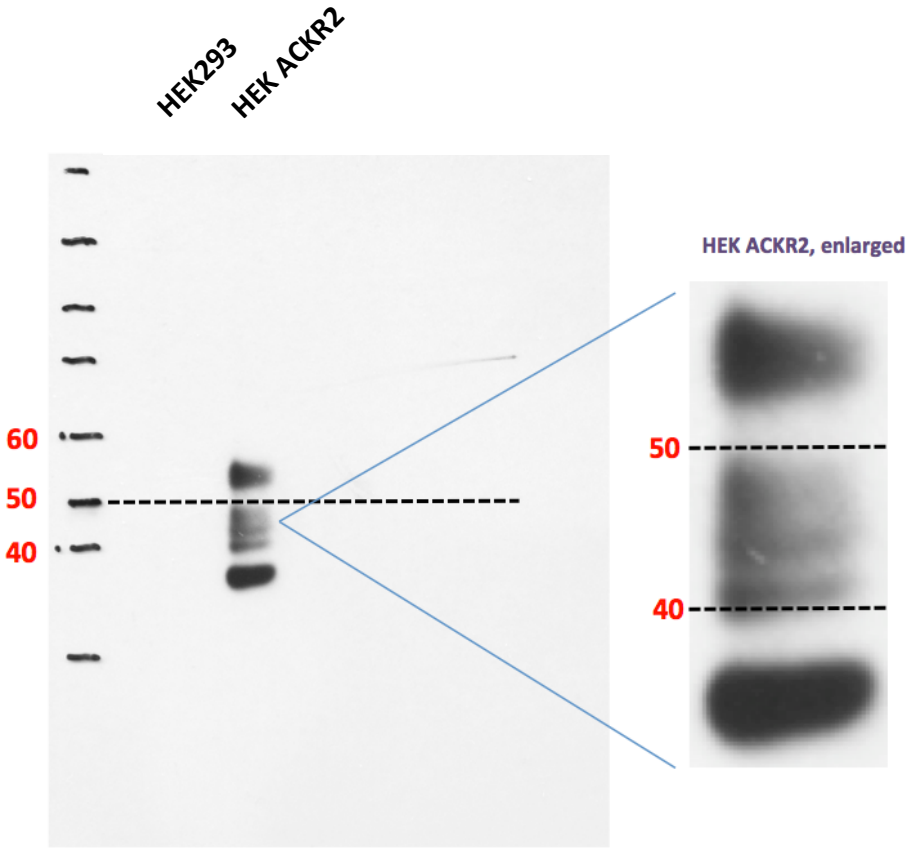

Figure 5.21 ACKR2 protein bands can be visualised using Western blotting.

ACKR2 antibody stain of Western blot, with protein lysate from HEK293 (no ACKR2, left lane) and ACKR2 transfected HEK293 cells (high ACKR2). Equal loading was assessed by Ponceau-S staining, and staining for β-tubulin. Data representative of 3 comparable experiments.

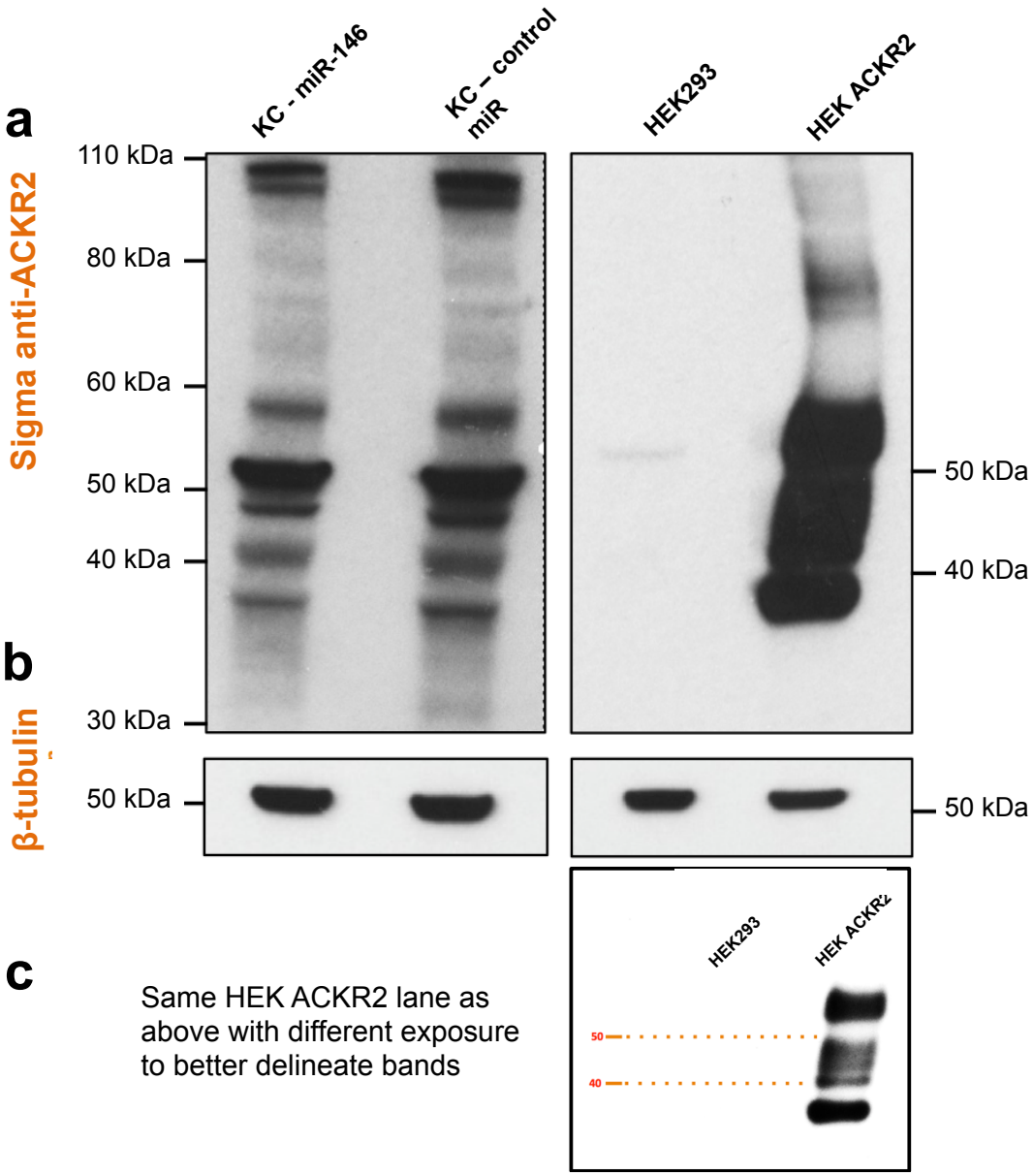

Figure 5.22 Reduced ACKR2 protein following transfection of KC with miR-146b.

Western blots of ACKR2 expression in KC 48h after transfection with scrambled control miR or miR-146b, compared to ß-tubulin (control). ACKR2 controls and transfected samples were run on the same gel – difference in exposure is due to coverage of HEK293 lanes with extra film to avoid over-exposure.

(a) Staining for ACKR2

(b) Staining for ß-tubulin as loading control

(c) ACKR2 staining for HEK293 lanes, with different exposure to better illustrate ACKR2-associated bands.

Data representative of two comparable experiments

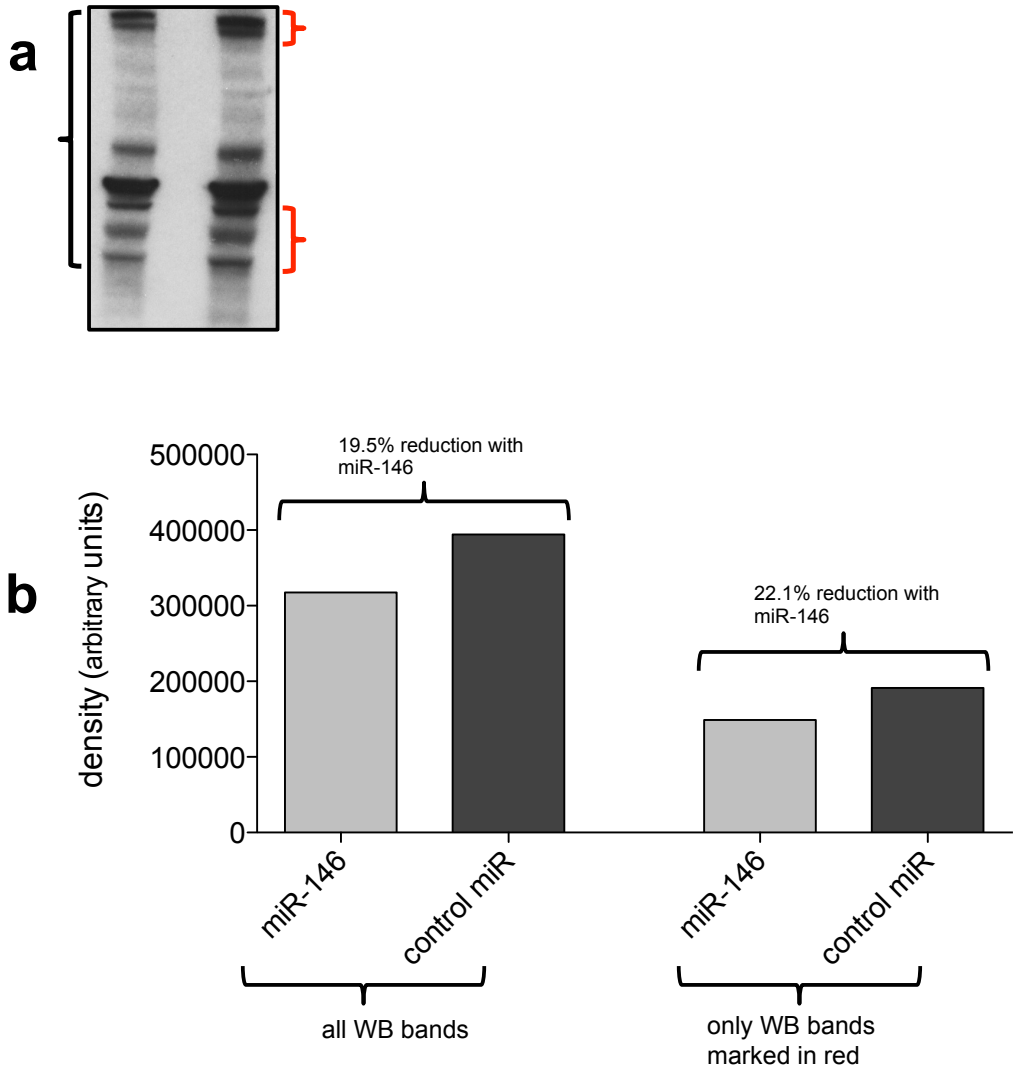

Figure 5.23 Reduced ACKR2 protein following transfection of KC with miR-146b as quantified through band densitometry.

Western blots quantified through band densitometry, with ACKR2 normalised to ß-tubulin band intensity, using two approaches illustrated in

(a) densitometry of all bands within black bracket, and bands most likely to represent ACKR2 within red brackets

(b) densitometry of Western blots of KC treated with either miR-146 or scrambled control miR

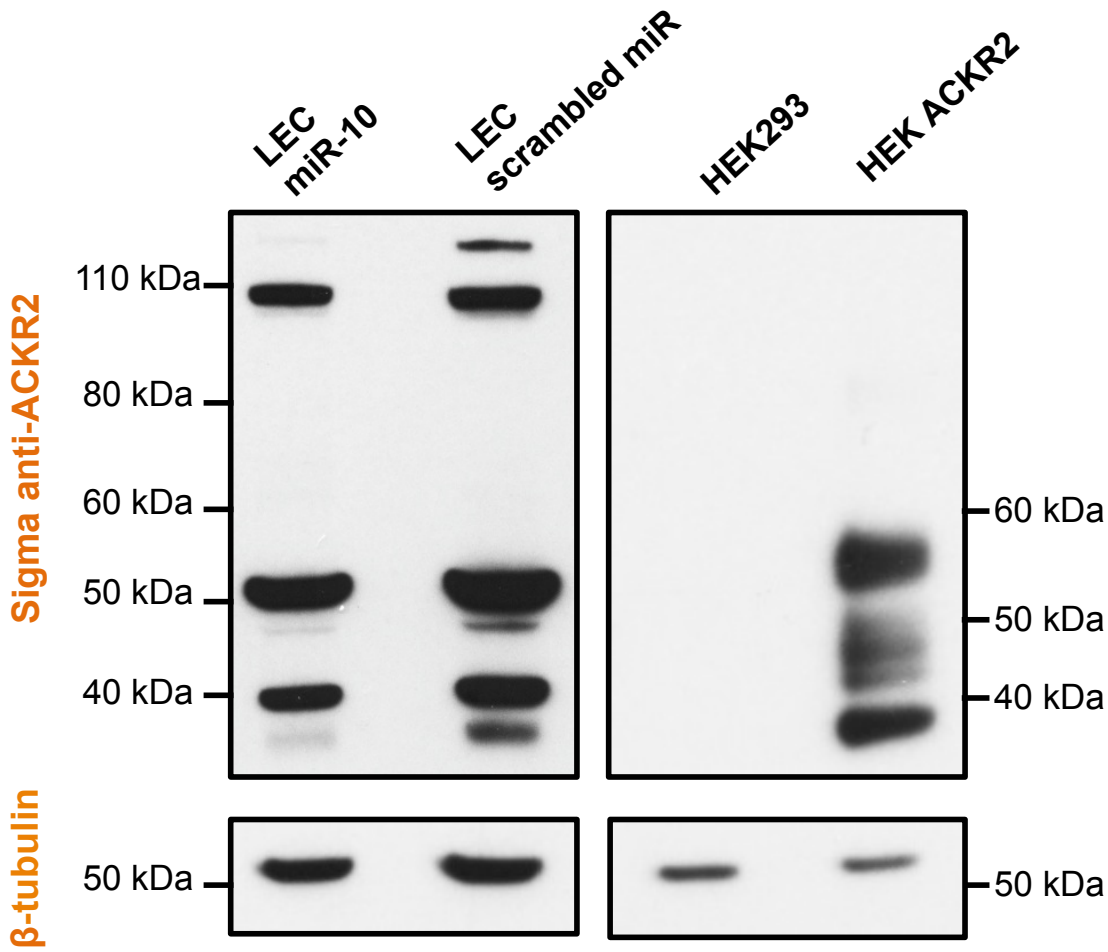

Figure 5.24 Reduced ACKR2 protein following transfection of LEC with miR-10b.

Western blots of ACKR2 expression in LEC 48h after transfection with scrambled control miR or miR-10b, compared to ß-tubulin (loading control). HEK293 ACKR2 positive and negative controls and transfected LEC samples were run on the same gel.

Data representative of two comparable experiments

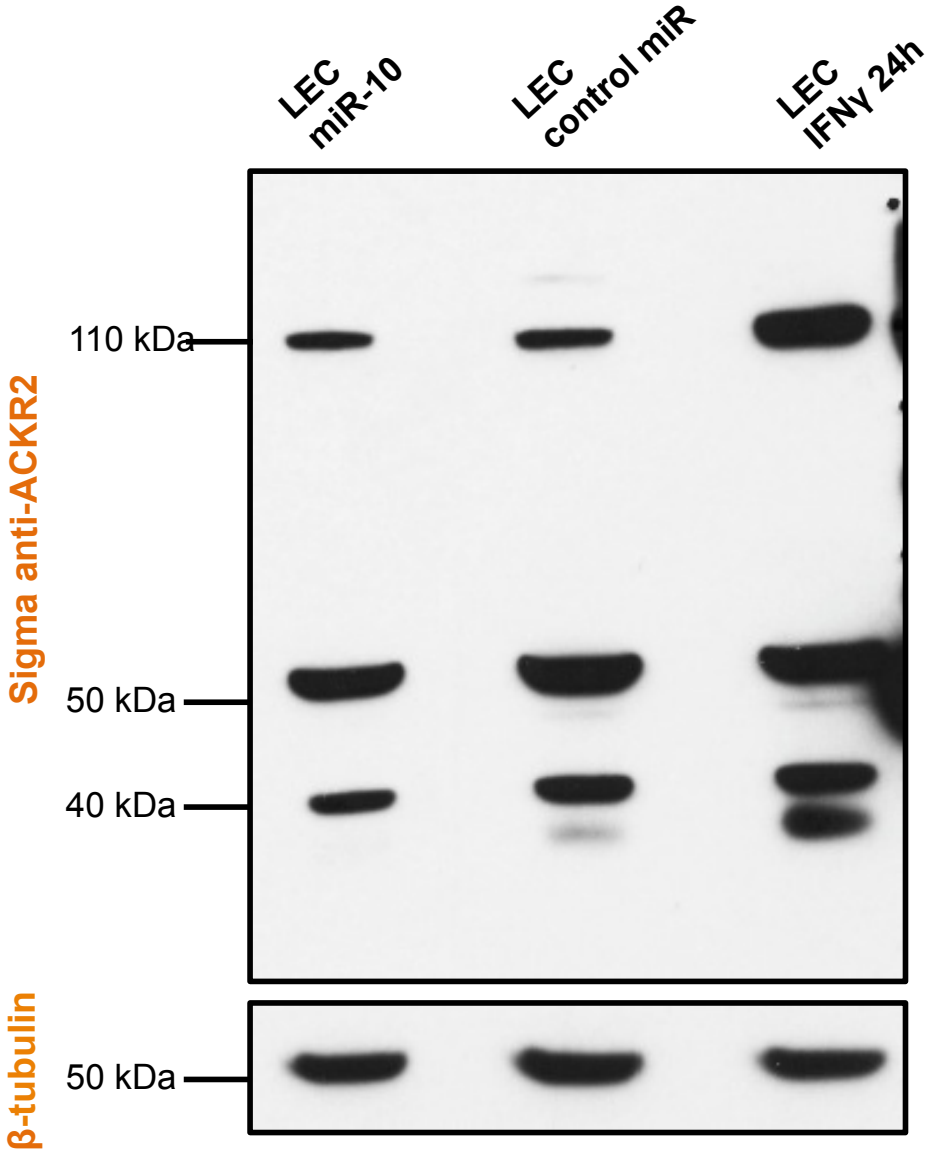

Figure 5.25 Reduced ACKR2 protein following transfection of LEC with miR-10b, and increased ACKR2 protein following treatment with IFNγ.

Western blots of ACKR2 expression in LEC 48h after transfection with scrambled control miR or miR-10b, compared to ß-tubulin (control). LEC treated with 100ng/ml IFNγ, to upregulate ACKR2, were used as a positive control.

Data representative of two comparable experiments (interferon treatment performed once)

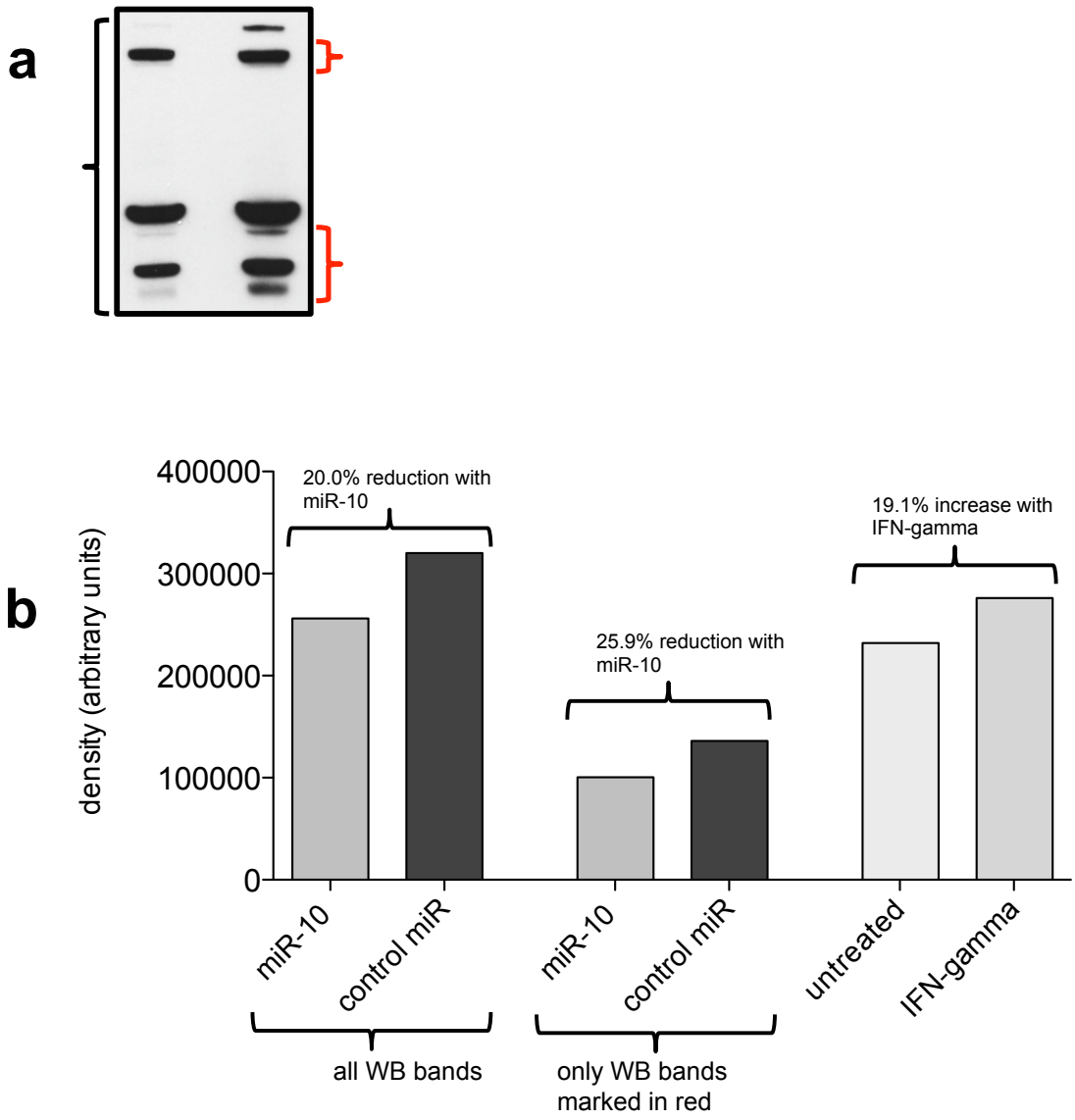

Figure 5.26 Reduced ACKR2 protein following transfection of LEC with miR-10b as quantified through band densitometry.

Western blots quantified through band densitometry, with ACKR2 normalised to ß-tubulin band intensity, using two approaches illustrated in

(a) densitometry of all bands within black bracket, and bands most likely to represent ACKR2 within red brackets

(b) densitometry of Western blots of LEC treated with either miR-10b or scrambled control miR, and LECs treated with IFNγ in order to upregulate ACKR2. All bands (equivalent of bands marked in red brackets above) used for densitometry of these samples.

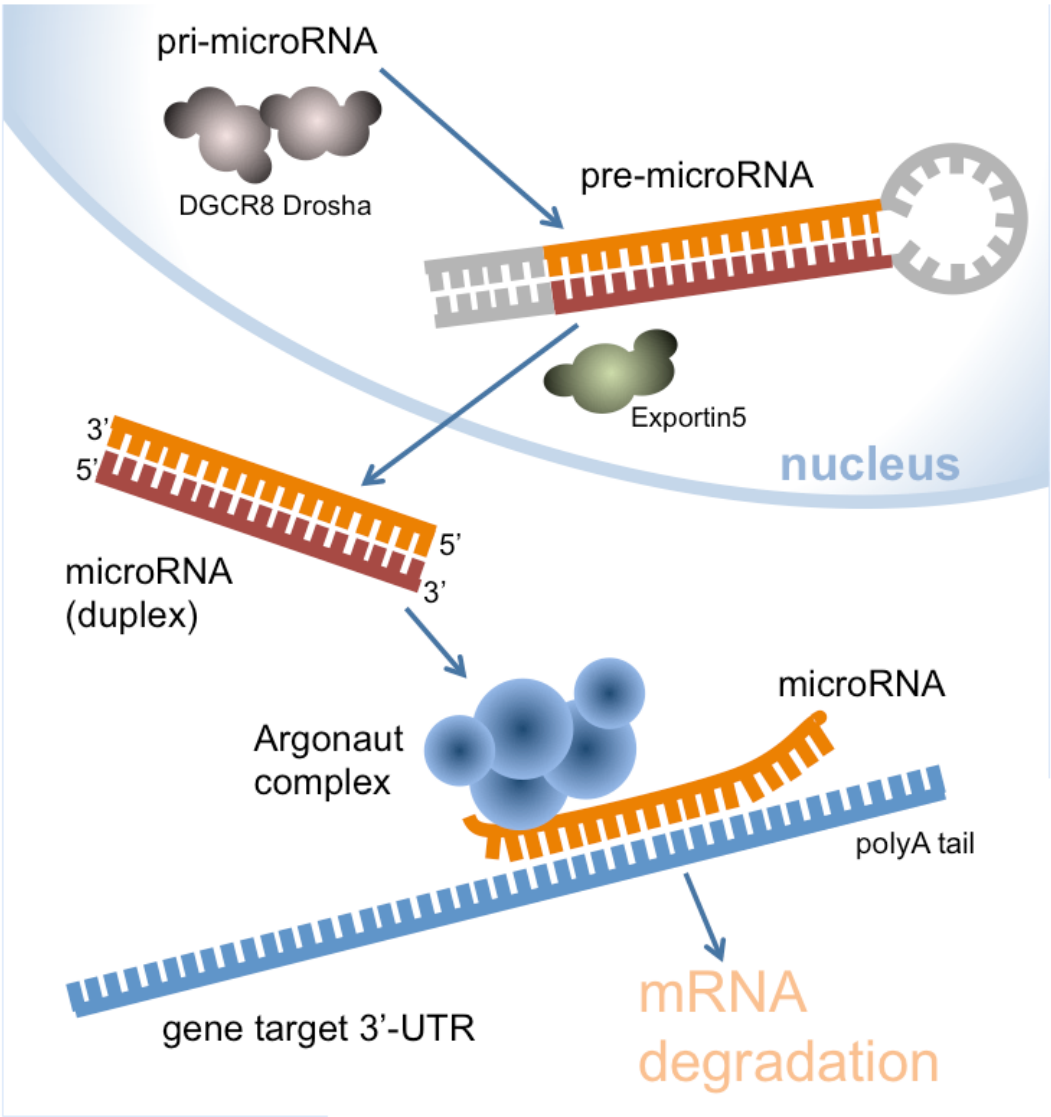

Supplementary Figure 5.1 Summary of miRNA biosynthesis
Compiled with information from; (Carthew & Sontheimer 2009; Kim et al. 2009). Pre-microRNA is synthesised in the nucleus with Exportin 5 facilitating its entry into the nucleus. There, cleavage of the pre-microRNA yields a microRNA duplex, after which the mature miRNA strand complexes with effector proteins (to form a so called RNA-induced silencing complex, RISC), whilst the complementary miRNA is degraded, miRNA, as part of the RISC will then interact with its mRNA target, leading eventually to mRNA degradation.

5.6 Summary Chapter 5

This chapter reports for the first time, the identification of microRNAs that bind directly to the ACKR2 3'-UTR and reduce expression of ACKR2 in primary human keratinocytes (KC) and lymphatic endothelial cells (LEC). Specifically, miR-146b downregulates ACKR2 in KC, and miR-10b downregulates ACKR2 in LEC, and are shown to bind directly to the ACKR2 3'-UTR.

Several cytokines are known to differentially regulate ACKR2 expression *in vitro*, and previous chapters in this thesis demonstrate a role for IFNγ in the upregulation of ACKR2 *in vivo*. However, the molecular mechanisms by which ACKR2 expression is regulated have not been determined. MicroRNAs are small RNA fragments that regulate gene expression at a post-transcriptional level, and have emerged as the most abundant class of gene regulators (Pasquinelli 2012). Previous array data demonstrated that a large number of microRNAs are differentially expressed in psoriasis (Sonkoly et al. 2007), but relatively little has been known about their potential roles in psoriasiform inflammation.

Bioinformatic databases exist that enable *in silico* predictions of which microRNAs may bind specific mRNA 3'-UTRs (Ekimler & Sahin 2014). Through the use of the database TargetScan, this thesis identified several microRNAs that were predicted to bind the ACKR2 3'-UTR *in silico*. Three of these were also differentially expressed in psoriasis in previously published array studies; miR-10, miR-146 and miR-203 (Sonkoly et al. 2007; Zibert et al. 2010). These microRNAs were selected for further study as possible negative regulators of ACKR2 expression. A protocol was subsequently developed in KC that would enable the successful transfection of primary human cells with microRNAs. Using previously validated miR-146 targets (IRAK1/TRAF6) successful transfection was confirmed using the developed protocol. KC and LEC were transfected with all three microRNAs, both singly and in combination, and data showed that miR-146a/b and miR-10b significantly downregulated ACKR2 mRNA expression in KC and LEC respectively; for this reason subsequent experiments were performed with miR-146 in KC and miR-10 in LEC. It is noteworthy that miR-10b has been shown to be upregulated in unaffected psoriatic skin (where ACKR2 expression is relatively high); it is

possible that ACKR2 expression would be yet higher without such upregulation, but further studies are required to determine the role of miR-10 *in vivo*. ACKR2 transcript was reduced by approximately one third in each cell type, which is in keeping with previous data of miR-induced mRNA repression (Bartel 2004; Bartel 2009). It is acknowledged that the absolute change in ACKR2 mRNA copy number is small, and the current experiments did not assess the biological significance of this change. Future work will need to determine whether the observed reduction in ACKR2 expression in KC and LEC does indeed translate into a difference in 1) ACKR2 ligand scavenging and 2) subsequent cell infiltration and inflammation. Furthermore, it is likely that there exists heterogeneity in KC responses to microRNA transfection, and for this reason, using a larger number of donors in the future would yield more robust results, and would enable the degree of heterogeneity to be determined.

Next, in order to confirm that the observed mRNA reduction was due to miR-146b/miR-10b binding directly to the ACKR2 3'-UTR, a dual-glo Luciferase assay was utilised. In brief, the ACKR2 3'-UTR was cloned into a dual-luciferase reporter vector, and stable HEK293 transfectants generated. HEK293 transfectants were subsequently transfected with microRNAs, and any reduction in bioluminescence upon addition of the substrate for Firefly luciferase would be indirectly proportional to direct microRNA binding of the ACKR2 3'UTR. Renilla luciferase bioluminescence was subsequently used for normalisation in the same experiments. Results confirmed that both miR-10b and miR-146b bind directly to the ACKR2 3'-UTR, which would be in keeping with the mRNA reduction previously demonstrated being due to a direct effect of microRNA binding to the ACKR2 3'-UTR.

Subsequently, the effect of microRNA on ACKR2 protein expression was determined by means of immunofluorescent microscopy. Primary human KC and LEC were transfected with miR-146b/miR-10b respectively as well as scrambled miR as control. In healthy KC transfected with miR control punctate ACKR2 staining was evident throughout the cytoplasm. This was in keeping with previous studies, that demonstrated that most ACKR2 protein (90%) is found in the cytoplasm (Blackburn et al. 2004). Transfection of the cells with miR-146b and miR-10b in KC and LEC respectively confirmed that

the microRNAs reduced ACKR2 expression in the cells, as suggested by the reduction in cytoplasmic ACKR2 staining 48 hours post transfection. These results were largely qualitative, and future repeat studies would be required in order to quantify the findings.

In order to quantify the reduction in ACKR2 protein, KC and LECs were again transfected with microRNAs, but this time the protein expression was assessed by Western blotting. In keeping with previously published studies, ACKR2 appeared not as a single band on Western Blotting, but as several bands, likely representing different states of glycosylation and dimerisation. Reduction in band density was assessed through densitometric analysis (adjusted to the ß–tubulin loading control). Transfection of miR-146b in KC and miR-10b in LEC was associated with a reduction of approximately 20% in Western Blot band intensity 48h post transfection, which is broadly in keeping with the degree of mRNA reduction observed with QPCR in this thesis. One limitation of the above experiments is that there was no assessment of the functional effect of the reduction in ACKR2 mRNA and protein. As ACKR2 has a high capacity for chemokine scavenging through re-cycling (Galliera, Galliera, et al. 2004), it could be that compensatory mechanism will come into play, enabling more rapid cycling, thus overcoming the reduction in ACKR2 protein in the cytoplasm. It is acknowledged that the effect of microRNA transfection on ACKR2 expression in KC and LEC appears relatively modest, as assessed by Q-PCR, immunofluorescent microscopy and Western Blots. It is unclear whether the observed differences are fully reproducible, and whether they translate into a biologically meaningful change in ACKR2 function, and further experiments will need to assess in detail the effect that microRNAs have on chemokine scavenging and overall inflammation. A further limitation of the above experiments, is that microRNA transfection possibly delivers supraphysiological levels of microRNAs. Thus, whilst the data demonstrate that the microRNAs bind the ACKR2 3'-UTR and reduce ACKR2 mRNA expression *in vitro*, the role of these microRNAs *in vivo* cannot be determined through these experiments alone.

CHAPTER 5

6 Tensile stretching of inflamed KC and LEC differentially regulates expression of ACKR2.

6.1 Contents

6.2 Hypothesis

6.3 Aims

6.4 Introduction

6.4.1 An *in vitro* model of repeated tensile trauma of primary human keratinocytes.

6.4.2 Tensile trauma of inflamed KC led to a rapid reduction in ACKR2 mRNA expression.

6.4.3 Tensile trauma of inflamed KC led to a significant increase in miR-146a and miR-146b expression.

6.4.4 Tensile trauma of LEC did not affect ACKR2 expression.

6.4.5 Incisional trauma of remote unaffected skin of mice in the IMQ mouse model of psoriasiform inflammation led to a downregulation of ACKR2.

6.6 Summary Chapter 6

6.2 Hypothesis

- Tensile trauma of skin cells downregulates ACKR2 expression

6.3 Aims

The aims of this chapter were to;

- Develop a model whereby the effect of tensile stress on primary human skin cells that express ACKR2 could be assessed
- Assess the effect of tensile stress on primary human cells
- Determine whether expression of ACKR2 interacting miRs correlate with tensile trauma

6.4 Introduction

As previously discussed, published data have demonstrated that ACKR2 expression is relatively deficient in psoriatic plaques (Singh et al. 2012). Additionally, it has previously been shown by us that tape stripping of clinically unaffected skin in patients with psoriasis leads to a rapid reduction of ACKR2 transcript expression in the skin (Singh et al. 2012). This finding is of particular relevance, as it might provide a possible mechanism for a phenomenon described in psoriasis called 'koebnerisation'. Koebnerisation is well-documented in psoriasis, and is a process by which simple trauma to unaffected skin of those with psoriasis, can trigger the development of psoriatic plaques at the site of trauma (Weiss et al. 2002; Camargo et al. 2013). Several forms of trauma can lead to koebnerisation, including surgical incisions, as well as uni- and bi-axial skin stretching (Alolabi et al. 2011) (Verma 2009) (Reid Vender & Ronald Vender 2015). In many patients, psoriatic lesions tend to develop at those cutaneous sites that most regularly receive minor trauma, such as the elbows. This, coupled with our previous observations that; 1) in the absence of ACKR2, cutaneous inflammation is exaggerated and 2) tape stripping leads to a rapid downregulation of ACKR2 in human skin, led to the hypothesis that trauma-induced downregulation of ACKR2 could be one trigger that precipitates the development of an inflammatory cutaneous lesion in psoriatic patients. The mechanism(s) by which this trauma-induced downregulation occurs, might provide insights into the molecular mechanism by which ACKR2 downregulation occurs in plaques.

6.4.1 An *in vitro* model of repeated tensile trauma of primary human keratinocytes.

Tape stripping of clinically unaffected human skin of patients with psoriasis leads to a rapid downregulation of ACKR2. However, the effect of tape stripping on healthy skin is two-fold; 1) it causes removal of the stratum corneum and damages the barrier function of skin and 2) It induces mild trauma of the skin. Due to report of stretching triggering koebnerisation (Verma 2009) (Reid Vender & Ronald Vender 2015), and as psoriasis has a particular predilection for sites that undergo repeated stretching in daily life (e.g. knees, elbows, skin folds, see Figure 1.4), emphasis was initially placed

on the effect of tensile trauma on the expression of ACKR2 in skin cells. In order to specifically determine the effect of *tensile* cell trauma on ACKR2 expression, a reductionist *in vitro* model was developed that would enable the effect of repeated tensile trauma on ACKR2 expression in primary human cells to be studied. The model developed was based on the FlexCell™ International FX5000 machine, whereby primary human cells are grown on silicone membranes in a 6-well format. The membrane can subsequently be subjected to repeated bi-axial cyclical tension *in vitro*, with pre-determined degree of tension, stretch wave-form, and cycle number (this model is summarised in Figures 6.1 and 6.2).

Experimental data presented in previous chapters demonstrated that KC and LEC can be successfully grown as confluent monolayers on uncoated polycarbonate plastic, as per the cell provider's instructions (PromoCell GmbH, Heidelberg, Germany). However, it was noted during the optimisation steps in this chapter that neither KC nor LEC adhered to uncoated silicon membranes (images of LECs grown on different substrates in Figure 6.3, demonstrating that LECs form confluent monolayers on polycarbonate and fibronectin coated silicone, but fail to adhere on silicone even when coated with attachment factor). KC and LEC required Collagen 1 and Fibronectin coated silicone respectively, in order to adhere (and critically, remained fully adherent after 12h of cyclical stretching). In order to ensure that growth on these alternative substrates had no unexpected effects on ACKR2 expression, KC and LECs were grown on Collagen 1 and Fibronectin respectively, and baseline ACKR2 expression determined by QPCR. Data showed that there was a modest but significant increase in KC ACKR2 expression (Figure 6.4a), and a decrease in LEC ACKR2 expression where cells were grown on coated silicon as compared to uncoated polycarbonate tissue culture plates (Figure 6.4b).

6.4.2 Tensile trauma of inflamed KC leads to a rapid reduction in ACKR2 mRNA expression.

In order to examine the effect of tensile trauma on KC, confluent KC monolayers grown on Collagen I coated silicon were subjected to stretching for 12h during which the membrane was stretched by 15% every 0.8 seconds

(0.8Hz) (Figure 6.2). Cells were rested for a further 12h (broadly similar to the time point used in tape stripping experiments in humans (Singh et al. 2012)) before lysis and RNA extraction. QPCR data showed no difference in ACKR2 expression between healthy primary human KC stretched for this duration of time, and non-stretched control KC (Figure 6.5a).

It should be noted that these primary human cells are derived from healthy donors and are grown in the absence of typical psoriasis-associated factors. Psoriasis patients have elevated T-cell cytokines including IFNγ that correlates with elevated ACKR2 in unaffected skin. To better model human psoriasis where KCs exist in the context of systemic inflammation, KCs were treated with either tissue culture supernatant from activated human T-cells or recombinant IFNγ and then exposed to tensile stress for 12h at 0.8Hz. In contrast to non-inflamed KC (Figure 6.5a), tensile trauma of T-cell supernatant pre-treated KC led to a significant decrease in ACKR2 expression (Figures 6.5b). This was also the case for IFNγ pre-treated KC, suggesting that KC with elevated ACKR2 display tensile stress induced downregulation of expression.

In order to determine whether the observed effect was due to IFNγ in the T-cell supernatant, T-cell supernatant was incubated with anti-IFNγ antibodies prior to being used to stimulate KC. However, treatment of the T-cell supernatant with IFNγ neutralising antibodies did not diminish this effect, suggesting that soluble T-cell products in addition to IFNγ can mediate ACKR2 upregulation (Figure 6.5b). It remains to be determined what the factors are, beyond IFNγ that upregulate ACKR2, and enable ACKR2 downregulation upon application of tensile stress. This can be achieved e.g. through testing of specific T-cell cytokines, or systematic neutralisation of likely cytokine mediators in active T-cell supernatant.

6.4.3 Tensile trauma of inflamed KC led to a significant increase in miR-146a and miR-146b expression.

In this thesis (Chapter 4), it has previously been shown that miR-146a/b bind directly to the ACKR2 3'-UTR and downregulate ACKR2 mRNA expression. miR-146 is also upregulated in psoriatic lesions according to previous studies (Sonkoly et al. 2007; Zibert et al. 2010). In order to determine whether

there was a possible link between these observations, miR-146a/b expression levels were quantified by QPCR in inflamed KCs, and were expressed as fold-change relative to non-inflamed healthy KC controls. Where inflamed KC were subjected to tensile trauma, there was an over 100-fold induction of miR-146a and a lesser (albeit still substantial and significant) induction of miR-146b (Figure 6, black bars), relative to static KC (Figure 6.6, grey bars). Given the demonstrated effect that these microRNAs have on ACKR2 expression, it is thus possible that the reduction of ACKR2 expression in inflamed KC that follows tensile trauma is mediated, at least in part, through upregulation of miR-146a/b. These experiments did not however assess whether the observed association between elevated miR-146/ACKR2 is causative, and future studies will need to repeat these experiments in the presence of anti-miR-146 in order to determine its role in the downregulation of ACKR2 in inflamed KC upon flexing.

6.4.4 Tensile trauma of LEC did not affect ACKR2 expression.

As shown above, flexing of KC pre-treated with both IFNγ and tissue culture supernatant from activated human T-cells was associated with a reduction in the expression of ACKR2. However, flexing did not affect ACKR2 expression in KC where ACKR2 expression had not been induced in this manner. Thus, it was appropriate to similarly induce ACKR2 expression in LEC prior to tensile trauma. Therefore, in order to study the effect of flexing on LEC, first the response of KC and LEC to key psoriasis associated cytokines was compared (Figures 6.7a-b). The data revealed that, in keeping with previously published data, LECs express higher amounts of ACKR2 mRNA compared to KC at rest, and that KC and LEC differ in their responsiveness to key pro-inflammatory cytokines (Figures 6.7a-b). Specifically, the response of LEC to IFNγ is more modest (albeit still significant, Figure 6.7b), with the strongest single cytokine inducer of ACKR2 expression in LEC amongst the cytokines tested being IL-6 (Figure 6.7b). Future experiments will however need to include the Th17 cytokine IL-17 as a key psoriasis-associated cytokine, which was not included in these experiments. Next the response of LEC to tissue culture supernatant from activated human T-cells was assessed (Figure 6.7c). Supernatant from non-activated T-cells had no effect on ACKR2

expression in LEC, but active T-cell supernatant significantly upregulated expression of ACKR2 (Figure 6.7c).

Next, having demonstrated that both IFNγ and T-cell supernatant upregulated ACKR2 in LECs, experiments were designed to assess the effect of flexing on LECs, that were untreated, or pre-treated with IFNγ (Figure 6.8a) and activated T-cell supernatant (Figure 8b), prior to flexing for 12h at 0.8Hz. Data showed that there was no effect on ACKR2 expression in LECs from flexing in LECs that were untreated, IFNγ stimulated or stimulated with T-cell supernatant (Figures 6.8a-b). Thus, the response of inflamed KC and LEC to tensile stress appears to be different, even where cells have been similarly pre-treated. This is in keeping with the results in previous chapters in this thesis, in which the major pathological finding exhibited by ACKR2-deficient mouse skin is the aberrant positioning of inflammatory T-cells in the epidermis.

6.4.5 Incisional trauma of remote unaffected skin of mice in the IMQ mouse model of psoriasiform inflammation led to a downregulation of ACKR2.

Previous chapters demonstrated that human psoriatic expression patterns of ACKR2 could be successfully replicated in a modified form of the IMQ mouse model of psoriasiform inflammation. Specifically, application of IMQ to flank skin on one side plus systemically administered IFNγ together caused an upregulation of ACKR2 in remote unaffected skin. As discussed above, previously published data also showed that tape stripping of unaffected human psoriatic skin (where ACKR2 expression is high) led to a rapid reduction in ACKR2 transcript levels (Singh et al. 2012).

As described above, *in vitro* stretching of inflamed KCs led to a downregulation of ACKR2. Thus, in order to examine whether cutaneous trauma to psoriatic mouse skin could similarly lead to ACKR2 downregulation, mice were treated with IMQ to one flank plus systemic IFNγ in order to upregulate remote ACKR2 (the experimental protocol is schematically represented in Figure 6.9a) and the effect of trauma on ACKR2 expression determined. To do this a second site on the contralateral flank was then subjected to superficial incisional trauma (just down to the dermis)

using a sterile surgical blade, and the expression of ACKR2 determined by means of QPCR. Data showed that incisional trauma *in vivo* led to a rapid (within 24h) reduction of ACKR2 expression. These results parallel the results observed upon tape stripping in patients with psoriasis. Thus, data suggest that trauma induced modulation of ACKR2 can in principle be successfully modelled in mice, which if developed further would enable the further study of the mechanisms that underpin trauma induced differential ACKR2 expression *in vivo*. However, the presented data were generated from one *in vivo* experiment, and larger experiments are required in order to be able to draw firmer conclusions about the effects of trauma in the context of a mouse model of psoriasis. Importantly, it is also acknowledged that incisional trauma does differ significantly from tensile trauma, but the work was undertaken within the restrictions of the available applicable Home Office licences. It would also be helpful to determine the role of microRNAs in the regulation of murine ACKR2 expression in this context. However, there are no clear miR-146 orthologs in mice, and the murine ACKR2 3'-UTR is significantly different to the human equivalent, and is therefore likely regulated by a set of microRNAs that are different to that in humans.

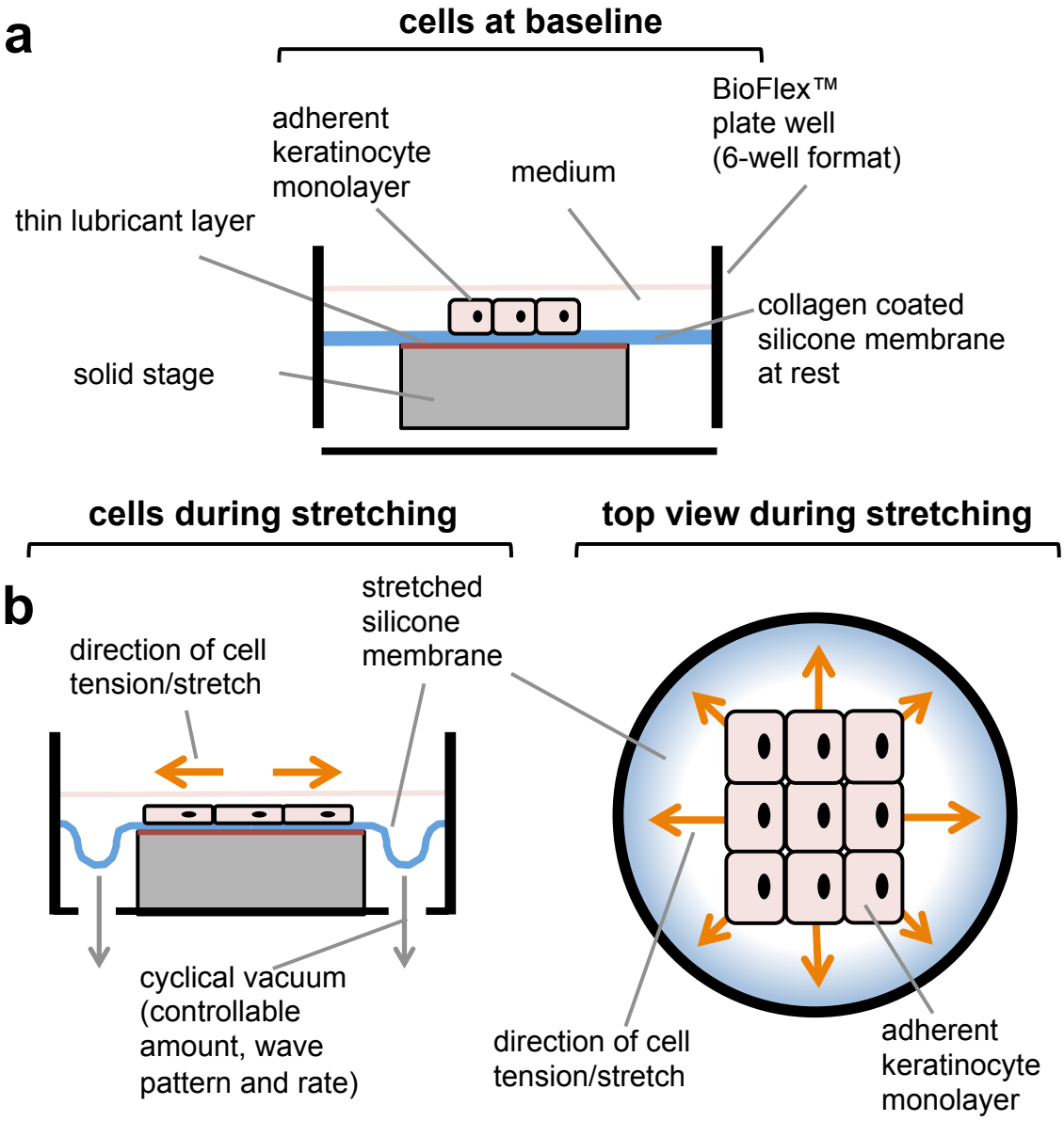

Figure 6.1 Schematic diagram of the cell flexing system used in this study.

Schematic representation of the FLexCell™/BioFlex™ cell tension/flexion system.

(c) Cells were grown as confluent monolayers on coated silicone membranes (Collagen 1 for KC, Fibronectin for LEC)

(d) Cyclical tension was applied to the silicone membrane by means of adjustable vacuum (12h at 0.8Hz)

(e) Top view of individual chamber (6-well format) upon application of tensile stress

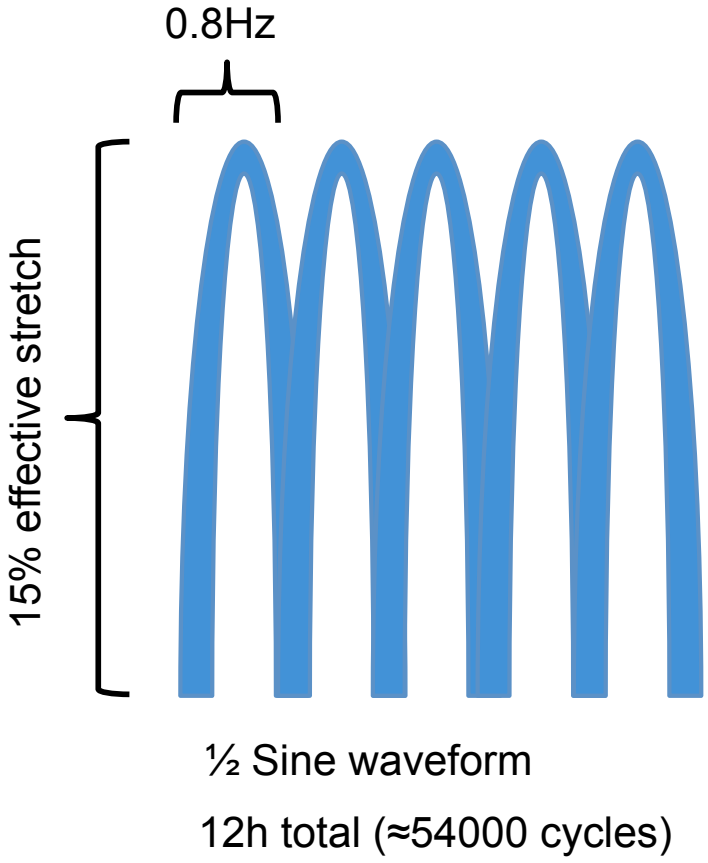

Figure 6.2 Diagrammatic representation of the waveform used for the application of tensile stress.

The FlexCell™ system enables adjustment of the duration, rate and waveform of the stretching applied. This study used a ½ sine waveform with 15% effective stretching of the membrane, at 0.8Hz for 12 hours.

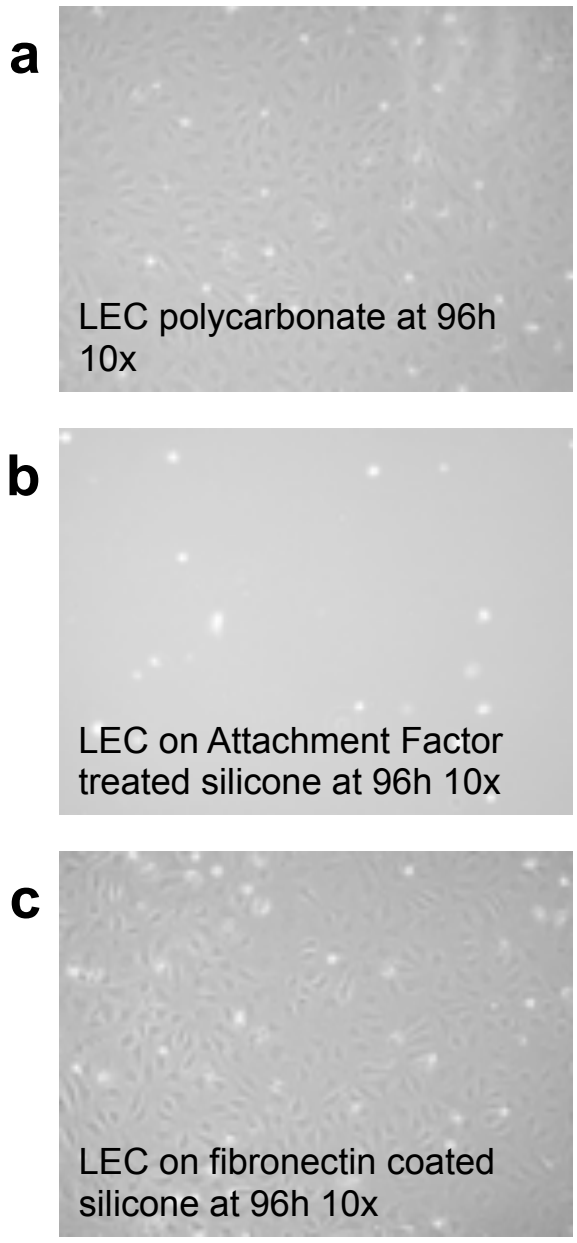

Figure 6.3 Representative bright field microscope images of primary human lymphatic endothelial cells (LEC) grown on different substrates.

(a) LEC grown as firmly adherent confluent monolayers on uncoated tissue culture polycarbonate (as per cell supplier's instructions)

(b) Image illustrating the failure of LECs to attach to silicone, even with the pre-treatment of the membrane with Attachment Factor (Sigma). LECs also failed to attach to untreated silicone.

(c) Image illustrating firm adhesion of LEC to Fibronectin coated silicone. Cells were always inspected at the end of experiments to ensure that they remained attached.

Data from one experiment, with n=3 wells per substrate.

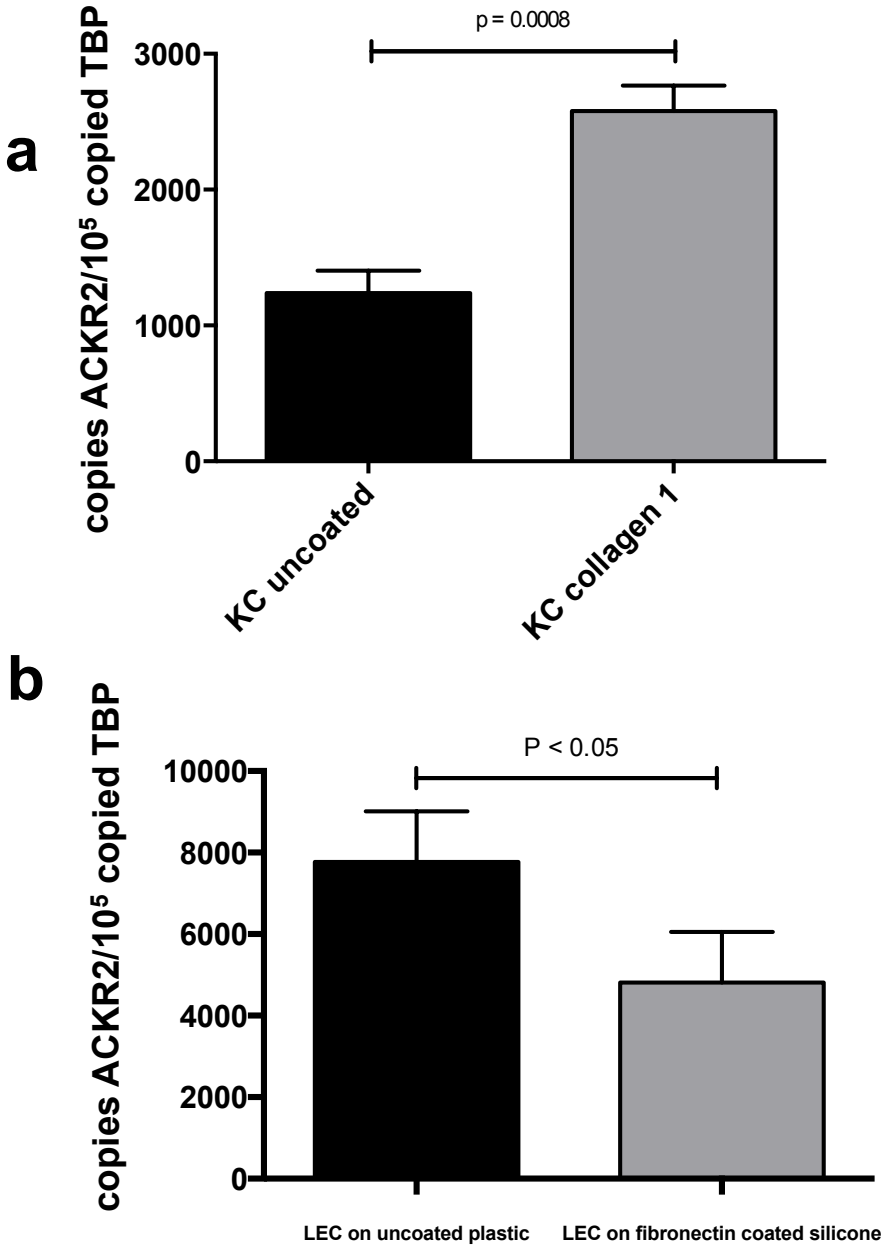

Figure 6.4 Effect of cell growth on Collagen 1 and Fibronectin on ACKR2 expression.

Absolute quantification of ACKR2 mRNA, normalised to TBP in;

(a) Healthy human primary KC grown on Collagen 1 coated silicone for 96 hours.

(b) Healthy human primary LEC grown on Fibronectin coated silicone for 96 hours.

Significance was assessed using Student's t-test. Data derived from one experiment, with n=3 wells per substrate.

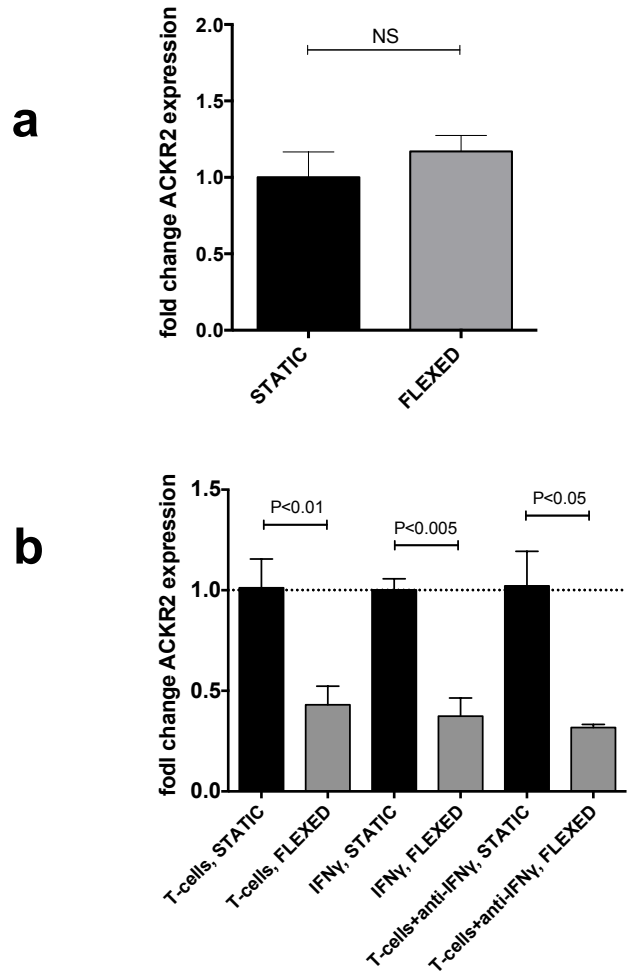

Figure 6.5 Effect of tensile stress on ACKR2 expression by primary human keratinocytes (KC).

Absolute quantification of ACKR2 mRNA, normalised to TBP, in keratinocytes

(a) Healthy human primary KC that remained static, or were subjected to tensile stress (flexed) at 0.8Hz for 12h, and then allowed to rest for 12h prior to cell lysis and RNA extraction.

(b) Healthy human primary KC that remained static, or were subjected to tensile stress (flexed) at 0.8Hz for 12h, and then allowed to rest for 12h prior to cell lysis and RNA extraction. KC were treated with either ***1)*** tissue culture supernatant from activated human T-cells (1:8 dilution in fresh medium), ***2)*** 100ng/ml recombinant human IFNγ, or ***3)*** tissue culture supernatant from activated human T-cells plus neutralising anti-IFNγ antibodies, overnight prior to flexing at 0.8Hz for 12hours. Black bars; non-flexed static controls, grey bars flexed cells.

Significance was assessed using One-way ANOVA. N=3 wells. Data representative of two comparable experiments (anti-interferon antibodies used once).

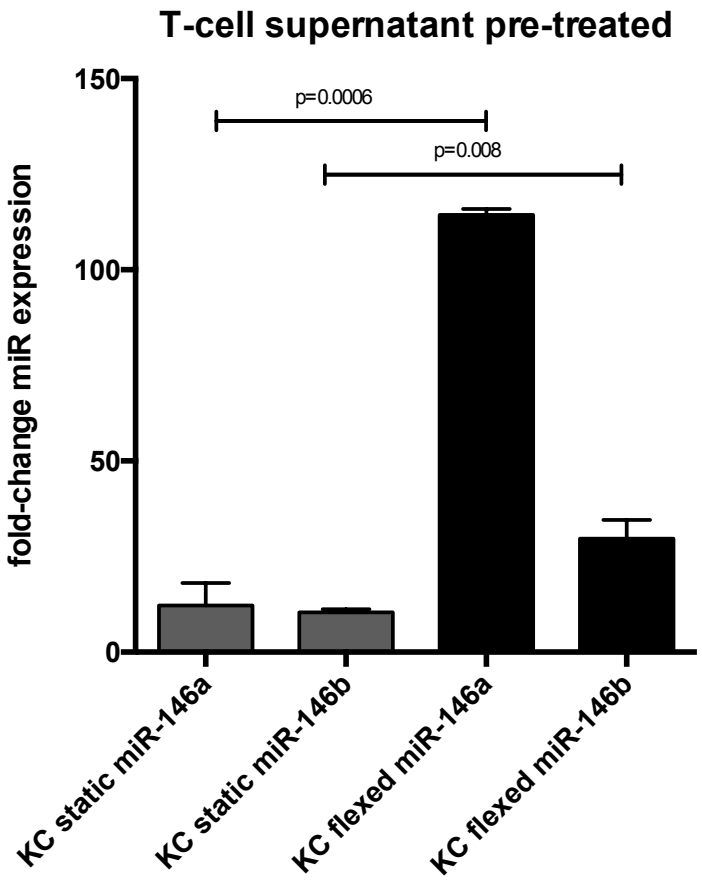

Figure 6.6 Effect of tensile stress on miR-146 expression in inflamed keratinocytes.

Fold change in miR-146a and miR-146b expression as assessed by QPCR, and normalised to scrambled miR treated static KCs. KC were treated with tissue culture supernatant from activated human T-cells (1:8 dilution in fresh medium) overnight prior to flexing at 0.8Hz for 12hours. Experiment performed once.

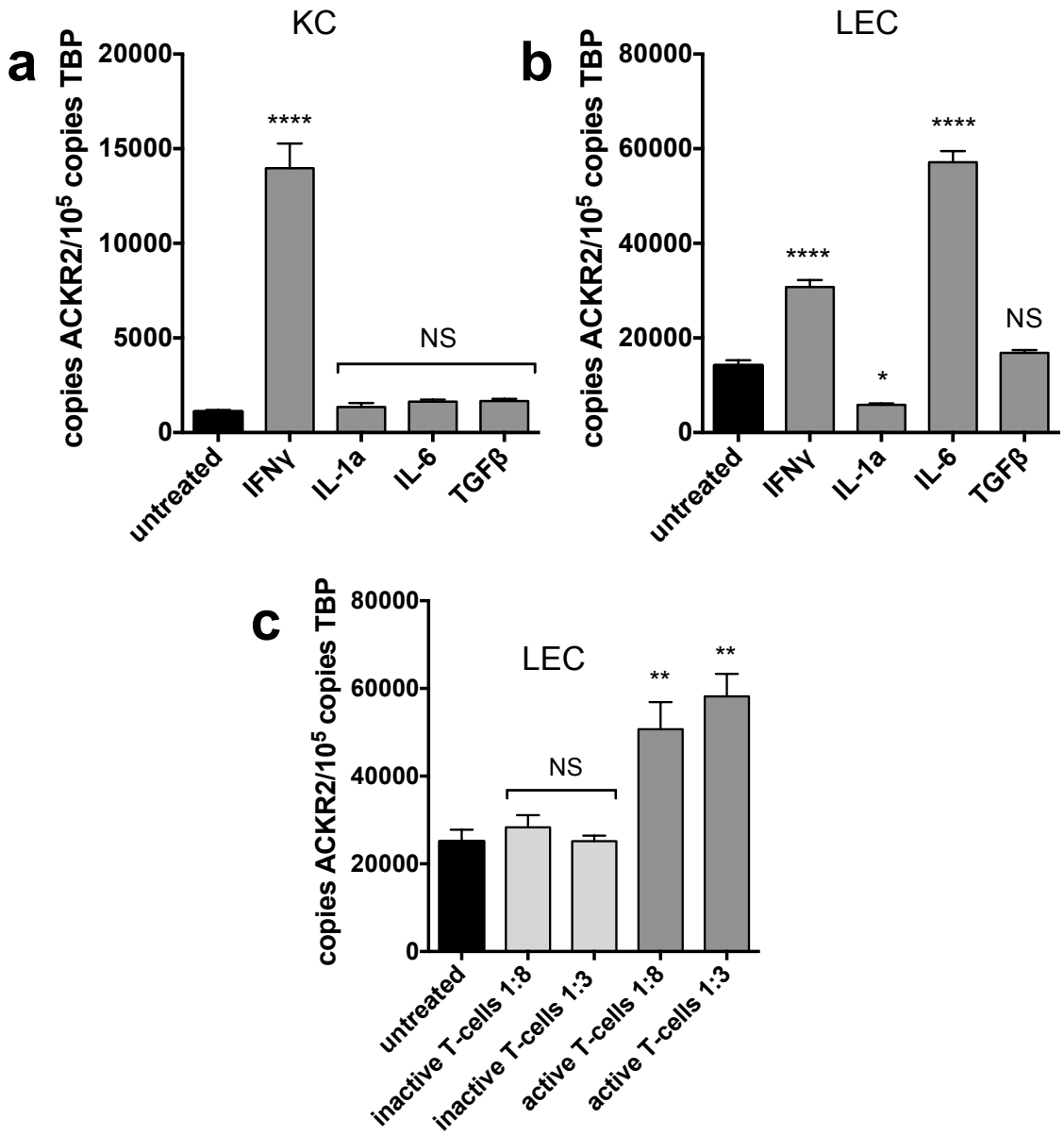

Figure 6.7 Cytokine treatment of healthy human primary keratinocytes and lymphatic endothelial cells.

Absolute quantification of ACKR2 mRNA, normalised to TBP following

(a) Treatment of healthy primary human keratinocytes with cytokine for 24 hours with IFNγ 10ng/ml; IL-1α 10ng/ml; IL-6 2ng/ml (pre-complexed with 10ng/ml sIL-6R); TGF-β 10ng/ml.

(b) Treatment of healthy primary human lymphatic endothelial cells (LEC) for 24 hours with IFNγ 10ng/ml; IL-1α 10ng/ml; IL-6 2ng/ml (pre-complexed with 10ng/ml sIL-6R); TGF-β 10ng/ml.

(c) Treatment of LEC with tissue culture supernatant from activated and inactive human T-cells (dilutions as indicated in figure)

Statistics: one-way ANOVA with Tukey's multiple comparisons test. * $P<0.05$, ** $P<0.01$, **** $P<0.0001$. Each experiment performed once, n=3 wells per treatment.

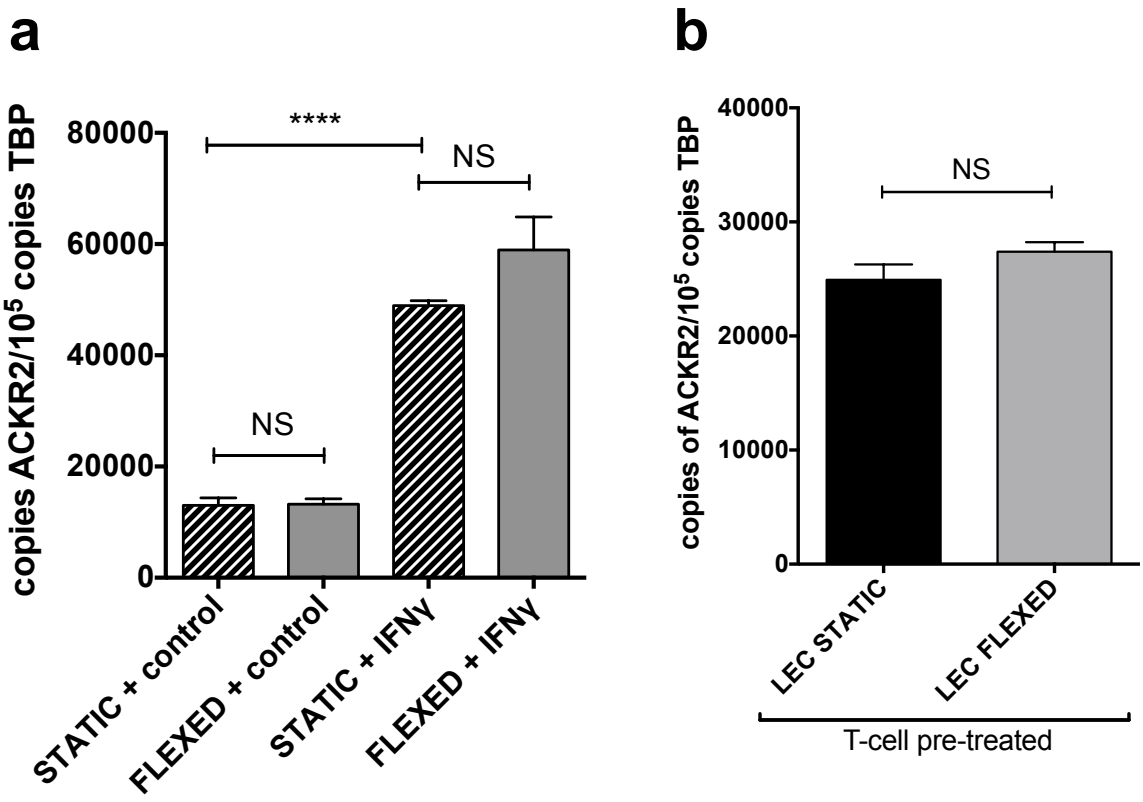

Figure 6.8 Effect of tensile stress on ACKR2 expression by lymphatic endothelial cells.

Absolute quantification of ACKR2 mRNA levels in lymphatic endothelial cells (LEC), normalised to TBP following

(a) no treatment, or treatment of LEC with IFNγ at 100ng/ml overnight, prior to flexing at 0.8Hz for 12h.

(b) Treatment of healthy primary LEC overnight with tissue culture supernatant from activated human T-cells (diluted 1:8 with fresh medium) prior to flexing.

Statistics: (a) one-way ANOVA with Tukey's multiple comparisons test and (b) Student's t-test. **** $P<0.0001$. Experiment performed once.

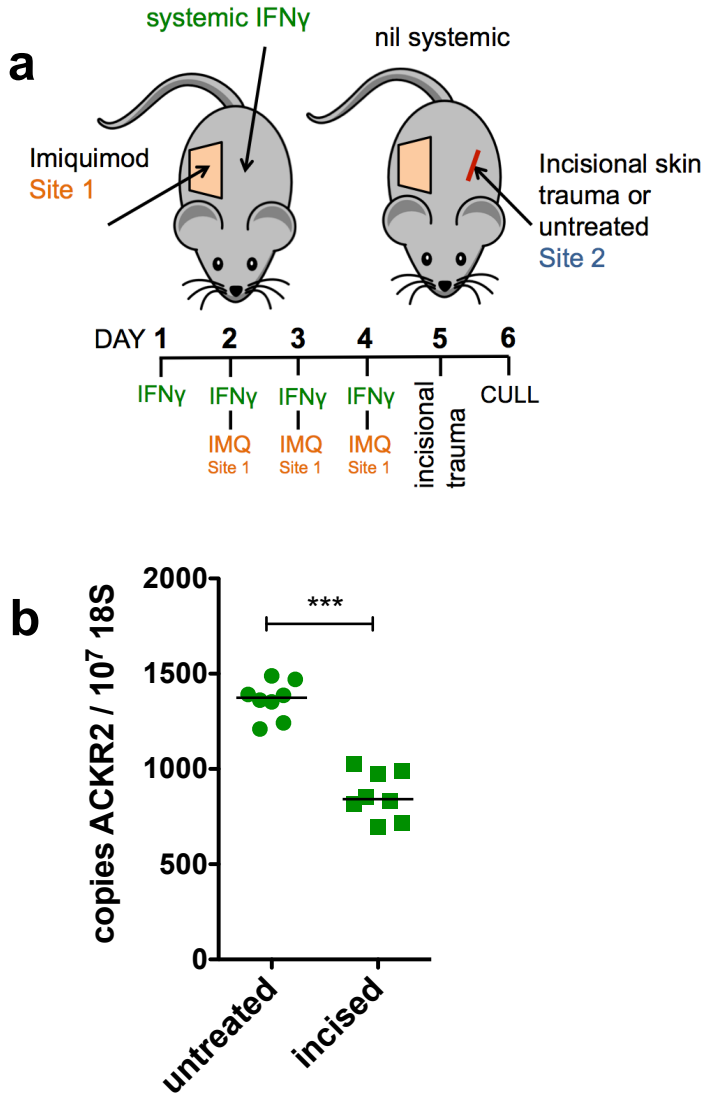

Figure 6.9. Effect of incisional skin trauma *in vivo* on ACKR2 expression

(a) Diagrammatic representation of the experimental design. One shaved mouse flank was treated with topical imiquimod (Aldara™ cream) daily for 3 days, with concurrent systemic IFNγ injections at 20,000U twice daily as indicated. This protocol had been previously shown to significantly upregulate ACKR2 expression in remote contralateral flank skin. Subsequently, and area was incised (down to superficial dermis), and the mice culled 24 hours later. Similarly treated mice that had not had their skin incised acted as a negative control.

(b) Absolute quantification of ACKR2 mRNA normalised to 18S in untreated whole mouse skin and incised skin.

Statistics: Paired Student's t-test *** $P<0.005$. The data presented represents one experiment.

6.5 Summary Chapter 6

This chapter reports for the first time that tensile trauma of inflamed human KC leads to a rapid reduction in ACKR2 expression. Concurrently, it reports that tensile trauma substantially upregulated the psoriasis-associated miR-146. This miR was shown, in the previous chapter, to bind the ACKR2 3'-UTR and downregulated ACKR2 in keratinocytes (KC).

Previous studies have shown that expression of ACKR2 is elevated in clinically unaffected skin of patients with psoriasis. Concurrently, expression of ACKR2 is relatively deficient in psoriatic plaques, although the mechanism for this downregulation had not been elucidated. Indeed, previous chapters of this thesis demonstrated that a lack of ACKR2 *in vivo* enables unrestricted CD3+ T-cell entry into the epidermis, and enhanced psoriasiform inflammation. Previous work has shown that tape stripping of unaffected psoriatic skin in humans leads to a rapid (24h) downregulation of ACKR2 expression in the traumatised skin.

Importantly, trauma as a downregulator of ACKR2 expression could provide, for the first time, a mechanism for so called koebnerisation. Koebnerisation is a phenomenon that has been described in psoriasis (and some other skin conditions) where trauma to unaffected skin leads to the development of skin lesions associated with the underlying condition. Furthermore, it is noteworthy, that psoriatic plaques tend to have a predilection for body sites that undergo repeated (tensile) stress due to day-to-day movement, e.g. elbows and knees. For these reasons, this chapter set out to examine the effect of tensile trauma on ACKR2 expression in the main ACKR2 expressing cells in the skin; keratinocytes (KC) and lymphatic endothelial cells (LEC). To enable this, a reductionist *in vitro* model of tensile skin trauma was developed, that enabled the study of tensile stress in isolation. It is however acknowledged that skin trauma has many elements, including compressive force, whilst incisional trauma is associated with complex wound repair processes.

In order to study the effect of cell tension on ACKR2 expression, the FlexCell™ FX5000 system was used, which enables repeated cyclical stretching of cells grown on flexible silicon membranes. Using this approach, both KC and LEC were subjected to tensile trauma, but this was found to

have no effect on ACKR2 expression in healthy cells. However, psoriasis is widely considered to be a systemic inflammatory disorder, with significant changes also in apparently unaffected skin (Xie et al. 2014). Furthermore, there are elevated levels of Th1/Th17 cytokines in the circulation of patients with psoriasis (need reference). Thus, in order to better recapitulate the *in vivo* situation, KC and LEC were both pre-treated with IFNγ or conditioned medium from activated human T-cells, both of which are known to upregulate ACKR2. When such inflamed KC and LECs were subjected to the same degree of tensile trauma, there was a rapid and significant reduction in ACKR2 expression in KC but not in LEC. These results are in keeping with cyclical tensile trauma in the context of inflammation reducing ACKR2 expression on KC.

Additionally, the preceding chapter of this thesis demonstrated that the psoriasis-associated miR-146 bound directly to the 3'-UTR of ACKR2 and downregulated its expression at transcript and protein level. Results in this chapter demonstrated that there was a substantial and significant increase in the expression of miR-146a/b in inflamed KC that had been subjected to tensile trauma, as compared to static KC. It is possible that it is this upregulation of miR-146a/b that drives the downregulation of ACKR2, although further studies (e.g. using antagomirs in similar future experiments) are required to ascertain whether this association is causative. Critically, these findings outlined in this and previous chapters provide for the first time a possible molecular mechanism for koebnerisation. It is hypothesised that cutaneous trauma leads to a rapid downregulation of ACKR2 in apparently unaffected skin; the downregulation in turn enables unrestricted T-cell recruitment (due to deficient ACKR2 scavenging of pro-inflammatory CC-chemokines), and unrestricted inflammation.

Whilst it is known that tape stripping of human unaffected psoriatic skin leads to a downregulation of ACKR2, there have been no animal models in which this can be further studied. In this chapter, preliminary results show that incisional trauma led to a rapid downregulation of ACKR2 in apparently unaffected skin of mice, in the well-established IMQ mouse model of psoriasis. The model outlined in this chapter, if further developed and validated, might enable the detailed study of koebnerisation *in vivo* in the

future. It is additionally noteworthy, that IFNγ administered systemically in a mouse model of psoriasis in previous chapters, was associated with reduced psoriasiform inflammation in WT, but not ACKR2 deficient mice. It is thus possible, that trauma to skin cells in the context of IFNγ associated inflammation, would lead to a reduction of ACKR2 expression and thus enhanced inflammation. This hypothesis is still to be explored *in vivo* in future studies.

CHAPTER 7

7 General discussion

Chemokines are chemotactic cytokines and have emerged as the principal regulators of leukocyte migration and inflammation (Griffith, Sokol & Luster 2014). The atypical chemokine receptor 2 (ACKR2, formerly D6) binds most pro-inflammatory CC-chemokines, but in contrast to conventional chemokine receptors, does not signal through G proteins upon ligand binding. Instead, ACKR2 internalises and helps degrade CC-chemokines. In doing so, ACKR2 acts as a chemokine scavenger that has a known role in regulating inflammation *in vivo* (Weber et al 2004). In the absence of ACKR2, inflammatory responses are dysfunctional in a number of *in vivo* models, although the mechanistic basis by which ACKR2 functions is still to be clarified (Di Liberto et al. 2008; Nibbs & Graham 2013; Nibbs et al. 2007; Berres et al. 2009).

Previous studies have shown a marked difference in ACKR2 expression in human psoriatic plaque skin, as compared to apparently unaffected skin from the same individuals. ACKR2 is particularly highly expressed in basal epidermal keratinocytes (KC) in non-lesional skin of psoriatic patients (Singh et al. 2012). Given the capacity of ACKR2 for scavenging pro-inflammatory CC-chemokines, it was hypothesised that high ACKR2 expression protects against inflammation. In contrast, it was hypothesised that reduced ACKR2 expression in psoriatic patients could lead to exaggerated responses to exogenous inflammatory cues and thus precipitate the development of a psoriasiform plaque. One such known exogenous cue is trauma, which can trigger the development of psoriatic lesions (so called *koebnerisation*) in some patients. Indeed, we have previously shown trauma to psoriatic skin to trigger a rapid down-regulation of ACKR2 expression in the skin (Singh et al. 2012).

In order to study the role of ACKR2 *in vivo*, a mouse model suitable for assessing differential ACKR2 expression in skin was established. Specifically, the well-established imiquimod (IMQ) mouse model was chosen as the basis for this model, as it shares key similarities with human psoriasis, enables the induction of psoriasiform plaques at specific skin sites, and is typically conducted in the same strain into which ACKR2-/-

mice are back-crossed (C57BL/6) (van der Fits et al. 2009). In this model, repeated application of the imiquimod cream Aldara™ leads to the rapid induction of psoriasiform skin plaques in wild-type (WT) C57BL/6 mice (van der Fits et al. 2009). In order to examine whether human ACKR2 expression patterns could be replicated in the IMQ model, ACKR2 mRNA expression was determined in whole skin. Data showed that ACKR2 expression in IMQ treated mouse skin was reduced (analogous to the relative ACKR2 deficiency seen in human psoriatic plaques (M. D. Singh et al. 2012)). Additional *ex vivo* whole mouse explant studies suggested that the active drug imiquimod, rather than another component of Aldara™ cream alone, can reduce ACKR2 expression in a dose-dependent manner. This is of significance, as there is an increasing recognition that Aldara™ cream modulates immune responses through other mechanisms than that induced by imiquimod alone (Walter et al. 2013).

In order to study, in detail, the dynamics of psoriasiform skin changes in this mouse model, a new scoring system of severity of psoriasiform inflammation was developed. This was broadly based on the human Psoriasis Area Severity Index (Fredriksson & Pettersson 1978), and is henceforth termed mPASI (0=normal skin, 12=most severe inflammation). Though some scoring systems of psoriasiform change in mice have been used in the literature, the criteria for scoring are often inadequately detailed/lacking altogether, and the scores are not validated against objective histopathological changes (van der Fits et al. 2009). In order to validate the mPASI defined here, the score was shown to significantly correlate with both epidermal thickening and KC hyperproliferation (as measured by staining for the cell proliferation marker Ki67). This is in keeping with the novel mPASI being a reliable clinical marker of histological features seen in psoriasiform inflammation *in vivo*.

IMQ induced rapid psoriasiform inflammation in WT C57BL/6 mice in these experiments. Whilst there are no differences in skin histology between ACKR2-/- and WT mice at rest (Nibbs et al. 2007), data showed that IMQ induced rapid psoriasiform skin changes that are significantly more severe in ACKR2-/- mice as compared to WT mice. Human psoriasis is characterised by both increased epidermal thickening, hyperkeratosis and

keratinocyte hyperproliferation (Griffiths & Barker 2007). In keeping with human psoriasis, IMQ treatment in mice led to significant epidermal thickening (acanthosis), enhanced hyperkeratosis and enhanced KC proliferation in ACKR2-/- and WT mice. Importantly, quantification of histological skin changes demonstrated significantly more severe psoriasis-associated changes in ACKR2-/- as compared to WT mice. Furthermore, the mPASI score increased more quickly, and reached a higher total, in ACKR2-/- as compared to WT mice. Overall, these results are in keeping with ACKR2 playing a role in limiting psoriasiform inflammation in a human disease-relevant murine model of psoriasis.

Psoriasis is increasingly considered to be a systemic condition, associated with excess cardiovascular and hepato-metabolic co-morbidities (Di Meglio et al. 2014; Roberts et al. 2014). For instance, prognosis of those with psoriasis is significantly worse following a myocardial infarction (Ahlehoff et al. 2011), and there is an increased prevalence of fatty liver disease in those with psoriasis (Roberts et al. 2014). Additionally, previous work on the IMQ model showed an enlargement of the spleen of mice treated with IMQ (van der Fits et al. 2009). For these reason, ACKR2 mRNA expression was additionally assessed in the heart, liver, spleen and skin draining lymph nodes in mice. Results showed a significant upregulation of ACKR2 in the heart and liver at day 7 in this model. Also, there was a significant increase in ACKR2 mRNA in non-draining (contralateral) inguinal lymph nodes of mice treated with IMQ, though this increase was small. In contrast, ACKR2 expression in the spleen is significantly reduced both at Days 4 and 7 in this model. The functional implications of these findings have yet to be determined and it will be important to explore whether reduced ACKR2 in remote tissues affect predisposition to inflammatory disorders. Relatively poor prognosis following a myocardial infarction (as seen in psoriasis (Ahlehoff et al. 2011)) may indicate aberrant regulation of inflammation, and it is possible that whilst ACKR2 expression is increased in e.g. the heart and liver in order to help limit inflammation, this increase may be insufficient to adequately limit inflammation. Additionally, it would be helpful to determine the precise site within the heart and liver where ACKR2 expression is increased, which may provide

insights into the possible functional relevance of its differential regulation in these organs. This is however not achievable at present e.g. through immunohistochemistry, as no antibodies are available that reliably detect ACKR2 in mice. One possibility would be to perform laser capture of specific tissue compartments, on which QPCR for ACKR2 transcript could be performed. Additionally, it would be interesting to induce inflammation in the heart and liver of mice in which ACKR2 expression has been induced, to assess the functional relevance of these observations *in vivo*. It should also be highlighted that whilst psoriasis is a chronic life-long disorder in humans, the observations here are over a relatively short period (7 days), and further longer-term time points would give us a better understanding of the long-term effects of skin inflammation on heart and liver tissue ACKR2 expression. Assessing the relevance of reduced ACKR2 expression in the spleen is more challenging, as a considerable amount of transcript is likely derived from leukocytes. These in turn are known to express ACKR2 (Graham & Locati 2013), and their migratory and heterogeneous nature makes analysis of ACKR2 expression in the spleen (and indeed lymph nodes) challenging.

Psoriasis pathology is a T-cell (notably Th1/Th17) driven condition (Di Meglio et al. 2014). In order to examine T-cells in the mouse IMQ model of psoriasis, mouse skin was stained for CD3+ T-cells and the effect of ACKR2 on T-cell positioning determined. Previous studies have shown that there are no significant differences between ACKR2-/- and WT mice at rest (Jamieson et al. 2005). Results here showed that whole skin CD3+ T-cell numbers are increased in the skin of both ACKR2-/- and WT mice upon treatment with IMQ. However, whilst CD3+ cells were largely excluded from the epidermis in WT mice, a high proportion of CD3+ T-cells were able to migrate and become positioned in the epidermis at both day 4 and 7 in ACKR2-/- mice in this model. Indeed, psoriasiform inflammation is critically dependent on T-cell migration from the dermis into the epidermis *in vivo* (Conrad et al. 2007), and these data suggest that ACKR2 plays a role in excluding CD3+ T-cells from the epidermis. These data suggest, for the first time, that ACKR2 plays a role in excluding T-cells from the epidermis during (IMQ-induced) psoriasiform inflammation.

Whilst previous studies have shown that the application of the phorbol ester TPA onto dorsal skin of ACKR2-/- mice leads to more florid inflammation compared to WT mice and a relative T-cell exclusion from the epidermis (Jamieson et al. 2005). However, whilst TPA that used in that particular study is an irritant, it does not induce inflammation that resembles psoriasis in C57BL/6 mice (either WT or ACKR2-/-).

The mechanism by which ACKR2 regulates the above observed T-cell epidermal localisation is not known. However, it is known that ACKR2 is predominantly expressed in basal epidermis/KCs (Singh et al. 2012), and that ACKR2 has the capacity to scavenge pro-inflammatory CC-chemokines (Weber et al 2004). KCs form a confluent proliferating cell layer that separates the dermis from the epidermis. CC-chemokines released in the epidermis thus need to form a chemotactic gradient that extends past the basal KCs, and into the dermis, in order to effectively recruit CC-chemokine receptor expressing leukocytes into the epidermis. It was hypothesised that ACKR2 expression by KCs creates defined areas of skin tissue that lack bioavailable inflammatory CC-chemokines, and so preventing the influx of leukocytes. In order to test whether ACKR2 expressed by KC can limit T cell migration past the dermal-epidermal interface, we established a novel *in vitro* model of T-cell migration. Whilst numerous chemokines are associated with psoriasis, CCL5 was selected as it is 1) associated with psoriasis pathogenesis and 2) is known to bind ACKR2 and 3) can attract inflammatory T-cells (CCL20 was not chosen for study as it is not bound by ACKR2). Data presented here suggest that high-ACKR2 expressing cells (both ACKR2 transfected HEK293 cells and IFNγ treated primary human KC), when placed between a CCL5 containing collagen matrix and T cells, restricted T-cell migration towards the CCL5 stimulus. In contrast, where ACKR2 expression is absent (HEK293 cells) or low (resting primary human KCs), T-cell migration and directionality towards the source of CCL5 across the cellular layer appears unaffected. This would in keeping with ACKR2 acting to prevent the free formation of a chemotactic CCL5 gradient, however, this experiments was performed once, and should be repeated to ensure the results are reproducible before drawing firm conclusions.

These observations in turn would tie in with the *in vivo* observations, that CD3+ T-cells are excluded from the epidermis in psoriasiform inflammation where ACKR2 is expressed, but can enter unrestricted in ACKR2-/- mice. It would be helpful for such experiments to be repeated with a broader range of psoriasis associated CC-chemokines that are also known to bind ACKR2 in order to more comprehensively understand in which contexts ACKR2 expression can restrict epidermal T-cell entry in the manner described above.

ACKR2 expression is relatively deficient in psoriatic plaques (Singh et al. 2012), and it has been shown in this thesis that a lack of ACKR2 is associated with more severe psoriasiform inflammation. In order to understand the molecular mechanism by which ACKR2 expression is negatively regulated, microRNAs were identified *in silico* that were predicted to bind the ACKR2 3'-UTR and that were shown to be differentially regulated in previous publications. MicroRNAs are, in the main, negative regulators of gene expression, bind the 3'-UTR of their mRNA target and lead to its degradation (Pasquinelli 2012). Data showed that miR-146 and miR-10 reduce ACKR2 mRNA and protein expression in keratinocytes (KC) and lymphatic endothelial cells (LEC) respectively and that they bind directly to the ACKR2 3'-UTR. The functional significance of the degree of reduction is however unknown. This is the first time a negative regulator of ACKR2 expression has been identified.

Our previous data additionally showed that simple skin trauma (in the form of tape stripping, where adhesive tape is repeatedly attached to skin and peeled off) of clinically unaffected human skin in patients with psoriasis, reduced ACKR2 mRNA expression (Singh et al. 2012). Additionally, it is recognised that psoriatic plaques have a predilection for skin that undergoes repeated tension, e.g. skin overlying elbows and knees (Lebwohl 2003). An *in vitro* model was therefore developed that enabled the study of the effect of tensile trauma on primary human skin cells. Results showed that tensile trauma of inflamed KC led to a rapid downregulation of ACKR2 expression. Additionally, there was a concurrent substantial and significant (>100-fold) upregulation of miR-146 in such cells that have been subjected to tensile stress. It is possible that miR-146

upregulation is a mechanism by which ACKR2 expression is reduced focally in skin that has been traumatised. It would be helpful to determine the causality of this association, for instance through the use of antagomirs to inhibit miR-146 upregulation upon the application of tensile cell stress. Whilst reductionist tensile stress experiments *in vitro* provide insights into the specific effects of tensile stress on cells, they will not fully capture the complex cell-cell interactions *in vivo*. Preliminary *in vivo* experiments in mice did however also suggest that trauma to skin (albeit in the form of incisional injury, rather than tape stripping), where ACKR2 expression had been previously induced, led to a rapid downregulation of ACKR2 expression. This provides the basis of an animal model in which negative ACKR2 regulation (and koebnerisation) can be studied *in vivo*, and could be expanded to test specifically the effect of tensile trauma *in vivo*. However, this model needs to be further validated and developed.

Experiments were, in general, conducted such that multiple techniques were used to demonstrate a specific finding. For instance, the effect of microRNAs on ACKR2 expression was demonstrated by Q-PCR of primary human cells, by immunocytochemistry of primary cell monolayers and by Western blotting (Chapter 5). It is acknowledged however, that where specific experiments were performed once in the thesis, the results should be treated with some caution. Indeed, it is important for further experiments to be undertaken to ascertain their reproducibility, before drawing firm conclusions. For experiments that assayed gene expression, further repeats would also enable more reliable comments to be made about the extent of up/down-regulation e.g. for Western blot experiments and immunocytochemistry (Chapter 5). This is also the case for leukocyte migration experiments in Chapter 3.

For cell culture experiments (Chapters 5 and 6), all experiments were performed as 3 replicates (e.g. tissue culture wells, tissue culture flasks), and individual biological samples analysed by quadruplicate by Q-PCR. However, it should be borne in mind that there are inherent biological differences between individuals, and though cell culture experiments were in general performed with primary cells from at least two different

human donors, increased donor numbers would have enabled a more thorough assessment on whether the presented data are generalizable.

In the laboratory where this work was performed, no litter-mates were available for the ACKR2-/- mice used (Chapters 3, 4 and 6). The control mice were therefore purchased, and it is acknowledged that (although they were one the same strain) differences could exist between the ACKR2-/- and purchased WT in terms of e.g. microbiota, diet and living environment prior to the experiments. Attempts were made to limit this source of bias, through co-housing the mice for at least one week prior to experiments. In future experiments, it would be helpful to breed and house control littermates alongside ACKR2-/- mice, to reduce this potential confounding variable.

For many experiments, ACKR2-/- numbers available were extremely limited (due to substantial difficulties with breeding adequate mouse numbers, and multiple users in the group). In particular, for key experiments where ACKR2-/- and WT mice were directly compared (Chapter 4) it would be important to repeat experiments more times, in order to ascertain reproducibility.

Current therapeutic strategies generally block T-cells and/or T-cell derived cytokines with variable specificity (Di Meglio et al. 2014). Though many of these are effective in alleviating symptoms, almost all anti-psoriatic therapies currently available are broadly immunosuppressive, and thus are associated with related averse effects, including increased risk of systemic infections and cancer (Di Meglio et al. 2014). The findings and hypotheses presented herein provide a novel means of limiting inflammation; by developing specific inducers of ACKR2 function, it may become possible to limit T-cell entry into the epidermis and thus the development of psoriasiform skin lesions. The rationale for such an approach is clearly demonstrated by the presented *in vivo* experiments, in which induced ACKR2 expression appeared to protect against psoriasiform inflammation. Such a therapeutic strategy would have the benefit of leaving the inherent function of T-cells intact (unlike most current therapies); instead targeting inflammation through modulating the T-cell

positioning in tissues. A topically applied agent capable of enhancing ACKR2 function would likely limit this effect largely to the skin, reducing potential adverse effects yet further. Such a future therapeutic approach would enhance (or at least maintain) the body's apparent endogenous means for limiting the spread of inflammation, that appear to fail at focal sites (e.g. through trauma), thus leading to exaggerated inflammation and plaque development.

Together, the presented data support the notion that ACKR2 induction may limit psoriasiform inflammation. However, further experimental work is required before the therapeutic potential of ACKR2 modulation in this context can be fully understood. It is particularly necessary to repeat experiments where ACKR2-/- and WT mice are directly compared, with further experimental repeats, including larger numbers of mice to ascertain reproducibility. Additionally, future experiments need to focus on functional effects of differential ACKR2 expression; e.g. data presented herein suggest certain microRNAs *in vitro* downregulate ACKR2 to a degree, and separate preliminary data also suggest that skin trauma in psoriasiform inflammation may downregulate ACKR2. However, these particular studies were not functional, and future experiments need to ascertain the effect of this downregulation on ACKR2 function *in vivo*.

Furthermore, though IFNγ was used as a tool to induce ACKR2 *in vivo*, using IFNγ as a therapeutic strategy in psoriasis is fraught with difficulty due to likely pro-inflammatory off§-target effects. Instead, it would be necessary to develop an agonist of ACKR2 function (rather than merely expression), that is capable of scavenging CC-chemokines *in vivo*. A high-throughput screening assay enabling the screening of validated compound libraries would be helpful. It would be particularly useful to perform such a screen in either primary cells, or *in vitro* skin equivalents, to better replicate the *in vivo* human situation. Identified compounds would subsequently provide a powerful tool for further studying the therapeutic potential for ACKR2 modulation both *in vitro* (e.g. update assays) and *in vivo*. It is noted however, that differences between mice and humans in terms of ACKR2 regulation, which are poorly defined, may provide particular challenges. Furthermore, the regulation of ACKR2 function is

not well understood and it is difficult to predict the pharmacological nature of such an agonist, through a small molecule compound could potentially be topically administered to skin, thus limiting systemic side effects.

The data presented herein suggests that ACKR2 may play a role in determining the positioning of T-cell in skin, and that this is associated with differences in the degree of inflammation. A causative link is possible, but has not been proven. Future studies will need to study the functional significance of T-cell positioning, both in terms of e.g. inflammatory chemokines/cytokines produced, but also in terms of T-cell cross-talk with other key psoriasis associated cells, including keratinocytes and dendritic cells. Critically also, little is known about what chemokines drive the early and chronic phases of psoriasis pathogenesis, and a better understanding of the role of chemokines (and in particular CC-chemokine ligands of ACKR2) would be pivotal in determining the therapeutic potential of ACKR2 modulation.

The presented data suggest that focal inflammation, modulates inflammatory responses in remote skin through modulation of ACKR2 expression. However, these changes are likely to occur over longer periods of time than that studied here; therefore, it would also be important to determine whether the differences noted between wild type and ACKR null mice are also apparent over a longer period of time. In addition, the observed effect of focal inflammation on remote skin needs to be studied in greater detail. It would additionally be particularly interesting to determine the effect of focal inflammation on resident T-cell populations in remote skin, and how any such changes may affect subsequent inflammatory processes.

Together, results presented in this thesis provide novel insights into the role of ACKR2 in psoriasiform inflammation, which are summarised schematically in Figure 7.1. ACKR2 plays a role in restricting epidermal T-cell entry and thus psoriasiform inflammation. Critically, the data provide a mechanism whereby spread of inflammation is restricted; one site of skin inflammation, leads to the upregulation of ACKR2 in remote unaffected skin, likely through soluble Th1/Th17 cytokines, and in

particular circulating IFNγ. This upregulation prevents the spread of psoriasiform inflammation to those sites. This upregulation can however be overcome by tensile trauma, that leads to a rapid downregulation of ACKR2 in keratinocytes. Specifically, microRNAs act as negative regulators of ACKR2, with tensile trauma being one factor that leads to the upregulation of microRNAs capable of downregulating ACKR2 expression. The findings presented provide a rationale for developing specific agonists of ACKR2 function, for the treatment and prevention of psoriasiform inflammation.

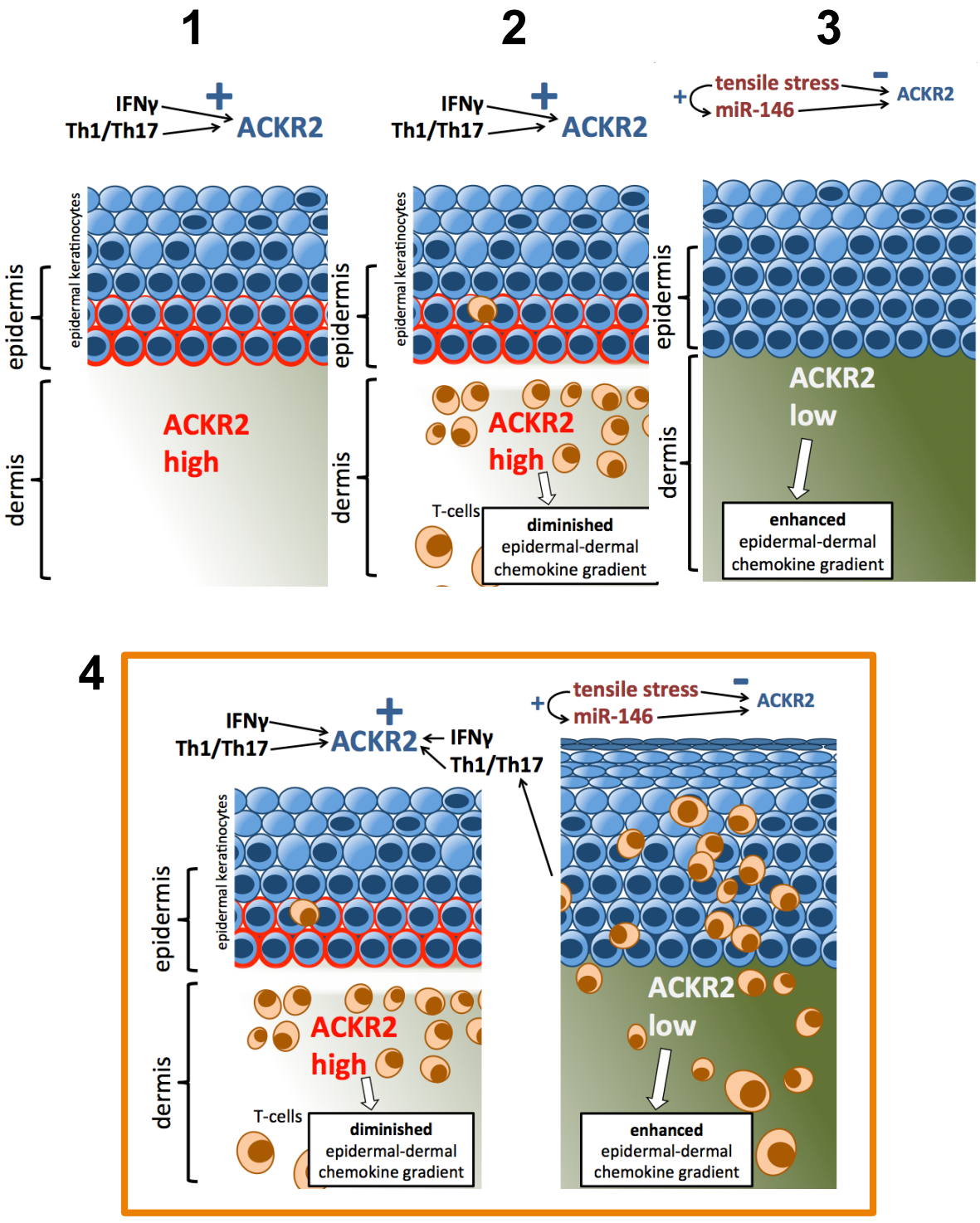

Figure 7.1 Schematic summary of main findings.

1) ACKR2 expression is increased in epidermal keratinocytes (KC) represented in red
2) Where basal epidermal KC ACKR2 expression is high, this leads to a clearance of epidermal-dermal chemotactic CC-chemokine gradients (clearance moss green shading). This limits CD3+ T-cell (orange ovals) entry into the epidermis.
3) Where ACKR2 is deficient (e.g. due to tensile trauma, miR-146), this leads to unrestricted chemotactic chemokine gradient formation (dark green)
4) This leads to enhanced CD3+ migration into the epidermis, release of pro-inflammatory factors, epidermal hyperproliferation, thickening and typical psoriasiform changes. Systemic release of Th1/Th17 cytokines will act to upregulate ACKR2 expression at remote skin sites. This in turn, protects such remote sites from the spread of psoriasiform inflammation

List of references

Aggarwal, S. et al., 2003. Interleukin-23 Promotes a Distinct CD4 T Cell Activation State Characterized by the Production of Interleukin-17. *Journal of Biological Chemistry*, 278(3), pp.1910–1914.

Ahlehoff, O. et al., 2011. Prognosis following first-time myocardial infarction in patients with psoriasis: a Danish nationwide cohort study. *Journal of Internal Medicine*, 270(3), pp.237–244.

Ainali, C. et al., 2012. Transcriptome classification reveals molecular subtypes in psoriasis. *BMC Genomics*, 13(1), p.472.

Albanesi, C. et al., 2009. Chemerin expression marks early psoriatic skin lesions and correlates with plasmacytoid dendritic cell recruitment. *Journal of Experimental Medicine*, 206(1), pp.249–258.

Almutawa, F. et al., 2013. Systematic Review of UV-Based Therapy for Psoriasis. *American Journal of Clinical Dermatology*, 14(2), pp.87–109.

Alolabi, N. et al 2011. The Koebner phenomenon and breast reconstruction: Psoriasis eruption along the surgical incision. *The Canadian journal of plastic surgery = Journal canadien de chirurgie plastique*, 19(4), pp.143–144.

Arai, H. et al 1997. Chemotaxis in a lymphocyte cell line transfected with C-C chemokine receptor 2B: evidence that directed migration is mediated by betagamma dimers released by activation of Galphai-coupled receptors. *Proceedings of the National Academy of Sciences of the United States of America*, 94(26), pp.14495–14499.

Arakawa, A. et al., 2015. Melanocyte antigen triggers autoimmunity in human psoriasis. *Journal of Experimental Medicine*, 212(13), pp.2203–2212.

Astarita, J. et al., 2012. Transcriptional profiling of stroma from inflamed and resting lymph nodes defines immunological hallmarks. *Nature Immunology*, 13(5), pp.499–510.

Ayala, F., 2007. Clinical presentation of psoriasis. *Reumatismo*, 59 Suppl 1, pp.40–45.

Bachelerie, F. et al., 2015. An atypical addition to the chemokine receptor nomenclature: IUPHAR Review 15. *British Journal of Pharmacology*, 172(16), pp.3945–3949.

Bachelerie, F. et al., 2000. New nomenclature for atypical chemokine receptors. *Nature Immunology*, 15(3), pp.207–208.

Baerveldt, E.M. et al., 2013. Ustekinumab improves psoriasis-related

gene expression in noninvolved psoriatic skin without inhibition of the antimicrobial response. *British Journal of Dermatology*, 168(5), pp.990–998.

Bailey, E.E. et al., 2012. Combination Treatments for Psoriasis: A Systematic Review and Meta-analysis. *Archives of dermatology*, 148(4), pp.511–522.

Bajoghli, B., 2013. Evolution and function of chemokine receptors in the immune system of lower vertebrates. *European Journal of Immunology*, 43(7), pp.1686–1692.

Baldwin, H.M. et al., 2013. Microarray Analyses Demonstrate the Involvement of Type I Interferons in Psoriasiform Pathology Development in D6-deficient Mice. *Journal of Biological Chemistry*, 288(51), pp.36473–36483.

Barker, J.N. et al., 1991. Keratinocytes as initiators of inflammation. *Lancet*, 337(8735), pp.211–214.

Bartel, D.P., 2004. MicroRNAs: genomics, biogenesis, mechanism, and function. *Cell*, 116(2), pp.281–297.

Bartel, D.P., 2009. MicroRNAs: Target Recognition and Regulatory Functions. *Cell*, 136(2), pp.215–233.

Baurecht, H. et al., 2015. Genome-wide comparative analysis of atopic dermatitis and psoriasis gives insight into opposing genetic mechanisms. *American Journal of Human Genetics*, 96(1), pp.104–120.

Bazzan, E. et al., 2013. Expression of the Atypical Chemokine Receptor D6 in Human Alveolar Macrophages in COPD. *CHEST Journal*, 143(1), pp.98–106.

Benechet, A.P., Menon, M. & Khanna, K.M., 2014. Visualizing T Cell Migration in situ. *Frontiers in Immunology*, 5(2), p.363.

Berres, M.-L. et al., 2009. The chemokine scavenging receptor D6 limits acute toxic liver injury in vivo. *Biological chemistry*, 390(10), pp.1039–1045.

Biondi Oriente, C. et al., 1989. Psoriasis and psoriatic arthritis. Dermatological and rheumatological co-operative clinical report. *Acta dermato-venereologica. Supplementum*, 146, pp.69–71.

Blackburn, P.E. et al., 2004. Purification and biochemical characterization of the D6 chemokine receptor. *Biochemical Journal*, 379(2), pp.263–272.

Boehncke, W.-H. & Schön, M.P., 2007. Animal models of psoriasis. *Clinics in dermatology*, 25(6), pp.596–605.

Boehncke, W.H. & Boehncke, W.H., 2005. The Psoriasis SCID Mouse Model: A Tool for Drug Discovery? In *link.springer.com*. Ernst Schering Research Foundation Workshop. Springer Berlin Heidelberg, pp. 213–234.

Boehncke, W.H. et al., 1996. Pulling the trigger on psoriasis. *Nature*, 379(6568), pp.777–777.

Bogunovic, M. et al., 2006. Identification of a radio-resistant and cycling dermal dendritic cell population in mice and men. *Journal of Experimental Medicine*, 203(12), pp.2627–2638.

Bondeva, T., 1998. Bifurcation of Lipid and Protein Kinase Signals of PI3K to the Protein Kinases PKB and MAPK. *Science*, 282(5387), pp.293–296.

Bonecchi, R. et al., 2004. Differential Recognition and Scavenging of Native and Truncated Macrophage-Derived Chemokine (Macrophage-Derived Chemokine/CC Chemokine Ligand 22) by the D6 Decoy Receptor. *The Journal of Immunology*, 172(8), pp.4972–4976.

Bonecchi, R. et al., 2008. Regulation of D6 chemokine scavenging activity by ligand- and Rab11-dependent surface up-regulation. *Blood*, 112(3), pp.493–503.

Bonini, J.A. & Steiner, D.F., 1997. Molecular cloning and expression of a novel rat CC-chemokine receptor (rCCR10rR) that binds MCP-1 and MIP-1beta with high affinity. *DNA and cell biology*, 16(9), pp.1023–1030.

Bonini, J.A. et al., 1997. Cloning, expression, and chromosomal mapping of a novel human CC-chemokine receptor (CCR10) that displays high-affinity binding for MCP-1 and MCP-3. *DNA and cell biology*, 16(10), pp.1249–1256.

Bordon, Y. et al., 2009. The Atypical Chemokine Receptor D6 Contributes to the Development of Experimental Colitis. *The Journal of Immunology*, 182(8), pp.5032–5040.

Borkowski, A.W. & Gallo, R.L., 2011. The Coordinated Response of the Physical and Antimicrobial Peptide Barriers of the Skin. *The Journal of investigative dermatology*, 131(2), pp.285–287.

Borroni, E.M. et al., 2013. ß-Arrestin-Dependent Activation of the Cofilin Pathway Is Required for the Scavenging Activity of the Atypical Chemokine Receptor D6. *Science signaling*, 6(273), p.ra30.

Bos, J.D. et al., 1983. Immunocompetent cells in psoriasis. In situ immunophenotyping by monoclonal antibodies. *Archives of Dermatological Research*, 275(3), pp.181–189.

Boyman, O. et al., 2004. Spontaneous development of psoriasis in a

new animal model shows an essential role for resident T cells and tumor necrosis factor-alpha. *The Journal of experimental medicine*, 199(5), pp.731–736.

Boyman, O. et al., 2007. The pathogenic role of tissue-resident immune cells in psoriasis. *Trends in immunology*, 28(2), pp.51–57.

Braun, A. et al., 2011. Afferent lymph–derived T cells and DCs use different chemokine receptor CCR7–dependent routes for entry into the lymph node and intranodal migration. *Nature Immunology*, 12(9), pp.879–887.

Bunting, M.D. et al., 2013. CCX-CKR deficiency alters thymic stroma impairing thymocyte development and promoting autoimmunity. *Blood*, 121(1), pp.118–128.

Burns, J.M. et al., 2006. A novel chemokine receptor for SDF-1 and I-TAC involved in cell survival, cell adhesion, and tumor development. *The Journal of experimental medicine*, 203(9), pp.2201–2213.

Cai, Y. et al., 2011. Pivotal role of dermal IL-17-producing γδ T cells in skin inflammation. *Immunity*, 35(4), pp.596–610.

Camargo, C.M.D.S. et al., 2013. Isomorphic phenomenon of Koebner: Facts and controversies. *Clinics in dermatology*, 31(6), pp.741–749.

Canals, M. et al., 2012. Ubiquitination of CXCR7 Controls Receptor Trafficking B. C. B. Ko, ed. *PLoS ONE*, 7(3), p.e34192.

Cantini, F. et al., 2015. Guidance for the management of patients with latent tuberculosis infection requiring biologic therapy in rheumatology and dermatology clinical practice. *Autoimmunity reviews*, 14(6), pp.503–509.

Capon, F. et al., 2007. Sequence variants in the genes for the interleukin-23 receptor (IL23R) and its ligand (IL12B) confer protection against psoriasis. *Human Genetics*, 122(2), pp.201–206.

Carthew, R.W. & Sontheimer, E.J., 2009. Origins and Mechanisms of miRNAs and siRNAs. *Cell*, 136(4), pp.642–655.

Chan, J.R. et al., 2006. IL-23 stimulates epidermal hyperplasia via TNF and IL-20R2-dependent mechanisms with implications for psoriasis pathogenesis. *Journal of Experimental Medicine*, 203(12), pp.2577–2587.

Chaudhuri, A. et al., 1994. Expression of the Duffy antigen in K562 cells. Evidence that it is the human erythrocyte chemokine receptor. *The Journal of biological chemistry*, 269(11), pp.7835–7838.

Chen, H. et al., 2011. A genetic risk score combining ten psoriasis risk

loci improves disease prediction. T. Mailund, ed. *PLoS ONE*, 6(4), p.e19454.

Cheuk, S. et al., 2014. Epidermal Th22 and Tc17 cells form a localized disease memory in clinically healed psoriasis. *The Journal of Immunology*, 192(7), pp.3111–3120.

Chollet, J.L. et al., 1999. Development of a topically active imiquimod formulation. *Pharmaceutical development and technology*, 4(1), pp.35–43.

Choy, D.F. et al., 2012. Comparative transcriptomic analyses of atopic dermatitis and psoriasis reveal shared neutrophilic inflammation. *The Journal of allergy and clinical immunology*, 130(6), pp.1335–43.e5.

Christophers, E., Metzler, G. & Röcken, M., 2014. Bimodal immune activation in psoriasis. *The British journal of dermatology*, 170(1), pp.59–65.

Clark, R.A., 2015. Resident memory T cells in human health and disease. *Science Translational Medicine*, 7(269), p.269rv1.

Clark, R.A., 2009. Skin-Resident T Cells: The Ups and Downs of On Site Immunity. *Journal of Investigative Dermatology*, 130(2), pp.362–370.

Clark, R.A. et al., 2006. The Vast Majority of CLA+ T Cells Are Resident in Normal Skin. *The Journal of Immunology*, 176(7), pp.4431–4439.

Clop, A. et al., 2013. An In-Depth Characterization of the Major Psoriasis Susceptibility Locus Identifies Candidate Susceptibility Alleles within an HLA-C Enhancer Element G. Novelli, ed. *PLoS ONE*, 8(8), p.e71690.

Codullo, V. et al., 2011. An investigation of the inflammatory cytokine and chemokine network in systemic sclerosis. *Annals of the Rheumatic Diseases*, 70(6), pp.1115–1121.

Comerford, I. et al., 2010. The atypical chemokine receptor CCX-CKR scavenges homeostatic chemokines in circulation and tissues and suppresses Th17 responses. *Blood*, 116(20), pp.4130–4140.

Comerford, I. et al., 2006. The chemokine receptor CCX-CKR mediates effective scavenging of CCL19in vitro. *European Journal of Immunology*, 36(7), pp.1904–1916.

Conrad, C. et al., 2007. Alpha1beta1 integrin is crucial for accumulation of epidermal T cells and the development of psoriasis. *Nature Medicine*, 13(7), pp.836–842.

Costa, C., Incio, J. & Soares, R., 2007. Angiogenesis and chronic inflammation: cause or consequence? *Angiogenesis*, 10(3), pp.149–

166.

Cotsapas, C. et al., 2011. Pervasive Sharing of Genetic Effects in Autoimmune Disease E. T. Dermitzakis, ed. *PLoS Genetics*, 7(8), p.e1002254.

Decaillot, F.M. et al., 2011. CXCR7/CXCR4 Heterodimer Constitutively Recruits -Arrestin to Enhance Cell Migration. *Journal of Biological Chemistry*, 286(37), pp.32188–32197.

Deleuran, M. et al., 1996. Localization of monocyte chemotactic and activating factor (MCAF/MCP-1) in psoriasis. *Journal of dermatological science*, 13(3), pp.228–236.

Devi, S. et al., 2013. Neutrophil mobilization via plerixafor-mediated CXCR4 inhibition arises from lung demargination and blockade of neutrophil homing to the bone marrow. *Journal of Experimental Medicine*, 210(11), pp.2321–2336.

DeVries, M.E. et al., 2005. Defining the Origins and Evolution of the Chemokine/Chemokine Receptor System. *The Journal of Immunology*, 176(1), pp.401–415.

Di Cesare, A., Di Meglio, P. & Nestle, F.O., 2009. The IL-23/Th17 Axis in the Immunopathogenesis of Psoriasis. *Journal of Investigative Dermatology*, 129(6), pp.1339–1350.

Di Lernia, V. et al., 2014. Familial aggregation of moderate to severe plaque psoriasis. *Clinical and experimental dermatology*, 39(7), pp.801–805.

Di Liberto, D. et al., 2008. Role of the chemokine decoy receptor D6 in balancing inflammation, immune activation, and antimicrobial resistance in Mycobacterium tuberculosis infection. *Journal of Experimental Medicine*, 205(9), pp.2075–2084.

Di Meglio, P. & Duarte, J.H., 2013. CD8 T Cells and IFN-γ Emerge as Critical Players for Psoriasis in a Novel Model of Mouse Psoriasiform Skin Inflammation. *Journal of Investigative Dermatology*, 133(4), pp.871–874.

Di Meglio, P., Perera, G.K. & Nestle, F.O., 2011. The multitasking organ: recent insights into skin immune function. *Immunity*, 35(6), pp.857–869.

Di Meglio, P., Villanova, F. & Nestle, F.O., 2014. Psoriasis. *Cold Spring Harbor perspectives in medicine*, 4(8), pp.a015354–a015354.

Diani, M., Altomare, G. & Reali, E., 2015. T cell responses in psoriasis and psoriatic arthritis. *Autoimmunity reviews*, 14(4), pp.286–292.

Diluvio, L. et al., 2006. Identical TCR -Chain Rearrangements in Streptococcal Angina and Skin Lesions of Patients with Psoriasis

Vulgaris. *The Journal of Immunology*, 176(11), pp.7104–7111.

Dohlman, H.G., 2015. Thematic Minireview Series: Cell Biology of G Protein Signaling. *Journal of Biological Chemistry*, 290(11), pp.6679–6680.

Drobits, B. et al., 2012. Imiquimod clears tumors in mice independent of adaptive immunity by converting pDCs into tumor-killing effector cells. *The Journal of Clinical Investigation*, 122(2), pp.575–585.

Duffin, K.C. et al., 2009. Genome-wide scan reveals association of psoriasis with IL-23 and NF-κB pathways. *Nature Genetics*, 41(2), pp.199–204.

Durham, A.L. et al., 2016. Targeted anti-inflammatory therapeutics in asthma and chronic obstructive lung disease. *Translational Research*, 167(1), pp.192–203.

Dustin, M.L. et al., 1988. Adhesion of T lymphoblasts to epidermal keratinocytes is regulated by interferon gamma and is mediated by intercellular adhesion molecule 1 (ICAM-1). *The Journal of experimental medicine*, 167(4), pp.1323–1340.

Eberle, F.C. et al., 2016. Recent advances in understanding psoriasis. *F1000Research*, 5, p.770.

Ekimler, S. & Sahin, K., 2014. Computational Methods for MicroRNA Target Prediction. *Genes*, 5(3), pp.671–683.

Elder, J.T. et al., 1993. Cyclosporin A rapidly inhibits epidermal cytokine expression in psoriasis lesions, but not in cytokine-stimulated cultured keratinocytes. *The Journal of investigative dermatology*, 101(6), pp.761–766.

Ellis, C.N. et al., 1991. Cyclosporine for plaque-type psoriasis. Results of a multidose, double-blind trial. *The New England journal of medicine*, 324(5), pp.277–284.

Enamandram, M. & Kimball, A.B., 2013. Psoriasis Epidemiology: The Interplay of Genes and the Environment. *The Journal of investigative dermatology*, 133(2), pp.287–289.

Eulalio, A. & Mano, M., 2015. MicroRNA Screening and the Quest for Biologically Relevant Targets. *Journal of biomolecular screening*.

Eyerich, S. et al., 2009. Th22 cells represent a distinct human T cell subset involved in epidermal immunity and remodeling. *The Journal of Clinical Investigation*, 119(12), pp.3573–3585.

Fanti, P.A. et al., 2006. Generalized psoriasis induced by topical treatment of actinic keratosis with imiquimod. *International journal of dermatology*, 45(12), pp.1464–1465.

Ferguson, S.S. et al., 1996. Role of beta-arrestin in mediating agonist-promoted G protein-coupled receptor internalization. *Science*, 271(5247), pp.363–366.

Fierlbeck, G. & Rassner, G., 1990. Treatment of psoriasis and psoriatic arthritis with interferon gamma. *The Journal of investigative dermatology*, 95(6 Suppl), pp.138S–141S.

Flier, J. et al., 2001. Differential expression of CXCR3 targeting chemokines CXCL10, CXCL9, and CXCL11 in different types of skin inflammation. *The Journal of pathology*, 194(4), pp.398–405.

Flutter, B. & Nestle, F.O., 2013. TLRs to cytokines: mechanistic insights from the imiquimod mouse model of psoriasis. *European Journal of Immunology*, 43(12), pp.3138–3146.

Fontenot, J.D., Gavin, M.A. & Rudensky, A.Y., 2003. Foxp3 programs the development and function of CD4+CD25+ regulatory T cells. *Nature Immunology*, 4(4), pp.330–336.

Ford, L.B. et al., 2014. Characterization of Conventional and Atypical Receptors for the Chemokine CCL2 on Mouse Leukocytes. *The Journal of Immunology*, 193(1), pp.400–411.

Forster, R. et al., 1999. CCR7 coordinates the primary immune response by establishing functional microenvironments in secondary lymphoid organs. *Cell*, 99(1), pp.23–33.

Foster, C.A. et al., 1990. Human epidermal T cells predominantly belong to the lineage expressing alpha/beta T cell receptor. *The Journal of experimental medicine*, 171(4), pp.997–1013.

Fra, A.M. et al., 2003. Cutting edge: scavenging of inflammatory CC chemokines by the promiscuous putatively silent chemokine receptor D6. *Journal of immunology (Baltimore, Md. : 1950)*, 170(5), pp.2279–2282.

Fraki, J.E., Briggaman, R.A. & Lazarus, G.S., 1982. Uninvolved skin from psoriatic patients develops signs of involved psoriatic skin after being grafted onto nude mice. *Science*, 215(4533), pp.685–687.

Fredriksson, T. & Pettersson, U., 1978. Severe psoriasis--oral therapy with a new retinoid. *Dermatologic Surgery*, 157(4), pp.238–244.

Fuentes-Duculan, J. et al., 2010. A Subpopulation of CD163-Positive Macrophages Is Classically Activated in Psoriasis. *Journal of Investigative Dermatology*, 130(10), pp.2412–2422.

Funamoto, S. et al., 2002. Spatial and Temporal Regulation of 3-Phosphoinositides by PI 3-Kinase and PTEN Mediates Chemotaxis. *Cell*, 109(5), pp.611–623.

Galliera, E., Galliera, E., et al., 2004. ß-Arrestin-dependent Constitutive Internalization of the Human Chemokine Decoy Receptor D6. *Journal of Biological Chemistry*, 279(24), pp.25590–25597.

Galliera, E., Jala, V.R., et al., 2004. ß-Arrestin-dependent Constitutive Internalization of the Human Chemokine Decoy Receptor D6. *The Journal of biological chemistry*, 279(24), pp.25590–25597.

Ganguly, D. et al., 2009. Self-RNA-antimicrobial peptide complexes activate human dendritic cells through TLR7 and TLR8. *Journal of Experimental Medicine*, 206(9), pp.1983–1994.

Ganguly, D. et al., 2013. The role of dendritic cells in autoimmunity. *Nature Reviews Immunology*, 13(8), pp.566–577.

Gardner, L. et al., 2004. The human Duffy antigen binds selected inflammatory but not homeostatic chemokines. *Biochemical and Biophysical Research Communications*, 321(2), pp.306–312.

Geisse, J. et al., 2004. Imiquimod 5% cream for the treatment of superficial basal cell carcinoma: results from two phase III, randomized, vehicle-controlled studies. *Journal of the American Academy of Dermatology*, 50(5), pp.722–733.

Gelfand, J.M. et al., 2005. Prevalence and treatment of psoriasis in the United Kingdom: a population-based study. *Archives of dermatology*, 141(12), pp.1537–1541.

Germain, R.N., Robey, E.A. & Cahalan, M.D., 2012. A decade of imaging cellular motility and interaction dynamics in the immune system. *Science*, 336(6089), pp.1676–1681.

Ghoreschi, K. et al., 2011. Modulation of Innate and Adaptive Immune Responses by Tofacitinib (CP-690,550). *The Journal of Immunology*, 186(7), pp.4234–4243.

Gibson, S.J. et al., 2002. Plasmacytoid dendritic cells produce cytokines and mature in response to the TLR7 agonists, imiquimod and resiquimod. *Cellular Immunology*, 218(1-2), pp.74–86.

Gilliet, M. et al., 2004. Psoriasis Triggered by Toll-like Receptor 7 Agonist Imiquimod in the Presence of Dermal Plasmacytoid Dendritic Cell Precursors. *Archives of dermatology*, 140(12), pp.1490–1495.

Glitzner, E. et al., 2014. Specific roles for dendritic cell subsets during initiation and progression of psoriasis. *EMBO Molecular Medicine*, 6(10), pp.1312–1327.

Goodman, W.A., Cooper, K.D. & McCormick, T.S., 2012. Regulation generation: the suppressive functions of human regulatory T cells. *Critical reviews in immunology*, 32(1), pp.65–79.

Gosling, J. et al., 2000. Cutting edge: identification of a novel chemokine receptor that binds dendritic cell- and T cell-active chemokines including ELC, SLC, and TECK. *Journal of immunology (Baltimore, Md. : 1950)*, 164(6), pp.2851–2856.

Gottlieb, A.B. et al., 2003. Pharmacodynamic and pharmacokinetic response to anti-tumor necrosis factor-alpha monoclonal antibody (infliximab) treatment of moderate to severe psoriasis vulgaris. *Journal of the American Academy of Dermatology*, 48(1), pp.68–75.

Gottlieb, A.B. et al., 2005. TNF inhibition rapidly down-regulates multiple proinflammatory pathways in psoriasis plaques. *Journal of immunology (Baltimore, Md. : 1950)*, 175(4), pp.2721–2729.

Gottlieb, S.L. et al., 1995. Response of psoriasis to a lymphocyte-selective toxin (DAB389IL-2) suggests a primary immune, but not keratinocyte, pathogenic basis. *Nature Medicine*, 1(5), pp.442–447.

Graham, G.J. & Locati, M., 2013. Regulation of the immune and inflammatory responses by the “atypical” chemokine receptor D6. E. S. White & A. R. Mantovani, eds. *The Journal of pathology*, 229(2), pp.168–175.

Graham, G.J. & McKimmie, C.S., 2006. Chemokine scavenging by D6: a movable feast? *Trends in immunology*, 27(8), pp.381–386.

Graham, G.J. et al., 2012. The biochemistry and biology of the atypical chemokine receptors. *Immunology Letters*, 145(1-2), pp.30–38.

Griffith, J.W., Sokol, C.L. & Luster, A.D., 2014. Chemokines and chemokine receptors: positioning cells for host defense and immunity. *Annual Review of Immunology*, 32, pp.659–702.

Griffiths, C.E.M. & Barker, J.N.W.N., 2007. Pathogenesis and clinical features of psoriasis. *Lancet*, 370(9583), pp.263–271.

Griffiths, C.E.M. et al., 2015. Comparison of ixekizumab with etanercept or placebo in moderate-to-severe psoriasis (UNCOVER-2 and UNCOVER-3): results from two phase 3 randomised trials. *The Lancet*, 386(9993), pp.541–551.

Grillo-Ardila, C.F. et al., 1996. *Imiquimod for anogenital warts in non-immunocompromised adults* C. F. Grillo-Ardila, ed., Chichester, UK: John Wiley & Sons, Ltd.

Gudjonsson, J.E. et al., 2006. Distinct clinical differences between HLA-Cw*0602 positive and negative psoriasis patients--an analysis of 1019 HLA-C- and HLA-B-typed patients. *The Journal of investigative dermatology*, 126(4), pp.740–745.

Gudjonsson, J.E., Johnston, A., Dyson, M., Valdimarsson, H. & Elder, J.T., 2007. Mouse models of psoriasis. *Journal of Investigative*

Dermatology, 127(6), pp.1292–1308.

Guerrero-Aspizua, S. et al., 2010. Development of a Bioengineered Skin-Humanized Mouse Model for Psoriasis. *The American Journal of Pathology*, 177(6), pp.3112–3124.

Gunderson, A.J. et al., 2012. CD8+ T Cells Mediate RAS-Induced Psoriasis-Like Skin Inflammation through IFN-γ. *Journal of Investigative Dermatology*, 133(4), pp.955–963.

Gustafson, C.J. et al., 2012. Combination Therapy in Psoriasis. *American Journal of Clinical Dermatology*, 14(1), pp.9–25.

Halioua, B. et al., 2015. Extent of misconceptions, negative prejudices and discriminatory behaviour to psoriasis patients in France. *Journal of the European Academy of Dermatology and Venereology*, 30(4), pp.n/a–n/a.

Hampton, P.J. et al., 2012. Lithium regulates keratinocyte proliferation via glycogen synthase kinase 3 and NFAT2 (nuclear factor of activated T cells 2). *Journal of Cellular Physiology*, 227(4), pp.1529–1537.

Haniffa, M., Gunawan, M. & Jardine, L., 2015. Human skin dendritic cells in health and disease. *Journal of dermatological science*, 77(2), pp.85–92.

Hansell, C.A.H., Hurson, C.E. & Nibbs, R.J.B., 2011. DARC and D6: silent partners in chemokine regulation? *Immunology and cell biology*, 89(2), pp.197–206.

Hansell, C.A.H., Schiering, C., et al., 2011. Universal expression and dual function of the atypical chemokine receptor D6 on innate-like B cells in mice. *Blood*, 117(20), pp.5413–5424.

Harper, E.G. et al., 2009. Th17 Cytokines Stimulate CCL20 Expression in Keratinocytes In Vitro and In Vivo: Implications for Psoriasis Pathogenesis. *Journal of Investigative Dermatology*, 129(9), pp.2175–2183.

Hedrick, M.N. et al., 2009. CCR6 is required for IL-23-induced psoriasis-like inflammation in mice. *The Journal of Clinical Investigation*, 119(8), pp.2317–2329.

Heinzel, K., Benz, C. & Bleul, C.C., 2007. A silent chemokine receptor regulates steady-state leukocyte homing in vivo. *Proceedings of the National Academy of Sciences*, 104(20), pp.8421–8426.

Hewit, K.D. et al., 2014. The N-terminal Region of the Atypical Chemokine Receptor ACKR2 Is a Key Determinant of Ligand Binding. *jbc.org*.

Hébert, H.L. et al., 2015. Identification of loci associated with late-

onset psoriasis using dense genotyping of immune-related regions. *The British journal of dermatology*, 172(4), pp.933–939.

Hirsch, E. et al., 2000. Central role for G protein-coupled phosphoinositide 3-kinase gamma in inflammation. *Science*, 287(5455), pp.1049–1053.

Hoffmann, F. et al., 2012. Rapid Uptake and Degradation of CXCL12 Depend on CXCR7 Carboxyl-terminal Serine/Threonine Residues. *The Journal of biological chemistry*.

Homey, B. et al., 2002. CCL27-CCR10 interactions regulate T cell-mediated skin inflammation. *Nature Medicine*, 8(2), pp.157–165.

Horuk, R. et al., 1993. The human erythrocyte inflammatory peptide (chemokine) receptor. Biochemical characterization, solubilization, and development of a binding assay for the soluble receptor. *Biochemistry*, 32(22), pp.5733–5738.

Hundhausen, C. et al., 2011. Allele-Specific Cytokine Responses at the HLA-C Locus: Implications for Psoriasis. *The Journal of investigative dermatology*, 132(3), pp.635–641.

Jamieson, T. et al., 2005. The chemokine receptor D6 limits the inflammatory response in vivo. *Nature Immunology*, 6(4), pp.403–411.

Jayo, M.J., Zanolli, M.D. & Jayo, J.M., 1988. Psoriatic plaques in Macaca fascicularis. *Veterinary pathology*, 25(4), pp.282–285.

Johnson, Z., Proudfoot, A.E. & Handel, T.M., 2005. Interaction of chemokines and glycosaminoglycans: a new twist in the regulation of chemokine function with opportunities for therapeutic intervention. *Cytokine and Growth Factor Reviews*, 16(6), pp.625–636.

Johnson-Huang, L.M. et al., 2012. A Single Intradermal Injection of IFN-γ Induces an Inflammatory State in Both Non-Lesional Psoriatic and Healthy Skin. *Journal of Investigative Dermatology*, 132(4), pp.1177–1187.

Kadowaki, N. et al., 2001. Subsets of human dendritic cell precursors express different toll-like receptors and respond to different microbial antigens. *The Journal of experimental medicine*, 194(6), pp.863–869.

Kim, V.N., Han, J. & Siomi, M.C., 2009. Biogenesis of small RNAs in animals. *Nature Reviews Molecular Cell Biology*, 10(2), pp.126–139.

Koenen, H.J.P.M. et al., 2008. Human CD25highFoxp3pos regulatory T cells differentiate into IL-17-producing cells. *Blood*, 112(6), pp.2340–2352.

Kuang, Y. et al., 1996. Selective G protein coupling by C-C chemokine receptors. *The Journal of biological chemistry*, 271(8), pp.3975–3978.

Kvist, P.H. et al., 2009. Comparison of the effects of vitamin D products in a psoriasis plaque test and a murine psoriasis xenograft model. *Journal of Translational Medicine*, 7(1), p.107.

Lagane, B. et al., 2005. Mutation of the DRY motif reveals different structural requirements for the CC chemokine receptor 5-mediated signaling and receptor endocytosis. *Molecular Pharmacology*, 67(6), pp.1966–1976.

Laggner, U. et al., 2011. Identification of a Novel Proinflammatory Human Skin-Homing V 9V 2 T Cell Subset with a Potential Role in Psoriasis. *The Journal of Immunology*, 187(5), pp.2783–2793.

Lande, R. et al., 2015. Cationic antimicrobial peptides in psoriatic skin cooperate to break innate tolerance to self-DNA. *European Journal of Immunology*, 45(1), pp.203–213.

Lande, R. et al., 2007. Plasmacytoid dendritic cells sense self-DNA coupled with antimicrobial peptide. *Nature*, 449(7162), pp.564–569.

Lande, R. et al., 2014. The antimicrobial peptide LL37 is a T-cell autoantigen in psoriasis. *Nature communications*, 5, p.5621.

Langenes, V. et al., 2013. Expression of the chemokine decoy receptor D6 is decreased in colon adenocarcinomas. *Cancer Immunology, Immunotherapy*, 62(11), pp.1687–1695.

Laudanna, C. et al., 2002. Rapid leukocyte integrin activation by chemokines. *Immunological reviews*, 186(1), pp.37–46.

Lebwohl, M., 2003. Psoriasis. *The Lancet*, 361(9364), pp.1197–1204.

Lee, E. et al., 2004. Increased expression of interleukin 23 p19 and p40 in lesional skin of patients with psoriasis vulgaris. *The Journal of experimental medicine*, 199(1), pp.125–130.

Lee, K.M. et al., 2011. D6 facilitates cellular migration and fluid flow to lymph nodes by suppressing lymphatic congestion. *Blood*, 118(23), pp.6220–6229.

Lee, K.M. et al., 2014. The chemokine receptors ACKR2 and CCR2 reciprocally regulate lymphatic vessel density. *The EMBO journal*, 33(21), pp.2564–2580.

Leonardi, C. et al., 2015. Efficacy and Safety of Calcipotriene Plus Betamethasone Dipropionate Aerosol Foam in Patients With Psoriasis Vulgaris--a Randomized Phase III Study (PSO-FAST). *Journal of drugs in dermatology : JDD*, 14(12), pp.1468–1477.

Leonardi, C. et al., 2011. The Long-Term Safety of Adalimumab Treatment in Moderate to Severe Psoriasis. *American Journal of Clinical Dermatology*, 12(5), pp.321–337.

Ley, K. et al., 2007. Getting to the site of inflammation: the leukocyte adhesion cascade updated. *Nature Reviews Immunology*, 7(9), pp.678–689.

Li, W.-Q. et al., 2013. Interactions between adiposity and genetic polymorphisms on the risk of psoriasis. *British Journal of Dermatology*, 168(3), pp.639–642.

Lin, A.M. et al., 2011. Mast Cells and Neutrophils Release IL-17 through Extracellular Trap Formation in Psoriasis. *The Journal of Immunology*, 187(1), pp.490–500.

Lowe, N.J. et al., 1981. Psoriasiform dermatosis in a rhesus monkey. *The Journal of investigative dermatology*, 76(2), pp.141–143.

Lowes, M.A. et al., 2005. Increase in TNF-alpha and inducible nitric oxide synthase-expressing dendritic cells in psoriasis and reduction with efalizumab (anti-CD11a). *Proceedings of the National Academy of Sciences of the United States of America*, 102(52), pp.19057–19062.

Lowes, M.A. et al., 2013. The IL-23/T17 pathogenic axis in psoriasis is amplified by keratinocyte responses. *Trends in immunology*, 34(4), pp.174–181.

Lowes, M.A., Suárez-Fariñas, M. & Krueger, J.G., 2014. Immunology of Psoriasis. *Annual Review of Immunology*, 32(1), pp.227–255.

Lucas, B. et al., 2015. CCRL1/ACKR4 is expressed in key thymic microenvironments but is dispensable for T lymphopoiesis at steady state in adult mice. *European Journal of Immunology*, 45(2), pp.574–583.

Luker, K.E. et al., 2010. Constitutive and chemokine-dependent internalization and recycling of CXCR7 in breast cancer cells to degrade chemokine ligands. *Oncogene*, 29(32), pp.4599–4610.

Luster, A.D., 1998. Chemokines--chemotactic cytokines that mediate inflammation. *The New England journal of medicine*, 338(7), pp.436–445.

Lønnberg, A.S. et al., 2013. Heritability of psoriasis in a large twin sample. *The British journal of dermatology*, 169(2), pp.412–416.

Mabuchi, T. et al., 2012. Chemokine receptors in the pathogenesis and therapy of psoriasis. *Journal of dermatological science*, 65(1), pp.4–11.

Madigan, J. et al., 2010. Chemokine scavenger D6 is expressed by

trophoblasts and aids the survival of mouse embryos transferred into allogeneic recipients. *The Journal of Immunology*, 184(6), pp.3202–3212.

Marcelo, C.L. & Tomich, J., 1983. Cyclic AMP, glucocorticoid, and retinoid modulation of in vitro keratinocyte growth. *The Journal of investigative dermatology*, 81(1 Suppl), pp.64s–8s.

Markham, A., 2016. Ixekizumab: First Global Approval. *Drugs*, 76(8), pp.901–905.

Marrakchi, S. et al., 2011. Interleukin-36–Receptor Antagonist Deficiency and Generalized Pustular Psoriasis. *The New England journal of medicine*, 365(7), pp.620–628.

Marsland, B.J. et al., 2005. CCL19 and CCL21 Induce a Potent Proinflammatory Differentiation Program in Licensed Dendritic Cells. *Immunity*, 22(4), pp.493–505.

Masopust, D. & Schenkel, J.M., 2013. The integration of T cell migration, differentiation and function. *Nature Reviews Immunology*, 13(5), pp.309–320.

McCulloch, C.V. et al., 2008. Multiple roles for the C-terminal tail of the chemokine scavenger D6. *The Journal of biological chemistry*, 283(12), pp.7972–7982.

McCully, M.L. et al., 2012. Epidermis instructs skin homing receptor expression in human T cells. *Blood*, 120(23), pp.4591–4598.

McKimmie, C.S. & Graham, G.J., 2006. Leucocyte expression of the chemokine scavenger D6. *Biochemical Society Transactions*, 34(Pt 6), pp.1002–1004.

McKimmie, C.S. et al., 2013. An analysis of the function and expression of D6 on lymphatic endothelial cells. *Blood*, 121(18), pp.3768–3777.

McKimmie, C.S. et al., 2008. Hemopoietic Cell Expression of the Chemokine Decoy Receptor D6 Is Dynamic and Regulated by GATA1. *The Journal of Immunology*, 181(5), pp.3353–3363.

Mei, J. et al., 2010. CXCL5 regulates chemokine scavenging and pulmonary host defense to bacterial infection. *Immunity*, 33(1), pp.106–117.

Menter, A. et al., 2008. Adalimumab therapy for moderate to severe psoriasis: A randomized, controlled phase III trial. *Journal of the American Academy of Dermatology*, 58(1), pp.106–115.

Merad, M. et al., 2002. Langerhans cells renew in the skin throughout life under steady-state conditions. *Nature Immunology*, 3(12), pp.1135–1141.

Miller, L.H. et al., 1976. The resistance factor to Plasmodium vivax in blacks. The Duffy-blood-group genotype, FyFy. *The New England journal of medicine*, 295(6), pp.302–304.

Mizutani, H. et al., 2003. Animal models of psoriasis and pustular psoriasis. *Archives of Dermatological Research*, 295 Suppl 1, pp.S67–8.

Mora, J.R., 2005. Reciprocal and dynamic control of CD8 T cell homing by dendritic cells from skin- and gut-associated lymphoid tissues. *Journal of Experimental Medicine*, 201(2), pp.303–316.

Morales, J. et al., 1999. CTACK, a skin-associated chemokine that preferentially attracts skin-homing memory T cells. *Proceedings of the National Academy of Sciences of the United States of America*, 96(25), pp.14470–14475.

Morhenn, V.B., 1987. Use of Recombinant Interferon Gamma Administered Intramuscularly for the Treatment of Psoriasis. *Archives of dermatology*, 123(12), pp.1633–1637.

Morizane, S. & Gallo, R.L., 2012. Antimicrobial peptides in the pathogenesis of psoriasis. *J Dermatol*, 39(3), pp.225–230.

Murphy, P.M. et al., 2000. International Union of Pharmacology. XXII. Nomenclature for Chemokine Receptors. *Pharmacology Reviews*.

Müller, A.J. et al., 2012. CD4+ T cells rely on a cytokine gradient to control intracellular pathogens beyond sites of antigen presentation. *Immunity*, 37(1), pp.147–157.

Nair et al., 2006. Sequence and haplotype analysis supports HLA-C as the psoriasis susceptibility 1 gene. *American Journal of Human Genetics*, 78(5), pp.827–851.

Nakatsuji, T. & Gallo, R.L., 2011. Antimicrobial Peptides: Old Molecules with New Ideas. *The Journal of investigative dermatology*, 132(3), pp.887–895.

Naumann, U. et al., 2010. CXCR7 Functions as a Scavenger for CXCL12 and CXCL11 G. Pockley, ed. *PLoS ONE*, 5(2), p.e9175.

Neote, K. et al., 1994. Functional and biochemical analysis of the cloned Duffy antigen: identity with the red blood cell chemokine receptor. *Blood*, 84(1), pp.44–52.

Neptune, E.R., Iiri, T. & Bourne, H.R., 1999. G i Is Not Required for Chemotaxis Mediated by Gi-coupled Receptors. *Journal of Biological Chemistry*, 274(5), pp.2824–2828.

Nestle, F.O. & Nickoloff, B.J., 2006. Animal models of psoriasis: a brief update. *Journal of the European Academy of Dermatology and Venereology*, 20(s2), pp.24–27.

Nestle, F.O. et al., 2005. Plasmacytoid predendritic cells initiate psoriasis through interferon- production. *Journal of Experimental Medicine*, 202(1), pp.135–143.

Nestle, F.O., Di Meglio, P., et al., 2009. Skin immune sentinels in health and disease. *Nature Reviews Immunology*, 9(10), pp.679–691.

Nestle, F.O., Kaplan, D.H. & Barker, J., 2009. Psoriasis. *The New England journal of medicine*, 361(5), pp.496–509.

Nestle, F.O., Turka, L.A. & Nickoloff, B.J., 1994. Characterization of dermal dendritic cells in psoriasis. Autostimulation of T lymphocytes and induction of Th1 type cytokines. *Journal of Clinical Investigation*, 94(1), pp.202–209.

Nibbs, R.J. et al., 1999. LD78beta, a non-allelic variant of human MIP-1alpha (LD78alpha), has enhanced receptor interactions and potent HIV suppressive activity. *The Journal of biological chemistry*, 274(25), pp.17478–17483.

Nibbs, R.J. et al., 2001. The beta-chemokine receptor D6 is expressed by lymphatic endothelium and a subset of vascular tumors. *The American Journal of Pathology*, 158(3), pp.867–877.

Nibbs, R.J., Wylie, S.M., Pragnell, I.B., et al., 1997. Cloning and characterization of a novel murine beta chemokine receptor, D6. Comparison to three other related macrophage inflammatory protein-1alpha receptors, CCR-1, CCR-3, and CCR-5. *The Journal of biological chemistry*, 272(19), pp.12495–12504.

Nibbs, R.J.B. & Graham, G.J., 2013. Immune regulation by atypical chemokine receptors. *Nature Reviews Immunology*, 13(11), pp.815–829.

Nibbs, R.J.B. et al., 2007. The atypical chemokine receptor D6 suppresses the development of chemically induced skin tumors. *Journal of Clinical Investigation*, 117(7), pp.1884–1892.

Nibbs, R.J.B., Wylie, S.M., Yang, J., et al., 1997. Cloning and Characterization of a Novel Promiscuous Human beta -Chemokine Receptor D6. *Journal of Biological Chemistry*, 272(51), pp.32078–32083.

Nickoloff, B.J. & Nestle, F.O., 2004. Recent insights into the immunopathogenesis of psoriasis provide new therapeutic opportunities. *Journal of Clinical Investigation*, 113(12), pp.1664–1675.

Niggli, V., 2000. A membrane-permeant ester of phosphatidylinositol 3, 4, 5-trisphosphate (PIP 3) is an activator of human neutrophil migration. *FEBS letters*, 473(2), pp.217–221.

Nograles, K.E. et al., 2008. Th17 cytokines interleukin (IL)-17 and IL-22

modulate distinct inflammatory and keratinocyte-response pathways. *British Journal of Dermatology*, 159(5), pp.1092–1102.

Nomiyama, H. & Yoshie, O., 2015. Functional roles of evolutionary conserved motifs and residues in vertebrate chemokine receptors. *Journal of Leukocyte Biology*, 97(1), pp.39–47.

Nomiyama, H., Osada, N. & Yoshie, O., 2013. Systematic classification of vertebrate chemokines based on conserved synteny and evolutionary history. *Genes to cells : devoted to molecular & cellular mechanisms*, 18(1), pp.1–16.

O'Boyle, G. et al., 2009. Anti-inflammatory therapy by intravenous delivery of non-heparan sulfate-binding CXCL12. *The FASEB Journal*, 23(11), pp.3906–3916.

O'Brien, M. & Koo, J., 2006. The mechanism of lithium and beta-blocking agents in inducing and exacerbating psoriasis. *Journal of drugs in dermatology : JDD*, 5(5), pp.426–432.

Oberle, N. et al., 2007. Rapid suppression of cytokine transcription in human CD4+CD25 T cells by CD4+Foxp3+ regulatory T cells: independence of IL-2 consumption, TGF-beta, and various inhibitors of TCR signaling. *Journal of immunology (Baltimore, Md. : 1950)*, 179(6), pp.3578–3587.

Oh, C.J., Das, K.M. & Gottlieb, A.B., 2000. Treatment with anti-tumor necrosis factor α (TNF-α) monoclonal antibody dramatically decreases the clinical activity of psoriasis lesions. *Journal of the American Academy of Dermatology*, 42(5), pp.829–830.

Ohtsuki, M. et al., 2014. Secukinumab efficacy and safety in Japanese patients with moderate-to-severe plaque psoriasis: Subanalysis from ERASURE, a randomized, placebo-controlled, phase 3 study. *J Dermatol*, 41(12), pp.1039–1046.

Oka, A. et al., 2012. Current understanding of human genetics and genetic analysis of psoriasis. *The Journal of Dermatology*, 39(3), pp.231–241.

Onoufriadis, A. et al., 2011. Mutations in IL36RN/IL1F5 Are Associated with the Severe Episodic Inflammatory Skin Disease Known as Generalized Pustular Psoriasis. *The American Journal of Human Genetics*, 89(3), pp.432–437.

Oppenheim, J.J. & Yang, D., 2005. Alarmins: chemotactic activators of immune responses. *Current Opinion in Immunology*, 17(4), pp.359–365.

Oppmann, B. et al., 2000. Novel p19 protein engages IL-12p40 to form a cytokine, IL-23, with biological activities similar as well as distinct from IL-12. *Immunity*, 13(5), pp.715–725.

Ortega, C. et al., 2009. IL-17-producing CD8+ T lymphocytes from psoriasis skin plaques are cytotoxic effector cells that secrete Th17-related cytokines. *Journal of Leukocyte Biology*, 86(2), pp.435–443.

Osório, F. et al., 2012. Anti-TNF-Alpha Induced Psoriasiform Eruptions with Severe Scalp Involvement and Alopecia: Report of Five Cases and Review of the Literature. *Dermatology*, 225(2), pp.163–167.

Pablos, J.L. et al., 1999. Stromal-cell derived factor is expressed by dendritic cells and endothelium in human skin. *The American Journal of Pathology*, 155(5), pp.1577–1586.

Pantelyushin, S., Haak, S., Ingold, B., Kulig, P., Heppner, F.L., Navarini, A.A. & Becher, B., 2012. Rorγt+ innate lymphocytes and γδ T cells initiate psoriasiform plaque formation in mice. *The Journal of Clinical Investigation*, 122(6), pp.2252–2256.

Papp, K., Cather, J.C., et al., 2012. Efficacy of apremilast in the treatment of moderate to severe psoriasis: a randomised controlled trial. *The Lancet*, 380(9843), pp.738–746.

Papp, K.A. et al., 2005. A global phase III randomized controlled trial of etanercept in psoriasis: safety, efficacy, and effect of dose reduction. *British Journal of Dermatology*, 152(6), pp.1304–1312.

Papp, K.A. et al., 2008. Efficacy and safety of ustekinumab, a human interleukin-12/23 monoclonal antibody, in patients with psoriasis: 52-week results from a randomised, double-blind, placebo-controlled trial (PHOENIX 2). *Lancet*, 371(9625), pp.1675–1684.

Papp, K.A. et al., 2013. Long-term safety of ustekinumab in patients with moderate-to-severe psoriasis: final results from 5 years of follow-up. *British Journal of Dermatology*, 168(4), pp.844–854.

Papp, K.A., Menter, A., et al., 2012. Efficacy and safety of tofacitinib, an oral Janus kinase inhibitor, in the treatment of psoriasis: a Phase 2b randomized placebo-controlled dose-ranging study. *British Journal of Dermatology*, 167(3), pp.668–677.

Parisi, R. et al., 2012. Global Epidemiology of Psoriasis: A Systematic Review of Incidence and Prevalence. *The Journal of investigative dermatology*, 133(2), pp.377–385.

Pasquinelli, A.E., 2012. MicroRNAs and their targets: recognition, regulation and an emerging reciprocal relationship. *Nature Reviews Genetics*, 13(4), pp.271–282.

Patel, U. et al., 2011. Imiquimod 5% cream induced psoriasis: a case report, summary of the literature and mechanism. *British Journal of Dermatology*, 164(3), pp.670–672.

Paul, C. et al., 2010. Evidence-based recommendations to assess

psoriasis severity: systematic literature review and expert opinion of a panel of dermatologists. *Journal of the European Academy of Dermatology and Venereology*, 24, pp.2–9.

Perera, G.K., Di Meglio, P. & Nestle, F.O., 2012. Psoriasis. *Annual Review of Pathology: Mechanisms of Disease*, 7, pp.385–422.

Petersein, C. et al., 2014. Impact of lithium alone and in combination with antidepressants on cytokine production in vitro. *Journal of Neural Transmission*, 122(1), pp.109–122.

Piskin, G. et al., 2006. In Vitro and In Situ Expression of IL-23 by Keratinocytes in Healthy Skin and Psoriasis Lesions: Enhanced Expression in Psoriatic Skin. *The Journal of Immunology*, 176(3), pp.1908–1915.

Primo, M.N. et al., 2012. Regulation of pro-inflammatory cytokines TNFα and IL24 by microRNA-203 in primary keratinocytes. *Cytokine*, 60(3), pp.741–748.

Puig, L., 2015. PASI90 response: the new standard in therapeutic efficacy for psoriasis. *Journal of the European Academy of Dermatology and Venereology : JEADV*, 29(4), pp.645–648.

Rajagopal, S. et al., 2010. ß-arrestin- but not G protein-mediated signaling by the "decoy" receptor CXCR7. *Proceedings of the National Academy of Sciences*, 107(2), pp.628–632.

Rajan, N. & Langtry, J.A.A., 2006. Generalized exacerbation of psoriasis associated with imiquimod cream treatment of superficial basal cell carcinomas. *Clinical and experimental dermatology*, 31(1), pp.140–141.

Randolph, G.J., Ochando, J. & Partida-Sánchez, S., 2008. Migration of dendritic cell subsets and their precursors. *Annual Review of Immunology*, 26(1), pp.293–316.

Raychaudhuri, S.P. et al., 1999. Upregulation of RANTES in psoriatic keratinocytes: a possible pathogenic mechanism for psoriasis. *Acta Dermato Venereologica*, 79(1), pp.9–11.

Reich, K. et al., 2015. Evidence That a Neutrophil-Keratinocyte Crosstalk Is an Early Target of IL-17A Inhibition in Psoriasis. *Experimental Dermatology*, pp.n/a–n/a.

Rink, I. et al., 2015. A Haptotaxis Assay for Leukocytes Based on Surface-Bound Chemokine Gradients. *Journal of Immunology*.

Riveira-Munoz, E. et al., 2010. Meta-Analysis Confirms the LCE3C_LCE3B Deletion as a Risk Factor for Psoriasis in Several Ethnic Groups and Finds Interaction with HLA-Cw6. *Journal of Investigative Dermatology*, 131(5), pp.1105–1109.

Roberts, K.K. et al., 2014. The prevalence of NAFLD and NASH among patients with psoriasis in a tertiary care dermatology and rheumatology clinic. *Alimentary Pharmacology & Therapeutics*, pp.n/a–n/a.

Rossi, D. & Zlotnik, A., 2000. The Biology of Chemokines and their Receptors. *dx.doi.org*.

Rot, A., 1993. Neutrophil attractant/activation protein-1 (interleukin-8) inducesin vitro neutrophil migration by haptotactic mechanism. *European Journal of Immunology*, 23(1), pp.303–306.

Rot, A. & Andrian, von, U.H., 2004. Chemokines in innate and adaptive host defense: basic chemokinese grammar for immune cells. *Annual Review of Immunology*, 22(1), pp.891–928.

Rot, A. et al., 2013. Cell-Autonomous Regulation of Neutrophil Migration by the D6 Chemokine Decoy Receptor. *The Journal of Immunology*, 190(12), pp.6450–6456.

Rothstein, B.E. et al., 2016. Apremilast and Secukinumab Combined Therapy in a Patient With Recalcitrant Plaque Psoriasis. *Journal of drugs in dermatology : JDD*, 15(5), pp.648–649.

Saba, R., Sorensen, D.L. & Booth, S.A., 2014. MicroRNA-146a: A Dominant, Negative Regulator of the Innate Immune Response. *Frontiers in Immunology*, 5(7), p.197.

Sadhu, C. et al., 2003. Essential Role of Phosphoinositide 3-Kinase in Neutrophil Directional Movement. *The Journal of Immunology*, 170(5), pp.2647–2654.

Savino, B. et al., 2009. Recognition versus adaptive up-regulation and degradation of CC chemokines by the chemokine decoy receptor D6 are determined by their N-terminal sequence. *Journal of Biological Chemistry*, 284(38), pp.26207–26215.

Scallon, B. et al., 2002. Binding and functional comparisons of two types of tumor necrosis factor antagonists. *The Journal of pharmacology and experimental therapeutics*, 301(2), pp.418–426.

Schafer, P.H. et al., 2009. Apremilast, a cAMP phosphodiesterase-4 inhibitor, demonstrates anti-inflammatory activity in vitro and in a model of psoriasis. *British Journal of Pharmacology*, 159(4), pp.842–855.

Schall, T.J. & Proudfoot, A.E.I., 2011. Overcoming hurdles in developing successful drugs targeting chemokine receptors. *Nature Reviews Immunology*, 11(5), pp.355–363.

Schlaak, J.F. et al., 1994. T cells involved in psoriasis vulgaris belong to the Th1 subset. *The Journal of investigative dermatology*, 102(2), pp.145–149.

Schmitt, J. et al., 2014. Efficacy and safety of systemic treatments for moderate-to-severe psoriasis: meta-analysis of randomized controlled trials. *British Journal of Dermatology*, 170(2), pp.274–303.

Schön, M.P. & Schön, M., 2007. Imiquimod: mode of action. *The British journal of dermatology*, 157 Suppl 2, pp.8–13.

Schulz, O. et al., 2016. Chemokines and Chemokine Receptors in Lymphoid Tissue Dynamics. *Annual Review of Immunology*, 34(1), pp.203–242.

Shevach, E.M., 2009. Mechanisms of foxp3+ T regulatory cell-mediated suppression. *Immunity*, 30(5), pp.636–645.

Singh, A. et al., 2015. The Interaction of Heparin Tetrasaccharides with Chemokine CCL5 Is Modulated by Sulfation Pattern and pH. *Journal of Biological Chemistry*, 290(25), pp.15421–15436.

Singh, M.D. et al., 2012. Elevated Expression of the Chemokine-Scavenging Receptor D6 Is Associated with Impaired Lesion Development in Psoriasis. *The American Journal of Pathology*, 181(4), pp.1158–1164.

Singh, T.P., Lee, C.H. & Farber, J.M., 2013. Chemokine receptors in psoriasis. *Expert opinion on therapeutic targets*, 17(12), pp.1405–1422.

Sivamani, R.K. et al., 2012. Biologic Therapies in the Treatment of Psoriasis: A Comprehensive Evidence-Based Basic Science and Clinical Review and a Practical Guide to Tuberculosis Monitoring. *Clinical Reviews in Allergy & Immunology*, 44(2), pp.121–140.

Smith, C.H. et al., 2009. British Association of Dermatologists' guidelines for biologic interventions for psoriasis 2009. *British Journal of Dermatology*, 161(5), pp.987–1019.

Snowden, J.A. & Heaton, D.C., 1997. Development of psoriasis after syngeneic bone marrow transplant from psoriatic donor: further evidence for adoptive autoimmunity. *The British journal of dermatology*, 137(1), pp.130–132.

So, L. & Fruman, D.A., 2012. PI3K signalling in B- and T-lymphocytes: new developments and therapeutic advances. *Biochemical Journal*, 442(3), pp.465–481.

Sokol, C.L. & Luster, A.D., 2015. The Chemokine System in Innate Immunity. *Cold Spring Harbor perspectives in biology*, 7(5).

Sonkoly, E. et al., 2007. MicroRNAs: Novel Regulators Involved in the Pathogenesis of Psoriasis? J. Zimmer, ed. *PLoS ONE*, 2(7), p.e610.

Sonkoly, E. et al., 2009. Protein Kinase C-Dependent Upregulation of

miR-203 Induces the Differentiation of Human Keratinocytes. *Journal of Investigative Dermatology*, 130(1), pp.124–134.

Stevens, S.R. et al., 1998. Long-term effectiveness and safety of recombinant human interferon gamma therapy for atopic dermatitis despite unchanged serum IgE levels. *Archives of dermatology*, 134(7), pp.799–804.

Storelli, S. et al., 2007. Synthesis and Structure-Activity Relationships of 3H-Quinazolin-4-ones and 3H-Pyrido[2,3-d]pyrimidin-4-ones as CXCR3 receptor antagonists. *Archiv der Pharmazie*, 340(6), pp.281–291.

Strange, A. et al., 2010. A genome-wide association study identifies new psoriasis susceptibility loci and an interaction between HLA-C and ERAP1. *Nature Genetics*, 42(11), pp.985–990.

Stuart, P.E. et al., 2012. Association of β-Defensin Copy Number and Psoriasis in Three Cohorts of European Origin. *The Journal of investigative dermatology*, 132(10), pp.2407–2413.

Suffee, N. et al., 2011. Angiogenic properties of the chemokine RANTES/CCL5. *Biochemical Society Transactions*, 39(6), pp.1649–1653.

Sugiyama, H. et al., 2005. Dysfunctional blood and target tissue CD4+CD25high regulatory T cells in psoriasis: mechanism underlying unrestrained pathogenic effector T cell proliferation. *Journal of immunology (Baltimore, Md. : 1950)*, 174(1), pp.164–173.

Sundberg, J.P. & King, L.E., 1996. Mouse mutations as animal models and biomedical tools for dermatological research. *The Journal of investigative dermatology*, 106(2), pp.368–376.

Sundberg, J.P. et al., 1990. Inherited mouse mutations as models of human adnexal, cornification, and papulosquamous dermatoses. *Journal of Investigative Dermatology*, 95(5 Suppl), pp.62S–63S.

Sutton, C.E. et al., 2009. Interleukin-1 and IL-23 Induce Innate IL-17 Production from γδ T Cells, Amplifying Th17 Responses and Autoimmunity. *Immunity*, 31(2), pp.331–341.

Suzuki, E. et al., 2014. The IL-23/IL-17 axis in psoriatic arthritis. *Autoimmunity reviews*, 13(4-5), pp.496–502.

Sweeney, C.M., Tobin, A.-M. & Kirby, B., 2011. Innate immunity in the pathogenesis of psoriasis. *Archives of Dermatological Research*, 303(10), pp.691–705.

Swindell et al., 2014. Cellular dissection of psoriasis for transcriptome analyses and the post-GWAS era. *BMC medical genomics*, 7(1), p.27.

Swindell et al., 2011. Genome-wide expression profiling of five mouse models identifies similarities and differences with human psoriasis. *PLoS ONE*, 6(4), p.e18266.

Szabo, M.C. et al., 1995. Chemokine class differences in binding to the Duffy antigen-erythrocyte chemokine receptor. *The Journal of biological chemistry*, 270(43), pp.25348–25351.

Szeimies, R.-M. et al., 2004. Imiquimod 5% cream for the treatment of actinic keratosis: results from a phase III, randomized, double-blind, vehicle-controlled, clinical trial with histology. *Journal of the American Academy of Dermatology*, 51(4), pp.547–555.

Takekoshi, T. et al., 2013. CXCR4 Negatively Regulates Keratinocyte Proliferation in IL-23-Mediated Psoriasiform Dermatitis. *The Journal of investigative dermatology*, 133(11), pp.2530–2537.

Tan et al., 2013. Structure of the CCR5 chemokine receptor-HIV entry inhibitor maraviroc complex. *Science*, 341(6152), pp.1387–1390.

Tan, C.S. & Koralnik, I.J., 2010. Progressive multifocal leukoencephalopathy and other disorders caused by JC virus: clinical features and pathogenesis. *The Lancet Neurology*, 9(4), pp.425–437.

Tang, H. et al., 2013. A large-scale screen for coding variants predisposing to psoriasis. *Nature Genetics*, 46(1), pp.45–50.

Teoh, P.J. et al., 2014. Atypical chemokine receptor ACKR2 mediates chemokine scavenging by primary human trophoblasts and can regulate fetal growth, placental structure, and neonatal mortality in mice. *The Journal of Immunology*, 193(10), pp.5218–5228.

Terui, T., Ozawa, M. & Tagami, H., 2000. Role of neutrophils in induction of acute inflammation in T-cell-mediated immune dermatosis, psoriasis: a neutrophil-associated inflammation-boosting loop. *Experimental Dermatology*, 9(1), pp.1–10.

Thelen, M., 2001. Dancing to the tune of chemokines. *Nature Immunology*, 2(2), pp.129–134.

Tiilikainen, A. et al., 1980. Psoriasis and HLA-Cw6. *The British journal of dermatology*, 102(2), pp.179–184.

Townson, J.R. & Nibbs, R.J.B., 2002. Characterization of mouse CCX-CKR, a receptor for the lymphocyte-attracting chemokines TECK/mCCL25, SLC/mCCL21 and MIP-3beta/mCCL19: comparison to human CCX-CKR. *European Journal of Immunology*, 32(5), pp.1230–1241.

Tsoi, L.C. et al., 2012. Identification of 15 new psoriasis susceptibility loci highlights the role of innate immunity. *Nature Genetics*, 44(12), pp.1341–1348.

Ueyama, A. et al., 2014. Mechanism of pathogenesis of imiquimod-induced skin inflammation in the mouse: A role for interferon-alpha in dendritic cell activation by imiquimod. *J Dermatol*, 41(2), pp.135–143.

Ulvmar, M.H. et al., 2014. The atypical chemokine receptor CCRL1 shapes functional CCL21 gradients in lymph nodes. *Nature Immunology*, 15(7), pp.623–630.

Urosevic, M. et al., 2005. Disease-Independent Skin Recruitment and Activation of Plasmacytoid Predendritic Cells Following Imiquimod Treatment. *JNCI Journal of the National Cancer Institute*, 97(15), pp.1143–1153.

Valladeau, J. et al., 2000. Langerin, a Novel C-Type Lectin Specific to Langerhans Cells, Is an Endocytic Receptor that Induces the Formation of Birbeck Granules. *Immunity*, 12(1), pp.71–81.

Van Belle, A.B. et al., 2012. IL-22 is required for imiquimod-induced psoriasiform skin inflammation in mice. *The Journal of Immunology*, 188(1), pp.462–469.

Van Belle, A.B. et al., IL-22 Is Required for Imiquimod-Induced Psoriasiform Skin Inflammation in Mice. *Journal of Immunology*.

van den Bogaard, E.H. et al., 2013. Crosstalk Between Keratinocytes and T-cells in a 3D Microenvironment: A Model to Study Inflammatory Skin Diseases. *Journal of Investigative Dermatology*, 134(3), pp.719–727.

van der Fits, L. et al., 2009. Imiquimod-induced psoriasis-like skin inflammation in mice is mediated via the IL-23/IL-17 axis. *The Journal of Immunology*, 182(9), pp.5836–5845.

van der Fits, L. et al., Imiquimod-Induced Psoriasis-Like Skin Inflammation in Mice Is Mediated via the IL-23/IL-17 Axis. *jimmunol.org*.

Vasudevan, S., Tong, Y. & Steitz, J.A., 2007. Switching from repression to activation: microRNAs can up-regulate translation. *Science*, 318(5858), pp.1931–1934.

Vender, Reid & Vender, Ronald, 2015. Paradoxical, Cupping-Induced Localized Psoriasis: A Koebner Phenomenon. *Journal of cutaneous medicine and surgery*, 19(3), pp.320–322.

Verma, S.B., 2009. Striae: stretching the long list of precipitating factors for â¤˜true koebnerizationâ¤™ of vitiligo, lichen planus and psoriasis. *Clinical and experimental dermatology*, 34(8), pp.880–883.

Vestergaard, C. et al., 2004. Expression of CCR2 on Monocytes and Macrophages in Chronically Inflamed Skin in Atopic Dermatitis and

Psoriasis. *Acta Dermato Venereologica*, 84(5), pp.353–358.

Vetrano, S. et al., 2010. The lymphatic system controls intestinal inflammation and inflammation-associated Colon Cancer through the chemokine decoy receptor D6. *Gut*, 59(2), pp.197–206.

Veys, E.M., Menkes, C.J. & Emery, P., 1997. A randomized, double-blind study comparing twenty-four-week treatment with recombinant interferon-gamma versus placebo in the treatment of rheumatoid arthritis. *Arthritis & Rheumatism*, 40(1), pp.62–68.

Villadsen, L.S. et al., 2003. Resolution of psoriasis upon blockade of IL-15 biological activity in a xenograft mouse model. *Journal of Clinical Investigation*, 112(10), pp.1571–1580.

Vinter, H., Iversen, L. & Steiniche, T., 2014. Aldara-induced skin inflammation-studies of psoriasis patients. *British Journal of …*.

Wagner, L. et al., 1998. beta-Chemokines are released from HIV-1-specific cytolytic T-cell granules complexed to proteoglycans. *Nature*, 391(6670), pp.908–911.

Walter, A. et al., 2013. Aldara activates TLR7-independent immune defence. *Nature communications*, 4, pp.1560–1560.

Warren, R.B. et al., 2015. Differential Drug Survival of Biologic Therapies for the Treatment of Psoriasis: A Prospective Observational Cohort Study from the British Association of Dermatologists Biologic Interventions Register (BADBIR). *Journal of Investigative Dermatology*, 135(11), pp.2632–2640.

Watanabe, R. et al., 2015. Human skin is protected by four functionally and phenotypically discrete populations of resident and recirculating memory T cells. *Science Translational Medicine*, 7(279), pp.279ra39–279ra39.

Watts, A.O. et al., 2013. ß-Arrestin recruitment and G protein signaling by the atypical human chemokine decoy receptor CCX-CKR. *Journal of Biological Chemistry*, 288(10), pp.7169–7181.

Weber, M. et al., 2013. Interstitial dendritic cell guidance by haptotactic chemokine gradients. *Science*, 339(6117), pp.328–332.

Weber, M., Blair, E., Simpson, C.V., O'Hara, M., Blackburn, P.E., Rot, A., Graham, G.J. & Nibbs, R.J.B., 2004. The chemokine receptor D6 constitutively traffics to and from the cell surface to internalize and degrade chemokines. *Molecular Biology of the Cell*, 15(5), pp.2492–2508.

Weiss, G., Shemer, A. & Trau, H., 2002. The Koebner phenomenon: review of the literature. *Journal of the European Academy of Dermatology and Venereology : JEADV*, 16(3), pp.241–248.

Weitz, J.E. & Ritchlin, C.T., 2013. Mechanistic Insights from Animal Models of Psoriasis and Psoriatic Arthritis. *Current Rheumatology Reports*, 15(11), pp.377–7.

Weninger, W., Biro, M. & Jain, R., 2014. Leukocyte migration in the interstitial space of non-lymphoid organs. *Nature Reviews Immunology*, 14(4), pp.232–246.

Wiederholt, T. et al., 2008. Genetic variations of the chemokine scavenger receptor D6 are associated with liver inflammation in chronic hepatitis C. *Human Immunology*, 69(12), pp.861–866.

Wimley, W.C., 2010. Describing the Mechanism of Antimicrobial Peptide Action with the Interfacial Activity Model. *ACS Chemical Biology*, 5(10), pp.905–917.

Witt, D.P. & Lander, A.D., 1994. Differential binding of chemokines to glycosaminoglycan subpopulations. *Current biology : CB*, 4(5), pp.394–400.

Wolf, R., Shechter, H. & Brenner, S., 1994. Induction of psoriasiform changes in guinea pig skin by propranolol. *International journal of dermatology*, 33(11), pp.811–814.

Wolfram, J.A. et al., 2009. Keratinocyte but Not Endothelial Cell-Specific Overexpression of Tie2 Leads to the Development of Psoriasis. *The American Journal of Pathology*, 174(4), pp.1443–1458.

Woolf, E. et al., 2007. Lymph node chemokines promote sustained T lymphocyte motility without triggering stable integrin adhesiveness in the absence of shear forces. *Nature Immunology*, 8(10), pp.1076–1085.

Wrone-Smith, T. & Nickoloff, B.J., 1996. Dermal injection of immunocytes induces psoriasis. *Journal of Clinical Investigation*, 98(8), pp.1878–1887.

Wu, J.K., Siller, G. & Strutton, G., 2004. Psoriasis induced by topical imiquimod. *Australasian Journal of Dermatology*, 45(1), pp.47–50.

Wu, S. et al., 2014. Hypertension, Antihypertensive Medication Use, and Risk of Psoriasis. *JAMA Dermatology*, 150(9), pp.957–963.

Xia, J. & Zhang, W., 2014. A meta-analysis revealed insights into the sources, conservation and impact of microRNA 5'-isoforms in four model species. *Nucleic Acids Research*, 42(3), pp.1427–1441.

Xie, S. et al., 2014. Comparisons of gene expression in normal, lesional, and non-lesional psoriatic skin using DNA microarray techniques. *International journal of dermatology*, 53(10), pp.1213–1220.

Xue, X. et al., 2011. Microbiota downregulates dendritic cell

expression of miR-10a, which targets IL-12/IL-23p40. *The Journal of Immunology*, 187(11), pp.5879–5886.

Zaba, L.C. et al., 2007. Amelioration of epidermal hyperplasia by TNF inhibition is associated with reduced Th17 responses. *Journal of Experimental Medicine*, 204(13), pp.3183–3194.

Zaba, L.C. et al., 2008. Psoriasis Is Characterized by Accumulation of Immunostimulatory and Th1/Th17 Cell-Polarizing Myeloid Dendritic Cells. *The Journal of investigative dermatology*, 129(1), pp.79–88.

Zibert, J.R. et al., 2010. MicroRNAs and potential target interactions in psoriasis. *Journal of dermatological science*, 58(3), pp.177–185.

Zlotnik, A. & Yoshie, O., 2000. Chemokines: a new classification system and their role in immunity. *Immunity*, 12(2), pp.121–127.

Zlotnik, A. & Yoshie, O., 2012. The chemokine superfamily revisited. *Immunity*, 36(5), pp.705–716.

Zuo, X. et al., 2015. Whole-exome SNP array identifies 15 new susceptibility loci for psoriasis. *Nature communications*, 6, pp.6793.